



# Molecularly imprinted polymers for the miniaturized analysis of drug and neurotransmitter traces in biological samples

Thomas Bouvarel

## ► To cite this version:

Thomas Bouvarel. Molecularly imprinted polymers for the miniaturized analysis of drug and neurotransmitter traces in biological samples. Polymers. Sorbonne Université, 2020. English. NNT : 2020SORUS274 . tel-03414212

**HAL Id: tel-03414212**

<https://theses.hal.science/tel-03414212>

Submitted on 4 Nov 2021

**HAL** is a multi-disciplinary open access archive for the deposit and dissemination of scientific research documents, whether they are published or not. The documents may come from teaching and research institutions in France or abroad, or from public or private research centers.

L'archive ouverte pluridisciplinaire **HAL**, est destinée au dépôt et à la diffusion de documents scientifiques de niveau recherche, publiés ou non, émanant des établissements d'enseignement et de recherche français ou étrangers, des laboratoires publics ou privés.

## THESE DE DOCTORAT DE SORBONNE UNIVERSITÉ

**ED 388**

Spécialité Chimie Analytique

Présentée par

**Thomas BOUVAREL**

Pour obtenir le grade de

**Docteur de Sorbonne université**

---

**Polymères à empreintes moléculaires pour l'analyse miniaturisée de traces de stupéfiants et de neurotransmetteurs dans des échantillons biologiques**

---

Thèse dirigée par Mme Valérie Pichon

Soutenue le 27 novembre 2020, devant le jury composé de :

<b>M. Jérôme RANDON</b> , Professeur, Université Claude Bernard Lyon 1	Rapporteur
<b>M<sup>me</sup> Jeanne-Bernadette TSE SUM BUI</b> , Ingénieur de recherche CNRS, HDR, Université de Technologie de Compiègne	Rapporteur
<b>M. Ludovic BELLOT-GURLET</b> , Professeur, Sorbonne université, Paris	Examinateur
<b>M<sup>me</sup> Bérangère CLAUDE</b> , Maître de conférences, Université d'Orléans	Examinateur
<b>M<sup>me</sup> Nathalie DELAUNAY</b> , Chargé de recherche CNRS, HDR, ESPCI Paris	Membre invitée
<b>M<sup>me</sup> Valérie PICHON</b> , Professeur, Sorbonne université, Paris	Directrice de thèse



## Remerciements

Ce projet de thèse a été réalisé au Laboratoire des Sciences Analytiques, Bioanalytiques et Miniaturisation (LSABM) de l'ESPCI Paris.

Je tiens, tout d'abord, à exprimer ma gratitude au Docteur Jeanne-Bernadette Tse Sum Bui ainsi qu'au Professeur Jérôme Randon pour avoir accepté de juger la qualité de mes travaux en tant que rapporteurs. Mes remerciements vont également au Docteur Bérangère Claude et au Professeur Ludovic Bellot-Gurlet pour leur implication et pour le temps qu'ils ont consacré à l'examen de ce manuscrit.

Mes remerciements vont bien évidemment à mon directeur de thèse, le Professeur Valérie Pichon ainsi qu'à mon encadrante, le Docteur Nathalie Delaunay pour m'avoir donné l'opportunité de mener à bien ce projet de thèse. Je les remercie chaleureusement pour leur encadrement, leur disponibilité, leurs conseils ainsi que leur soutien pendant ces trois années. Je ne saurai oublier ce temps passé avec elles, et j'espère que nos chemins se recroiseront.

Un grand merci aux permanents de ce laboratoire, Mélanie Cohen, Audrey Combès, José Dugay, Patrice Legeay, Didier Thiébaut et Jérôme Vial, qui m'ont apporté leur aide chacun à leur façon à des moments clés de ma thèse, sans oublier Patrick Sassié parti à la retraite. Un remerciement spécial à Isabelle Borsenberger et Hélène Dodier pour leur disponibilité et leur gentillesse à toute épreuve.

Je remercie tous les membres du LSABM pour les bons moments que j'ai passés au cours de ces années. Je remercie tout particulièrement Anastasia, Faïza, Florine, Marine, Pauline, Christophe, Clément, Romain et Stan pour leur bonne humeur, leur soutien et sans qui cette thèse n'aurait pas été la même. Mes pensées vont également aux anciens doctorants de ce laboratoire, Lorena, Maud, Sara, Julien et Vincent.

Un immense merci à tous mes amis qui m'ont accompagné tout au long de ces années. Merci à Mahaluxmy, Cédric, Elliot, Guillaume, Jonny, Maxime, Mickael et Ugo, groupe de la première heure de fac qui s'est étoffé au fil du temps pour former cette bande si unique et spéciale. Merci à Anne et Christophe pour ces années fantastiques d'études mais surtout de rigolades. Merci à Agathe B. et Jeanne pour ce trio formidable que nous formons. Merci à Adriana, Agathe L., Astrid, Carla, Hortense, Marie, Miya, Sophie, Sophie-Anne, Antoine D. et Antoine L. qui sont à mes côtés depuis de nombreuses

années et je l'espère le seront pour de nombreuses autres. Enfin, merci à Raoul, nous avons vécu tellement d'aventures depuis notre enfance, tu es simplement toi mais tu es un ami merveilleux.

Je veux remercier ma famille pour avoir rendu ces trois années de thèse inoubliables. Merci à mes parents, Sylvie et Pierre, pour leur confiance, leurs encouragements, leur soutien indéfectible mais avant tout leur patience. Un gigantesque merci à Mariette et Bertrand qui m'apportent bien plus qu'ils ne le pensent tout en faisant part à mon égard d'une tendresse et d'une générosité sans commune mesure.

Finalement, je dédie ce manuscrit à Aliette et Etienne Meurisse, ainsi qu'à Laurence† et Jacques† Bouvarel.

## **AVERTISSEMENT AU LECTEUR**

Cette thèse est rédigée comme une succession de chapitres, dont certains sont construits sur la structure d'articles (publiés ou soumis) pouvant se lire indépendamment. Ceci engendre des changements entre la langue française et anglaise ainsi que quelques redondances.



## TABLES DES MATIERES

<b>LISTES DES PUBLICATIONS ET COMMUNICATIONS .....</b>	<b>11</b>
PUBLICATIONS.....	11
COMMUNICATIONS ORALES .....	11
Symposiums internationaux.....	11
Symposiums nationaux .....	12
COMMUNICATIONS PAR AFFICHE .....	12
<b>LISTE DES ABREVIATIONS.....</b>	<b>15</b>
<b>INTRODUCTION GENERALE .....</b>	<b>17</b>
<b>CHAPITRE I – Etat de l'art sur les polymères à empreintes moléculaires dans des dispositifs d'extraction et de séparation miniaturisés .....</b>	<b>25</b>
Review : Molecularly imprinted polymers in miniaturized extraction and separation devices.....	27
I.1. Abstract.....	27
I.2. Introduction.....	28
I.3. Generalities on MIP synthesis .....	29
I.4. Open-tubular MIP .....	31
I.4.1. Preparation of open tubular MIP.....	31
I.4.2. Open tubular MIPs applied to separation in CEC and nanoLC.....	36
I.4.3. Open tubular MIPs in solid-phase extraction .....	38
I.5. MIP particles packed in capillary or chip channel .....	39
I.5.1. Packing of particles .....	39
I.5.2. Separation in CEC and nanoLC on particles-based MIPs .....	45
I.5.3. Particles-based MIP in solid-phase extraction.....	47
I.6. Monolithic MIPs.....	48
I.6.1. <i>In situ</i> synthesis of monolithic MIPs .....	49
I.6.1.1. Organic monolithic MIPs.....	49
I.6.1.2. Hybrid organic-inorganic monolith .....	51
I.6.2. Surface imprinting of a MIP on a core monolith.....	58
I.6.3. Monolithic MIPs for separations in CEC and nanoLC.....	62
I.6.4. Monolithic MIPs in extraction.....	71

I.6.4.1. Pipette tips .....	71
I.6.4.2. Capillaries .....	76
I.6.4.3. Chip microchannels.....	84
I.7. Conclusion .....	85

<b>CHAPITRE II – Monolithes à empreintes moléculaires couplés à la nano-chromatographie en phase liquide pour l'extraction sélective de la cocaïne.....</b>	<b>91</b>
II.1. Présentation des molécules d'intérêt.....	91
II.1.1. La cocaïne et sa toxicité .....	92
II.1.2. Pharmacocinétique et métabolisme de la cocaïne dans le corps humain .....	93
II.1.3. Propriétés physico-chimiques de la cocaïne et de la BZE .....	95
II.1.4. Matrices biologiques utilisées pour doser la cocaïne et la BZE .....	95
II.2. MIP pour l'extraction de la cocaïne et la BZE obtenu par une synthèse en bloc en format conventionnel.....	96
II.3. Vers une miniaturisation de l'étape d'extraction sélective de la cocaïne et de la BZE et son couplage en ligne avec la nanoLC.....	100
Article 1 : Selective extraction of cocaine from biological samples with a miniaturized monolithic molecularly imprinted polymer and on-line analysis in nano-liquid chromatography.....	100
II.3.1. Introduction .....	104
II.3.2. Experimental .....	106
II.3.2.1. Chemicals and reagents .....	106
II.3.2.2. In situ preparation of the monolithic polymers .....	106
II.3.2.3. Characterization of the monolithic MIP by SEM and nanoLC .....	107
II.3.2.4. NanoLC-UV analysis of cocaine and benzoylecgonine .....	108
II.3.2.5. On-line coupling of MIP or NIP extraction with nanoLC-UV analysis.....	109
II.3.2.6. Preparation of plasma and saliva samples.....	110
II.3.3. Results and discussion .....	110
II.3.3.1. Preliminary studies for the choice of the reagents.....	110
II.3.3.2. Evaluation of the selectivity studying retention properties in nanoLC.....	113
II.3.3.3. On-line coupling of the capillary containing the monolithic MIP and the nanoLC-UV system .....	115
II.3.3.4. Optimization of the on-line MIP extraction and nanoLC-UV analysis protocol .....	116
II.3.3.5. Applications to biological samples.....	119
II.3.4. Conclusion.....	123
II.3.5. Etude complémentaire en vue d'améliorer la rétention de la BZE .....	124

II.4. Conclusion .....	125
------------------------	-----

**CHAPITRE III – Monolithes à empreintes moléculaires pour la détection directe de la benzoylecgonine .....129**

Article 2 : Simplified miniaturized set-up based on molecularly imprinted polymer for the determination of benzoylecgonine in urine samples.....	131
III.1. Abstract.....	131
III.2. Introduction.....	132
III.3. Experimental.....	134
III.3.1.Chemicals and reagents .....	134
III.3.2. <i>In situ</i> preparation of the monolithic polymers.....	134
III.3.3.Characterization of the monoliths by SEM and nanoLC .....	135
III.3.4.On-line coupling of MIP or NIP extraction with direct UV detection .....	136
III.3.5.Preparation of biological samples.....	138
III.4. Results and discussion .....	138
III.4.1.Preliminary study on the potential of an on-line set-up for direct extraction and detection of BZE .....	138
III.4.2.Study of the synthesis conditions .....	141
III.4.3.Evaluation of the selectivity studying retention properties in nanoLC .....	143
III.4.4.Optimization of the on-line MIP extraction and UV detection analysis protocol.....	145
III.4.5.Applications to urinary samples.....	149
III.5. Conclusion .....	151

**CHAPITRE IV – Transfert de savoir-faire pour la production d'un monolithe à empreintes moléculaires pour l'extraction sélective et miniaturisée de neurotransmetteurs .....155**

IV.1. Présentation des composés d'intérêt.....	156
IV.2. Etat de l'art sur les MIP pour l'extraction exhaustive non miniaturisée de l'éphédrine, la méthyléphédrine, la dopamine, l'octopamine et la synéphrine .....	157
IV.3.Synthèse de monolithes imprimés miniaturisés avec l'éphédrine et premières caractérisations .....	163
IV.3.1. Evaluation de la perméabilité des monolithes.....	164
IV.3.2. Evaluation de la sélectivité des monolithes à base de TRIM .....	166
IV.4.Séparation analytique de l'éphédrine et de ses analogues structuraux .....	167
IV.4.1. Séparation HILIC au format conventionnel .....	168

IV.4.2. Séparation avec une phase stationnaire PGC au format conventionnel et transfert de méthode .....	170
IV.5. Conclusion .....	173
<b>CONCLUSION GENERALE ET PERSPECTIVES.....</b>	<b>177</b>
<b>ANNEXES.....</b>	<b>I</b>
Annexe 1 : Structure chimique des réactifs .....	III
Annexe 2 : Protocole de synthèse d'un MIP dans un capillaire .....	IV
Annexe 3 : Supplementary materials – Chapitre II - Article 1 .....	VI
Annexe 4 : Supplementary materials – Chapitre III - Article 2 .....	VIII
Annexe 5 : Conditions expérimentales pour la synthèse et la caractérisation des monolithes imprimés miniaturisés avec l'éphédrine .....	XI
Annexe 6 : Méthode d'analyse LC-UV pour l'éphédrine et ses analogues structuraux .....	XIII
<b>LISTE DES TABLEAUX ET FIGURES .....</b>	<b>XVII</b>
Liste des figures .....	XVII
Liste des tableaux .....	XXI
<b>REFERENCES.....</b>	<b>XXIII</b>

## LISTES DES PUBLICATIONS ET COMMUNICATIONS

### PUBLICATIONS

**T. Bouvarel**, N. Delaunay, V. Pichon “Selective extraction of cocaine from biological samples with a miniaturized monolithic molecularly imprinted polymer and on-line analysis in nano-liquid chromatography” *Analytica Chimica Acta*, 1096 (2020) 89-99.

**T. Bouvarel**, N. Delaunay, V. Pichon “Simplified miniaturized set-up based on molecularly imprinted polymer for the determination of benzoylecgonine in urine sample” (en correction).

**T. Bouvarel**, N. Delaunay, V. Pichon “Molecularly imprinted polymers in miniaturized extraction and separation devices” (en correction).

### COMMUNICATIONS ORALES

#### Symposiums internationaux

**A. Combès**, P. Kadirvel, **T. Bouvarel**, L. Renault, L. Bordron, V. Pichon. “Development of molecular imprinted polymers for the monitoring of emerging pollutants and their metabolites in water” ISC 2018, 32<sup>nd</sup> International Symposium on Chromatography, Cannes-Mandelieu, France, 23-27 Septembre 2018.

**T. Bouvarel**, S. Perche pied, A. Combès, N. Delaunay, **V. Pichon** “Miniaturized and selective extraction sorbents coupled on-line to nanoLC for the determination of target analytes at the trace level in complex samples” Euroanalysis XX, Istanbul, Turquie, 1-5 Septembre 2019.

**T. Bouvarel**, S. Perche pied, A. Combès, N. Delaunay, **V. Pichon** “Miniaturized selective extraction devices for trace analysis in complex samples” HTC 16, 16<sup>th</sup> International Symposium on Hyphenated Techniques in Chromatography and Separation technology, Ghent, Belgique, 29-31 Janvier 2020.

**T. Bouvarel**, N. Delaunay, V. Pichon “Monolithic molecularly imprinted polymer and nano-liquid chromatography for on-line miniaturized trace analysis in biological fluids” HTC 16, 16<sup>th</sup> International

Symposium on Hyphenated Techniques in Chromatography and Separation technology, Ghent, Belgique, 29-31 Janvier 2020.

## Symposiums nationaux

**T. Bouvarel**, N. Delaunay, V. Pichon “Synthèse *in situ* d'un polymère à empreintes moléculaires dans un capillaire et couplage en ligne à la nano-chromatographie en phase liquide pour l'extraction sélective de molécules de fluides biologiques” SEP 2019, 13<sup>ème</sup> Congrès Francophone sur les Sciences Séparatives et les Couplages de l'AfSep, Paris, France, 25-28 Mars 2019 (Flash présentation).

**T. Bouvarel**, N. Delaunay, V. Pichon “Synthèse *in situ* d'un polymère à empreintes moléculaires dans un capillaire et couplage en ligne à la nano-chromatographie en phase liquide pour l'extraction sélective de stupéfiants dans des fluides biologiques” 1<sup>ère</sup> Ecole Thématische du Club Jeunes de l'AfSep, Montpellier, France, 13-15 Mai 2019.

**T. Bouvarel**, N. Delaunay, V. Pichon “*In situ* synthesis of a molecularly imprinted polymer in a capillary and on-line coupling to nano-liquid chromatography for the selective extraction of narcotic drugs in biological fluids” Journée des doctorants de l'Ecole Doctorale 388, Paris, France, 24 Juin 2019.

**T. Bouvarel**, N. Delaunay, V. Pichon “Polymères à empreintes moléculaires miniaturisés pour l'analyse de stupéfiants et de neurotransmetteurs dans des échantillons biologiques de très faibles volumes” Journée du Club Ile-de-France de l'association francophone des sciences séparatives (AfSep) : Analyses de mélanges complexes, Paris, France, 20 Novembre 2019.

## COMMUNICATIONS PAR AFFICHE

**T. Bouvarel**, A. Combès, N. Delaunay, V. Pichon. “Selective extraction of cocaine and benzoylecgonine from a biological sample using a monolithic imprinted capillary coupled on-line with nano-liquid chromatography” ISC 2018, 32<sup>nd</sup> International Symposium on Chromatography, Cannes-Mandelieu, France, 23-27 Septembre 2018.

**T. Bouvarel**, N. Delaunay, V. Pichon “Synthèse *in situ* d'un polymère à empreintes moléculaires dans un capillaire et couplage en ligne à la nano-chromatographie en phase liquide pour l'extraction

sélective de molécules de fluides biologiques” SEP 2019, 13<sup>ème</sup> Congrès Francophone sur les Sciences Séparatives et les Couplages de l’AfSep, Paris, France, 25-28 Mars 2019.

**T. Bouvarel**, N. Delaunay, V. Pichon “*In situ* synthesis of a molecularly imprinted monolith in a capillary and on-line coupling to nano-liquid chromatography for the selective extraction of cocaine and its metabolite from biological fluids” HPLC 2019, 48<sup>th</sup> International Symposium on High-Performance Liquid Phase Separations and Related Techniques, Milan, Italie, 16-20 Juin 2019.



## LISTE DES ABREVIATIONS

AA :	Acide acrylique (Acrylic acid)
ACN :	Acétonitrile (Acetonitrile)
Ag/GO :	Oxyde de graphène modifié à l'argent (Silver-modified graphene oxide)
AIBN :	Azo-N,N'-diisobutyronitrile
APTMS :	3-Aminopropyltriméthoxysilane (3-Aminopropyltrimethoxysilane)
BZE :	Benzoylécgonine
CE :	Électrophorèse capillaire (Capillary electrophoresis)
CEC :	Electrochromatographie capillaire (Capillary electrochromatography)
CIP :	Polymère imprimé à coordination métallique (Coordination imprinted polymer)
CL :	Agent de réticulation (Cross-linking agent)
COC :	Cocaïne (Cocaine)
CV :	Coefficient de variation
DCM :	Dichlorométhane (Dichloromethane)
DMC :	5,7-Diméthoxycoumarine (5,7-Dimethoxycoumarin)
DMSO :	Diméthylsulfoxyde (Dimethyl sulfoxide)
EF :	Facteur d'enrichissement (Enrichment factor)
EGDMA :	Ethylène glycol diméthacrylate (Ethylene glycol dimethacrylate)
EOF :	Flux électroosmotique (Electroosmotic flow)
EtOH :	Ethanol
HEMA :	2-Hydroxyéthyl méthacrylate (2-Hydroxyethyl methacrylate)
IA :	Acide itaconique (Itaconic acid)
i.d. :	Diamètre interne (Internal diameter)
IF :	Facteur d'impression (Imprinting factor)
K :	Perméabilité (Permeability)
k :	Facteur de rétention (Retention factor)
LC :	Chromatographie en phase liquide (Liquid chromatography)
LIF :	Fluorescence induite par laser (Laser induced fluorescence)
LOD :	Limite de détection (Limit of detection)
LOQ :	Limite de quantification (Limit of quantification)
M :	Monomère (Monomer)
MAA :	Acide méthacrylique (Methacrylic acid)
MBAA :	N,N'-Méthylènebis(acrylamide) (N,N'-Methylenebis(acrylamide))

MeOH :	Méthanol (Methanol)
MIP :	Polymère à empreintes moléculaires (Molecularly imprinted polymer)
N :	Efficacité <i>ou</i> Nombre de plateaux théoriques (Efficiency)
nanoLC :	Nano-chromatographie en phase liquide (Nano-liquid chromatography)
NIP :	Polymère non imprimé (Non-imprinted polymer)
P :	Solvant porogène (Porogen)
PDMS :	Poly(diméthylsiloxane) (Poly(dimethylsiloxane))
POSS :	Oligomère polyédrique de silsesquioxane (Polyhedral oligomeric silsesquioxanes)
R% :	Rendement (Recovery)
R <sub>s</sub> :	Résolution (Resolution)
RSD :	Ecart type relatif (Relative standard deviation)
SDS-PAGE :	Électrophorèse sur gel de polyacrylamide en présence de dodécylsulfate de sodium (Sodium dodecyl sulfate polyacrylamide gel electrophoresis)
SEM :	Microscopie électronique à balayage (Scanning electron microscopy)
SGO :	Oxyde de graphène silanisé (Silanized graphene oxide)
SPE :	Extraction en phase solide (Solid phase extraction)
T :	Molécule empreinte (Template)
t <sub>r</sub> :	Temps de rétention (Retention time)
TEOS :	Tétraéthyl orthosilicate (Tetraethyl orthosilicate)
TFA :	Trifluoroacetic acid (Acide trifluoroacétique)
THP :	Tétrahydropalmatine (Tetrahydropalmatine)
TMOS :	Tétraméthyl orthosilicate (Tetramethyl orthosilicate)
TRIM :	Triméthylolpropane triméthacrylate (Trimethylolpropane trimethacrylate)
UV :	Ultra-violet (Ultraviolet)
VP :	Vinylpyridine
α :	Sélectivité (Selectivity)
γ-MAPES :	3-(Triéthoxysilyl)propyl méthacrylate (3-(Triethoxysilyl)propyl methacrylate)
γ-MAPS :	3-(Triméthoxysilyl)propyl méthacrylate (3-(Trimethoxysilyl)propyl methacrylate)
μ-TAS :	Système d'analyse micro-totale (Micro total analysis system)

## INTRODUCTION GENERALE

Quel que soit le domaine d'application (clinique, agroalimentaire, environnemental, toxicologique...), les défis de la chimie analytique sont multiples. L'analyste se trouve confronté à des analytes d'intérêt de natures très hétéroclites, présents à des teneurs variables, bien que souvent à l'état de traces ou d'ultra-traces ( $\text{ng mL}^{-1}$  ou  $\text{pg mL}^{-1}$ ) dans des échantillons complexes, comme dans le cas des échantillons biologiques. En dépit de ces contraintes, les méthodes d'analyse doivent être fiables, rapides, bon marché et respectueuses de l'environnement. Pour faire face à ces défis, l'analyste peut compter sur diverses techniques performantes pour la séparation telles que la chromatographie et l'électrophorèse capillaire. Cependant, dans certains cas, ces méthodes ne suffisent pas à surmonter la complexité de l'échantillon. Des modes de détection sensibles et spécifiques, comme la spectrométrie de masse, peuvent alors être couplés aux techniques séparatives, conduisant à des progrès considérables pour l'analyse de traces dans des échantillons complexes. Toutefois, l'utilisation de la spectrométrie de masse pour l'analyse d'échantillons complexes n'est pas toujours simple sur le plan de la quantification puisque des effets de matrices, *i.e.* phénomènes de suppression ou d'augmentation des signaux, peuvent être observés dus à la présence de certains interférents dans l'échantillon affectant l'ionisation des analytes, pouvant conduire à des interprétations erronées. Une attention particulière est donc à porter au traitement de l'échantillon puisqu'il peut permettre de préconcentrer les analytes d'intérêt tout en éliminant ces interférents de manière à s'affranchir des effets de matrice.

Un essor de la miniaturisation des systèmes analytiques a été observé ces dernières années, avec comme but ultime l'intégration des diverses étapes de l'analyse (traitement de l'échantillon, séparation, détection) dans un dispositif unique pour former un microsystème analytique ( $\mu$ -TAS, Micro Total Analysis System). Cette tendance se justifie par la nécessité de réduire les temps d'analyse et les quantités d'échantillon et de réactifs utilisées, mais aussi par la possibilité d'automatisation et de portabilité permettant de mener des analyses de terrain. Dans le domaine du traitement de l'échantillon, cette évolution vers des approches et systèmes miniaturisés est également en cours.

Parmi les techniques de traitement de l'échantillon, l'extraction sur phase solide (SPE, Solid Phase Extraction) est l'une des méthodes couramment utilisées pour extraire des composés à partir d'échantillons liquides ou d'extraits de matrices solides. De nombreux types de supports tels que des silices greffées ou des phases polymériques ont été développés et différents dispositifs microfluidiques ont démontré la possibilité de miniaturiser ces supports. Cependant, l'extraction sur ces supports classiques est le résultat d'interactions non sélectives, généralement dépendantes uniquement de la

polarité des molécules, et aboutissant ainsi à la co-extraction de composés ayant une polarité similaire à celle des analytes ciblés. Pour pallier ce manque de sélectivité, différents supports d'extraction générant un mécanisme de reconnaissance moléculaire ont été développés.

Une première approche consiste à utiliser des supports greffés avec des biomolécules : les immunoadsorbants (IS) et les oligoadsorbants (OS). Un IS est constitué d'anticorps immobilisés sur le support solide et dirigés contre un antigène, l'analyte cible. La très forte affinité de l'interaction antigène-anticorps fondée sur une reconnaissance stérique et fonctionnelle confère aux IS une sélectivité très élevée. Toutefois, les durées élevées de production des anticorps (de 6 mois à un an) et de régénération (24-48h) sont un facteur très limitant. Un OS, quant à lui, est basé sur l'immobilisation d'aptamères, qui sont des oligonucléotides de longueur comprise entre 20 et 60 bases dont certaines séquences peuvent présenter une très forte affinité pour un analyte cible. Les aptamères ont pour principal avantage de pouvoir être synthétisés par voie chimique et de pouvoir être rapidement régénérés contrairement aux anticorps. Cependant, un nombre limité de séquences est, à ce jour, disponible. De plus, ces deux types de supports greffés sont onéreux et nécessitent des conditions de stockage drastiques pour assurer leur stabilité.

Une autre stratégie consiste à utiliser des outils biomimétiques ayant une sélectivité similaire, les polymères à empreintes moléculaires (MIP, Molecularly Imprinted Polymer). Ces supports sont des polymères possédant des cavités avec une complémentarité stérique et fonctionnelle vis-à-vis de la molécule cible. Ils offrent de nombreux avantages, notamment une stabilité chimique et thermique. La synthèse des MIP s'avère relativement facile et rapide pour une grande variété d'applications telles que les systèmes d'administration de médicaments, les capteurs, les catalyseurs biomimétiques en synthèse organique ou la séparation d'analogues structuraux et d'énanthiomères. L'utilisation des MIP comme support d'extraction sélectif a été décrite pour la première fois par Sellergren et ses collaborateurs en 1994 pour l'extraction de la pentamidine dans l'urine. Depuis lors, l'intérêt pour ce domaine s'est accru, que ce soit pour la reconnaissance selective de petites molécules (médicaments, pesticides, polluants environnementaux ...), de protéines, ou même de micro-organismes.

Comme pour la chimie analytique en général, la miniaturisation des MIP présente les avantages cités précédemment, et de surcroit lorsque la molécule empreinte indispensable à la synthèse des MIP est onéreuse, réglementée ou difficile à synthétiser. Un grand nombre de travaux témoigne de la possibilité d'introduire des phases imprimées dans des dispositifs analytiques miniaturisés par la synthèse de films minces ou par le remplissage de particules dans des capillaires ou des puces conçues à cet effet. Une autre approche consiste en la synthèse de phases poreuses monolithiques directement à l'intérieur de capillaires ou de micro-canaux de puces. Les monolithes,

apparus au début des années 1990, sont en effet un moyen de surmonter les contraintes liées à l'utilisation de particules (immobilisation, remplissage homogène) ou de films minces (faible quantité de phase). Ils possèdent également une surface spécifique élevée et une grande perméabilité. Tous ces avantages font donc des MIP monolithiques des supports sélectifs de choix pour la miniaturisation de l'étape de traitement de l'échantillon et son intégration dans un dispositif  $\mu$ -TAS.

L'objectif de cette thèse est donc d'élaborer une approche miniaturisée sélective *via* le développement de MIP monolithiques pour l'analyse de traces dans des échantillons biologiques. Pour cela, la cocaïne et son métabolite principal, la benzoylecgonine (BZE), ont été sélectionnés comme molécules modèles puisque la synthèse d'un MIP sélectif a déjà été décrite dans la littérature au format conventionnel. Ainsi, il a été possible de tirer des enseignements de la mise au point de ce dernier afin d'orienter notre stratégie pour la synthèse d'un monolithe imprimé miniaturisé. Cependant, le changement de format opéré durant ce travail de thèse n'est pas seulement une réduction des dimensions, mais implique également un changement des conditions de polymérisation afin d'obtenir un MIP suffisamment perméable et rétentif. Par conséquent, une caractérisation des MIP monolithiques miniaturisés a été nécessaire en termes de perméabilité, capacité, sélectivité, rendement d'extraction et répétabilité de synthèse et d'utilisation. Par la suite, un dispositif couplant en ligne le MIP monolithique avec la nano-chromatographie en phase liquide (nanoLC) a été mis en place et les protocoles d'analyse ont été optimisés afin de promouvoir la sélectivité du système permettant la détection de cocaïne dans des échantillons de salive et de plasma humain. Dans un effort constant de miniaturisation des dispositifs analytiques, il a été possible de tirer avantage de la sélectivité fournie par le MIP monolithique afin de réduire notre montage en éliminant la colonne analytique de nanoLC pour réaliser la détection directe en ligne de la BZE dans des échantillons urinaires. Puis, en exploitant le savoir-faire acquis au cours des différentes synthèses, de nouveaux supports imprimés miniaturisés ont été synthétisés afin de cibler des neurotransmetteurs et leurs analogues structuraux.



---

## **PARTIE BIBLIOGRAPHIQUE**

---



## **CHAPITRE I**

**Etat de l'art sur les polymères à empreintes moléculaires  
dans des dispositifs d'extraction et de séparation  
miniaturisés**



## **CHAPITRE I – Etat de l'art sur les polymères à empreintes moléculaires dans des dispositifs d'extraction et de séparation miniaturisés**

De nombreux travaux portant sur la miniaturisation des dispositifs analytiques ont été menés avec pour objectif final l'intégration de toutes les étapes constituant l'analyse (préparation de l'échantillon, séparation et détection) dans un microsystème analytique unique ( $\mu$ -TAS). Cette évolution actuelle se justifie non seulement par le coût de certains réactifs mais aussi par la nécessité constante de gagner en temps d'analyse pour ainsi augmenter la cadence analytique. Il est également possible de développer des outils portables permettant des analyses de terrain. Cependant, la réduction du pouvoir séparatif lié à la diminution des dimensions de séparation est problématique compte tenu de la complexité des échantillons réels ainsi que des faibles niveaux de concentration parfois ciblés. L'intégration d'une étape de traitement de l'échantillon sélective s'avère alors indispensable afin de faire face à ces contraintes et les MIP constituent une approche très intéressante.

Ce chapitre est consacré à l'état de l'art concernant la miniaturisation des MIP destinés à des dispositifs d'extraction ou de séparation. Différentes approches permettant leur intégration dans des systèmes miniaturisés y sont présentées telles que des films fins à la surface de capillaires ou canaux de microsystèmes, le remplissage et l'immobilisation de particules de MIP ou la synthèse *in situ* de MIP monolithiques. Les voies de synthèse, ainsi que les choix raisonnés des différents réactifs décrits dans la littérature sont présentés. Une attention particulière est également portée sur la caractérisation de la sélectivité dans des applications d'extraction exhaustive ou de séparation en électrochromatographie capillaire ou en nano-chromatographie en phase liquide.

Ce chapitre se présente sous la forme d'une revue, en cours de soumission : « Molecularly imprinted polymers in miniaturized extraction and separation devices », T. Bouvarel, N. Delaunay, V. Pichon.



---

## **Review : Molecularly imprinted polymers in miniaturized extraction and separation devices**

Thomas Bouvarel<sup>a</sup>, Nathalie Delaunay<sup>a</sup>, Valérie Pichon<sup>a,b</sup>

<sup>a</sup> Laboratoire des Sciences Analytiques, Bioanalytiques et Miniaturisation - UMR Chimie Biologie Innovation 8231, ESPCI Paris, CNRS, PSL University, 75005 Paris, France

<sup>b</sup> Sorbonne Université, 75005 Paris, France

---

### **I.1. Abstract**

Molecularly imprinted polymers are highly selective and cost-effective materials, which have attracted significant interest in various areas such as sample pretreatment and chromatographic and electrophoretic separations. This review aims to present the state of the art concerning the miniaturization of these materials in order to meet the societal demand for reliable, fast, cheap, and solvent/sample saving analyses. The polymerization route specificities for the production of miniaturized molecularly imprinted polymers such as open tubular, packed particles, magnetic nanoparticles, and *in situ* imprinted monoliths are investigated. Their performances as selective supports in solid phase extraction and as stationary phases in electrochromatography and liquid chromatography, as well as their possible perspectives are discussed.

## I.2. Introduction

Molecularly imprinted polymers (MIPs) are synthetic materials possessing specific cavities with steric and functional complementarity towards a template molecule and involving a retention mechanism based on molecular recognition for analyte recognition or discrimination of chemical species of similar structure. MIPs can be considered as synthetic supports mimicking immunosorbents or oligosorbents as they provided similar selectivity. The concept of MIP was first described in 1931 by Polyakov [1], using silica matrices, showing preferential binding capacity to a specific solvent in a mixture. In 1972 Wulff and Sarhan described an imprinted polymeric material for enantiomeric separation of racemates [2]. MIPs offer many advantages including chemical and thermal stability but also easy, cheap, and rapid preparation for a wide variety of applications related to chemical and biological molecules. They have been already successfully applied in several fields, such as drug delivery [3–5], sensors [6–9], or biomimetic catalyst in organic synthesis [10]. However, MIPs were also widely used as stationary phase in liquid chromatography (LC) [11–13] and electrochromatography (CEC) [12–15] for separations of structural analogs and enantiomers [16,17] or as sorbent for extraction, whether for the selective recognition of small molecules, such as drugs, pesticides, or other environmental pollutants [18–24], of proteins [25–27], or even of microorganisms [28].

In the extraction and separation fields, while early works used MIPs in the form of particles of more or less controlled sizes into disposable extraction cartridges or columns, depending on the application, many recent studies have shown that they can be produced on a miniaturized scale as thin films or monoliths. Preparation of the MIP in miniaturized format allows the reduction of the required amount of template which is often the most expensive reagent involved in the synthesis process [29]. More generally, the potential benefits of miniaturization are numerous, following the principle that small-scale processes consume less time, sample, and reagents and thus reduce the analysis costs, as well as the amount of waste [30]. In order to limit this reagent consumption and to tend towards well-defined small particle sizes, many groups have worked on the production of nanoparticles coated with a thin layer of polymers mainly used for extraction in dispersive mode as recently reported [18], the purified extract being generally analyzed by conventional methods. However, in order to make the most of this miniaturization, all the different steps of the analytical procedure must be miniaturized and, if possible, integrated into a single device in order to move towards the concept of micro total analytical system ( $\mu$ -TAS) introduced by Manz *et al.* [31] in the 90's and also called lab-on-chip.

Among the miniaturized separation methods available, capillary electrophoresis (CE) and liquid phase nanochromatography (nanoLC) are predominantly employed. Therefore, for the integration of

MIPs as a stationary phase for separation or upstream as an extraction sorbent, it is quite understandable that the preferred format for miniaturized MIPs has consisted in introducing them in a privileged way in fused-silica capillaries. There are multiple approaches for preparing a MIP in a capillary. The MIP can be available as particles of various sizes (down to nanoparticles and with possibly magnetic properties) held in the capillary. It is also possible to synthesize MIPs inside the capillary in the form of a thin porous film following an approach called open tubular or of a porous monolith filling the entire section of the capillary. This last approach that appeared in the early 1990s in the conventional format was first dedicated to the preparation of stationary phases of different polarities for separation purposes [32–36]. It was first reported in the capillary format in 1997 by Schweitz *et al.* for chiral separations [37,38] before being applied to extraction purposes [39]. The approach based on the synthesis of a monolith is a way of overcoming the constraints related to the use of particles (immobilization, homogeneous packing...) or thin films (low amount of phase), while providing a high specific surface area and a high permeability [40].

Other formats of miniaturized MIPs have also been developed such as pipette tips [41] or fibers [42–44] for solid-phase microextraction although they are exclusively reserved for extraction applications. Finally, in order to go further in the miniaturization and integration of MIPs into the overall analysis procedure and thus respond to the μ-TAS concept previously mentioned, many groups have taken an interest in the integration of MIPs on a chip using approaches similar to those used to prepare capillaries.

Based on the published works on miniaturized MIPs for extraction and separation purposes, this paper aims first to present and discuss the different ways in which miniaturized MIPs can be prepared for use as extraction or separation media in capillary or on-chip format. Their potential as a stationary phase for separation in CEC and nanoLC will be presented and, in a second step, as a sorbent for selective solid phase extraction (SPE) will be discussed. However, since this review focuses exclusively on exhaustive extraction, applications such as solid phase microextraction and dispersive solid phase extraction will not be covered.

### I.3. Generalities on MIP synthesis

MIP synthesis generally consists first of a complexation in solution of a template molecule with functional monomers *via* non-covalent bonds. A cross-linker and an initiator are then introduced to generate polymerization of the monomers around the template, either by thermal (T) or photochemical (UV) initiation. After polymerization, the template molecules are removed by extensive

washing steps, resulting in available cavities complementary to the template in terms of shape, size, and position of functional groups.

In most cases, target analytes are very often used as templates. As expected, the structure and functionality of the target analytes define the properties of the binding sites, ensuring optimal recognition during the extraction or separation process. However, the complete removal of the template molecules from the MIP can be incomplete or difficult to achieve despite extensive washing steps with large volumes. The residual template leakage from the MIP can lead to erroneous quantification, especially when applied in trace analysis. In this case, the use of a structural analog as template during the MIP synthesis that can be distinguished from the target analyte during its determination, especially by chromatographic methods, constitutes an easy way to limit the risk and is called dummy approach [39,45–49]. In the case where multiple compounds having similar structures are targeted, syntheses using dual templates were reported to improve the polymer's ability to selectively and simultaneously trap the compounds [50–52].

Despite the wide variety of targets and templates employed, reagents used for the polymerization are recurrent. Among them, the functional monomers generally chosen are methacrylic acid (MAA), acrylic acid (AA), itaconic acid (IA), 2-hydroxyethyl methacrylate (HEMA), or vinylpyridine (VP) [18]. The most commonly used cross-linkers are bifunctional ethylene glycol dimethacrylate (EGDMA) and divinylbenzene or trifunctional trimethylolpropane trimethacrylate (TRIM). In order to promote formation of the template-monomer complex, the polymerization solvent is selected to promote the desired interactions, *i.e.* hydrogen bonds and electrostatic interactions for example. Therefore, it is better in this case to employ, whenever possible, a weakly polar and aprotic solvent such as toluene, dichloromethane (DCM), chloroform, and acetonitrile (ACN) or a mixture of them.

The performance of a MIP is related to the occurrence of cavities that promote highly selective interactions between the polymer and target compounds. In most of the works, a non-imprinted polymer (NIP) is synthesized with exactly the same conditions as MIP except that the template is omitted. This control polymer, that does not possess any specific cavities, is studied in parallel during the MIP characterization. Because of the use of the same reagents, this non-imprinted support allows the evaluation of the contribution of the non-specific interactions occurring between a given compound and the NIP surface that exist also at the MIP surface. Therefore, the comparison of the retention of a compound on the MIP and its NIP allows the evaluation of the relative contribution of the cavities and the surface to the retention of a compound on a MIP, and thus of the selectivity

broaden by the MIP and its analytical conditions of use (mobile phase composition or extraction protocol).

The reagents and synthesis conditions (T vs UV, T values, ...) affect MIP properties, *i.e.* specific surface area, porosity, mechanical strength, non-specific interactions, etc... Depending on the chosen application, it is possible to obtain the MIP in different formats, either as a monolith which can be then ground if necessary, particles or nanoparticles, or a film.

## I.4. Open-tubular MIP

### I.4.1. Preparation of open tubular MIP

The first miniaturized MIPs were synthesized as a porous thin film on the inner surface of a capillary [53,54]. Until today, numerous MIPs prepared following such an open tubular approach in capillaries have been reported as shown in **Table 1**.

Before starting the synthesis, most of these studies reported the use of 3-(trimethoxysilyl)propyl methacrylate ( $\gamma$ -MAPS) in a first step to ensure the future anchoring of the film to the inner wall of the capillary [51,54–65]. This reagent has a trifunctional silane group that can bind the silica wall of the capillary as well as a function that will participate to the polymerization of the MIP.

The reagents predominantly used are MAA coupled with the cross-linker EGDMA and an initiation with Azobisisobutyronitrile (AIBN), either thermally [51,54–58,60–63] or photochemically [59,64–66]. The most commonly employed porogens are ACN [51,54–58,60,64–66] and toluene [54,59,61,63,66] with the addition of small amount of isoctane [51,55,61,63] or decanol [59] to increase the specific surface area, or even 2-propanol [56–58] to ensure the complete dissolution of each reagent. Wu *et al.* employed a special ternary porogen system (toluene, isoctane, and DMSO) to solve the solubility problem and obtain an open tubular MIP layer specific for D-zopiclone, a very polar compound [63]. The MIP morphology and separation performance were dramatically varied with a little change of DMSO composition in the porogen. Indeed, the best result was obtained when the DMSO composition was 30% while for a 33.3% content the capillary was clogged. In order to control the film thickness, a thermal initiation (from 50 to 75°C) and a short polymerization time (from 10 min to 4 h) are adopted [51,54–57,59–63]. In some publications a pressure is applied after the polymerization to shrink the polymer into a thin film against the capillary wall [54,59,60].

The first evaluation of a MIP thin film consists generally in observing the inner section of the capillary by scanning electron microscopy (SEM) to check the homogeneity of the material and its good anchorage. This also makes possible to determine the approximate thickness of the film, which ranges from 0.1 to a few micrometers with a single study up to 10  $\mu\text{m}$ .

The dimensions of the devices fluctuate significantly, but it is possible to observe some trends depending on the chosen application. The open tubular MIPs for CEC or nanoLC applications are mainly produced in capillaries of 25 [51,54–56] and 50  $\mu\text{m}$  of internal diameter (i.d.) [57–59,66], although larger diameters of 75 [60] and 100  $\mu\text{m}$  [61–63] can be found. For extraction applications, i.d. of the capillaries are 100  $\mu\text{m}$  [64,65]. Concerning the lengths of the MIPs, they are heterogeneous in separations with a range from 5 to 50 cm for most of the cases, while for extraction applications, they range from few millimeters to several centimeters.

**Table 1.** Conditions of synthesis and performances of MIPs in open tubular format.

Target*	M/CL/Solvent (v:v)	T/M/CL (mol/mol/mol)	Dimensions (L (l) x i.d. x t) **	$\alpha$	$R_s$	N (plates/m)	RSD	Ref.
<b>CEC applications</b>								
Adenosine, Thymine, Guanine, Cytosine (9-Ethyladenine)	MAA/EGDMA/ACN	1/12/18	70 cm (50) x 75 $\mu\text{m}$ x -	-	-	2,600-75,300	$t_r$ : < 6,69% (n = 7)	[60]
<u>R,S-Amlodipine</u>	MAA+MA0702/MAM/Toluene: Isooctane (90:10)	1/4+4.7/4	47.5 cm (37) x 100 $\mu\text{m}$ x 0.1- 0.2 $\mu\text{m}$	-	14.8	35,300 (R) 31,700 (S)	$t_r$ , N, $R_s$ : < 3.32% (n = ?) $t_r$ , N, $R_s$ : < 3.01% ( $n_{B/B} = ?$ )	[61]
<u>R,S-Amlodipine</u>	MAA/Ov-POSS/Chloroform	1/3/1.5	47.5 cm (37) x 100 $\mu\text{m}$ x 0.1- 0.2 $\mu\text{m}$	2.60	33.0	77,600 (R) 54,000 (S)	$t_r$ : 0.80-1.29% ( $n_{B/B} = ?$ ) N: 2.57-4.06% ( $n_{B/B} = ?$ ) $R_s$ : 2.08% ( $n_{B/B} = ?$ )	[62]
<u>Boc-D,L-Trp</u>	AA/EGDMA/ACN:Isooctane (96:4)	1/4/20	8 cm (-) x 25 $\mu\text{m}$ x 2.5 $\mu\text{m}$	-	1.3	-	$t_r$ : 1.0-1.2% (n = 3) $t_r$ : 2.5-3.2% ( $n_{D/D} = 3$ ) $t_r$ : 3.3-3.6% ( $n_{C/C} = 3$ )	[55]
<u>Dansyl-D,L-phenylalanine</u>	MAA+VP/EGDMA/Toluene:ACN (87.5:12.5)	1/7.4+7.4/36.3	100 cm (85) x 25 $\mu\text{m}$ x -	-	-	248,600 (D) 8,00 (L)	EOF: 2.2% (n = 6)	[54]
<u>R,S-Ketoprofen</u>	MAA+4-SSA/EGDMA/ACN: 2-Propanol (90:10)	1/4.8+0.5/15.4	100 cm (91.4) x 25 $\mu\text{m}$ x 1-4 $\mu\text{m}$	-	4.0	1,130,000 (R) 460,000 (S)	N: < 2.2% ( $n_{B/B} = 3$ )	[56]
<u>R,S-Ketoprofen</u>	MAA+4-SSA/EGDMA/ACN: 2-Propanol (90:10)	1/4.8+0.5/15.4	36.4 cm (28) x 50 $\mu\text{m}$ x 1-4 $\mu\text{m}$	-	10.5	156,000 (R) 10,000 (S)	$R_s$ , N: < 3.5% ( $n_{B/B} = 3$ ) $R_s$ , N: < 3% ( $n_{D/D} = 3$ )	[57]
Phospholipids (S-Ketoprofen)	MAA+4-SSA/EGDMA/ACN: 2-Propanol (90:10)	1/4.8+0.5/15.4	30 cm (-) x 50 $\mu\text{m}$ x -	-	-	-	$t_r$ : 2.80-4.44% (n = ?)	[58]
<u>R,S-Propanolol</u>	MAA/TRIM/DCM	1/8/8	35 cm (26.5) x 25-50 $\mu\text{m}$ x 0.15- 2 $\mu\text{m}$	-	-	-	-	[66]

Target*	M/CL/Solvent (v:v)	T/M/CL (mol/mol/mol)	Dimensions (L (l) x i.d. x t) **	$\alpha$	$R_s$	N (plates/m)	RSD	Ref.
D,L-Tyrosine, D,L-Tryptophan	AA/EGDMA/ACN:Isooctane (96:4)	1+3/16/80	6 cm (-) x 25 $\mu\text{m}$ x 2 $\mu\text{m}$	-	1.0 1.0	-	tr: 1.2-1.8% (n = 6) tr: 2.4-2.7% ( $n_{D/D} = 6$ ) tr: 3.8-5.2% ( $n_{C/C} = 6$ )	[51]
D,L-Zopiclone	MAA/EGDMA/Toluene:Isooctane: DMSO (50:20:30)	1/4.6/17.4	50 cm (36) x 100 $\mu\text{m}$ x 1-10 $\mu\text{m}$	-	5.4	37,900 (L) 21,400 (D)	EOF: 4.4% (n = 5) N: 4.8% (n = 5) N: 8.1% ( $n_{C/C} = 3$ )	[63]
<b>nanoLC applications</b>								
Dansyl-D,L- phenylalanine	MAA+VP/EGDMA/Toluene:ACN (87.5:12.5)	1/8+8/39.2	100 cm (85) x 25 $\mu\text{m}$ x -		79,900 (D) 15,700 (L)	-	-	[54]
R,S-Ketoprofen	VP/EGDMA/Toluene:Decanol (25:75)	1/1.1/8.3	60 cm (60) x 50 $\mu\text{m}$ x 0.8 $\mu\text{m}$	1.28	0.5	6,004 (R) 3,495 (S)	-	[59]

Target*	M/CL/Solvent (v:v)	T/M/CL (mol/mol/mol)	Dimensions (L x i.d. x t) **	$V_p$	Medium	Selectivity (MIP/NIP)	EF	Recovery	RSD on recovery	Ref.
<b>SPE application with CE separation – on-line mode</b>										
Bisphenol A	MAA/EGDMA/ACN	1/4/20	5 cm x 100 $\mu\text{m}$ x -	-	Tap water (Direct injection) River water, Beverage, Urine (Diluted x1.1)	-	-	87-109%	2.0-5.6%	[65]
Methyltestosterone	MAA/EGDMA/ACN	1/4/20	3 mm x 100 $\mu\text{m}$ x -	15.3 $\mu\text{L}$	Urine (Diluted x1.1)	-	200 ***	-	-	[64]

\* Template indicated in bracket when different from target or underlined for a mixture of targets.

\*\* L (l) x i.d. x t: total length (effective length in cm) x internal diameter x MIP thickness.

\*\*\* Results obtained in pure medium.

4-SSA: 4-styrenesulfonic acid; Boc-Trp: N-(tert-Butoxycarbonyl)-tryptophan; DCM: Dichloromethane; EF: Enrichment factor; EOF: Electroosmotic flow; MA0702: Methacryllsobutyl polyhedral oligomeric silsesquioxanes; MAM: 2-Methacrylamidopropyl methacrylate; N: Efficiency;  $n_{B/B}$ : Batch-to-batch;  $n_{C/C}$ : Column-to-column;  $n_{D/D}$ : Day-to-day; Ov-POSS: Octavinyl-modified polyhedral oligomeric silsesquioxanes;  $R_s$ : Resolution; RSD: Relative standard deviation;  $t_r$ : Retention time;  $V_p$ : Percolation volume;  $\alpha$ : Selectivity.

#### I.4.2. Open tubular MIPs applied to separation in CEC and nanoLC

The MIPs synthesized with the open tubular approach were mainly used as stationary phases in CEC or nanoLC. Indeed, this approach brings several advantages since it benefits from low back pressure and fast mass transfer kinetic. In order to evaluate the MIP performances, different parameters can be measured such as selectivity  $\alpha$ , resolution  $R_s$  or efficiency  $N$  and are reported in **Table 1**. A large majority of publications dealing with open tubular MIPs for CEC [51,54–57,61–63,66] or LC [54,59] have been dedicated to the separation of enantiomers. In this case, high resolution or selectivity values resulting from a stronger retention of the enantiomer used as template clearly indicate the contribution of the specific cavities in the retention mechanism.

Tan *et al.* were the first to use an open tubular MIP for the baseline enantioseparation of dansyl-D,L-phenylalanine in both CEC and nanoLC modes [54]. Shortly after, a S-propranolol imprinted poly(MAA-co-TRIM) film was produced with a thickness of 0.15-2  $\mu\text{m}$  allowing also a baseline enantioseparation by CEC [66].

Zhao *et al.* [61] exploited the advantages of the addition of a polyhedral oligomeric silsesquioxane (POSS) as monomer to improve the MIP performances by taking advantage of rigidity reinforcement at the molecular level. Indeed, this hybrid organic-inorganic MIP was applied to the CEC enantioseparation of amlodipine and an average efficiency  $N$  of  $3.35 \times 10^4$  plates  $\text{m}^{-1}$  together with a resolution ( $R_s$ ) of 14.84 were obtained. A POSS-free MIP was also synthesized to evaluate the contribution of POSS, but separation performances were lower ( $N = 11,300$  plates  $\text{m}^{-1}$ ;  $R_s = 7.63$ ), which demonstrated the superiority of the POSS-based MIP. Special care was taken to the study of the stability with a set of 200 injections without change in the chromatograms. Intra-day and batch-to-batch RSD ( $n = 3$ ) values lower than 3% for the resolution were determined.

MIPs were also used in open tubular CEC for non-chiral separation of structural analogs such as nucleotide bases [60] or profen drugs [56]. However, this type of application requires the use of a NIP. Indeed, in chiral separation a high resolution reveals the presence of cavities, but for the separation of analogs of different polarities, the presence of cavities can only be proven by using a NIP.

Zaidi *et al.* performed both chiral separation of ketoprofen and non-chiral separations of naproxen, ibuprofen, and fenoprofen in long capillaries (1, 2, or 3 m x 50  $\mu\text{m}$  i.d.) with a MIP approximately 1-4  $\mu\text{m}$  thick [56]. The synthesis conditions were the results of a previous study in shorter capillary that incorporated 4-styrenesulfonic acid in the imprinted poly(MAA-co-EGDMA) to enable a strong and stable electroosmotic flow (EOF) at the optimized pH [57]. The enantioseparation

as well as non-chiral separation of profen drugs were successfully accomplished on each column, as shown in **Figure 1**, with a resolution of 4.0 for the ketoprofen racemic with the capillary of 1 m length and an impressive average efficiency of 1,000,000 plates m<sup>-1</sup>. A batch-to-batch RSD ( $n = 3$ ) lower than 2.3% for the efficiency was observed, indicating a very good synthesis repeatability despite the long length of the capillaries.

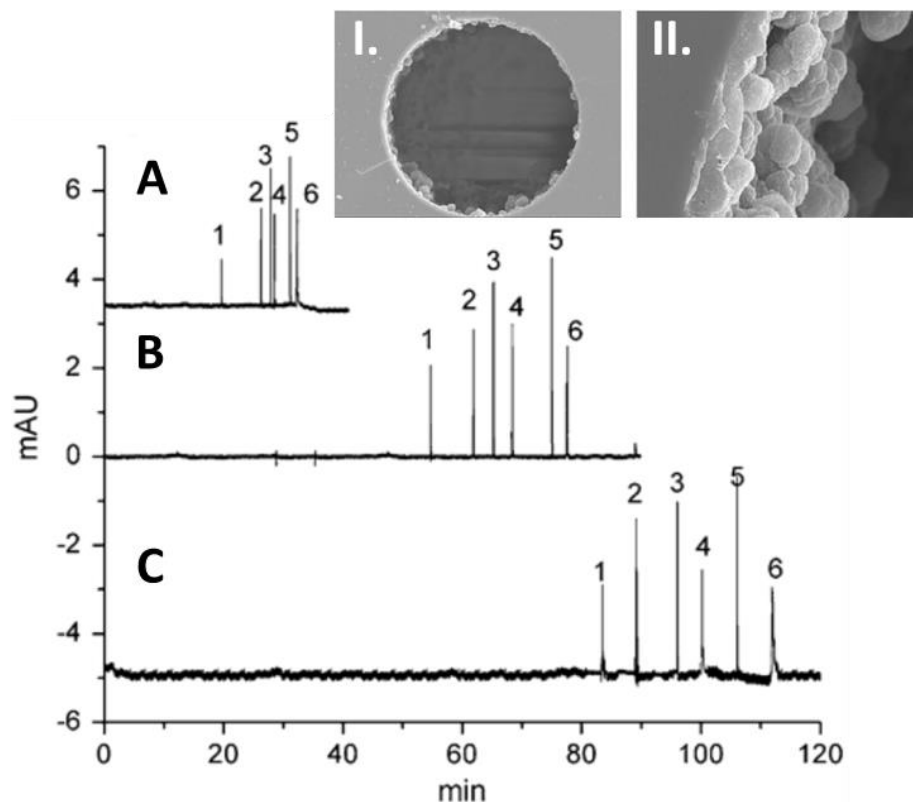


**Figure 1.** Open tubular CEC separation with a MIP stationary phase in a capillary (50  $\mu\text{m}$  i.d.) with a length of 1 m (A), 2 m (B), and 3 m (C). CEC conditions: ACN/sodium acetate 60 mM at pH 3.5 (92/8 (v/v)), applied voltage of +30 kV, UV detection at 214 nm. Peaks attribution: Acetone (1), Racemic naproxen (2), Racemic ibuprofen (3), Racemic fenoprofen (4), R-ketoprofen (5), and S-ketoprofen (6). Scanning electron micrograph of the MIP synthesized with S-ketoprofen in the capillary cross section (I) and enlargement in the region of the capillary wall (II). Adapted from [56].

An atypical device was proposed by Jang *et al.* by interfacing a S-ketoprofen imprinted poly(MAA-co-4-styrenesulfonic acid-co-EGDMA) open-tubular capillary with a nanospray interface utilizing a sheath flow for electrospray ionization and tandem mass spectrometry, in order to simultaneously separate and characterize phospholipids in human urinary lipid extracts [58]. The

phospholipids were separated by their acyl chain length and polar head groups, allowing the identification of 18 of them. However, the selectivity remains to be demonstrated since no NIP was synthesized.

Qu *et al.* developed a dual-template L-tyrosine and L-tryptophan imprinted poly(AA-co-EGDMA) for CEC multiple enantioseparation [51]. However, the authors decided to go further by integrating the fused-silica capillary containing the open tubular MIP phase (6 cm length, 25 µm i.d., and MIP layer about 2 µm thick) inside a poly(dimethylsiloxane) (PDMS) chip with a carbon fiber microdisk electrode for detection. The separation was performed with simultaneous baseline separation for both racemic tyrosine and tryptophan within 120 s with  $R_s$  values of 1.02 and 1.00, respectively. It is also important to highlight the effort that was made in determining RSDs ( $n = 6$ ) of retention time and peak area for run-to-run (1.2-1.8% and 2.6-3.9%, respectively), day-to-day (2.4-2.7% and 4.3-7.1%, respectively), and chip-to-chip (3.8-5.2% and 5.9-8.8%, respectively), suggesting that the method had good stability and repeatability but also that the imprinted chips had good manufacturing reproducibility. The same team produced also a hybrid microchip with a capillary (8 cm length, 25 µm i.d., and MIP layer about 2.5 µm thick) containing a N-(tert-Butoxycarbonyl)-L-tryptophan imprinted poly(AA-co-EGDMA) film [55]. A resolution of 1.27 was achieved in 75 s. The same effort was made on the determination of the RSD values ( $n = 3$ ) of retention time and peak area of 1.0-2.1% for run-to-run, 2.5-6.7 for day-to-day, and 3.3-8.8% for chip-to-chip, demonstrating once again the good manufacturing of the device as well as the good reproducibility and stability.

#### I.4.3. Open tubular MIPs in solid-phase extraction

For its use in extraction, the open tubular approach suffers from a low surface-to-volume ratio. Indeed, the amount of MIP represents only a small part of the volume of the capillary and therefore the resulting limited capacities seem particularly problematic for such an application. A MIP film was used as SPE sorbent by constituting an in-line concentrator (5 cm x 100 µm i.d. with an unknown film thickness) directly inside the capillary of a CE-UV system for the determination of bisphenol A [65]. The extraction was first carried out and then a plug of MeOH as eluent solvent was injected at the inlet end at a height of 7 cm. Finally, a voltage of 15 kV was applied to operate the CE analysis. After optimization of the MIP-SPE-CE method, real samples (tap water, river water, beverage, and urine) spiked with bisphenol A from 10 to 500 ng mL<sup>-1</sup> were applied and RSD for recovery of 86.7-108.6% were obtained in the range of 2.0-5.6%. The LOD was evaluated in pure medium at 0.8 ng mL<sup>-1</sup> which is over 100-fold better than that of direct CE determination. Although the percolated sample volume was not indicated, this means that a significant enrichment factor was obtained.

Another shorter concentrator was formed (3 mm x 100 µm i.d. with an unknown film thickness) with methyltestosterone imprinted poly(MAA-co-EGDMA) coupled in-line with CE-UV [64]. By comparing the CE signal with and without SPE in pure medium on model analytes, *i.e.* epitestosterone, methyltestosterone, and testosterone acetate, an enrichment factor of about 200 was calculated. In addition, the theoretical plate numbers were  $1.60 \times 10^4$  and  $1.88 \times 10^4$  for methyltestosterone with and without in-line extraction, respectively, which indicated a restrained loss of separation efficiency due to the SPE process. Finally, the authors indicated that the coated MIP layer maintained good operational performance after more than 100 cycles.

Nevertheless, if the enrichment was proven in both studies, the evaluation of non-selective interactions was not fully considered because the synthesis of a NIP was not reported. Moreover, it is worthwhile to notice that it is quite unusual to select a capillary with a so high internal diameter (*i.e.* 100 µm) with the open tubular approach. Indeed, small values such as 10 or 25 µm are in general preferred to favor the diffusion of the compounds from the inner liquid phase to the solid phase present only on the capillary surface, and thus the interactions with the support.

## I.5. MIP particles packed in capillary or chip channel

### I.5.1. Packing of particles

Miniaturized MIP devices can also be prepared by packing MIP particles in capillaries or in microchannels of chips (**Table 2**) [67–75]. By filling the entire section of the capillary or channel, it allows the overcoming of the lack of capacity of the open tubular format. The synthesis is generally first carried out in bulk and the MIP is next crushed and sieved during several cycles, giving rise of MIP particles with diameters between 50 and 110 µm. The heterogeneity induced by this synthesis method may represent a first drawback since it may be damaging for separation purposes.

Since this format is based on the same synthesis method as conventional MIPs, the recurrent reagents used are MAA and EGDMA as monomer and cross-linking agent, respectively [67–69]. Even if the synthesis path is simple and very diversified, the typical yield of useful particles is less than 50% [76].

Another inconvenience is the need of frits or restrictions to maintain particles. Frits are tricky to obtain as they should withstand high pressures, be porous enough, and should not be too long or interact with the analytes [14]. In addition, the presence of frits is propitious to the generation of air

bubbles. Numerous other methods were adopted to immobilize particles such as the use of acrylamide gel inside capillary [69] or using particles with diameters of 55-57 µm similar to the i.d. of the separation capillary (50 or 75 µm i.d.) in order to generate an agglomerate just before the separation capillary without frits [70,71]. Concerning chip device, the particles can be immobilized by designing micro-cell containing the particles of larger dimensions than the other channels of the chip and thus generating a restriction [67,68].

Considering the difficulties to maintain particles in capillaries or channels by the previously described methods, it could have been interesting to have information related to the filling repeatability by measuring its impact on the efficiency for devices dedicated to separation or on peak area for extraction devices. This has only been discussed once [71] by Moreno-González *et al.* who studied the repeatability after constructing three MIP concentrators by inserting the capillary containing the MIP particles (2 mm x 150 µm i.d.) and the one dedicated to the CE separation (130 cm x 50 µm i.d.) into a teflon tube. The relative standard deviation (RSD) ( $n = 10$ ) values of peak areas of ten consecutive injections ranged from 3.4 to 9.8% and for the three different concentrators ranged from 5.1 to 10.4%.

**Table 2.** Conditions of synthesis and performances of MIPs particles.

Target	MIP material (Diameter)	Immobilization method	Dimensions	V <sub>P</sub>	Medium	Selectivity (MIP/NIP)	Recovery	RSD	Ref.
<b>SPE applications</b>									
Atrazine DEA DIA DEIA	SupelMIP Triazine (55 µm)	Capillary restriction (75 µm i.d.)	Fused silica capillary (2 mm x 150 µm i.d.)	2.7 µL	Urine (Dil. x1.008)	-	92-102%	Recovery: 9-11% (n = 3) Area: 0.7-17.9% (n = 3) Area: 2.2-21.8% (n <sub>D/D</sub> = 3)	[70]
Danofloxacin Sarafloxacin Difloxacin Enrofloxacin Ciprofloxacin Flumequine Marbofloxacin Oxolinic acid	SupelMIP Quinolones (57 µm)	Capillary restriction (50 µm i.d.)	Fused silica capillary (2 mm x 150 µm i.d.)	22 µL	Milk (Precipitation & dilution)	-	70-102.3%	Recovery: 3-12% (n = 6) Area: 3-12% (n = 3) Area: 6.6-15% (n <sub>D/D</sub> = 3)	[71]
Z-L-Phe-OH-NBD	Poly(MAA-VP-co-EGDMA) < 110 µm)	Channel restriction (105 µm i.d.)	Chip channel (220 µm i.d.)	20 µL	Pure medium	Adsorption: 61/18%	-	-	[68]
Terbutaline	Poly(MAA-co-EGDMA) < 50 µm)	Channel restriction (200 µm x 150 µm)	Chip micro-cell (10 cm x 1 mm x 500 µm)	12 µL	Human serum (Filtration)	-	98-108%	Signal intensity: 3.6% (n = 7)	[67]
Target	MIP material (Diameter)	Immobilization method	Dimensions	R <sub>s</sub>	N (plates/m)		RSD	Ref.	
<b>CEC applications</b>									
D,L-Phenylalanine	Poly(MAA-co-EGDMA) (2-10 µm)	Acrylamide gel frits (3 mm x 75 µm)	Fused silica capillary (20 cm x 75 µm i.d.)	1.43	-		-	-	[69]

\* Template underlined for a mixture of targets.

DEA: Desethylatrazine; DIA : Desisopropylatrazine; DEIA: Desethyldesisopropylatrazine ;  $n_{D/D}$ : Day-to-day; RSD: Relative standard deviation;  $V_p$ : Percolation volume; Z-L-Phe-OH-NBD: Z-L-phenylalanine-nitrobenzoxadiazole.

More homogeneous MIP particles can be obtained by imprinting the surface of core particles [77,78]. This approach has contributed to the strong expansion of the use of MIP particles in dispersive solid phase extraction as recently reviewed [18,79–81]. In most cases, the core sorbents are particles with magnetic properties to facilitate the extraction workflow by replacing the long and tedious centrifugation step by the application of magnetic field to recover the particles. These properties were also exploited to immobilize MIP particles into miniaturized separation or extraction devices by applying an external magnetic field, thus eliminating the necessity of frits.

For this purpose, particles of different natures, mainly  $\text{Fe}_3\text{O}_4$  particles [73–75] as shown in **Table 3** with diameters between 25 and 385 nm were selected. After activating the surface of the magnetic nanoparticles with  $\gamma$ -MAPS as in open tubular synthesis, a MIP film is synthesized either using conventional reagents such as MAA and EGDMA [72] or by exploiting the self-polymerization of dopamine [73] and norepinephrine [74,75]. Using scanning and transmission electron microscopy observations, the authors reported film thicknesses ranging from 6 to 8 nm for the imprinted poly(dopamine) and poly(norepinephrine), and of 87-88 nm for the imprinted poly(MAA-co-EGDMA). Finally, the MIP magnetic nanoparticles were directly filled in chip channels (18  $\mu\text{m}$  deep  $\times$  50  $\mu\text{m}$  wide) [73–75] or introduced into capillary of 25  $\mu\text{m}$  i.d. which was then integrated into a chip [72]. The part occupied by the particles can be tuned according to the magnet and corresponds to a length ranging from 5 mm to 2 cm.

**Table 3.** Conditions of synthesis and performances of MIPs by imprinting the surface of core particles.

Target*	MIP material (Thickness)	Nanoparticles core (Diameter)	Dimensions	R <sub>s</sub>	N (plates/m)	RSD	Ref.
<b>CEC applications</b>							
<u>D,L-Histidine</u>	Poly(Norepinephrine) (7-8 nm)	Fe <sub>3</sub> O <sub>4</sub> particles ( $\simeq$ 385 nm)	PDMS channel (2 cm x 50 $\mu$ m x 18 $\mu$ m )	1.63	-	-	[75]
<u>R,S-Mandelic acid</u>				1.82	3,200 (S) 5,400 (R)	t <sub>r</sub> : 2.3-2.5% (n = 6) t <sub>r</sub> : 3.3-4.6% (n <sub>C/C</sub> = 3)	
<u>D,L-Tryptophan</u>	Poly(Norepinephrine) (6 nm)	Fe <sub>3</sub> O <sub>4</sub> particles ( $\simeq$ 100 nm)	PDMS channel (1 cm x 50 $\mu$ m x 18 $\mu$ m )	1.84	128,000 (D) 183,000 (L)	t <sub>r</sub> : 1.8-2.2% (n = 6) t <sub>r</sub> : 4.2-4.7% (n <sub>B/B</sub> = 3)	[74]
<u>D,L-Tryptophan</u>	Poly(Dopamine) (8 nm)	Fe <sub>3</sub> O <sub>4</sub> particles ( $\simeq$ 130 nm)	PDMS channel (2 cm x 50 $\mu$ m x 18 $\mu$ m )	1.65	78,500 (D) 175,000 (L)	t <sub>r</sub> : 1.6-1.8% (n = 6) t <sub>r</sub> : 3.9-4.2% (n <sub>B/B</sub> = 3)	[73]
<u>R,S-Ofloxacin</u>	Poly(MAA-co-EGDMA) (87-88 nm)	Commercial hydroxyl group modified superparamagnetic nanospheres ( $\simeq$ 25 nm)	Fused silica capillary (5 mm x 25 $\mu$ m i.d.)	1.46	-	t <sub>r</sub> : 1.1-1.2% (n = 3) t <sub>r</sub> : 2.3-2.5% (n <sub>D/D</sub> = 3) t <sub>r</sub> : 4.3-5.6% (n <sub>C/C</sub> = 3)	[72]

\* Template underlined for a mixture of targets.

N: Efficiency; n<sub>B/B</sub>: Batch-to-batch; n<sub>C/C</sub>: Column-to-column; n<sub>D/D</sub>: Day-to-day; PDMS: Poly(dimethylsiloxane); R<sub>s</sub>: Resolution; RSD: Relative standard deviation;

t<sub>r</sub>: Retention time.

### 1.5.2. Separation in CEC and nanoLC on particles-based MIPs

The heterogeneous MIP particles prepared by bulk process are known to exhibit lower separation performance than stationary phases prepared by other methods due to the irregularity of shape of such MIP particles obtained by grinding and sieving steps [12]. Thus, the number of publications on the implementation of these phases for separation is significantly reduced.

Lin *et al.* developed an imprinted poly(MAA-co-EGDMA) for the enantioseparation of phenylalanine in CEC [69]. MIP particles with size distribution between 2 and 10 µm were packed in a 75 µm i.d. capillary with a length of 20 cm and immobilized with 3 mm length frits made of an acrylamide gel. A resolution of 1.43 between the two enantiomers was obtained. However, no information on the repeatability and lifetime of the system is available.

Even if the nanoparticles can fill the entire section of the channel, it turns out that the selective MIP layer represents only a small part at the surface of the core magnetic particle. This allows the limitation of the diffusion of the compounds within the particles and thus promotes the separation efficiency. Qu *et al.* [72] designed a microfluidic device for rapid enantioseparation of ofloxacin by CEC on chip. As shown in **Figure 2**, the device was based on a PDMS chip containing a fused-silica capillary with 25 µm of i.d. as separation channel filled with NPs coated by an imprinted poly(MAA-co-EGDMA) localized in the capillary to a defined place by applying an external magnetic field. It was found that the tunable length was optimal for 5 mm and led to a resolution of 1.46 with an analysis time of 195 s. As it can be seen on the chromatograms, a baseline enantioseparation was achieved with the MIP particles and not with the NIP ones or an empty capillary, which demonstrates the selectivity of the MIP support. They determined RSD values ( $n = 3$ ) of retention time and peak area for run-to-run (1.1-1.2% and 1.5-2.1%, respectively), day-to-day (2.3-2.5% and 3.4-5.5%, respectively), and chip-to-chip (4.3-5.6% and 7.2-8.3%, respectively) suggesting a good stability, precision, and fabrication reproducibility.

With the same objective, Wang *et al.* employed an L-tryptophan imprinted poly(dopamine) film on Fe<sub>3</sub>O<sub>4</sub> nanoparticles [73]. The separation efficiency obtained with these MIP nanoparticles (packing length of 2 cm) was calculated to be about  $7.85 \times 10^4$  and  $1.75 \times 10^5$  plates m<sup>-1</sup> for D and L-tryptophan, respectively. The resolution was about 1.65 while no baseline separation was accomplished with NIP and the analysis time was inferior to 1 min. The RSD values of the system for run-to-run, day-to-day, and chip-to-chip were less than 5% for the retention times. Furthermore, the stability of MIP particles was demonstrated by storing them at 4°C for at least two weeks with no obvious effect on the analysis performance. However, after one month of storage the resolution was

lowered to 91% of the initial value. The analytical performances were further improved by replacing the poly(dopamine) coating by a poly(norepinephrine) one and a resolution of 1.84 was obtained with efficiencies estimated to be about  $1.28 \times 10^5$  and  $1.83 \times 10^5$  plates m<sup>-1</sup> for D- and L-tryptophan, respectively, for a packing length of 1 cm [74]. Repeatability results were similar in both studies. The use of a mixture of nanoparticles resulting from the same synthesis route with three different templates (S-ofloxacin, L-tryptophan, and S-binaphthol) was also reported to carry out the separation of different kinds of chiral analytes (amino acids, drugs, and industrial catalytic samples) simultaneously within 120 s in a single run [74].

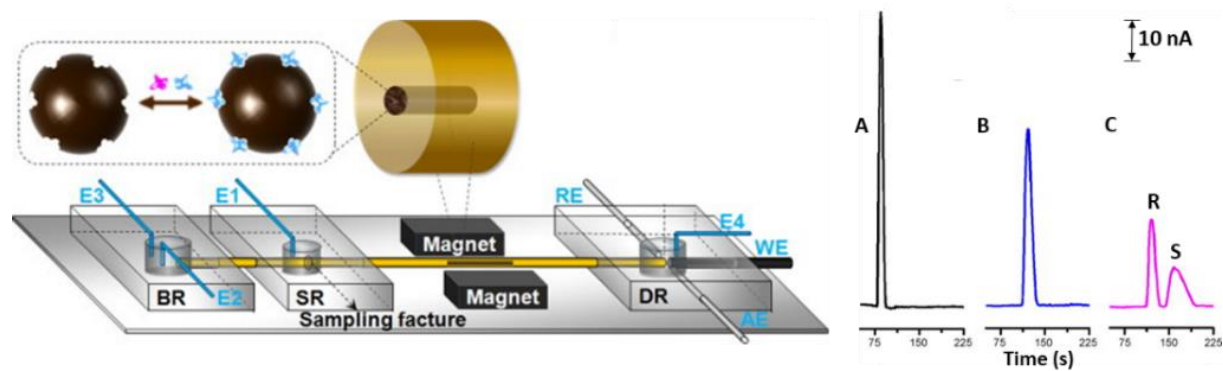


**Figure 2.** (Left) MIP magnetic nanoparticles used in a chip device and (Right) chromatograms of the CEC separation of R,S-ofloxacin in a microchannel empty (A) or filled with a NIP (B) or a MIP (C). CEC conditions: ACN/acetate buffer 40 mM at pH 4.0 (9/1 (v/v)), detection potential of +1.0 V, injection voltage of 200 V for 2 s and separation voltage of 1200 V. AE: Auxiliary electrode; BR: Buffer reservoir; DR: Detection reservoir; E1, E2, E3, and E4: Electrodes for applying sampling and separation voltages; RE: Reference electrode; SR: Sample reservoir; WE: Working electrode. Adapted from [72].

A similar chip was constructed with a R-mandelic acid imprinted poly(norepinephrine) film [75]. A resolution of 1.82 was obtained and the separation efficiencies were calculated to be  $3.2 \times 10^3$  and  $5.4 \times 10^3$  plates m<sup>-1</sup> for S- and R-mandelic acid, respectively. The run-to-run repeatability was evaluated with RSD ( $n = 6$ ) of 2.3-2.5% and 3.1-3.6% on retention times and peak areas, respectively. The good reproducibility of the manufacturing process was also checked with RSD ( $n = 3$ ) of 3.3-4.6% on retention times. Finally, the authors proposed a know-how transfer, this time using L-histidine as template molecule, allowing to perform the enantiomer separation with a resolution of 1.63 [75].

### **I.5.3. Particles-based MIP in solid-phase extraction**

In solid phase extraction, the trend is the opposite of separation applications. Indeed, the MIP film obtained by surface imprinting being marginal compared to the size of the core particle on which it is synthesized, this type of media may lead to capacity too limited for extraction purposes in case of high contamination, as previously with the open tubular format. However, the particles obtained by bulk synthesis are integrally made of MIP and therefore the capacity provided by these particles is of obvious interest for this type of applications.

A chemiluminescence micro flow chip was developed, using 2 mg of imprinted poly(MAA-co-EGDMA) as selective extraction sorbent for the direct determination of terbutaline in human serum [67]. The particles (< 50 µm) were introduced into the micro-cell (10 mm long, 1 mm wide, and 0.5 mm deep) and immobilized by channel restriction (200 µm x 150µm). Injections of 12 µL of filtered serum were performed on the MIP but no results on the NIP were discussed and it is therefore difficult to evaluate the real selectivity contribution of the cavities on the retention process. The lifetime of the device was evaluated to be limited at 100 runs in one month before a decrease in the chemiluminescence intensity as a possible consequence of the binding site destruction by the shrinkage of the MIP.

Similarly, Z-L-phenylalanine-nitrobenzoxadiazole imprinted poly(MAA-VP-co-EGDMA) particles were packed in a channel having an i.d. of 220 µm in a poly(methylvinylsiloxane) chip and immobilized *via* a restriction channel (105 µm i.d.) [68]. The imprinted effects were evaluated by loading 20 µL of a  $1.10^{-6}$  mol L<sup>-1</sup> of Z-L-phenylalanine-nitrobenzoxadiazole in acetonitrile (porogen of the synthesis) and on-line detected by laser induced fluorescence (LIF). The adsorption percentage was 61% for MIP and 18% for NIP, suggesting that a selective retention was obtained on MIP within a shortened overall analysis time from 4 h to 10 min in contrast to conventional molecularly imprinting analysis in batchwise mode.

Another category of examples based on packing of MIP particles in miniaturized devices are based on the use of commercial MIPs as sorbent to carry out SPE coupled in-line with CE separation [70,71]. Lara *et al.* used MIP particles from SupelMIP™ SPE-Triazine (from Supelco) [70]. The concentrator was constructed in a first capillary (2 mm x 150 µm i.d. x 360 µm o.d.) that was then coupled *via* a Teflon tube (300 µm i.d.) to a second capillary (75 µm i.d. x 360 µm outer diameter (o.d.)) dedicated to the CE separation. Injections of water or urine spiked with atrazine and three metabolites gave higher recoveries on the MIP than on a commercial SPE support (Oasis® HLB particles, 60 µm). For the water solution, the signal obtained with the Oasis HLB concentrator was 0-42% of the signal

obtained with the MIP concentrator. On the other hand, for the urine sample, the quantitative comparison was not possible since no satisfactory results could be obtained on the Oasis HLB concentrator due to retention and competition of the endogenous compounds from the matrix. However, no NIP concentrator was built, making the evaluation of the selective contribution of the MIP incomplete. The RSD ( $n = 3$ ) of the peak areas for intra-day and inter-day precision in pure medium were 0.7-17.9% and 2.2-21.8%, respectively, and RSD ( $n = 3$ ) for recoveries were of 9-11% in urine samples.

The same group also proposed the introduction of commercial SupelMIP Quinolone particles (from Supelco) in the same concentrator coupled in-line with CE (50  $\mu\text{m}$  i.d. capillary) and mass spectrometry (MS) for the determination of eight regulated veterinary quinolones in bovine milk samples [71]. Repeatability was evaluated in milk samples and intra-day RSD ( $n = 6$ ) for peak areas of 3-12% was determined as well as inter-day RSD ( $n = 15$ ) of 6.6-15%. However, there is no NIP to assess the selectivity of this concentrator.

## I.6. Monolithic MIPs

Synthesis of monolithic MIPs can be addressed by different paths depending on the target and the sample. Based on the nature of the synthesis conditions, polymers are categorized into organic, inorganic, and organic-inorganic hybrid supports. Monolithic MIPs were first prepared at conventional format in 4.6 mm i.d. stainless-steel columns as reported by Ou *et al.* [82,83] and more recently by other groups [84-87]. However, miniaturized formats, such as pipette tips or capillaries, represent today most of the developments.

MIP monoliths were prepared in the whole section of miniaturized devices using organic and hybrid organic-inorganic monomers but also by surface imprinting on a core monolith. Since this review aims to list miniaturized monolithic MIPs in capillary or chip microchannel, a maximum i.d. value of 1 mm has been defined. In literature the dimensions of the devices fluctuate considerably, but it is possible to observe some trends depending on the chosen application. The monolithic MIPs in devices dedicated to separation purposes have a diameter ranging from 25 to 320  $\mu\text{m}$  with a majority at 100  $\mu\text{m}$  and their lengths fluctuate between 4 and 100 cm, which represents phase volumes ranging from 25 nL to 4  $\mu\text{L}$  (**Table 6**). Concerning the monolithic MIPs used for extraction purposes, their lengths range from 3 to 25 cm with a majority around 10 cm and with diameters varying between 100 and 530  $\mu\text{m}$  (**Table 8**). However, diameters smaller than 500  $\mu\text{m}$  are exclusively used for applications with off-line sodium dodecyl sulfate polyacrylamide gel electrophoresis (SDS-PAGE) analysis [88,89] or

with on-line LC analysis [45,49,90–92]. Therefore, monolith phase volumes from 7 to 20  $\mu\text{L}$  were used for extraction with off-line mode separation while for on-line couplings they cover a large range from 400 nL to 22  $\mu\text{L}$ . Some MIPs used as extraction sorbent were also prepared in pipette tips with phase volumes from 10 to 100  $\mu\text{L}$  (**Table 7**).

### I.6.1. *In situ* synthesis of monolithic MIPs

#### I.6.1.1. Organic monolithic MIPs

As for the largest scale, miniaturized monolithic MIPs were mainly synthesized using organic monomers because numerous types of monomers are available and because of the simplicity of the polymerization procedure [11]. Organic polymers benefit also from an excellent stability at different pH and their surface chemistry and porosity can be tuned [40] that is favorable for their *in situ* synthesis in capillaries or channels.

As illustrated by **Table 4**, most of miniaturized monolithic MIP syntheses were carried out in fused-silica capillaries that must first be activated to ensure the anchorage of the monolith at their inner surface. As for open tubular,  $\gamma$ -MAPS is the favored compound although other reagents such as 3-(triethoxysilyl)propyl methacrylate ( $\gamma$ -MAPES) [39,45,46,93] or vinyltrimethoxsilane [94] were also sometimes used. SEM observations can be used to verify the correct anchorage of the imprinted monolith after its *in situ* polymerization. Furthermore, it is a fairly easy and quick technique to set up to observe the influence of some parameters such as solvents [95–97] or monomers [47,50] on the morphology of the monolith, *i.e.* the presence of macropores that ensure its permeability which is an important parameter to consider.

As summarized in **Table 4**, target analytes are still predominantly used as templates even if the dummy approach was reported by different groups [39,45,46,93] for the same reason as previously mentioned (**Section I.3**). As for MIP synthesis in bulk, MAA is the most commonly used functional monomer usually copolymerized with EGDMA as cross-linker, but AA [39,45,46,97] and VP [39,45,46,95,98] were sometimes preferred. The T/M/CL ratio is highly variable but a preponderance of publications works with a molar ratio of 1/4/20 [90,99–104]. Finally, miniaturized organic monolithic MIPs are mainly prepared by free radical polymerization with AIBN that allows either a photochemical or thermal initiation.

The choice of porogen is one of the key factors and is the biggest change from classical bulk synthesis. Indeed, in addition to solubilizing template and all reagents and promoting interactions

between the template and the functional monomers, it must lead to large pores to obtain good flow-through property, *i.e.* a high permeability [105]. For all these reasons, syntheses with a single solvent as porogen are rarely reported unlike to the use of a mixture of several solvents. A conventional solvent is selected, such as predominantly ACN or toluene, to solubilize the template and promote polar non-covalent interactions between functional monomers and template. Then, another solvent is added, such as dodecanol [39,45,46,95,98–101,104,106,107] or isoctane [37,90,92,97,103,108,109], for its ability to produce large pores due to earlier onset phase separation. Appropriate ratios of each solvent are then adjusted to set the solubility, polarity, and the ability to generate pores to a satisfactory degree.

To evaluate the flow-through property of the monolithic MIP in a capillary a simple process was described that consists of setting the pressure to 1 MPa on a solvent and for a defined time of flow-out of 30 s, 30 s-1 min, and more than 1 min, the permeability was characterized as high, good, and low, respectively [48,96,110,111]. However, this evaluation does not provide a quantitative value and depends considerably on the solvent viscosity, temperature, and of the diameter and length of the MIP. It seems that this technique can only be used for screening tests with identical capillary sizes. However permeability can be easily measured and calculated by the Darcy's law [49,89–91,112–114] formulated with the following equation:

$$K = \frac{4\eta LF}{\pi d_i^2 \Delta P} \quad (\textbf{Equation 1})$$

K is the permeability ( $\text{m}^2$ ), F is the mobile phase flow rate ( $\text{m}^3 \text{s}^{-1}$ ),  $\eta$  is the mobile phase viscosity ( $\text{Pa s}$ ), L is the capillary length (m), S is the section ( $\text{m}^2$ ), and  $\Delta P$  is the back pressure (Pa) generated by the monolithic MIP in the capillary or channel. The measured permeabilities reported in literature cover a wide range from  $3.3 \times 10^{-15}$  to  $7.2 \times 10^{-11} \text{ m}^2$ . Some of these publications have shown the influence of the solvent ratio on permeability [89,90], while others have shown the influence of the synthesis temperature [49].

Since the potential of a MIP is related to cavities promoting highly selective interactions that should be absent in its NIP, other physical characterizations can be done as described in **Table 4**. Nitrogen adsorption porosimetry can measure the surface area [88,89,93,110,112–115] or pore volume [89,93,116] of monolithic MIPs/NIPs. Some publications present results obtained by Fourier transform infrared [47,48,52,89,91,92,94,96,97,110,111,113–119] or solid-state UV-vis [47,97,110,116,117] to determine the characteristic functions and chemical groups that make up the MIP and NIP. By comparing the spectra before and after the template removal, it is possible to confirm

that this step was successfully completed. Finally, Zhang *et al.* [92] characterized the resistance of the synthesized monolith through a thermogravimetric analysis and solvent resistance. However, all these measurements are obtained with a monolith synthesized in larger dimensions and are therefore not fully representative of the miniaturized monolith really synthesized in a capillary or channel.

Recently, new innovative materials have been introduced in syntheses to improve the performances of the MIPs [47,52,117–119]. For example, Liang *et al.* incorporated carbon quantum dots in the polymerization mixture [47]. Those nanomaterials were employed due to green synthesis, easy functionalization, and low toxicity. Adsorption capacity for aflatoxin B<sub>1</sub> was determined by breakthrough curve and was significantly improved for the monolithic MIP prepared with quantum dots ( $0.442 \text{ ng mg}^{-1}$ ) compared to the MIP without ( $0.263 \text{ ng mg}^{-1}$ ) or the corresponding NIP ( $0.0917 \text{ ng mg}^{-1}$ ). The same group also proposed the use of multi-walled carbon nanotubes in the polymerization mixture as modifiers to improve again the adsorption performance based on large specific surface areas [119]. However, the high surface energy and the risk of agglomeration of the multi-walled carbon nanotubes forced the authors to functionalize them to increase their stability in solvents.  $\gamma$ -MAPS was therefore used to silanize them before synthesizing the coated imprinted monolith. In order to enhance the selectivity of the MIP it was decided to use acryloyl- $\beta$ -cyclodextrin with MAA as dual-functional monomers. Adsorption capacities for thiabendazole ( $58.01 \text{ ng mg}^{-1}$ ), and its analogues ( $57.25$  and  $50.84 \text{ ng mg}^{-1}$  for fuberidazole and carbendazim, respectively) were remarkably improved compared to the MIP prepared without the two additional reagents or the NIP [119]. Composite materials with silanized graphene oxide (SGO) [117,118] or silver-modified graphene oxide (Ag/GO) [52] were also employed to increase the adsorption capacity by their large specific surface areas. Among these studies, one combined SGO with a metal ion to obtain a coordination imprinted polymer (CIP) [117]. Indeed, the MIP was synthesized with Zn<sup>2+</sup>, which acts as a coordination center and forms a complex with the flumequine template molecule. As metal-coordination interactions are rarely affected by the solvent, since the binding interactions are stronger than hydrogen bond and other Van der Waals forces, it helps to stabilize the template-monomer complex before the polymerization. These advantages resulted in a higher adsorption capacity for the SGO-CIP ( $61.74 \text{ ng mg}^{-1}$ ) than for SGO-MIP ( $36.02 \text{ ng mg}^{-1}$ ) or for CIP ( $28.76 \text{ ng mg}^{-1}$ ).

#### **I.6.1.2. Hybrid organic-inorganic monolith**

Although predominantly reported, organic monoliths exposed to different solvents may shrink or swell [40]. These perturbations may alter the morphology and the structure of the polymer network,

thus affecting its performances. Hybrid monolithic MIPs benefit from the advantageous features of both the organic (simple polymerization procedures but also tunable porosity and surface chemistry) and inorganic (excellent mechanical strength and good solvent resistance) based materials [40].

A first approach to synthesize hybrid supports was to use  $\gamma$ -MAPS, usually used for the anchorage of the monolith, also as a cross-linker [48,96,111,115,116]. Wang *et al.* even combined this reagent with a green solvent in a ternary porogen made of an ionic liquid (1-butyl-3-methylimidazolium hexafluorophosphate,  $\text{BMIM}^+\text{PF}_6^-$ ), acetonitrile, and chloroform [116]. Thus, a poly(MAA- $\gamma$ -MAPS) imprinted with S-naproxen was synthesized by a non-hydrolytic sol-gel process, an attractive alternative that does not require aging and drying steps at high temperatures but also avoids the cracking and shrinking phenomena. The ionic liquid has properties including a high ionic strength that could increase the rate of aggregation.

POSS, *i.e.* nano-building blocks with cage like architecture containing silicon and oxygen, was also proposed with EGDMA as co-cross-linkers and VP as monomer to get a hybrid monolithic MIP for baicalin with reinforced physical properties and enhanced adsorption capacity [91]. Both MIP and NIP showed an increased retention capacity compared to the same materials without POSS. The authors hypothesized that due to the different amounts of double bond per cross-linker molecule and different molecular volumes, the incorporation of the nanocage-like structure of POSS into the net composed of linear EGDMA, could increase the local density of polymerized monomers, which led to increased interaction towards the template.

Among these works, Lin *et al.* succeeded in synthesizing an hybrid monolithic MIP, where polycondensation and polymerization were subsequently carried out in a 25 cm x 75  $\mu\text{m}$  capillary, with lysozyme protein as template [89]. The poly(MAA-co-MBAA-TMOS)-based MIP allowed the combination of the rigidity from silica matrix and the flexibility from organic hydrogel.

**Table 4.** Conditions of *in situ* synthesis of monolithic MIPs in capillaries.

Target *	Activator	Monomer/CL/Solvent (v:v)	T/M/CL (mol/mol/mol)	Initiation	Physical characterizations	Ref.
<b>Organic monolith</b>						
<u>2,4-Aminopyridine</u>	$\gamma$ -MAPS	MAA/EGDMA/ACN	1/4/20	AIBN / 60°C, 12h	Average pore size: 0.1-5 $\mu$ m	[102]
<u>Dopamine</u> , Norepinephrine	$\gamma$ -MAPS	MAPA/EGDMA/EtOH:MeOH (60:40)	1/?/33.5	AIBN / 70°C, 40min	◦ Specific surface area: 8.9/8.7 $m^2 g^{-1}$ (MIP/NIP) ◦ $K = 7.16/6.04 \times 10^{-11} m^2$ (MIP/NIP)	[113]
<u>Histamine</u> , <u>Serotonin</u> + 3 analogs	$\gamma$ -MAPS	IA/EGDMA/DMF	1+1/5/18	AIBN / 55°C, 6h	-	[50]
(-)Norepinephrine, (+)-Norepinephrine + 5 analogs	$\gamma$ -MAPS	IA/EGDMA/DMF	1/9.2/19	AIBN / 65°C, 17min	-	[120]
<u>R,S-Ornidazole</u> , <u>R,S-Secnidazole</u>	$\gamma$ -MAPS	MAA+VP/EGDMA/Toluene:Dodecanol (10:90, w:w)	1/0.75+0.75/6	AIBN / 56°C, 20h	-	[95]
<u>R,S-Ornidazole</u> + 5 analogs	$\gamma$ -MAPS	HEMA+DMAEMA/EGDMA/Toluene: Dodecanol (12:88, w:w)	1/0.75+0.75/6	AIBN / 56°C, 24h	-	[106]
<u>D,L-Phenylalanine</u>			1/?/33		◦ Specific surface area: 9.3/8.7 $m^2 g^{-1}$ (MIP/NIP) ◦ $K = 1.521 \times 10^{-11} m^2$ (MIP)	
<u>D,L-Tryptophan</u>	$\gamma$ -MAPS	MAPA/EGDMA/EtOH:MeOH (60:40)	1/?/40.8	AIBN / 70°C, 40min	◦ Specific surface area: 9.0/8.7 $m^2 g^{-1}$ (MIP/NIP) ◦ $K = 1.644 \times 10^{-11} m^2$ (MIP)	[114]
<u>D,L-Tyrosine</u>			1/?/36.2		◦ Specific surface area: 9.1/8.7 $m^2 g^{-1}$ (MIP/NIP) ◦ $K = 1.676 \times 10^{-11} m^2$ (MIP)	
<u>R,S-Ropivacaine</u>	$\gamma$ -MAPS	MAA/TRIM/Toluene:Isooctane (99:1)	1/12/12	AIBN / UV, 350nm, -20°C, 16h	-	[37]

Target *	Activator	Monomer/CL/Solvent (v:v)	T/M/CL (mol/mol/mol)	Initiation	Physical characterizations	Ref.
R,S-TB		MAA/EGDMA/Toluene:Dodecanol (16:84)	1/3/20			
	$\gamma$ -MAPS			AIBN / 55°C, 10h	-	[107]
D,L-THP		MAA/EGDMA/Toluene:Dodecanol (12:88)	1/2/13			
Thiabendazole	$\gamma$ -MAPS	MAA/EGDMA/Toluene:Isooctane (96:4)	1/4/20	AIBN / UV, RT, 1.5h	-	[103]
Trietazine, Cyanazine	$\gamma$ -MAPS	MAPA/EGDMA/EtOH:MeOH (60:40)	1/?/12.2	AIBN / 70°C, 90min	<ul style="list-style-type: none"> <li>◦ Specific surface area: 9.1/8.7 m<sup>2</sup> g<sup>-1</sup> (MIP/NIP)</li> <li>◦ K = 7.03/6.04 × 10<sup>-11</sup> m<sup>2</sup> (MIP/NIP)</li> </ul>	[112]
D,L-Tyrosine	$\gamma$ -MAPS	AA/EGDMA/ACN:Isooctane (67:33)	1/4/40	AIBN / 60°C, 4h	-	[97]
D,L-Tyrosine + 4 analogs	$\gamma$ -MAPS	MAA+VP/EGDMA/Toluene:Dodecanol (20:80)	1/1.5+1.5/8.1	AIBN / 50°C, 12h	-	[98]
YPLG, Oxytocin	$\gamma$ -MAPS	MAA/EGDMA/ACN:Isooctane (96:4)	1/15/60	AIBN / 48°C, 3h	-	[108]
YPLG, YPGL	$\gamma$ -MAPS	MAA/EGDMA/ACN:Isooctane (96:4)	1/15/60	AIBN / 48°C, 3h	-	[109]
Aflatoxin B <sub>1</sub> (DMC)	APTES	MAA/EGDMA/Carbon quantum dots/MeOH:Toluene (80:20)	1/10/40	AIBN / 55°C, 6h	-	[47]
Auramine O	-	MAA/EGDMA/MeOH:Toluene: Dodecanol (20:20:60)	1/4/20	AIBN / UV, 365 nm, 10h	-	[104]
Bisphenol A, Nonyl phenol	-	MAA/EGDMA/(Ag/GO)/MeOH:Toluene (77:23)	1+1/10/60	AIBN / 60°C, 6h	-	[52]
Cannabidiol, $\Delta$ 9-THC	Vinyltrimethoxy silane	MAA/EGDMA/DCM	1/3/9	AIBN / 60°C, 24h	-	[94]

Target *	Activator	Monomer/CL/Solvent (v:v)	T/M/CL (mol/mol/mol)	Initiation	Physical characterizations	Ref.
Cocaine	$\gamma$ -MAPS	MAA/TRIM/ACN:Isooctane (90:10)	1/4/20	AIBN / 60°C, 24h	K = 3.3/3.7 x 10 <sup>-15</sup> m <sup>2</sup> (RSD: 3-17%, n = 3) (MIP/NIP)	[90]
Flumequine (Flumequine-Zn <sup>2+</sup> )	SGO	VP+IA/EGDMA/MeOH:H <sub>2</sub> O (85:15)	1/2+2/30	AIBN / 60°C, 24h	-	[117]
Fluoroquinolones (Pefloxacin methane sulphonate)	$\gamma$ -MAPES	MAA/DEGDMA/MeOH:H <sub>2</sub> O (77:23)	1/9.4/24.2	AIBN / 65°C, 16h	<ul style="list-style-type: none"> <li>◦ Specific surface area: 8.7/7.4 m<sup>2</sup> g<sup>-1</sup> (MIP/NIP)</li> <li>◦ Pore volume: 0.013 cm<sup>3</sup> g<sup>-1</sup> (MIP &amp; NIP)</li> <li>◦ Average pore size ≈ 5 <math>\mu</math>m</li> </ul>	[93]
8-OHdG (Guanosine)	$\gamma$ -MAPES	AA+VP/MBAA/Dodecanol:DMSO (50:50)	1/12.8+5.8/6.6	AIBN / 60°C, 18h	-	[39]
8-OHdG (Guanosine)	$\gamma$ -MAPES	AA+VP/MBAA/Dodecanol:DMSO (50:50)	1/13+9/7	AIBN / 60°C, 20h	-	[45]
Rhodamine B	-	MAA/EGDMA/SGO/MeOH:Toluene: Dodecanol (17:33:50)	1/4/30	AIBN / 60°C, 4h	-	[118]
Safranin T	-	MAA/EGDMA/MeOH:Toluene: Dodecanol (9:36:55)	1/4/20	AIBN / 60°C, 4h	-	[101]
<u>SQX + 4 analogs</u>	$\gamma$ -MAPS	MAA/EGDMA/DMF:para-Xylene: Isooctane (23:54:23)	1/9.7/23.6	AIBN / 60°C, 70h then 120°C, 2h	-	[92]
<u>Thiabendazole</u> + 2 analogs	-	MAA+A- $\beta$ -CD/EGDMA/SMWNT/ Toluene:MeOH:Dodecanol (33:17:50)	1/1+3.5/20	AIBN / 60°C, 4h	-	[119]
Auramine O	-	MAA/EGDMA/MeOH:Toluene: Dodecanol (20:20:60)	1/4/20	AIBN / UV, 365 nm, 10h	-	[100]
8-OHdG (Guanosine)	$\gamma$ -MAPES	AA+VP/MBAA/Dodecanol:DMSO (50:50)	1/13+6/7	AIBN / 60°C, 18h	-	[46]

Target *	Activator	Monomer/CL/Solvent (v:v)	T/M/CL (mol/mol/mol)	Initiation	Physical characterizations	Ref.
Rose bengal	-	MAA/EGDMA/MeOH:Toluene: Dodecanol (17:33:50)	1/4/20	AIBN / 55°C, 4.5h	-	[99]
<b>Organic-inorganic monolith</b>						
Acephate, Phosphamidon (4-DMPTABA)	-	MAA/ $\gamma$ -MAPS/MeOH:Toluene (60:40)	1/3/8.4	AIBN / 50°C, 18h	-	[48]
Baicalin	$\gamma$ -MAPS	VP/EGDMA+POSS/DMSO:1,4- Butanediol:Dodecanol (12.5:12.5:75)	1/4.2/9	AIBN / 60°C, 3h	$K = 3.38 \times 10^{-11} \text{ m}^2$ (MIP)	[91]
<u>Carbaryl + 2 analogs</u>	-	MAA/ $\gamma$ -MAPS/ACN:DCM (20:80)	1/6/8	AIBN / 50°C, 12h	<ul style="list-style-type: none"> <li>◦ Specific surface area: <math>5.72 \text{ cm}^2 \text{ g}^{-1}</math> (MIP)</li> <li>◦ Pore volume: <math>0.0152 \text{ m}^3 \text{ g}^{-1}</math> (MIP)</li> <li>◦ Average pore size: 4.98 nm</li> </ul>	[115]
Lysozyme	$\gamma$ -MAPS	AA/MBAA+TMOS/MeOH:H <sub>2</sub> O (62.5:37.5)	1/5500/344	AIBN / 60°C, 12h	<ul style="list-style-type: none"> <li>◦ Specific surface area: <math>90.45/39.35 \text{ m}^2 \text{ g}^{-1}</math> (MIP/NIP)</li> <li>◦ Pore volume: <math>0.078/0.03 \text{ cm}^3 \text{ g}^{-1}</math> (MIP/NIP)</li> <li>◦ Average pore size: 3.57/5.2 nm (MIP/NIP)</li> <li>◦ <math>K = 1.52/1.60 \times 10^{-14} \text{ m}^2</math> (MIP/NIP)</li> </ul>	[89]
<u>R,S-Naproxen</u>	-	MAA/ $\gamma$ -MAPS/BMIM <sup>+</sup> PF <sub>6</sub> <sup>-</sup> :ACN: Chloroform (4.5:11.2:84.3)	1/4.2/17.2	AIBN / 54°C, 6h	-	[116]
(S,R),(R,S),(S,S),(R,R)- Ractopamine	-	AA/ $\gamma$ -MAPS/MeOH:Toluene (60:40)	1/3.1/7.5	AIBN / 60°C, 24h	-	[96]
Trichlorfon	-	MAA/ $\gamma$ -MAPS/MeOH:Toluene (60:40)	1/2/8.4	AIBN / 50°C, 12h	-	[111]

\* Template indicated in bracket when different from target or underlined for a mixture of targets.

4-DMPTABA: 4-(dimethoxyphosphorothioylamino)butanoic acid; 8-OHdG: 8-Hydroxy-2'-deoxyguanosine; A- $\beta$ -CD: Acryloyl- $\beta$ -cyclodextrin; Ag/GO: Silver-modified graphene oxide; APTES: 3-Aminopropyltriethoxysilane; BMIM $^+$ PF $_6^-$ : 1-Butyl-3-methylimidazolium hexafluorophosphate; DCM: Dichloromethane; DEGDMA: Di(ethylene glycol) dimethacrylate; DMAEMA: 2-(Dimethylamino)ethyl methacrylate; DMC: 5,7-Dimethoxycoumarin; DMF: N,N-dimethylformamide; HEMA: 2-hydroxyethyl methacrylate; IA: Itaconic acid; K: Permeability; MBAA: N,N'-Methylenebis(acrylamide); MAPA: N-Methacryloyl-L-phenylalanine; POSS: Polyhedral oligomeric silsesquioxanes; RSD: Relative standard deviation; RT: Room temperature; SGO: Silanized graphene oxide; SMWNT: Silanized multi-walled carbon nanotube; SQX: Sulfaquinoxaline; TB: Tröger's base; THP: Tetrahydropalmatine; TMOS: Tetramethyl orthosilicate; YPGL: Tyrosine-Proline-Glycine-Leucine; YPLG: Tyrosine-Proline-Leucine-Glycine;  $\Delta$ 9-THC:  $\Delta$ 9-tetrahydrocannabinol;  $\gamma$ -MAPES: 3-(Triethoxysilyl)propyl methacrylate;  $\gamma$ -MAPS: 3-(Trimethoxysilyl)propyl methacrylate.

### I.6.2. Surface imprinting of a MIP on a core monolith

Instead filling the whole section of a capillary or a channel, MIP can be prepared at the surface of an organic or inorganic core monolith, as described in **Table 5**. This approach allows a direct synthesis of MIPs on the surface of a generic and optimized monolith by using a minimal amount of template. This approach also makes it possible to take advantage of the permeability and of the large specific surface area of the core monolith and thus to synthesize a MIP in closer to the conditions of bulk synthesis. This explains the absence of dodecanol and isoctane in the porogen composition for a large part of these works [49,110,121,122]. Nevertheless, the resulting volume of MIP phase is intermediate between the one obtained by open tubular approach involving a MIP film and by filling the entire section of the capillary by a monolithic MIP.

Many works employed the organic synthesis of poly(TRIM) as core monolith [49,76,122,123]. The only particularity is the synthesis in two separate steps. In the first one, TRIM reacts on itself to form the core monolith. Then, in the second one, template, monomer, cross-linker and solvents, the same as in conventional MIP synthesis, are introduced to produce the thin film of MIP on the core monolith. In the reported works, the polymerization was initiated with AIBN either thermally [49,123] or photochemically [76,122] but also with benzoin methyl ether under UV [49].

A poly(TMOS) core was formed by an inorganic sol-gel process [110,121]. The synthesis was carried out with a mixture of poly(ethylene glycol) in an acetic acid solution with a thermostated water bath at 40°C for 24 h. Next, the second step to synthesize the MIP layer is the same as for conventional organic MIP synthesis, in order to combine the advantages of both inorganic and organic approaches. Using the nitrogen adsorption porosimetry, He *et al.* demonstrated that the combination of this type of two-step synthesis with the use of an ionic liquid as porogen leads to an improvement of the surface area (102 and 109 m<sup>2</sup>/g without and with ionic liquid, respectively) [110].

For the selective capture and release of proteins, Wen *et al.* designed a thermally switchable MIP [124]. This system used the properties of the N-isopropylacrylamide employed in the synthesis, which is known for its significant changes in polarity at temperatures below and above its lower critical solution temperature (32°C) resulting from difference in entropy at both states. The properties of the specific cavities of the MIP can thus be thermally modified. First, a poly(glycidyl methacrylate-co-EGDMA) monolith was synthesized. The epoxy groups of the monolith reacted with ethylenediamine followed by functionalization with 2-bromoisobutyryl bromide to introduce the initiator for the atom transfer radical polymerization. Subsequently, a poly(N-isopropylacrylamide) layer imprinted with

myoglobin was synthesized onto the surface of the monolithic core by atom transfer radical polymerization.

Lin *et al.* [88] developed a monolith imprinted with a glycoprotein according to a three-step process described in **Figure 3**. First, a monolith of poly(4-vinylphenylboronic acid-co-pentaerythritol triacrylate) was synthesized in a 100 µm i.d. capillary pre-treated with  $\gamma$ -MAPS. The polymerization was achieved into a water bath at 75°C for 12 h and then horseradish peroxidase was immobilized as template by the complexation of its glycans by their diol moieties and the boronate functionalities of the core monolith allowing the orientation of the protein. Finally, a poly(dopamine) coating was performed on the monolithic skeleton to create the specific cavities around the immobilized glycoproteins.

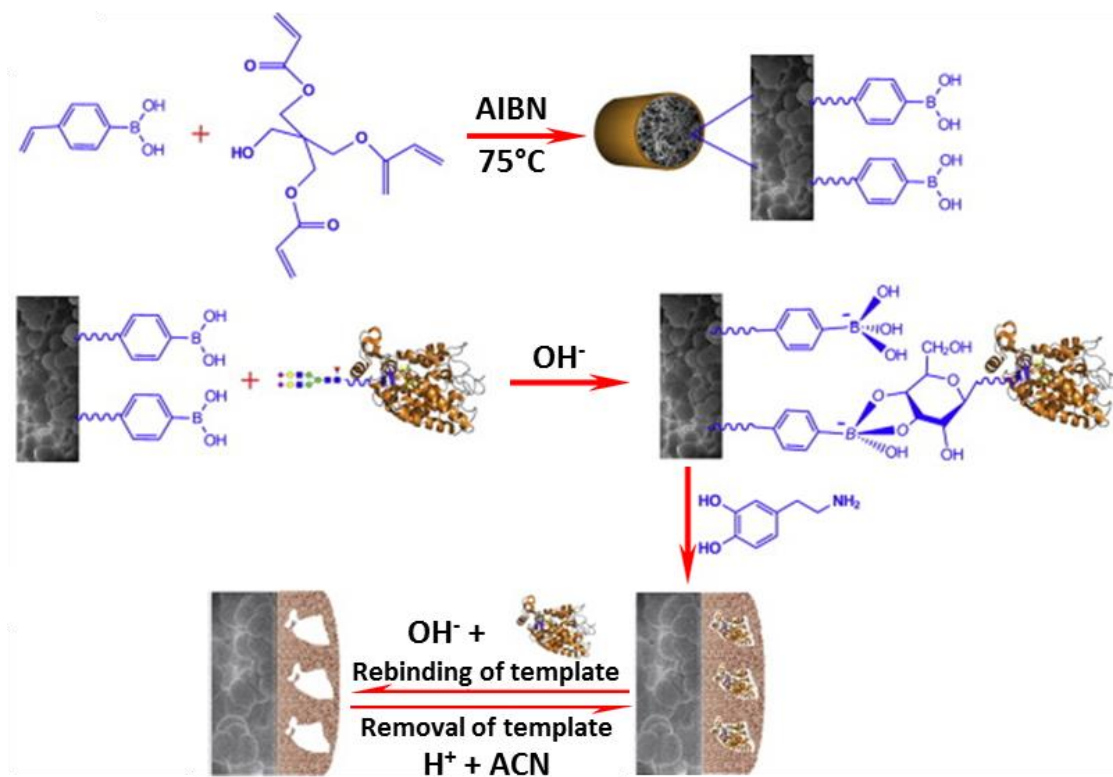


**Figure 3.** Preparation of a monolith imprinted with a glycoprotein, based on boronate functionalized monomer with poly(dopamine) coating, and its recognition mechanism toward glycoproteins.

Adapted from [88].

In the particular case of MIPs synthesized on a monolithic core, further information can be obtained from characterization techniques (porosity, specific surface or thickness of the MIP).

However, as visible in **Table 5**, these parameters are not sufficiently described which makes it difficult to compare surface imprinting of MIP on core monolith with other monolithic supports. SEM can give an estimated thickness of the monolithic MIP coating [88,123]. Elemental analysis can confirm the successful polymerization of the MIP on the core as it was done in the case of a MIP imprinted with amlodipine on a poly(TRIM) monolith [123] or to verify the successful polymerization of poly(dopamine) in the case of the MIP imprinted with glycoprotein [88]. It can also check each step of the synthesis of a MIP for myoglobin on a monolithic core [124]. Porosity was only documented once by Wei *et al.* who observed by conductivity a decrease in porosity from 0.849 to 0.759 after the synthesis of a poly(MAA-co-EGDMA) imprinted with S-amlodipine on a monolithic poly(TRIM) [123].

**Table 5.** Conditions of synthesis of MIPs by surface functionalization on core monolith.

Target *	Core monolith	T/M/CL (mol/mol/mol)	Monomer/CL/Solvent (v:v)	Initiation	Physical characterizations	Ref.
R,S-Amlodipine	Poly(TRIM)	1/4/20	MAA/EGDMA/Toluene:Isooctane (80:20)	AIBN / 53°C, 3h	◦ MIP thickness: 0.2µm ◦ Porosity: 0.849/0.759 (core monolith/MIP monolith)	[123]
Sulfamethazine	Poly(TMOS)	1/5.9/21.1	MAA/EGDMA/BMIM <sup>+</sup> PF <sub>6</sub> <sup>-</sup> :ACN:Toluene (6.25:31.25:62.5)	AIBN / 60°C, 30min	Specific surface area: 109 m <sup>2</sup> g <sup>-1</sup> (MIP)	[110]
D,L-THP	Poly(TMOS)	1/3.3/13.3	MAA/EGDMA/ACN	AIBN / 55°C, 40min	Average pore size ≈ 2 µm (Core monolith)	[121]
R,S-TB		1/0.4/16		AIBN / 55°C, 60min		
Bupivacaine	Poly(TRIM)	1/12/60	MAA/EGDMA/Toluene	AIBN / UV, 365nm, 1h	-	[76]
Bupivacaine, Mepivacaine, S-Ropivacaine	Poly(TRIM)	1/12/60	MAA/EGDMA/Toluene	AIBN / UV, 365nm, 1h	Specific surface area: 16.7 ± 0.5 m <sup>2</sup> g <sup>-1</sup> (n = 4) (core monolith)	[122]
Horseradish peroxidase	Poly(VPBA-co-PETA)		Dopamine/Sodium phosphate buffer	4°C, 12 h	Specific surface area: 8.62/5.5/0.1 m <sup>2</sup> g <sup>-1</sup> (core monolith/MIP/NIP)	[88]
Aflatoxins B <sub>1</sub> , B <sub>2</sub> , G <sub>1</sub> and G <sub>2</sub> (DMC)	Poly(TRIM)	0.3/4/20	MAA/EGDMA/Toluene	AIBN / 60°C, 24h AIBN / UV, 365nm, 1h, 0°C	K = 0.3-1.8/0.4-4.4 × 10 <sup>-14</sup> m <sup>2</sup> (MIP/NIP)	[49]

\* Template indicated in bracket when different from target or underlined for a mixture of targets.

BMIM<sup>+</sup>PF<sub>6</sub><sup>-</sup>: 1-Butyl-3-methylimidazolium hexafluorophosphate; DMC: 5,7-Dimethoxycoumarin; K: Permeability; PETA: Pentaerythritol triacrylate; TB: Tröger's base; THP: Tetrahydropalmatine; TMOS: Tetramethyl orthosilicate; VPBA: 4-vinylphenylboronic acid.

### I.6.3. Monolithic MIPs for separations in CEC and nanoLC

One of the major applications of miniaturized imprinted monoliths is as stationary phase in separation techniques such as in CEC and to a lesser extent in nanoLC. As visible in **Table 6**, a large number of publications indicated that they are particularly effective for the separation of enantiomers [37,95,96,98,102,106,107,114,116,120,121,123] and structural analogues [48,50,106,108–110,112,113,115,122]. For the enantiomeric separation, the resolution can be used in the same way as for the open tubular approach to highlight the contribution of the specific cavities. For the separation of structural analogs, the criterion that best reflects the MIP performance in CEC or nanoLC is the imprinting factor (IF) [50,76,88,89,108,110,112–115,122], that is a quantitative measurement of the selectivity of a MIP for a compound by comparing its behavior with that of the NIP for the same compound. It is defined as the ratio of the retention factors  $k$  of a compound on the MIP and NIP columns ( $IF = k_{MIP} / k_{NIP}$  with  $k = (t_r - t_0)/t_0$  where  $t_r$  is the retention time of the compound and  $t_0$  the retention time of a non-retained compound). It is also essential to pay attention to other figures of merit of the method, *i.e.* its repeatability whatever the synthesis or the separation, and the lifetime of the columns.

Miniaturized monolithic MIPs were mainly used in CEC for enantioseparation. Schweitz *et al.* [37] were the first to perform a chiral separation with a monolithic MIP in a capillary of 75 µm i.d.. An optimal ratio of monomers, template, and porogen solvent was determined to obtain a monolithic MIP possessing good flow-through characteristics, then, pH and organic solvent content of the mobile phase were optimized to separate R- and S-ropivacaine. However, no  $R_s$  was provided. Adding an ionic liquid in the porogen, Wang *et al.* [116] managed to get a MIP able to separate the chiral drug R,S-naproxen with a resolution higher than 8.

Two different stationary phases were developed by Ou *et al.* for the CEC separation of tetrahydropalmatine (THP) or Tröger's base, either an organic monolithic MIP [107] or an organic MIP layer on a silica-based core monolith [121]. Baseline separation was obtained with the organic monolithic MIP within 4 min by applying a voltage of 10 kV and an assisting pressure of 6 bar. The enantioseparation was also achieved with optimized conditions on the hybrid MIP with the same duration but led to better column efficiency and stability. In addition, the column-to-column and batch-to-batch repeatability was studied on retention times and EOF and RSD values ( $n = 3$ ) lower than 8% were obtained. Both types of supports were also evaluated in nanoLC and the retention of the two THP enantiomers was higher on the organic column than on the hybrid column, indicating a lower number of recognition sites in the MIP layer synthesized on the silica-based monolith. However, the

separation performances were superior on this hybrid MIP than on the organic monolith with a better peak symmetry and higher column efficiency, probably resulting from the thin layer of MIP that limits the diffusion phenomena in the stationary phase.

A MIP synthesized at the surface of a poly(TRIM) monolith was used for the CEC enantioseparation of amlodipine [123]. After having studied the influence of parameters such as the mobile phase composition, its pH value, and operating voltages, a strong recognition ability was obtained with a selectivity of 5.83 and a resolution of 7.99. The batch-to-batch RSDs ( $n = 3$ ) for the retention time, column efficiency, and resolution were 1.67, 4.75, and 3.61%, respectively.

Concerning the separation of structural analogues, as shown in **Figure 4**, an imprinted poly(*N*-methacryloyl-L-phenylalanine-co-EGDMA) was successfully applied for the separation of two triazine herbicides, the template trietazine and its analogue cyanazine, while no baseline separation was obtained on the corresponding NIP [112]. An IF of 2.10 was determined for the template. The same group developed a dopamine-imprinted monolithic MIP that gave an IF of 2.0 in pure medium and led to the separation of dopamine and its analog norepinephrine [113].

He *et al.* succeeded in screening sulfamethazine from a sulfonamide mixture [110]. For this, a MIP imprinted with sulfamethazine and synthesized on a poly(TMOS) core monolith was applied in pure medium and led to an IF higher than 3 in CEC. Cross-reactivity was tested with nine analogues and although they interacted less than the template with the support, IFs values between 1 and 2 demonstrated the separation potential of the support for the sulfonamides. In addition, column-to-column and batch-to-batch RSDs ( $n = 3$ ) were evaluated for the EOF and retention time of the thiourea and values lower than 14.5% were obtained.

Another work was done in the field of pesticides with an hybrid organic-inorganic monolithic MIP imprinted with carbaryl [115]. Three carbamates (carbaryl, fenobucarb, and metolcarb) were separated by CEC and led to IF of 7.57, 1.27, and 1.64, respectively. RSD values ( $n = 3$ ) for retention times lower than 2.1% and 4.5% for the run-to-run and the column-to-column repeatability, respectively, were measured. A dummy approach was employed for the synthesis of an hybrid organic-inorganic monolithic MIP employed for the simultaneous determination of acephate and phosphamidon in vegetables [48]. Intra-day ( $n = 5$ ) and inter-day (1, 3, 5, or 7 days) repeatability was studied and gave RSD for peak area of 2.1-4.7% and 3.9-7.4%, respectively. Moreover, the monolithic MIP column can be reused 15 times. However, the absence of a NIP prevents the evaluation of the selectivity really provided by this monolith.

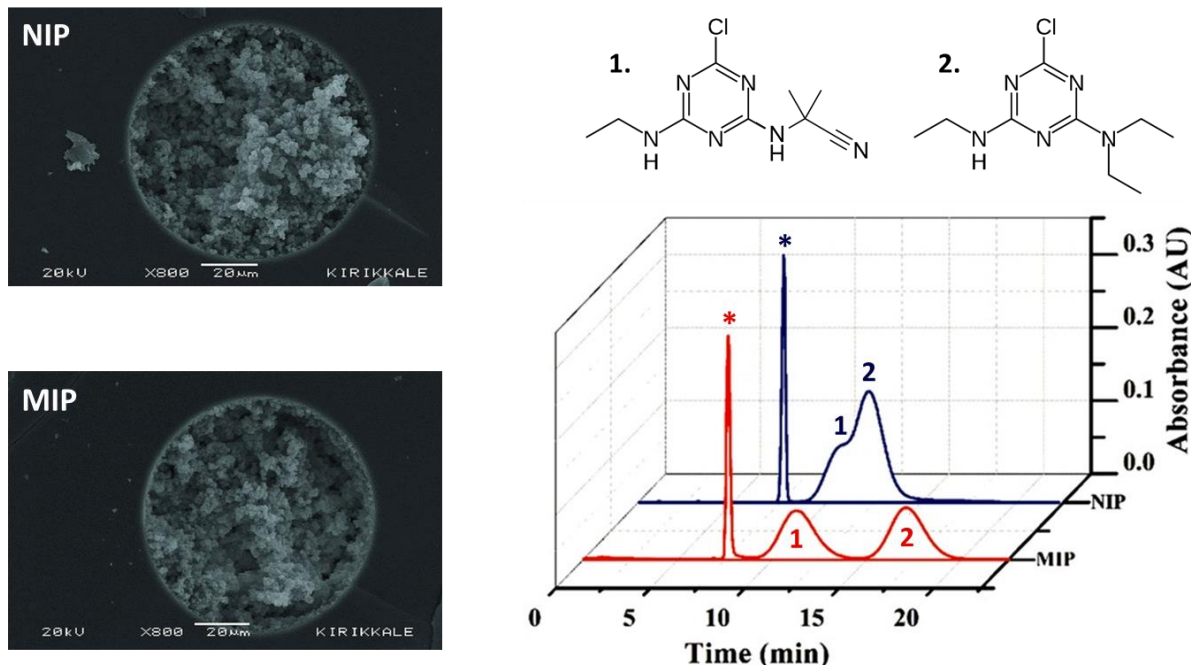


**Figure 4.** (Left) Scanning electron micrograph of the trietazine imprinted poly(MAPA-co-EGDMA) and the corresponding NIP and (Right) separation performance on the monolithic MIP and NIP for template trietazine (1), analog cyanazine (2), and thiourea (\*, unretained marker) at 1.0 mg/mL in aqueous media. CEC conditions: ACN/PBS buffer 10 mM at pH 11.0 (9/1 (v/v)), injection voltage of 5 kV for 30 s and separation voltage of +10 kV, UV detection at 214 nm. Adapted from [112].

Miniaturized imprinted monoliths were also applied to separate biological macromolecules. Zheng *et al.* [108] studied the selective retention in CEC of nonapeptide oxytocin based on the epitope approach with a monolithic MIP synthesized using the tetrapeptide YPLG (Tyrosine-Proline-Leucine-Glycine) as template. This pseudo-dummy approach allowed to obtain a template soluble in the synthesis medium. By optimizing the polymerization mixture, a good selectivity was obtained for oxytocin with an IF of 4.01 and a column efficiency of  $1.6952 \times 10^4$  plates m<sup>-1</sup> was achieved. To further investigate the selectivity of the MIP, a mixture of oxytocin and other proteins including BSA, bovine hemoglobin, ovalbumin, and lysozyme was analyzed. All proteins were co-eluted except oxytocin. A separation factor, defined as the ratio of the retention times of the oxytocin peak to that of the co-eluted compounds, of 4.45 was obtained on MIP in opposition to 2.33 on NIP, demonstrating the selectivity of such support. The same stationary phases were used for the CEC separation of the template YPLG and its analog YPGL (Tyrosine-Proline-Glycine-Leucine), showing good recognition ability and high selectivity for YPLG with a resolution of 3.72 between both compounds [109].

The MIP selectivity can also be very advantageous to determine a single compound present in a complex sample containing other analytes. For example, a hybrid organic-inorganic monolithic MIP allowed the determination by CEC-UV of traces of trichlorfon in vegetable extracts with a limit of detection (LOD, based on a signal-to-noise ratio of 3) and quantification (LOQ, based on a signal-to-noise ratio of 10) of 92.5 and 305.3  $\mu\text{g kg}^{-1}$ , respectively [111]. In another example, the quantification with a CEC-UV analysis of the fungicide thiabendazole in citrus extracts was realized with special effort in optimization of synthesis conditions of the MIP and separation performances [103]. In this case, the influence of the mobile phase composition, voltage, and temperature was first studied with a given MIP. Once optimum separation conditions were established, the concentration and ratio of the reagents in the polymerization mixture were optimized using a factorial experimental design with a Pareto chart showing the impact that each factor has on the response. However, this process is unusual, since it can be expected that the optimal separation conditions will also depend on the nature of the MIP stationary phase, which is optimized in a second step. Nevertheless, the optimized monolith imprinted with thiabendazole demonstrated to be suitable for the analysis of crude citrus sample extracts, allowing target to be unambiguously identified in less than 6 min with LOD of 0.04  $\text{mg kg}^{-1}$  and LOQ of 0.14  $\text{mg kg}^{-1}$ , *i.e.* below the established maximum residue limits for control of this fungicide.

Enantioseparation and separation of structural analogs can also be achieved simultaneously. Indeed, an organic monolith imprinted with (-)-norepinephrine allowed the CEC separation of six neurotransmitters and their enantiomers including dopamine, epinephrine, isoproterenol, octapamine, synephrine, and norepinephrine [120]. In pure medium, an average separation efficiency of  $9.8 \times 10^4$  plates  $\text{m}^{-1}$  was calculated and stability tests established that separation was still achieved after 2 months and more than 600 injections. CEC was also performed for spiked urine samples and neurotransmitters were still separated but the salts present in urine reduced drastically the chiral separation of all the analytes and only the template, norepinephrine, was enantioseparated.

The synthesis of monolithic MIPs in capillaries was a significant progress in miniaturization. Another objective is their integration into a  $\mu$ -TAS. In this context, a hybrid microsystem was described, based on the introduction into a chip of a capillary containing the MIP. A portable device was constructed by Qu *et al.* [97] for the CEC enantioseparation of D,L-tyrosine with a capillary of 25  $\mu\text{m}$  i.d. and 5 cm long containing a poly(AA-co-EGDMA) imprinted with L-tyrosine, coupled to a carbon fiber microdisk working electrode for amperometric detection. After the optimization of chiral separation conditions such as voltage, pH, concentration of acetate buffer in mobile phase, or sampling conditions, a resolution of 2.40 was achieved within 55 s. The RSDs ( $n = 6$ ) for retention time and peak area were 1.2-1.4 and 2.4-2.8% for run-to-run, 2.3-2.4 and 4.3-5.1% for day-to-day, and 3.2-4.2 and

5.8-6.8% for chip-to-chip, respectively, suggesting a good stability of MIP, but also that the MIP-based chips have a good manufacturing reproducibility. In addition, it can be noticed that these authors involved also the open tubular approach for CEC enantioseparation as described previously [51]. However, this approach led to lower separation performances for the same targets due to the low volume of MIP stationary phase in the capillary with a resolution of 1.02 for the enantioseparation of D,L-tyrosine.

As already mentioned, a few imprinted monoliths were also used in nanoLC [76,88,89,121,122]. Three supports were synthesized with different templates including bupivacaine, mepivacaine, and S-ropivacaine [122]. Very encouraging IFs were obtained (29, 14, and 43, respectively) with low retention on the monolithic NIP. However, the difficulties for authors in determining  $t_0$  makes the uncertainty of this parameter relatively large. IFs were calculated based on the center of gravity of the peaks, it is therefore necessary to put the results into perspective. This also illustrates the fact that the differences in flow profiles between CEC (flat) and LC (parabolic) will always be in favor of the separation in CEC.

**Table 6.** Performances of monolithic MIPs used as stationary phase for separation.

Target	Medium	Dimensions (L (l) x i.d.) *	$\alpha$	IF	$R_s$	N (plates/m)	RSD	Ref.
<b>CEC (Chiral separation)</b>								
2,4-Aminopyridine	Pure medium	31.2 cm (20) x 100 $\mu\text{m}$	-	-	-	-	$t_r$ : < 5% ( $n = 3$ )	[102]
R,S-Amlodipine	Pure medium	41.5 cm (30) x 100 $\mu\text{m}$	5.83	-	7.99	19,267 (R) 18,667 (S)	$t_r$ , N, Rs: < 5% ( $n = 5$ ) $t_r$ , N, Rs: < 4.75% ( $n_{B/B} = 3$ )	[123]
R,S-Naproxen	Pure medium	31.2 cm (20) x 100 $\mu\text{m}$	5.74	-	8.82	12,000 (S)	-	[116]
R,S-Ornidazole, R,S-Secnidazole	Ornidazole tablets (ACN extract)	52 cm (30) x 100 $\mu\text{m}$	1.78 1.45	-	-	-	$t_r$ , EOF: < 3.3% ( $n_{D/D} = 5$ ) $t_r$ , EOF: < 6% ( $n_{C/C} = 3$ ) $t_r$ , EOF: < 6% ( $n_{B/B} = 3$ )	[95]
D,L-Phenylalanine	Pure medium	38 cm (30) x 100 $\mu\text{m}$	-	> 2.0	-	-	$t_r$ : < 10% ( $n_{C/C} = ?$ )	[114]
(S,R),(R,S),(S,S),(R,R)- Ractopamine	Pure medium	- (-) x 100 $\mu\text{m}$	-	-	-	-	-	[96]
R,S-Ropivacaine	Pure medium	100 cm (91.5) x 75 $\mu\text{m}$	-	-	-	-	-	[37]
R,S-TB	Pure medium	33 cm (24.5) x 75 $\mu\text{m}$	-	-	1.56	-	EOF: < 5% ( $n = 3$ ) EOF: < 8% ( $n_{C/C} = 3$ )	[107]
D,L-THP					1.43			
R,S-TB	Pure medium	33 cm (8.5) x 75 $\mu\text{m}$	-	-	-	-	$t_r$ , EOF: < 2.2% ( $n = 3$ ) $t_r$ , EOF: < 4.7% ( $n_{C/C} = 3$ ) $t_r$ , EOF: < 6.3% ( $n_{B/B} = 3$ )	[121]
D,L-THP					1.08	19,857 (D) 3,993 (L)		

Target	Medium	Dimensions (L (l) x i.d.) *	$\alpha$	IF	$R_s$	N (plates/m)	RSD	Ref.
D,L-Tyrosine	Pure medium	5 cm (-) x 25 $\mu\text{m}$	-	-	2.40	-	$t_r$ : 1.2-1.4% ( $n = 6$ ) $t_r$ : 2.3-2.4% ( $n_{D/D} = 6$ ) $t_r$ : 3.2-4.2% ( $n_{C/C} = 6$ )	[97]
D,L-Tyrosine	Pure medium	38 cm (30) x 100 $\mu\text{m}$	-	> 2.0	-	-	$t_r$ : < 10% ( $n_{C/C} = ?$ )	[114]
D,L-Tryptophan								
<b>CEC (Analog separation)</b>								
Acephate, Phosphamidon	Cucumber, Letuce ( $\text{H}_2\text{O}$ extract)	55 cm (44) x 75 $\mu\text{m}$	-	-	-	-	Area: 1.5-4.6% ( $n = 3$ ) Area: 3.9-7.4% ( $n_{D/D} = 4$ )	[48]
Carbaryl, Fenobucarb, Metolcarb	Pure medium	30.2 cm (15) x 100 $\mu\text{m}$	4.62- 5.96	7.57 (Car) 1.27 (Fen) 1.64 (Met)	-	-	$t_r$ : < 2.1% ( $n = 3$ ) $\alpha$ : < 5.1% ( $n = 3$ ) $t_r$ : < 4.5% ( $n_{C/C} = 3$ ) $\alpha$ : < 10.3% ( $n_{C/C} = 3$ )	[115]
Dopamine	Banana ( $\text{MeOH}$ extract)	36 cm (27) x 100 $\mu\text{m}$	-	2.0	-	-	$t_r$ : 0.87-1.74% ( $n = 3$ )* $t_r$ : 0.69-1.96% ( $n_{B/B} = 3$ )*	[113]
Histamine, Serotonin, Dopamine, Histidine, 5-HT	Pure medium	48.4 cm (40) x 100 $\mu\text{m}$	-	1.6-6.7	3.4	60,100 (Histamine) 56,500 (Serotonin)	$t_r$ : < 1.1% ( $n = 5$ ) N, $R_s$ , IF, $t_r$ : < 3.2% ( $n_{B/B} = 3$ )	[50]
Sulfamethazine	Pure medium	- (-) x 100 $\mu\text{m}$	-	3.04	-	-	EOF: < 5.7% ( $n = 3$ ) $t_r$ , EOF: < 9.1% ( $n_{C/C} = 3$ ) $t_r$ , EOF: < 14.5% ( $n_{B/B} = 3$ )	[110]
Thiabendazole	Citrus / Orange ( $\text{ACN}$ extract)	50 cm (8.5) x 100 $\mu\text{m}$	-	-	-	-	$t_r$ : 0.9-2.6% ( $n = 5$ )	[103]
Trichlorfon	Cucumber / Cauliflower / Leek ( $\text{H}_2\text{O}$ extract)	35 cm (27.5) x 100 $\mu\text{m}$	-	-	-	-	Area: 4.5% ( $n = 5$ )	[111]
Trietazine	Pure medium	36 cm (27) x 100 $\mu\text{m}$	-	2.10	-	-	-	[112]

Target	Medium	Dimensions (L (l) x i.d.) *	$\alpha$	IF	$R_s$	N (plates/m)	RSD	Ref.
YPLG, Oxytocin	Pure medium	31.2 cm (20) x 100 $\mu\text{m}$	-	4.50 4.01	-	22,995 (YPLG) 16,952 (Oxy)	$t_r$ : 3.16-4.07% (n = 5)	[108]
YPLG, YPGL	Pure medium	31.2 cm (20) x 100 $\mu\text{m}$	-	-	3.72	-	-	[109]
<b>CEC (Chiral + Analog separation)</b>								
( $\pm$ )-Norepinephrine, Dopamine, ( $\pm$ )- Epinephrine, (-)- Isoproterenol, ( $\pm$ ) Octopamine, ( $\pm$ )- Synephrine	Urine (Direct injection)	70 cm (50) x 75 $\mu\text{m}$	-	-	-	30,000- 180,000	$t_r$ : < 3.47% (n = 3)	[120]
R,S-Ornidazole, Metronidazole Secnidazole, Ronidazole, Tinidazole, Dimetridazole	Pure medium	51 cm (30) x 100 $\mu\text{m}$	-	-	0.38 (R/S) >1.21 (Analog)	60,000- 103,000	$t_r$ : < 6.1% ( $n_{C/C} = 3$ )	[106]
D,L-Tyrosine, D,L-Alanine, D,L-Phenylalanine, D,L- Tryptophan, Cbz-D,L- Tyrosine	Pure medium	- (-) x 100 $\mu\text{m}$	1.00- 2.64	-	-	-	$t_r$ : 1.34% (n = 5)	[98]
<b>nanoLC</b>								
Bupivacaine, Mepivacaine, S-Ropivacaine	Pure medium	5 cm x 100 $\mu\text{m}$	-	14-43	-	-	-	[122]
Bupivacaine	Pure medium	4 cm x 320 $\mu\text{m}$	-	2.5	-	-	-	[76]
Horseradish peroxidase	Pure medium	25 cm x 100 $\mu\text{m}$	-	2.76	-	-	k: 0.53% (n = 5) k: 4.07% ( $n_{B/B} = 3$ )	[88]

Target	Medium	Dimensions (L (l) x i.d.) *	$\alpha$	IF	$R_s$	N (plates/m)	RSD	Ref.
Lysozyme	Chicken egg white (Diluted x1000)	25 cm x 75 $\mu\text{m}$	-	1.91	-	-	k: 0.43% ( $n = 5$ ) k: 3.87% ( $n_{B/B} = 5$ )	[89]
D,L-THP	Pure medium	25 cm x 75 $\mu\text{m}$	-	-	-	-	-	[121]

\* L (l) x i.d.: total length (effective length for CEC in cm) x internal diameter.

5-HT: 5-Hydroxytryptophan; Cbz: Carboxybenzyl; EOF: Electroosmotic flow; IF: Imprinting factor; k: Retention factor; N: Efficiency;  $n_{B/B}$ : Batch-to-batch; nc/c: Column-to-column;  $n_{D/D}$ : Day-to-day;  $R_s$ : Resolution; RSD: Relative standard deviation; TB: Tröger's base; THP: Tetrahydropalmatine;  $t_r$ : Retention time; YPGL: Tyrosine-Proline-Glycine-Leucine; YPLG: Tyrosine-Proline-Leucine-Glycine;  $\alpha$ : Selectivity.

#### I.6.4. Monolithic MIPs in extraction

The monolithic approach for selective extraction is the most widely reported one, largely because of its advantages in terms of phase quantity compared to the open tubular, the easier preparation of the extraction set-up compared to packed bed particles that need frits or restriction, and the higher homogeneity of the stationary phase compared to the heterogeneous bulk particle approach that may affect the quality of the coupling of the MIP extraction with the separation method. Two major formats are favored for such applications with miniaturized monoliths, *i.e.* pipette tip that can be considered as a miniaturization of conventional SPE cartridge used off-line and capillaries that can be directly connected to separation methods.

##### I.6.4.1. Pipette tips

The *in situ* synthesis conditions of a monolithic MIP inside a pipette tip are described in **Table 7**. As shown in this table, the organic approach is the most widespread with synthesis conditions not so different from bulk. Indeed, the reagents used are mainly the same, *i.e.* MAA [125–128] and AA [129,130] as monomers and EGDMA [125–130] as cross-linker. Conventional molar ratios of template, monomer, and cross-linker (T/M/C) are used like 1/4/20 [125,127,128]. The most commonly employed porogens are MeOH [126,127,130] and toluene [125,128]. As in the case of monolithic MIPs in capillaries, it is possible to find the addition of small amount of isoctane [126] or dodecanol [125,128]. The synthesis protocol is almost similar to the bulk one, except that the reaction mixture has a small volume such as 10 [131], 40 [128], 60 [125,129], 90 [132], or 100 µL [127,130], which can therefore be contained in a pipette tip. However, the volume of the pipette tip employed is much less mentioned and is reported only as 100 µL [131] or 200 µL [128]. In this case, the MIP does not need to be anchored to the surface of the tip due to its shape and since the extraction protocols are always achieved with a unidirectional flow with relatively low working pressure. However, the synthesis conditions must be such that the resulting monolithic MIP has a sufficient permeability and an immobilization state so that the different solutions (i) can pass through it and (ii) not between the MIP and the pipette wall. To solve these problems, different approaches were described. For example, after its synthesis, the monolithic MIP was pressed by a glass rod to better fix it at the bottom of the tip [132]. The synthesis method was also improved by lifting the polymerization mixture during the polymerization step by an air pressure to avoid the fall of the monolith extremity, particularly brittle, from the pipette tip [129].

Pipette tip format only allows extraction with off-line analysis process, for which the performances are described in **Table 7**. Extraction protocol is simple and no specialized equipment is

required [35]. Typically, 1-10 mL of sample solution are loaded through the monolith while the elution is carried out with only few microliters. The evaporation step can then be suppressed [125,130] and the eluate can be directly injected into non-miniaturized chromatography since its dimension is therefore compatible with the order of magnitude of the eluate volume.

It is possible to apply the pipette tip extraction to various nature of samples, such as organic extracts of solids [127,128,130,131], diluted biological fluids [126,129], directly percolated waters [125], or juice samples after a simple filtration through a 0.45 µm filter [132]. For example, it was used for the determination of berberine in human plasma and urine, after a simple dilution step (factor 2) with an imprinted poly(AA-co-EGDMA) [129]. Recoveries were in the range of 90.6-103.2% with RSD values ( $n = 3$ ) lower than 4.7% and enrichment factors of about 9. Poly(MAA-co-EGDMA)-based MIPs in pipette tips were also developed for the determination of methomyl in various environmental waters with recoveries between 84.9 and 105.1% and RSD ( $n = 3$ ) lower than 9.0% [125] or of vanillin and methyl vanillin in milk powder (ACN extract) [127].

Another work targeted neuropeptides in cerebrospinal fluid by an epitope approach with a poly(MAA-co-EGDMA) imprinted with cholecystokinin-5 [126]. The proposed method was successfully applied for the simultaneous determination of the pentapeptide CCK5 (Gly-Trp-Met-Asp-Phe-NH<sub>2</sub>) and the octapeptide CCK8 (Asp-Tyr-Met-Gly-Trp-Met-Asp-Phe-NH<sub>2</sub>), which share the same sequence of five amino acids at their C-terminus. An enrichment factor of about 20 was calculated. In another example, the simultaneous extraction of six macrolide antibiotics from animal muscles was performed on a roxithromycin imprinted poly(MAA-co-EGDMA) and coupled to a LC-MS/MS analysis [128]. The authors carefully checked that this support provided higher recoveries (78.7-91.3%) than traditional C18 (70.7-82.7%) and HLB cartridges (62.7-82.7%).

Recently, a poly(APTMS-TEOS) imprinted with gallic acid was applied for orange juice samples [132]. This work is characterized by an optimization of the parameters (sample volume, sample flow rate, and pH) affecting the extraction recovery using an experimental design methodology. For their part, Cao *et al.* developed a resin-based monolith imprinted with dopamine hydrochloride for the selective extraction of three plant growth regulators, *i.e.* p-chlorophenoxyacetic acid, 1-naphthaleneacetic acid, and 2,4-dichlorophenoxyacetic acid, in bean sprouts extracts [131]. It is also worthwhile to notice that an organic-inorganic hybrid monolith imprinted with 2,4-dichlorophenoxyacetic acid was successfully applied with spiked rice extracts [130]. When the extraction on the MIP in the pipette tip was combined with an HPLC-DAD analysis, a linear dynamic range from 167 to 4167 µg kg<sup>-1</sup> and recoveries between 80.2 and 94.1% were determined.

All the previous works led to very satisfactory recoveries higher than 80% [125–132] but the main property a MIP must fulfill is selectivity. For this, the imprinted factor defined here as the ratio of the enrichment factor EF for a compound on the MIP and NIP under the same conditions ( $IF_1 = EF_{MIP} / EF_{NIP}$  with  $EF = C_{elu} / C_0$  where  $C_{elu}$  is the analyte concentration in eluent and  $C_0$  the initial concentration of analyte within the sample), and so-called  $IF_1$ , was used in pure medium either for the template [125,126,130] or analog compounds [126,127,130] as visible in **Table 7**. In another cases, another imprinted factor ( $IF_2$ ) was determined by measuring the binding capacity of the MIP and NIP ( $IF_2 = Q_{MIP} / Q_{NIP}$  where  $Q_{MIP}$  and  $Q_{NIP}$  are the adsorption capacity on MIP and NIP, respectively) [128,129,131].

Regarding the reproducibility of the methods developed, it was mainly evaluated by the intra- and inter-day precision obtained on the extraction recoveries [125,127,128,130–132]. However, no data related to the reproducibility of the synthesis of the different devices were reported. Very few articles studied the lifetime of the supports developed. Song *et al.* repeated several adsorption and elution SPE cycles with pork extracts to demonstrate that the MIP could be reused at least 20 times, with only a slight decrease in recovery (loss of less than 5%) [128]. For their part, Li *et al.* observed that the MIP could be reused to extract CCK peptides from cerebrospinal fluid for at least 100 times without significant change in the mean enrichment factor [126]. Nevertheless, the major problem with the MIPs in pipette tips is that they do not allow an on-line coupling with the analytical method, this limitation being solved by using monolith MIPs synthesized in a capillary or on-chip.

**Table 7.** Conditions of synthesis and performances of monolithic MIPs in pipette tips.

Target *	Monomer/CL/Solvent (v:v)	Dimensions ( $V_{\text{Poly}}$ , $V_{\text{Tip}}$ )	$V_p$	Medium	Selectivity (MIP/NIP) **	Recovery	RSD on recovery	Ref.
<u>Berberine</u>	AA/EGDMA/DMSO	60 µL, -	2 mL	Human plasma (Dil. x2), Urine (Dil. x2)	$IF_2 = 2.41$	90.6-103.2%	1.9-4.7% (n = 3)	[129]
<u>CCK5, CCK8</u>	MAA/EGDMA/MeOH:Isooctane (95.5:4.5)	-	2 mL	Human CSF (Chloroform extract)	$IF_1 = 4.2-4.5$	87.6-90.2%	3.2-3.9% (n = 3)	[126]
2,4-D, NAA, PCPA (Dopamine hydrochloride)	Melamine-urea-formaldehyde monolithic resin/MeOH	10 µL, 100 µL	1 mL	Bean sprouts (Lead acetate solution extract)	$IF_2 \approx 1.5$	89.8-98.8%	1.3-5.2% (n = 3) 4.0-6.4% ( $n_{D/D} = 3$ )	[131]
<u>2,4-D</u>	((AA/EGDMA)/(MTMS-γ-MAPS) (3/1, v/v))/MeOH	100 µL, -	3 mL	Rice (ACN extract)	$IF_1 = 3.29$	80.2-94.1%	5.1-7.9% (n = 5) 6.3-8.6% ( $n_{D/D} = 5$ )	[130]
<u>Gallic acid</u>	APTMS/TEOS/H <sub>2</sub> O:MeOH (24:76)	90 µL, -	6 mL	Orange juice	Extraction recovery ratio ≈ 3.3-6.1	92.0-100.5%	1.0-3.8% (n = 3) 1.6-4.5% ( $n_{D/D} = 5$ )	[132]
<u>Methomyl</u>	MAA/EGDMA/Toluene: Dodecanol (10:90)	60 µL, -	3 mL	Reservoir water, South Lake water, Farmland water, Waste water	$IF_1 = 2.26$	84.9-105.1%	3.0-9.0% (n = 3) 4.1% ( $n_{D/D} = 3$ )	[125]
Methyl vanillin, Vanillin (Nonylphenol)	MAA/EGDMA/MeOH	100 µL, -	3 mL	Infant milk powder (ACN extract)	$IF_1 = 2.04-3.56$	80-110%	0.04-3.55% (n = 3) < 3.62% ( $n_{D/D} = 4$ )	[127]
<u>Roxithromycin, Azithromycin, Clarithromycin, Erythromycin, Spiramycin, Tilmicosin, Tulathromycin</u>	MAA/EGDMA/Toluene: Dodecanol (1/6)	40 µL, 200 µL	5 mL	Chicken, Pork, Beef (ACN extract)	$IF_2 = 1.6-2.8$	76.1-92.8%	0.7-8.3% (n = 6) 1.1-10.4% ( $n_{D/D} = 18$ )	[128]

\* Template indicated in bracket when different from target or underlined for a mixture of targets.

\*\* Results obtained in pure medium.

$IF_1 = EF_{MIP} / EF_{NIP}$  with  $EF = C_{elu} / C_0$  where  $C_{elu}$  is the analyte concentration in eluent and  $C_0$  the initial concentration of analyte within the sample.

$IF_2 = Q_{MIP} / Q_{NIP}$  where  $Q_{MIP}$  and  $Q_{NIP}$  are the adsorption capacity on MIP and NIP, respectively.

2.4-D: 2,4-Dichlorophenoxyacetic acid; APTMS: 3-Aminopropyltriethoxysilane; CCK5: Pentapeptide cholecystokinin; CCK8: Octapeptide cholecystokinin; CSF: Cerebrospinal fluid; IF: Imprinting factor; MTMS: Methyltrimethoxysilane;  $n_{D/D}$ : Day-to-day; NAA: 1-Naphthaleneacetic acid; PCPA: p-Chlorophenoxyacetic acid; RSD: Relative standard deviation; TEOS: Tetraethyl orthosilicate;  $V_p$ : Volume of percolation;  $V_{Poly}$ : Volume of the polymerization mixture;  $V_{Tip}$ : Volume of the tip;  $\gamma$ -MAPS: 3-(Trimethoxysilyl)propyl methacrylate.

#### **I.6.4.2. Capillaries**

Miniaturized monolithic MIPs synthesized in capillaries were used for extraction of various targets such as drugs [90–93,117], biomarkers [39,45,46], proteins [88,89], dyes [99,101,104], fungicides [119], or toxins [47,49] in different complex matrices including urine [39,45,46], saliva [90], food [47,92,93,99,101,104,117,119], plant [91], or serum [88–90]. These studies are summarized in **Table 8**. Most of them deal with sample extracts diluted in solvents similar to the porogen used for the synthesis and thus adapted to develop the appropriate interactions between the target compound and the cavities. In this case, the target compounds are already concentrated in the extracts. This is why the essential property that is expected for MIP is the ability to purify the extract rather than to concentrate it. It is therefore essential that the MIP be selective. This can be confirmed as previously by studying the behavior of the target analyte(s) in parallel on the NIP ensuring that the study is carried out with the same sample and under the same conditions as those used for the MIP, the ratio of retention factors  $k$  between both sorbents allowing to calculate the IF [49,90,91,93]. Values between 2.2 and 3.4 were reported.

As shown in **Table 8**, most of the published works reported monolithic MIPs synthesized in 3.5–10 cm length and 500  $\mu\text{m}$  i.d. capillaries that were off-line used [39,47,93,101,104,117,119]. The percolated volumes ranged from 1 to 5 mL and are therefore similar to the volume percolated on SPE cartridges. The elution fraction recovered from the MIP after the extraction procedure was next injected mainly in conventional LC, *i.e.* on separation columns with an i.d. of 4.6 mm, or in CE. For example, Zheng *et al.* developed a monolith imprinted with pefloxacin for the selective extraction of four fluoroquinolones from milk samples [93]. In pure medium, an IF of 3.1 was determined by LC measurements for the template and, by comparing the adsorption capacity on MIP and NIP for different concentrations of the compounds in the loading solution, binding capacity of 36 and 23.5  $\mu\text{mol g}^{-1}$  were obtained, respectively. The selectivity was demonstrated by calculating the ratio of extraction recoveries between MIP and NIP for pefloxacin and the four other fluoroquinolones and values between 1.7 and 3.6 were obtained in pure medium. To highlight the performance of the monolithic MIP, extractions with a spiked milk sample on the miniaturized monolithic MIP and a C18 sorbent in a SPE cartridge were compared. While no interference was observed after the extraction on the MIP, several interfering peaks were observed after extraction on C18 due to non-specific interactions. However, the two protocols were not fully comparable, largely because of the diverging formats used.

A monolithic MIP in a capillary was used for the selective extraction of safranin T in wolfberry further analyzed by LC-LIF [101]. The capacity of the MIP and NIP monoliths were measured by breakthrough volume in pure medium as  $0.066$  and  $0.006 \mu\text{g mg}^{-1}$ , respectively. Moreover, a recovery of 80.7% was obtained on the MIP compared to 23.4% on the NIP in pure medium. An enrichment factor higher than 90 was calculated with a wolfberry sample by comparing chromatograms obtained before and after its extraction on MIP. In another example, Liang *et al.* extracted aflatoxin B<sub>1</sub> from peanut samples using carbon quantum dots coated with a dummy imprinted monolith and then analyzed by LC-FLD (fluorescence detection) [47]. The selectivity was demonstrated by plotting breakthrough curves based on injection volume and concentration leading to a capacity of  $0.442 \text{ ng mg}^{-1}$  for the MIP and  $0.0917 \text{ ng mg}^{-1}$  for the NIP. An enrichment factor of 71 led to a high sensitivity with a LOQ of  $0.393 \text{ ng mL}^{-1}$  in spiked peanut extracts.

Other works used monolithic MIPs with similar dimensions to the previous ones but with an off-line CE separation, allowing to achieve both extraction and separation steps at miniaturized scale [46,99]. A monolith imprinted with rose bengal was applied for its extraction in brown sugar prior to its analysis in CE-LIF [99]. According to the breakthrough curves, capacities of  $1.314 \mu\text{g mg}^{-1}$  and  $0.531 \mu\text{g mg}^{-1}$  were calculated in pure medium for MIP and NIP, respectively. A monolithic MIP was also developed for the extraction of urinary 8-Hydroxy-2'-deoxyguanosine, a biomarker of oxidative DNA damage, before an analysis by CE and electrochemical detection [46]. This method gave an enrichment factor of 73 and 41 in pure medium on MIP and NIP, respectively.

Monolithic MIPs synthesized in capillaries with smaller i.d. were also applied for extraction of biological macromolecules and off-line SDS-PAGE analyses [88,89]. A monolithic MIP was imprinted with horseradish peroxidase (45 kDa) in a capillary with an i.d. of  $100 \mu\text{m}$  and allowed to isolate it from spiked human sera diluted 500 times [88]. In pure medium, an IF of 2.76 was determined. Even if no data on NIP were available, the SDS-PAGE analysis revealed that the eluate fraction was purified from impurities such as human serum albumin, human transferring or immunoglobulin G. Another support using a one-pot method was also developed in a  $75 \mu\text{m}$  i.d. capillary to extract lysozyme (14.4 kDa) from spiked human sera diluted 500 times and the same purification result was observed after SDS-PAGE analysis [89].

As indicated in **Table 8**, another significant part of the studies focused on the on-line coupling of the extraction and separation steps. Although in most cases the i.d. of the LC separation columns was still conventional ( $4.6$  [45,91,92] or  $2.1 \text{ mm}$  [94]), the general trend is towards a reduction of the i.d. of the capillary containing the monolithic MIP compared with the ones used for off-line applications, with values between  $250$  and  $500 \mu\text{m}$  with capillary lengths between  $10$  and  $25 \text{ cm}$ . Zhang

*et al.* achieved trace analysis of antimicrobials (sulfaquinoxaline, sulfamethoxazole, mequindox, and quinocetone) in chicken, pork, and egg samples with a monolithic MIP imprinted with sulfaquinoxaline and coupled on-line to LC-UV [92]. The selectivity was demonstrated by a ratio of extraction recoveries on MIP and NIP between 1.8 and 4.3 for the five studied compounds contained in pure medium. Other on-line couplings of monolithic MIP with LC-UV were conducted, whether for the determination of urinary 8-Hydroxy-2'-deoxyguanosine [45] or of baicalin in *Scutellaria baicalensis* extracts, for which IF of 2.2 was determined by LC measurements in pure medium [91]. Finally, Marchioni *et al.* implemented a monolithic MIP imprinted with hydrogenated cannabidiol coupled on-line with LC-MS/MS to determine cannabinoids in plasma samples [94]. Adsorption experiments demonstrated the MIP selectivity with capacities 5 and 2.5 times higher on MIP than on NIP for cannabidiol and Δ9-tetrahydrocannabinol, respectively.

Szumski *et al.* were the first to propose an on-line device homogenizing the miniaturized dimensions of the extraction and separation steps [49]. They described the hyphenation of an extraction with a miniaturized monolithic MIP in a 100 μm i.d. capillary coupled on-line with nanoLC separation on a 180 μm i.d. capillary and LIF detection for the analysis of four aflatoxins (B<sub>1</sub>, B<sub>2</sub>, G<sub>1</sub>, and G<sub>2</sub>). The originality of this device resides in the fact that each step of the analytical protocol, *i.e.* extraction or separation, is connected with the detection. With the injection of 5 μL of a model solution of four aflatoxins, the signal of the analytes was detected during the extraction step on the NIP, while the majority of these analytes were observed after the separation step when the MIP was used. The comparison of both MIP and NIP supports highlighted the selective contribution of the MIP with IF values of 3.37 for the template 5,7-Dimethoxycoumarin (DMC) and 2.44 for aflatoxin B<sub>1</sub> in pure medium and obtained by LC measurements.

Recently, a work was conducted on a monolithic MIP imprinted with cocaine in a 100 μm i.d. capillary and coupled on-line to a 75 μm i.d. nanoLC column (**Figure 5**) [90]. The selectivity of the MIP was first demonstrated by obtaining IF values of  $3.2 \pm 0.5$  and  $2.2 \pm 0.3$  ( $n = 3$ ) for cocaine and its main metabolite (benzoylecgonine), respectively, in pure medium and by LC measurements. The nature and volume of the washing solution were carefully optimized in pure medium and then the determination of cocaine in biological fluids, *i.e.* plasma and saliva, was performed. **Figure 5** presents the chromatograms obtained using MIP and saliva or plasma samples with and without spiking. They can be compared to the ones obtained with the NIP and the same spiked saliva and plasma samples. The very low NIP retention confirms IF values measured in pure media. The very clean-baseline obtained using the MIP allows the easy determination of the cocaine with UV detection with a LOQ of 6.1 and

$14.5 \text{ ng mL}^{-1}$  while injecting only  $100 \text{ nL}$  of saliva or 2 times diluted plasma, respectively. Such small volumes illustrate the excellent sensitivity of the miniaturized analytical system.

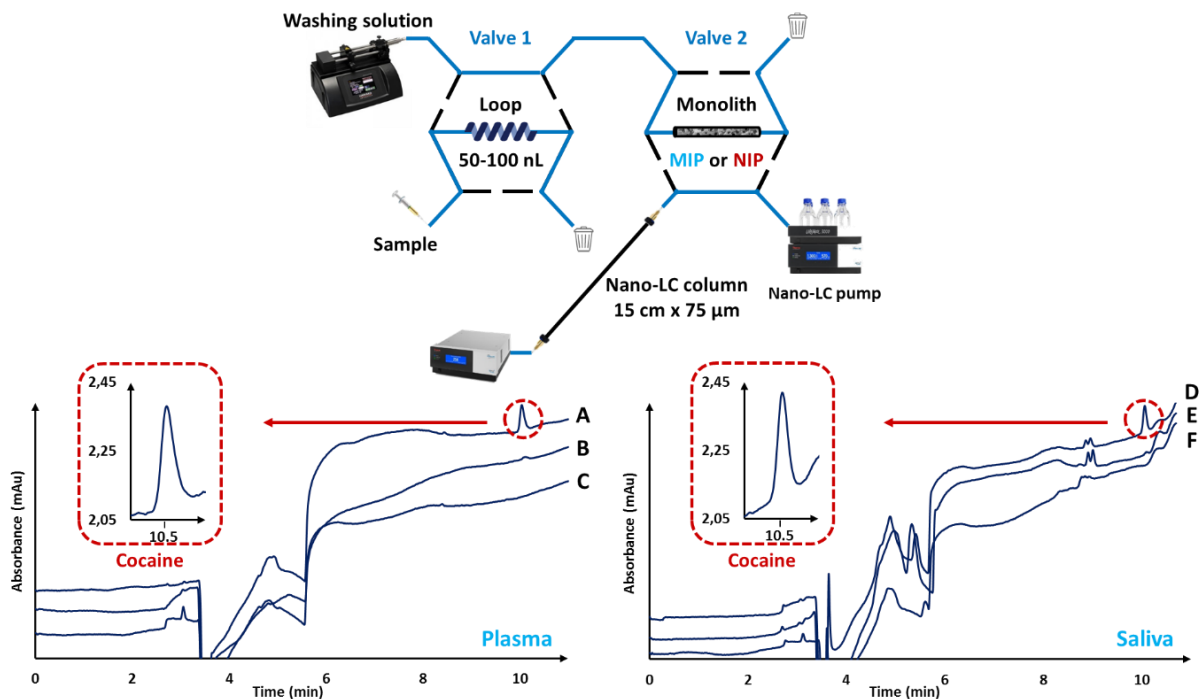


**Figure 5.** Set-up of the on-line coupling of the monolithic MIP/NIP ( $50 \text{ mm} \times 100 \mu\text{m}$  i.d.) with nanoLC-UV (Top). Chromatograms (Left) obtained after the extraction on MIP (A) and NIP (B) of  $50 \text{ nL}$  of plasma spiked with cocaine (equivalent to  $100 \text{ ng mL}^{-1}$  in plasma) compared to the blank plasma (C) on MIP and chromatograms (Right) obtained after the extraction on MIP (D) and NIP (E) of  $50 \text{ nL}$  of saliva spiked with  $50 \text{ ng mL}^{-1}$  of cocaine compared to the blank plasma (F) on MIP. Adapted from [90].

Finally, Wen *et al.* achieved a new step in miniaturization by developing an imprinted monolith for the selective capture of myoglobin directly coupled with UV detection and thus without using a separation step [124]. The binding capacities were monitored using a continuous pumping of a myoglobin solution ( $20 \text{ mg mL}^{-1}$ ) and were equal to  $1,641$  and  $705 \text{ mg g}^{-1}$  for the MIP and NIP, respectively. The MIP was able to selectively capture and release myoglobin from  $1 \mu\text{L}$  of a protein mixture in water containing myoglobin ( $1 \text{ mg mL}^{-1}$ ), lysozyme ( $0.5 \text{ mg mL}^{-1}$ ), and bovine serum albumin ( $0.5 \text{ mg mL}^{-1}$ ). The retention behavior of the MIP was controlled by temperature, which induces a change in solvation, due to the temperature-responsive properties of the poly(N-isopropylacrylamide) constituting the MIP. However, there is no quantitative data on the extraction recoveries and no applications with real samples.

The study of the repeatability of the MIP syntheses and analytical methods is very often omitted by the authors. When it was the case, most of the publications implemented the intra- and inter-day study on recoveries [45,47,93,99,101,117,119]. The reproducibility of the synthesis was rarely reported and consisted in comparing the results of the recoveries obtained in pure medium with MIPs from different batches and without giving any data for the NIPs [39,91–93]. Only two publications investigated the repeatability by comparing recoveries obtained with plasma samples and independently synthesized MIPs in capillaries [90,94]. The first one measured the permeability and IFs for independently synthesized MIPs with RSD ( $n = 3$ ) of 3-17% [90], and the second one measured the adsorption capacities for independently synthesized MIPs and NIPs with RSDs ( $n = 3$ ) of 2.3-5.0% [47]. At last, in order to reduce the analytical cost, the reusability of some MIPs was evaluated showing the possibility to use them at least 15 [47], 20 [119], 50 [39,93,94], or 100 times [92] with no significant changes in column backpressure and extraction efficiency, although these studies were conducted in pure medium.

**Table 8.** Performances of monolithic MIPs prepared in capillaries, used as extraction sorbent, and ordered by the successive separation methods.

Target	Medium	Dimensions (L x i.d.)	V <sub>P</sub>	Selectivity (MIP/NIP)	EF	Recovery	RSD on recovery	Ref.
<b>LC – off-line mode</b>								
Auramine O	Shrimp (MeOH extract)	10 cm x 500 µm	1.5 mL	Binding capacity: 0.722 / 0.147 µg mg <sup>-1</sup> *	73	90.5-92.4%	2.1-4.4% (n = 3)	[104]
Bisphenol A, Nonyl phenol	Fish (MeOH extract)	4 cm x 500 µm	8 mL	Binding capacity: 0.391 / 0.143 µg mg <sup>-1</sup> *	92-113	82-92%	2.2-4.2% (n = 5) 3.8-4.1% (n <sub>C/C</sub> = 3)	[52]
Aflatoxin B <sub>1</sub>	Peanut (MeOH/H <sub>2</sub> O extract, 80/20)	10 cm x 500 µm	5 mL	Binding capacity: 0.442 / 0.0917 ng mg <sup>-1</sup> *	71	79.5-91.2%	1.9-4.9% (n = 6) 1.2-3.8 (n <sub>D/D</sub> = 3)	[47]
Flumequine	Fish (ACN/ Acetic acid extract, 90/10)	10 cm x 500 µm	2.5 mL	Binding capacity: 61.74 / 8.00 ng mg <sup>-1</sup> *	40	80.6-95.2%	4.3-5.9% (n = 3) 3.8-5.4% (n <sub>D/D</sub> = 3)	[117]
Guanosine, 8-OHdG	Urine (ACN extract)	4.8 cm x 530 µm	1 mL	-	76-100 *	81-86%	< 3% (n = 3) 3.9% (n <sub>B/B</sub> = 5)	[39]
Ciprofloxacin, Difloxacin, Danofloxacin, Enrofloxacin	Milk (Dil. x10)	8 cm x 530 µm	1 mL	IF = 3.1 Binding capacity: 36.0 / 23.5 µmol g <sup>-1</sup> *	-	92-98%	1.8-4.8% (n = 5) 2.4-5.5% (n <sub>B/B</sub> = 4) * 1.9-5.9% (n <sub>D/D</sub> = 3)	[93]
Rhodamine B	Chili powder (H <sub>2</sub> O extract)	3.5 cm x 500 µm	8 mL	Binding capacity: 1.994 / 0.282 µg mg <sup>-1</sup> *	110	83-88%	3.2-4.0% (n = 3) 2.5-3.1% (n <sub>D/D</sub> = 6)	[118]
Safranin T	Wolfberry (MeOH extract)	10 cm x 500 µm	4 mL	Binding capacity: 66 / 6 ng mg <sup>-1</sup> *	> 90	91-93%	3.5-4.2% (n = 3) 3.4-3.9% (n <sub>D/D</sub> = 6) 3.4% (n <sub>C/C</sub> = 3)	[101]
Carbendazim, Thiabendazole Fuberidazole	Citrus (ACN extract)	8 cm x 500 µm	4 mL	Binding capacity: 58.01 / 10 ng mg <sup>-1</sup> *	9.4-23	84.9-98.4%	1.9-7.1% (n = 3) 2.5-8.1% (n <sub>D/D</sub> = 3)	[119]

Target	Medium	Dimensions (L x i.d.)	V <sub>P</sub>	Selectivity (MIP/NIP)	EF	Recovery	RSD on recovery	Ref.
<b>CE – off-line mode</b>								
8-OHdG	Urine (ACN extract)	4.8 cm x 530 µm	1 mL	-	73 (MIP) * 41 (NIP) *	85.4%	4.7% (n = 6)	[46]
Rose bengal	Brown sugar (MeOH extract)	10 cm x 500 µm	2 mL	Binding capacity: 1.314 / 0.531 µg mg <sup>-1</sup> *	64	90%	3.8-4.5% (n = 3) 3.6-4.0% (n <sub>D/D</sub> = 6)	[99]
<b>SDS-PAGE – off-line mode</b>								
Horseradish peroxidase	Human serum (Dil. x500)	25 cm x 100 µm	75 µL	Binding capacity: 4.56 / 1.65 µg mg <sup>-1</sup> *	-	-	-	[88]
Lysozyme	Human serum (Dil. x500)	25 cm x 75 µm	40 µL	Binding capacity: 3.864 / 2.015 µg mg <sup>-1</sup> *	-	-	-	[89]
<b>LC – on-line mode</b>								
Aflatoxins (B <sub>1</sub> , B <sub>2</sub> , G <sub>1</sub> , G <sub>2</sub> )	Pure medium	17 cm x 100 µm	5 µL	IF = 2.44-3.37	-	-	-	[49]
Baicalin	<i>Scutellaria baicalensis</i> (ACN/DMSO extract, 90/10)	25 cm x 250 µm	500 µL	IF = 2.2	-	-	-	[91]
Cannabidiol, Δ9-THC	Human plasma (Concentrated x6)	10 cm x 530 µm	10 µL	Binding capacity: 148.05 ng cm <sup>3</sup> / ≈ 5 times less *	-	-	1.0-13.08% (n = 3) 8.6-11.4% (n <sub>B/B</sub> = 3)	[94]
Cocaine	Human serum (Diluted x2) Saliva (Direct injection)	5 cm x 100 µm	50 -100 nL	IF = 3.2 ± 0.5 *	-	88.6-100.4%	1.2-11.1% (n = 3) 3.8-5.8% (n <sub>B/B</sub> = 3)	[90]
Myoglobin	Pure medium	- x 100 µm	1 µL	Binding capacity: 1641 / 705 µg mg <sup>-1</sup> *	-	-	-	[124]
8-OHdG	Urine (ACN extract)	14.5 cm x 250 µm	1 mL	-	102 *	81-84%	< 7.4% (n = 3) < 4.7% (n <sub>D/D</sub> = 4) *	[45]

Target	Medium	Dimensions (L x i.d.)	V <sub>P</sub>	Selectivity (MIP/NIP)	EF	Recovery	RSD on recovery	Ref.
SQX, SMZ, SMD, Mequindox, Quinocetone	Chicken, Pork, Egg (ACN/Toluene/n-Hexane extract)	12 cm x 320 µm		Extraction selectivity: 1.8-4.3 *	46-211 *	70-108%	1.9-8.5% (n = 3) 3.6-7.5% (n <sub>B/B</sub> = 3) *	[92]
<b>CE – on-line mode</b>								
Auramine O	Shrimp (MeOH extract)	2.7 cm x 500 µm	440 µL	Binding capacity: 0.722 / 0.147 µg mg <sup>-1</sup> *	12	90-93%	2.6-4.7% (n = 3)	[100]

\* Results obtained in pure medium.

$$IF = k_{MIP} / k_{NIP} \text{ with } k = (t_r - t_0) / t_0$$

8-OHdG: 8-Hydroxy-2'-deoxyguanosine; EF: Enrichment factor; IF: Imprinting factor; n<sub>B/B</sub>: Batch-to-batch; n<sub>C/C</sub>: Column-to-column; n<sub>D/D</sub>: Day-to-day; RSD: Relative standard deviation; SMD: Sulfametoxydiazine; SMZ: Sulfamethoxazole; SQX: Sulfaquinoxaline; V<sub>P</sub>: Volume of percolation; Δ9-THC: Δ9-tetrahydrocannabinol.

#### **I.6.4.3. Chip microchannels**

To date, as for their application in separation, only attempts to integrate monolithic MIPs by hybrid approaches, *i.e.* by introducing a capillary containing a MIP in a chip, were described in the literature [52,100,118]. For extraction purposes, broad capillaries of 500 µm i.d. were used to selectively extract compounds from large samples of 8 mL in off-line mode [52,118]. This group developed a microfluidic hybrid device integrating eight MIPs in parallel (4 cm x 500 µm i.d.) for the simultaneous determination of bisphenol A and nonyl phenol in spiked fish sample extracts [52]. IFs of bisphenol A and nonyl phenol were 2.6 and 2.9, respectively. Enrichment factors of 113 and 92 and LODs of 2.4 and 4.7 ng L<sup>-1</sup> were obtained for bisphenol A and nonyl phenol, respectively, for spiked fish sample extracts. Finally, RSD on recoveries between 3.8 and 4.1% were obtained for three chips and each MIP or chip could be reused at least 15 times. Unfortunately, the analyses of the purified extracts were next achieved off-chip by LC-FLD. Similarly, a SPE microfluidic glass/PDMS chip containing four monolithic MIPs in parallel (3.5 cm x 500 µm i.d.) that were synthesized with silanized graphene oxide was developed for the extraction of rhodamine B from chili powder [118]. The selectivity of the MIP within the chip was demonstrated with an IF of 7.07. The enrichment factor of the SPE procedure was equal to 110 in spiked chili powder sample extracts. Finally, the authors claimed that the hybrid chip can be reused 30 times without loss of performance and an RSD ( $n = 3$ ) of 3.4% was obtained for the recoveries from chip-to-chip. Again, the eluted fractions were analyzed off-chip by LC-FLD.

This group also proposed to combine this hybrid approach with a CE analysis on-chip for the determination of auramine O in spiked shrimp extracts [100]. For this, a capillary (2.7 cm x 500 µm i.d.) containing a monolithic MIP was introduced into a glass/PDMS device and coupled to a separation microchannel of 75 µm deep and 100 µm wide for on-line SPE-CE procedure and conductivity detection. The wide difference in capacities of MIP and NIP (0.722 and 0.147 µg mg<sup>-1</sup>, respectively) revealed the selective contribution of the MIP. A LOD of 2.5 µg mL<sup>-1</sup> was obtained in shrimp extracts and an enrichment factor of 12 was determined for an injection of 440 µL of a standard solution, but these results were given for off-line mode and unfortunately not for the on-line one. In addition, the concentration of the spiked extracts was of 5 µg mL<sup>-1</sup>, which is already high.

Therefore, many efforts remain to be made for the development of chips integrating MIP extraction, separation, and detection steps with an on-line mode, as it was the original purpose of the concept of µ-TAS. If the MIP selectivity is really high, one could even consider removing the separation step and thus simplify the chip device by only integrating the detection device.

## I.7. Conclusion

The current analytical chemistry literature is rich in works on miniaturized devices to meet the societal demand for reliable, fast, inexpensive, and low solvent/sample consuming analyses. All the steps of the analysis must be redesigned and the development of miniaturized selective sorbents such as MIPs is therefore essential for both extraction and separation applications. Various methods allowing the miniaturization of MIPs were referenced such as open tubular, packed particles, magnetic nanoparticles, and of course *in situ* synthesis of imprinted monoliths, which in the light of the diversity of applications proposed in this review seems to be the most complete approach.

Throughout the review, we highlighted the diversity of approaches leading to the preparation of monolithic MIP in capillaries or in chip microchannels with different combinations of templates, monomers, cross-linkers, and porogen solvents. The targets are of various natures and range from small molecules to glycoproteins. These devices have demonstrated great potential for separation and extraction applications. For the latter area, a significant progress has been made by the authors by having carried out applications with real samples such as biological, environmental, and food ones, although it appears that development in pure medium still concerns the majority of publications. However, the main aspect to be improved is the description of the repeatability of the syntheses and the lifetime of the systems, particularly when applying real samples, which are characteristics that have been insufficiently studied.

Further developments of *in situ* MIPs synthesized in capillaries can undoubtedly be expected. This approach is particularly interesting in view of the development of coupling integrating all the stages of analysis and tending towards lab-on-chip type systems. In the context of these developments, the high selectivity generated by the MIP is an obvious advantage. It allows a lower resolution requirement of the separation systems, whose length can be greatly reduced, and even allows to move towards systems where the MIP used as a support for selective concentration or retention will require just downstream the integration of a detection step.



---

## **PARTIE EXPERIMENTALE**

---



## **CHAPITRE II**

**Monolithes à empreintes moléculaires couplés à la nano-chromatographie en phase liquide pour l'extraction sélective de la cocaïne**



## CHAPITRE II – Monolithes à empreintes moléculaires couplés à la nano-chromatographie en phase liquide pour l'extraction sélective de la cocaïne

Dans le chapitre précédent, différentes approches de miniaturisation des MIP ont été décrites afin de pouvoir les utiliser dans le domaine soit de l'extraction soit de la séparation. Comme mentionné dans la revue, peu d'études portent sur la synthèse de monolithes imprimés à des fins d'extraction sélective couplée à une méthode de séparation elle aussi miniaturisée. Ce nombre est d'autant plus réduit pour les applications avec des échantillons réels. Par conséquent, nous nous sommes intéressés à la synthèse d'un MIP monolithique dans un capillaire pour extraire des composés avant leur analyse en ligne en nanoLC.

Pour mener à bien ce projet, il a fallu dans un premier temps sélectionner des molécules modèles. En raison des nombreux travaux précédemment menés dans le laboratoire [133,134], la cocaïne et son métabolite principal, la benzoylecgonine (BZE), dont les structures sont présentées **Figure 6**, ont été choisies. De plus, la miniaturisation des outils d'analyse pour ces deux molécules se justifie parfaitement en raison de leurs coûts et de la réglementation qui encadre leur utilisation à des fins de recherche.

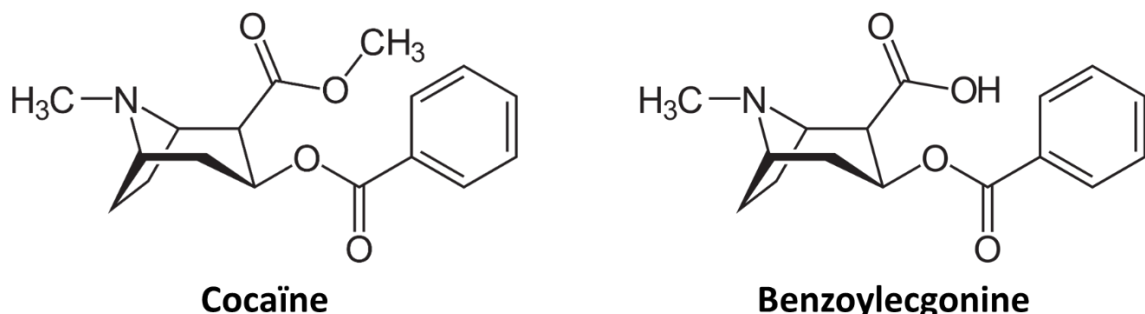


**Figure 6.** Structure chimique de la cocaïne et de la benzoylecgonine.

### II.1. Présentation des molécules d'intérêt

La cocaïne est un alcaloïde tropanique d'origine végétale résultant de l'extraction des feuilles du cocaïer, *Erythroxylum coca*, arbuste cultivé du côté Est de la cordillère des Andes au Pérou, en Bolivie et en Colombie. Il s'agit d'un psychotrope avec un fort pouvoir stimulant sur le système nerveux

central mais également un vasoconstricteur périphérique. Sa consommation est addictive et elle est classée comme stupéfiant par la convention unique sur les stupéfiants de l'Organisation des Nations Unis depuis 1961 [135]. Le rapport mondial sur les drogues de l'Office des Nations Unies contre la drogue et le crime estime qu'en 2018, la production mondiale a atteint une quantité d'environ 1 723 tonnes de cocaïne à un niveau de pureté de 100% [136]. La superficie totale consacrée à la culture du cocaïer s'élevait à 244 200 hectares, soit 342 017 terrains de football et il existerait 19 millions de consommateurs de cocaïne dans le monde.

### II.1.1. La cocaïne et sa toxicité

La cocaïne présente une toxicité profonde pour le système nerveux central et cardiovasculaire. En effet, elle stimule la libération de neurotransmetteurs, comme la dopamine et la sérotonine, dans la fente synaptique générant ainsi une réponse physiologique par l'activation des neurones postsynaptiques (**Figure 7 A et B**). En temps normal, cette réponse est régulée par la réabsorption des neurotransmetteurs par les neurones présynaptiques (**Figure 7 C**). Cependant, la cocaïne bloque cette recapture de dopamine et de sérotonine (**Figure 7 D**), ce qui empêche la régulation et induit l'accumulation de neurotransmetteurs, se traduisant par une stimulation [137].

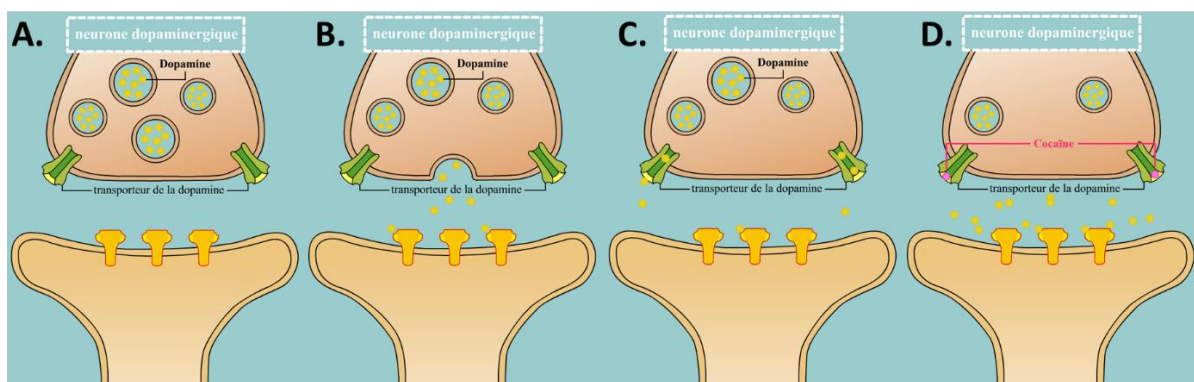


**Figure 7.** Mécanisme d'action de la cocaïne sur le système nerveux. Adapté de [138].

L'excès de sérotonine pourrait être lié à l'addiction à la cocaïne et à son effet de récompense. Par contre, c'est l'excès de dopamine qui semble être à l'origine de la majorité des symptômes du système nerveux central. Cela se traduit à faibles doses par une euphorie, une assurance accrue et une forte vivacité mais aussi par une agressivité, une désorientation, des insomnies et des hallucinations pour des doses plus élevées [139]. D'autre part, la cocaïne possède des propriétés de vasoconstricteur

et de bloqueur des canaux sodiques. Elle provoque donc à court terme des effets tels que l'augmentation du rythme cardiaque et de la fréquence respiratoire, et à long terme, la cocaïne peut entraîner des arythmies ventriculaires, des accidents vasculaires cérébraux, des infarctus et d'autres complications cardiovasculaires.

En France, la cocaïne de rue commercialisée illicitement présentait une pureté moyenne de 60% en 2018, d'après l'Institut national de la police scientifique [140]. Elle contient donc pour 40% un certain nombre de contaminants pouvant être des sous-produits de fabrication, des adultérants ou des diluants ajoutés intentionnellement, des alcaloïdes naturels et des produits résultant de la dégradation chimique de la cocaïne pouvant aggraver son effet toxique [141]. Certains, comme le sucre, le talc ou la féculle de maïs, permettent d'augmenter le volume de drogue disponible à moindre coût, mais peuvent provoquer des irritations des voies nasales, des fibroses pulmonaires ou des hypertensionns. Les adultérants sont également ajoutés à la cocaïne pour accroître la puissance de son effet ou diminuer ses effets secondaires [142]. Dans cette catégorie, on trouve souvent des anesthésiants locaux tels que la benzocaïne, la lidocaïne, la procaïne ou encore le lévamisol détecté dans 74% des saisies en France [140] et responsable de paresthésies et tremblements. Finalement, l'abus d'alcool en parallèle à la consommation de cocaïne génère du cocaéthylène ayant les mêmes effets que la cocaïne sur la pression sanguine, le rythme cardiaque et l'euphorie, mais avec une durée plus longue à laquelle il faut ajouter les effets supplémentaires de l'alcool. Par conséquent, le taux de mortalité des individus consommant simultanément les deux substances est plus élevé.

### **II.1.2. Pharmacocinétique et métabolisme de la cocaïne dans le corps humain**

Dans le corps humain, la cocaïne est rapidement métabolisée par des voies enzymatiques et non enzymatiques (**Figure 8**). Sa durée de demi-vie varie entre 0,5 et 1,5 h, mais peut aller parfois jusqu'à 4 h en fonction des habitudes de consommation, avec un allongement de cette période chez les utilisateurs chroniques [143]. Pour des doses habituelles de cocaïne, sa présence dans le sang est détectable pendant seulement 1 à 12 h [144]. Moins de 10% de la cocaïne sous sa forme originale est éliminée dans les urines, milieu dans lequel elle peut être détectée jusqu'à 5 h après la prise [145]. La pharmacocinétique de la cocaïne dépend de divers facteurs comme sa forme chimique, le mode de consommation, la génétique et la consommation simultanée d'alcool. On distingue deux voies métaboliques principales que sont l'hydrolyse, ayant lieu dans le sang et les tissus, et l'oxydation qui se produit principalement au niveau du foie.

Au pH physiologique ou basique, la cocaïne est soumise à une hydrolyse chimique spontanée de la fonction méthylester conduisant à la formation de la BZE. Ce métabolite peut également être obtenu par hydrolyse enzymatique faisant intervenir des carboxylestérases hépatiques de type 1 [146]. La BZE est un métabolite inactif n'ayant donc pas d'effet sur le système nerveux central mais il est toutefois important de noter ses propriétés de vasoconstricteur [139]. La BZE est le métabolite majoritaire détecté dans les urines et dans le sang et pour lequel les durées de détection sont, respectivement, de 48 à 96 h et de 12 à 24 h [144]. Sa durée de demi-vie d'élimination plasmatique est comprise entre 4 et 7 h [143]. Elle est excrétée dans les urines et représente entre 35 et 54% de la dose de cocaïne initiale [147]. Compte tenu de sa longue persistance dans l'organisme et de sa forte concentration, la BZE est utilisée comme marqueur principal d'une prise de cocaïne.

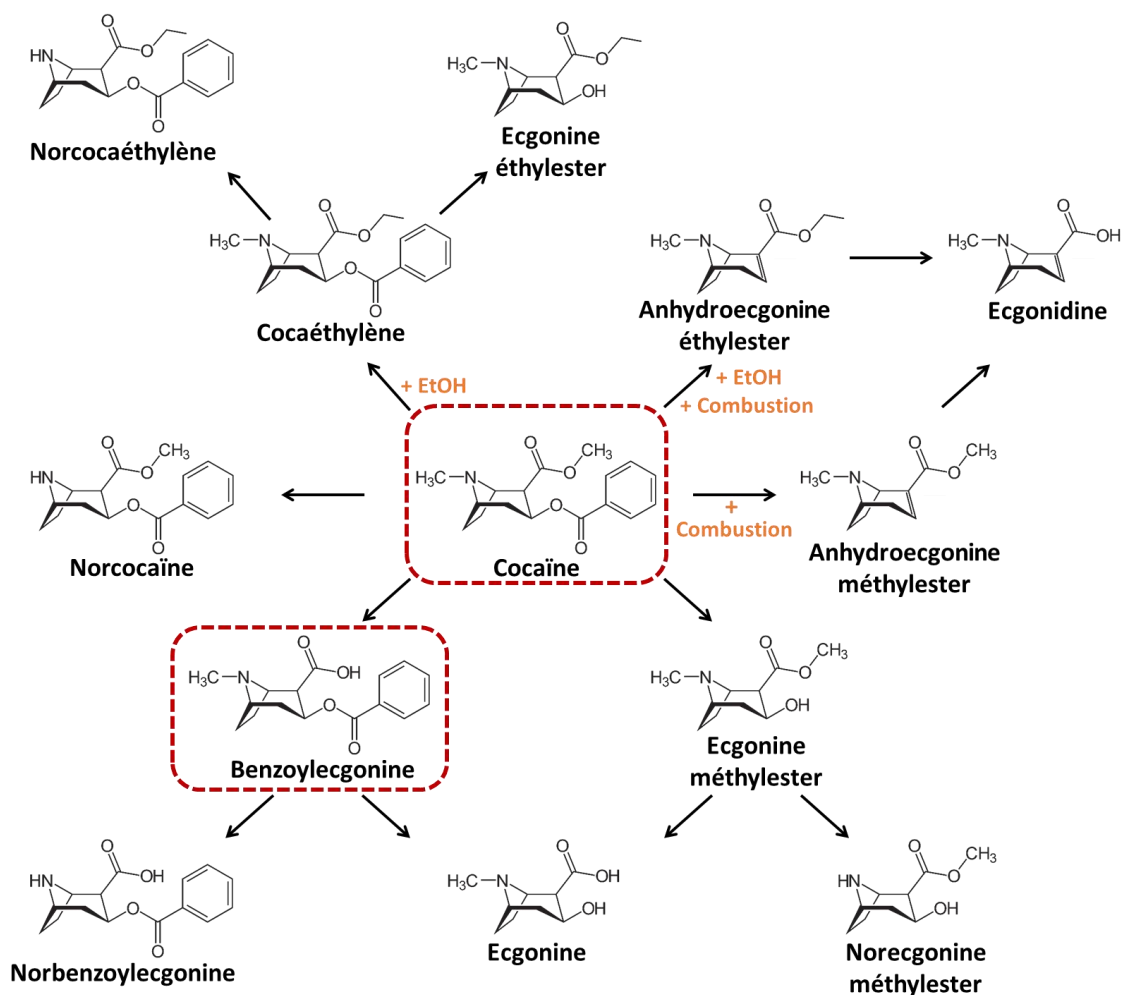


**Figure 8.** Principales voies métaboliques de la cocaïne dans le corps humain.

### II.1.3. Propriétés physico-chimiques de la cocaïne et de la BZE

La cocaïne est un ester formé d'acide benzoïque et d'un amino-alcool, l'ecgonine méthylester. Elle est constituée d'une région hydrophobe comprenant un noyau benzénique et d'une région hydrophile contenant la partie amine et une seconde fonction méthylester. Le logarithme de son coefficient de distribution octanol/eau ( $\log D_{\text{oct}}$ ) est de 3,08 [148], valeur qui diminue fortement lorsque la molécule est ionisée. En effet, la fonction amine tertiaire est une base faible et son  $pK_a$  est de 8,97 [148]. Les métabolites de la cocaïne sont constitués du même squelette de base et tous comportent par conséquent une fonction amine tertiaire ou secondaire dans le cas des métabolites N-déméthylés. Les  $pK_a$  de la fonction amine pour la cocaïne et son principal métabolite sont assez proches comme le montre le **Tableau 9**. Cette fonction base faible est donc fortement protonée dans les conditions physiologiques. Par ailleurs, la fonction méthylester de la cocaïne a subi une hydrolyse dans le cas de la BZE, qui est donc un composé zwitterionique puisqu'il possède une fonction acide carboxylique en plus de la fonction amine. Ce groupement acide est déprotoné au pH physiologique, ce qui donne une charge globalement nulle à la BZE dans ce cas, mais induit une diminution sensible de la valeur réelle de son coefficient de distribution octanol/eau.

**Tableau 9.** Valeurs des  $pK_a$  (fonction amine en gras) et des coefficients de distribution octanol/eau pour la cocaïne et son principal métabolite, la BZE [148].

Composé	M (g mol <sup>-1</sup> )	pKa	Log D <sub>oct</sub>
Cocaïne	303,35	<b>8,97</b>	3,08
Benzoylécgonine	289,33	3,35 / <b>10,82</b>	2,71

### II.1.4. Matrices biologiques utilisées pour doser la cocaïne et la BZE

L'analyse de la cocaïne et de la BZE peut se faire dans diverses matrices biologiques. Les plus courantes sont l'urine, le sang, la salive et les cheveux, mais la cocaïne a déjà été aussi quantifiée dans d'autres matrices telles que la sueur [149], les ongles [150], le méconium [151], le sébum, le sperme, les dents [152], le foie ou le cerveau [142].

En France, l'arrêté du 13 décembre 2016 fixe les modalités du dépistage, des analyses et des examens pour les substances témoignant de l'usage de stupéfiants [153]. Les minima des seuils de détection à atteindre sont présentés dans le **Tableau 10**. L'analyse de stupéfiants se fait généralement en deux étapes : une étape de dépistage pour identifier les substances stupéfiantes présentes et une étape de confirmation et de quantification en cas de dépistage positif.

**Tableau 10.** Durées de détectabilité et seuils de positivité pour la consommation de cocaïne en France dans les matrices biologiques couramment analysées [144,153,154].

Matrice	Composés recherchés	Durée de détectabilité	Seuil de positivité pour le dépistage (D) et la confirmation (C)
Urine	BZE	2-4 jours (usage occasionnel)	D : 300 ng.mL <sup>-1</sup>
		10-14 jours (usage intensif)	
Salive	Cocaïne	1-12 h	D : 10 ng.mL <sup>-1</sup> & C : 10 ng.mL <sup>-1</sup>
	BZE	12-24 h	
Sang	Cocaïne	1-12 h	C : 10 ng.mL <sup>-1</sup>
	BZE	12-24 h	

## II.2. MIP pour l'extraction de la cocaïne et la BZE obtenu par une synthèse en bloc en format conventionnel

Des études portant sur la synthèse en bloc en format conventionnel d'un MIP pour l'extraction sélective de la cocaïne et de la BZE ont déjà été réalisées au laboratoire [133,134]. Pour cela, un criblage des différentes conditions de synthèse a été effectué en changeant la nature des réactifs ainsi qu'en modifiant le mode d'initiation de la polymérisation, comme résumé dans le **Tableau 11**.

La sélectivité des différents MIP a été évaluée en comparant la rétention sur une cartouche SPE (25 mg de phase) de la cocaïne et de la BZE dans l'ACN dopé à 100 ng mL<sup>-1</sup> avec chacun leur NIP respectif mais également en comparant les divers MIP entre eux [133]. C'est pour cette raison, qu'une procédure d'extraction en milieu pur a été optimisée indépendamment pour chaque MIP (**Tableau 12**).

**Tableau 11.** Conditions de synthèse des MIP en bloc pour l'extraction de la cocaïne et la BZE [133].

Synthèse	Molécule empreinte	Monomère	Agent réticulant	Solvant	Initiation
1	Cocaïne	MAA	EGDMA	ACN	UV : 24 h, 15°C
2	Cocaïne	MAA	EGDMA	ACN	Thermique : 24 h, 60°C
3	Cocaïne	MAA	TRIM	DCM	UV : 24 h, 3°C puis Thermique : 24 h, 60°C
4	Cocaïne	MAA	EGDMA/DVB (30/70, v/v)	ACN	Thermique : 24 h, 60°C
5	Cocaïne	2-VP:MAA (1:1)	EGDMA	ACN	UV : 24 h, 15°C

**Tableau 12.** Conditions de lavage optimisées pour les différents MIP/NIP dans des cartouches remplies avec 25 mg de phase [133].

MIP/NIP	Lavage
1	1 mL ACN + 1 mL ACN/MeOH, 95/5 (v/v)
2	1 mL ACN + 1 mL ACN/MeOH, 99/1 (v/v)
3	1 mL ACN + 1 mL ACN/MeOH, 97,5/2,5 (v/v)
4	1 mL ACN
5	1 mL ACN/MeOH, 97,5/2,5 (v/v)

Les résultats alors obtenus sont reportés sous forme d'histogrammes en **Figure 9**. Ils contiennent les taux de récupération de chacun des analytes ciblés au cours des différentes étapes du protocole d'extraction (percolation, lavage et élution). Les meilleures sélectivités ont été obtenues avec la synthèse n°1 et 2 en utilisant la cocaïne en tant que molécule empreinte, le MAA comme monomère fonctionnel, l'EGDMA comme agent réticulant avec un ratio molaire de 1/4/20 respectivement pour chacun de ces éléments. En effet, des rendements supérieurs à 79% ont été obtenus pour la cocaïne et la BZE avec les deux MIP alors que pour les NIP les valeurs sont inférieures à 30%. Pour confirmer ces résultats et vérifier si la différence entre les profils observés sur les deux MIP est significative, la procédure d'extraction a été répétée trois fois sur les MIP n°1 et 2. Une plus

grande sélectivité a été obtenue pour les deux molécules sur le MIP n°1, *i.e.* synthèse avec initiation photochimique, que sur le MIP n°2 obtenu par polymérisation thermique. En effet, des rendements d'extraction de  $79 \pm 9\%$  et  $89 \pm 9\%$  ( $n = 3$ ) ont été obtenus respectivement pour la cocaïne et la BZE sur le MIP n°1, contre 0% et  $4 \pm 3\%$  sur le NIP n°1. En ce qui concerne le support n°2, des rendements d'extraction élevés ont également été obtenus sur le MIP (109 ± 3% et 84 ± 2%) pour les deux molécules mais la rétention sur le NIP correspondant était plus élevée, avec des valeurs de respectivement  $30 \pm 2\%$  et  $12 \pm 4\%$  pour la cocaïne et la BZE. Le MIP n°1 a donc été sélectionné pour étudier davantage ses performances et sa capacité pour la rétention de la cocaïne a été évaluée à  $8,96 \mu\text{mol g}^{-1}$ .

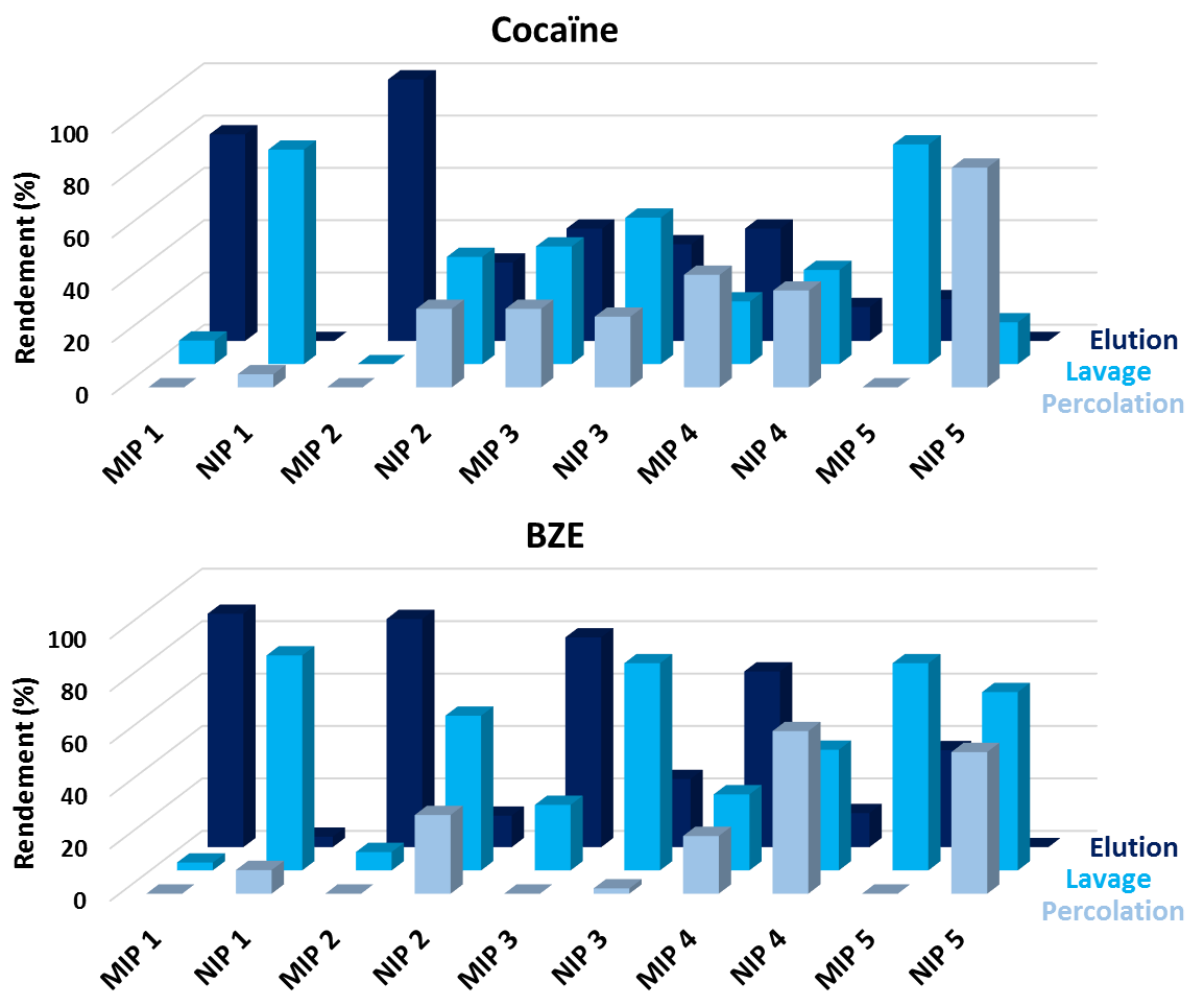


**Figure 9.** Profils d'élution de la cocaïne et de la BZE ( $100 \text{ ng mL}^{-1}$  dans ACN) obtenus sur les différents MIP et NIP synthétisés en appliquant les protocoles optimisés correspondants décrits dans le Tableau 12 [133].

La sélectivité du MIP n°1 a ensuite été évaluée en milieu réel avec des extraits de cheveux [133]. Pour cela, des échantillons de cheveux ont été décontaminés par incubations successives dans l'eau, un mélange H<sub>2</sub>O/MeOH (50/50, v/v) et le DCM, coupés en petits morceaux et extraits dans l'ACN avant d'être dopés avec de la cocaïne ou de la BZE. Les extraits de cheveux dopés à 4 ng mg<sup>-1</sup> ont été percolés avant un lavage avec 1 mL d'ACN et 1 mL d'un mélange ACN/MeOH (97,5/2,5 v/v), puis les analytes cibles ont été élus avec 2 mL de MeOH/acide acétique (95/5, v/v). Des rendements d'extraction sur le MIP de 89 ± 7% et 93 ± 5% (n = 3) ont été obtenus respectivement pour la cocaïne et la BZE, tandis que de faibles rendements entre 0 et 2% ont été obtenus en parallèle sur le NIP. L'élimination d'une majorité des interférents a donc été observée sur les chromatogrammes obtenus par LC-UV après extraction sur le MIP n°1 en comparaison avec un chromatogramme obtenu après une injection directe de l'extrait. Enfin, en associant la méthode développée avec une détection MS, des LOQ de 0,07 et 0,04 ng mg<sup>-1</sup> ont été respectivement calculées pour la cocaïne et la BZE.

Comme une grande sélectivité de la méthode d'extraction a été observée avec un extrait de cheveux, d'autres échantillons biologiques ont ensuite été étudiés. Le protocole d'extraction a alors été ré-optimisé en réduisant l'étape de lavage pour extraire sélectivement la cocaïne dans un échantillon de sérum humain dopé à 50 ng mL<sup>-1</sup> [134]. Un volume de 0,5 mL de sérum dilué avec de l'ACN (x2) a été percolé sur le MIP ou le NIP, suivi d'une étape de lavage avec 1 mL d'ACN et d'une élution avec 2,25 mL de MeOH/acide acétique 95/5% (v/v). Un rendement d'extraction de 96 ± 2% a été obtenu sur le MIP contre seulement 0,5 ± 0,8% sur le NIP (n = 3). En revanche, ce protocole n'a pas permis d'extraire la BZE de ce type d'échantillon (rendement inférieur à 5%). En effet, la polarité supérieure de la BZE par rapport à la cocaïne limite certainement le développement d'interactions hydrophobes participant à la rétention de la cocaïne sur le MIP lors de la percolation de l'échantillon hydro-organiques et avant l'étape de lavage permettant d'améliorer la sélectivité. La BZE possède également un groupement carboxylique qui peut provoquer une répulsion avec les résidus acides du MIP.

De ce fait, pour analyser l'urine, un protocole d'extraction liquide-liquide a été réalisé en amont de l'extraction sur le MIP avec des échantillons dopés à 100 ng mL<sup>-1</sup> avec de la cocaïne ou de la BZE [134]. Ensuite, 1 mL de l'extrait dans l'ACN a été percolé sur le MIP avant un lavage avec 1 mL d'ACN et 1 mL d'un mélange ACN/MeOH (97,5/2,5 v/v). L'élution a été réalisée avec 1,25 mL d'une solution de MeOH contenant 5% d'acide acétique. Des rendements totaux de 86% et 49% ont été obtenus respectivement pour la cocaïne et la BZE sur le MIP. En revanche, aucune rétention n'a été obtenue sur le NIP pour les deux analytes. Les fractions d'élution ont ensuite été analysées par LC/MS et des LOQ de 0,09 et 0,4 ng mL<sup>-1</sup> ont été déterminées respectivement pour la cocaïne et la BZE.

Une autre équipe a quant à elle étudié l'extraction sélective de la cocaïne dans des échantillons de salive en synthétisant un MIP en bloc avec les mêmes réactifs et ratio mais par initiation thermique (24 h, 60°C) [155]. Pour cela, un protocole d'extraction a été mis en place avec la percolation sur le MIP et le NIP de 1 mL d'un échantillon salivaire dopé à 200 ng mL<sup>-1</sup> avec de la cocaïne ainsi que différents interférents pouvant être détectés dans ce type d'échantillon (codéine, nicotine, diazépam, benzocaïne, succinate de doxylamine et chlorhydrate de diphenhydramine). Ensuite, l'étape de lavage a été optimisée et consistait en 1 mL d'eau et 1 mL de chloroforme. Enfin, la cocaïne retenue sur les supports a été élueée avec 1 mL d'acide acétique à 5 % (v/v) dans le MeOH. Les extraits ont été analysés en spectrométrie de mobilité ionique et des rendements de 85 ± 9% et 49 ± 15% ont été obtenus respectivement sur le MIP et le NIP pour la cocaïne. La méthode proposée a ainsi permis d'obtenir une LOD et une LOQ de respectivement 18 et 60 ng mL<sup>-1</sup>.

Les différentes études s'accordent donc sur les réactifs de synthèse pour obtenir un MIP sélectif mais il apparaît qu'après synthèse, les conditions d'utilisation devront être étudiées pour permettre le maintien de la rétention, notamment pour la BZE, tout en conservant la sélectivité.

### **II.3. Vers une miniaturisation de l'étape d'extraction sélective de la cocaïne et de la BZE et son couplage en ligne avec la nanoLC**

En s'inspirant des conditions établies pour les MIP en bloc, des synthèses ont été réalisées dans des capillaires de 100 µm de diamètre interne pour obtenir des monolithes imprimés capables de retenir sélectivement la cocaïne et la BZE. Différents ajustements de synthèse ont dû être réalisés afin de satisfaire les exigences de ce format miniaturisé.

Le monolithe imprimé le plus prometteur a été obtenu en utilisant le protocole décrit en **Annexe 2**, en sélectionnant la cocaïne comme molécule empreinte, le MAA en tant que monomère et le TRIM comme agent réticulant avec un ratio molaire de 1/4/20 respectivement pour ces trois éléments. La perméabilité du MIP monolithique a été caractérisée puis sa sélectivité a été démontrée en calculant les facteurs d'impression. Un montage a ensuite été réalisé afin de coupler en ligne l'extraction sur MIP avec une séparation en nanoLC. Les protocoles d'extraction et de séparation ont été optimisés afin d'exacerber la sélectivité de la méthode, avant son application à des échantillons biologiques. Il est à noter qu'une attention particulière a été apportée à la répétabilité des synthèses et des extractions.

Ce chapitre se présente sous la forme d'un article rédigé en anglais, publié dans *Analytica Chimica Acta* : « Selective extraction of cocaine from biological samples with a miniaturized monolithic molecularly imprinted polymer and on-line analysis in nano-liquid chromatography », T. Bouvarel, N. Delaunay, V. Pichon, *Analytica Chimica Acta*, 1096 (2020) 89-99.





# Selective extraction of cocaine from biological samples with a miniaturized monolithic molecularly imprinted polymer and on-line analysis in nano-liquid chromatography

Thomas Bouvarel <sup>a</sup>, Nathalie Delaunay <sup>a</sup>, Valérie Pichon <sup>a, b, \*</sup>

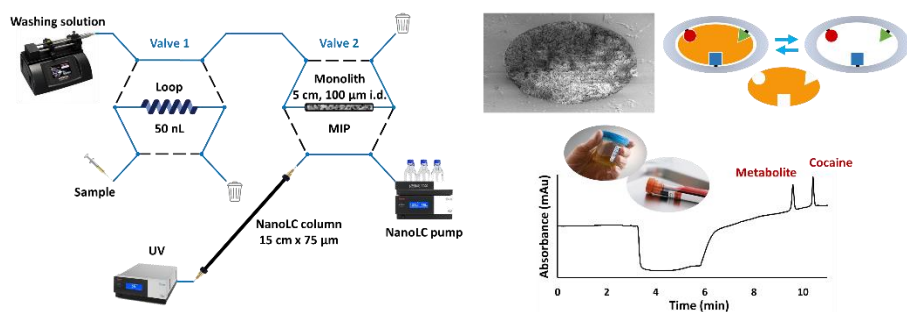
<sup>a</sup> Laboratoire des Sciences Analytiques, Bioanalytiques et Miniaturisation, UMR Chimie Biologie Innovation 8231, ESPCI Paris, CNRS, PSL University, 75005, Paris, France

<sup>b</sup> Sorbonne Université, 75005, Paris, France

## HIGHLIGHTS

- *In situ* synthesis of monolithic cocaine molecularly imprinted polymers in capillary.
- Characterizations of their permeability and selectivity optimization.
- Evaluation of the synthesis repeatability for independent syntheses.
- Optimization of the on-line monolithic MIP extraction and nanoLC separation.
- Trace analysis of cocaine in spiked human plasma and saliva with 50 nL and in 20 min.

## GRAPHICAL ABSTRACT



## ARTICLE INFO

### Article history:

Received 31 July 2019

Received in revised form

18 October 2019

Accepted 21 October 2019

Available online 23 October 2019

### Keywords:

Molecularly imprinted polymer

Monolith

On-line coupling

Cocaine

Human plasma

## ABSTRACT

We report the on-line coupling of a monolithic molecularly imprinted polymer to nano-liquid chromatography for the selective analysis of cocaine and its main metabolite, benzoylecgonine, in complex biological samples. After the screening of different synthesis conditions, a monolithic molecularly imprinted polymer was *in situ* synthesized into a 100 mm internal diameter fused-silica capillary using cocaine as template, methacrylic acid as functional monomer, and trimethylolpropane trimethacrylate as cross-linker. Scanning electron microscopy was used to assess the homogeneous morphology of the molecularly imprinted polymer and its permeability was measured. Its selectivity was evaluated by nano-liquid chromatography-ultraviolet, leading to imprinting factors of  $3.2 \pm 0.5$  and  $2.2 \pm 0.3$  for cocaine and benzoylecgonine, respectively, on polymers resulting from three independent syntheses, showing the high selectivity and the repeatability of the synthesis. After optimizing the extraction protocol to promote selectivity, the monolithic molecularly imprinted polymer was successfully on-line coupled with nano-liquid chromatography-ultraviolet for the direct extraction and analysis of cocaine present in spiked human plasma and saliva samples. The repeatability of the obtained extraction recovery, between 85.4 and 98.7% for a plasma sample spiked at  $100 \text{ ng mL}^{-1}$ , was high with relative standard deviation values lower than 5.8% for triplicate analyses on each of the three independently synthesized molecularly imprinted polymers. A linear calibration range was achieved between 100 and  $2000 \text{ ng mL}^{-1}$  ( $R^2 = 0.999$ ). Limits of quantification of  $14.5 \text{ ng mL}^{-1}$  and  $6.1 \text{ ng mL}^{-1}$  were achieved in plasma and saliva samples, respectively. The very clean-baseline of the resulting chromatogram illustrated the high selectivity brought by the monolithic molecularly imprinted polymer that allows the removal of a huge peak corresponding to the elution of interfering compounds and the easy determination of the target analyte in these complex biological samples.

### **II.3.1. Introduction**

Miniaturized analytical devices have matured considerably since the initial lab-on-a chip concept proposed by Manz in 1990 [31]. The potential benefits of miniaturization are enormous, following the principle that small-scale processes consume less time, samples, and reagents [30]. However, the miniaturization of the analytical system may result in loss of the separation power by the reduction of the separation lengths. This represents a serious limitation when target analytes are at trace levels in complex matrices. To overcome this problem, a selective sample pre-treatment step can be integrated into the miniaturized devices.

Solid-phase extraction (SPE) is a powerful method for the extraction and the purification of compounds contained in complex samples. However, the majority of the available sorbents mainly promotes the development of non-specific interactions during the extraction procedure that leads to the co-extraction of a huge amount of interfering compounds. This lack of selectivity has been at the origin of the development of molecular imprinted polymers (MIPs). MIPs are synthetic and selective sorbents that possess specific cavities designed for a target analyte, with a retention mechanism based on molecular recognition, similarly to immunosorbents [156,157] or oligo-sorbents [158,159]. They are used in several fields, such as sensors, catalysis, enantiomeric separations, and extraction [160].

The analysis of various organic compounds from complex samples assisted by MIP extraction and clean-up has been largely described in literature [105,161]. As for conventional SPE sorbents, MIPs have been mainly used off-line by packing MIPs particles into a cartridge between frits. For their on-line-coupling with conventional LC systems, some monolithic MIPs have been prepared in 4.6 mm internal diameter (i.d.) columns [86,87]. This approach was used to prepare a MIP column for HPLC separation [162,163] and did not require the covalent attachment of the MIP to the inner surface of the column since frits were used to maintain the sorbent in the column.

The miniaturization of MIPs for extraction is particularly attractive from a general point of view, and even more when templates or monomers are expensive or difficult to synthesize. For devices base on partition, MIPs can be nanoparticles, mainly used in dispersive SPE [164], a coating of a fiber or a thin film on the inner wall of a capillary for in-tube solid phase microextraction [42,44]. Concerning exhaustive extraction in SPE, MIP particles can be packed in a specially designed chip [67,68] or the surface of a core monolith can be grafted by MIP [49,123,124]. The *in situ* synthesis of a monolithic MIP filling the entire section and well-anchored at the capillary or chip channel surface can lead to higher capacity than the open-tubular approach to be applied to trace enrichment purposes.

Monolithic MIPs were first synthesized for capillary electrochromatography (CEC) [15,165,166], especially for chiral separations [14,16]. Recently, monolithic MIPs were also developed for off-line extractions in miniaturized devices, such as pipet-tips [126,127], hollow-fiber membrane [167], or 75 µm to 530 µm i.d. capillaries [39,45,47,89,91–93,99,101,117]. If the repeatability of the extraction was sometimes mentioned, the repeatability of the MIP synthesis has almost never been described. Besides, to our knowledge, only one work is related to the on-line coupling of a capillary containing a MIP (100 µm i.d.) with a capillary column (300 µm x 25 cm) [49]. The MIP was produced by a two-step process since it was synthesized at the surface of a monolith. The feasibility of the on-line coupling was demonstrated for the analysis of several aflatoxins. However, there is no application with real samples, no mention of synthesis repeatability, and the two-step synthesis procedure should give rise to a sorbent with a lower capacity than a direct *in situ* polymerization of a monolithic MIP.

The aim of the present work was the direct *in situ* synthesis of a monolithic MIP into a 100 µm i.d. capillary and its on-line coupling with nano-liquid chromatography (nanoLC) for the selective extraction of a target analyte from a biological fluid. For this proof-of-concept, cocaine was taken as a model molecule. Indeed, our group already synthesized MIPs in bulk for the selective extraction of cocaine and its metabolites, benzoylecgonine (BZE) and ecgonine methyl ester [133,134]. In these studies, cocaine was chosen as template molecule and various monomers, cross-linking agents, porogens, and initiation modes were evaluated. The most promising MIP was obtained with methacrylic acid (MAA) as monomer, ethylene glycol dimethacrylate (EGDMA) as cross-linker, and acetonitrile (ACN) as porogen. The bulk polymerization was initiated under UV using Azo-*N,N'*-diisobutyronitrile (AIBN) as initiator [133]. The resulting MIP monolith was grinded and resulting MIP particles were packed into SPE cartridges to selectively extract the target analytes from hair extracts [133] and urine samples [134] with high extraction recoveries of 89 ± 7% and 92 ± 15%, respectively, for cocaine. Another group synthesized a MIP with the same pathway to extract cocaine from saliva samples and quantify it by ion mobility spectrometry [155]. In all cases, MIPs exhibited good selectivity and high capacity.

The success of the *in situ* synthesis of a monolithic MIP relies on the presence of large pores to provide convective flow-through and of highly selective binding sites. The synthesis conditions must therefore be adapted to satisfy these two parameters. In this work, different synthesis conditions were screened and the resulting monoliths were first characterized by permeability measurements and by scanning electron microscopy (SEM). The most promising MIPs were then evaluated by studying their selectivity, comparing their retention factors with the ones of a non-imprinted polymer (NIP), *i.e.* a control polymer prepared in the same conditions but in absence of the template. After checking the

repeatability of the synthesis, the extraction on the monolithic MIP was coupled on-line with nanoLC-UV analysis. The volume and the composition of the solution ensuring both the transfer of the target analytes from the injection loop to the MIP and the removal of non-specific interactions were optimized using NIP. Finally, analyses of cocaine present in spiked plasma and saliva samples were carried out.

## **II.3.2.Experimental**

### ***II.3.2.1. Chemicals and reagents***

Cocaine base and stock solutions of  $1 \text{ mg mL}^{-1}$  of BZE in MeOH were provided by Sigma-Aldrich (Saint-Quentin-Fallavier, France). The working solutions at  $1 \text{ }\mu\text{g mL}^{-1}$  were obtained by dilution of the stock solution ( $1 \text{ mg mL}^{-1}$ ) in HPLC-grade ACN (Carlo Erba, Val-de-Reuil, France). These solutions were stored at  $-20^\circ\text{C}$ . MeOH, EtOH, and isoctane were purchased from Carlo Erba. Acetic acid and anhydrous ACN were provided by Sigma-Aldrich.  $1 \text{ M}$  NaOH and  $0.1 \text{ M}$  HCl were obtained using deionized water (Milli-Q purification system, Millipore, Molsheim, France) and Titrisol solution from Merck (Darmstadt, Germany).

MAA, EGDMA, trimethylolpropane trimethacrylate (TRIM), and 3-(trimethoxysilyl)propyl methacrylate ( $\gamma$ -MAPS) were purchased from Sigma-Aldrich. EGDMA was washed twice with an equal volume of a solution of 10% NaOH in deionized water, and then washed twice with an equal volume of water. Afterwards, it was dried using an equal volume of saturated NaCl solution and next over  $\text{Na}_2\text{SO}_4$ . Purified EGDMA and MAA were distilled under vacuum in order to remove inhibitors and stored at  $-20^\circ\text{C}$ . AIBN was purchased from Acros Organics (Noisy-le-Grand, France). AIBN, TRIM, and  $\gamma$ -MAPS were of satisfactory purity so they were used without further purification. Fused-silica capillaries with a UV transparent protecting fluorocarbon polymer coating (PTFE-coated silica capillaries,  $100 \text{ }\mu\text{m i.d.} \times 375 \text{ }\mu\text{m o.d.}$ ) were purchased from Polymicro Technologies (Photon Lines, Saint Germain-en-Laye, France).

### ***II.3.2.2. In situ preparation of the monolithic polymers***

The monolithic polymers were prepared *in situ* by a thermally initiated polymerization within fused-silica capillaries. Prior to polymerization, the inner wall of the capillaries was activated to anchor the monolith with  $\gamma$ -MAPS according to a procedure adapted from Hjertén [168]. Briefly, the capillaries were first rinsed with water, then activated by flushing  $1 \text{ M}$  NaOH for 30 min. After a washing step with

water, 0.1 M HCl was flushed for 30 min. The silanization was then achieved with 250 µL of γ-MAPS in 1 mL of EtOH, with a pH adjusted to 3.5 by acetic acid, for at least 1 h at room temperature. The capillaries were washed with EtOH and finally dried with nitrogen.

The template molecule (T: cocaine, 10 mg), functional monomer (M: MAA), cross-linking agent (CL: TRIM or EGDMA), and radical initiator (AIBN, 1.5% M+CL, %w/w) were dissolved in porogen (P: ACN containing 10% of isoctane) with a molar ratio T/M/CL of 1/4/20. Then the polymerization mixture was purged with nitrogen for 5 min to get rid of oxygen and introduced in the 15 cm-long capillaries. After sealing both ends of the capillaries with rubber septum, they were immersed in a thermostated water bath at 60°C. The thermal polymerization was allowed to proceed during 24 h. After polymerization, the capillary containing the monolithic MIP was connected to a nano-pump and rinsed at a flow rate of 200 nL min<sup>-1</sup> with a volume of ACN/acetic acid (98/2, v/v) corresponding to ten volumes of the empty capillary to remove the template molecules and other residual reagents. Before using a new monolithic MIP, in order to confirm the removal of the template, blanks were made to verify that the potential leaching of cocaine led to a concentration level below the LOD. The monolithic NIPs were obtained by performing the same procedure in the absence of the template. The resulting capillaries were cut to obtain 5 cm-long capillaries.

#### ***II.3.2.3. Characterization of the monolithic MIP by SEM and nanoLC***

The cross section of the capillaries containing the polymer was observed by SEM, with a FEI MAGELLAN 400 scanning electron microscope that operates with a beam energy comprised between 3 keV and 5 keV. Considering the support at our disposal to carry out the SEM observations, it was not possible to set the lens just above our capillaries, which means that the pictures were taken with a small angle, but it does not interfere with the observations we wanted to make concerning the monoliths. Permeability measurements were carried out with an Ultimate™ RSLCnano 3000 system (ThermoFisher Scientific, Le Pecq, France), composed of a nano-pump delivering 100% ACN ( $\eta = 0.316 \text{ mPa s}$  at 35°C) at a constant temperature of 35°C with different flow rates and allowing to record the generated back-pressure. The permeability was calculated using Darcy's law which expresses the permeability as a function of the applied flow rate:

$$K = \frac{4\eta LF}{\pi d_i^2 \Delta P} \quad (\text{Equation 1})$$

$K$  is the permeability ( $\text{m}^2$ ),  $F$  the applied flow rate ( $\text{m}^3 \text{s}^{-1}$ ),  $\eta$  the viscosity of the solvent ( $\text{Pa s}$ ),  $L$  the length of the capillary (m),  $\Delta P$  the measured back-pressure (Pa), and  $d_i$  the capillary inner diameter (m).

For retention studies, cocaine ( $25 \mu\text{g mL}^{-1}$ ) and BZE ( $25 \mu\text{g mL}^{-1}$ ) were injected on a nanoLC system composed of a six-port switching nano-valve (Cheminert nanovolume 6 ports 2 pos 1/32", manual CN2-4346, Vici Valco Instruments Inc. Co., Houston, TX, USA) connected to a home-made injection loop (50 nL), to a nano-pump (NCP-3200RS Nano Pump, ThermoFisher Scientific Dionex, controlled by Chromeleon 6.80 SR12), and to the MIP or NIP capillaries maintained at  $35^\circ\text{C}$  with a column oven (TCC 3000SD column compartment, ThermoFisher Scientific Dionex) connected to a diode array detector (VWD 3100 Detector, ThermoFisher Scientific Dionex) with a flow cell of 3 nL. Compounds were detected at 233 nm. The flow rate of ACN was set at  $200 \text{ nL min}^{-1}$ . The marker used to determine the dead volume was acetone. Retention factors  $k$  and imprinting factors (IF) were calculated using the following **Equation 2** and **Equation 3**:

$$\text{IF} = \frac{k_{\text{MIP}}}{k_{\text{NIP}}} \quad (\text{Equation 2})$$

where  $k_{\text{MIP}}$  and  $k_{\text{NIP}}$  are the retention factors obtained on the MIP and the NIP monolithic columns, respectively.

$$k = \frac{t_r - t_0}{t_0} \quad (\text{Equation 3})$$

where  $t_r$  and  $t_0$  are the retention times of cocaine or BZE and of acetone, respectively.

#### **II.3.2.4. NanoLC-UV analysis of cocaine and benzoylecgonine**

The nanoLC analyses of standards of cocaine and BZE were achieved using the same device as the one described in Part 2.3, replacing the MIP/NIP capillaries by the nanoLC column (Acclaim™ PepMap™ 100 C18, 150 x 0.075 mm, 3  $\mu\text{m}$ , ThermoFisher Scientific) and using an home-made injection loop of 50 nL. The separation was achieved at a flow-rate of  $200 \text{ nL min}^{-1}$  and a gradient based on ammonium formate 10 mM pH 3.1 adjusted with formic acid (A) and ACN (B). The gradient started with 10% B, increased to 25% B in 1.5 min, then reached 40% B in 5.6 min, increased to 80% B in 0.8 min, and remained for 2.4 min. Finally, the mobile phase composition was set back to 10% B to let the system equilibrate. Solutions composing the mobile phase were filtered by 0.45  $\mu\text{m}$  nylon

membrane filters purchased from Whatman (Maidstone, England) before using. The UV detection of cocaine and BZE was carried out at 233 nm.

#### **II.3.2.5. On-line coupling of MIP or NIP extraction with nanoLC-UV analysis**

The on-line set-up allowing the coupling of monolithic MIP/NIP to the nanoLC-UV device is presented in **Figure 10**. It consisted in a syringe pump (Standard Infuse/Withdraw PHD ULTRA™ 4400 Programmable Syringe Pump, Harvard apparatus, Les Ulis, France, Pump 1) connected to a six-port switching nano-valve. This valve, valve 1, was connected to a home-made injection loop (50 nL) and to another 6-port switching nano-valve. This second valve, valve 2, was connected to a nanoLC pump (Ultimate™ NanoFlow RSLC system, ThermoFisher Scientific Dionex, Pump 2), to the MIP or the NIP capillaries, and to the analytical column. All the connections were achieved with 26 µm i.d. fused-silica capillaries (Polymicro Technologies, 360 µm o.d.) and microtight unions PEEK (Upchurch Scientific).

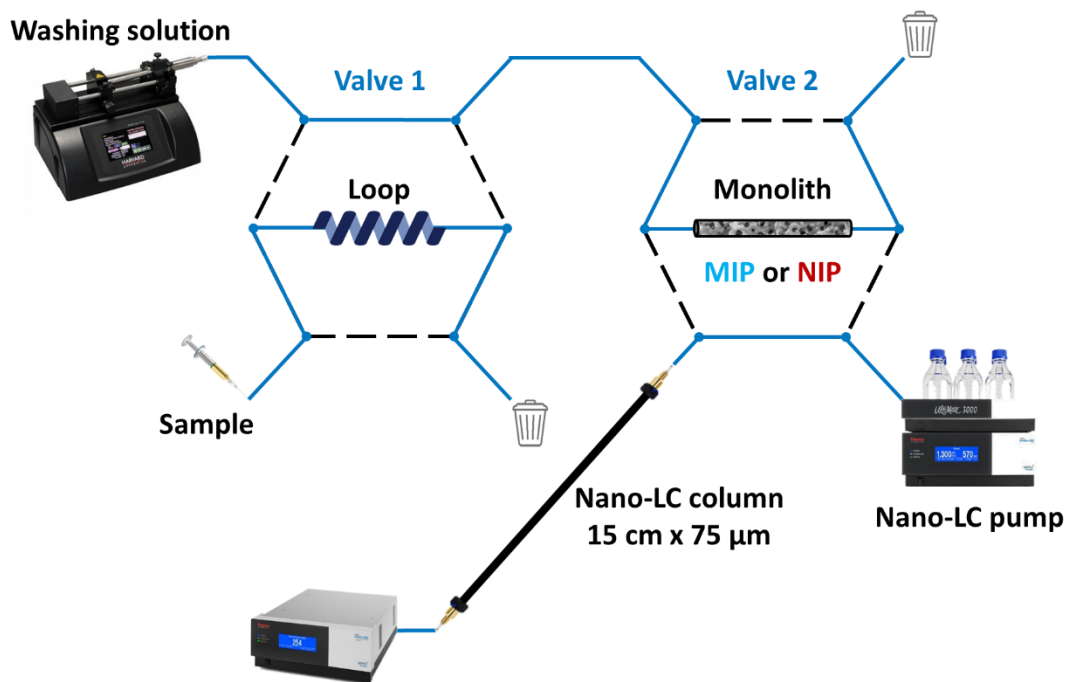


**Figure 10.** Set-up of the on-line coupling of the monolithic MIP/NIP (50 mm x 100 µm i.d.) with nanoLC-UV.

In the first step of the extraction procedure, sample was loaded onto the loop (valve 1). In parallel, the analytical column was conditioned with mobile phase. In a second step, the valve 1 was

switched in order to transfer the sample to the monolithic MIP/NIP extraction capillary (50 mm x 100 µm) using a washing solvent, a H<sub>2</sub>O/ACN mixture with optimized volume and composition as mentioned in **Section II.3.3.4**, delivered by the syringe pump through the sample loop at a flow rate of 200 nL min<sup>-1</sup>. At the last step, the valve 2 was switched allowing thus the transfer of the trapped compounds from the monolithic MIP/NIP to the nanoLC analytical column by the mobile phase delivered by the nanoLC pump. After each analysis, the MIP/NIP capillaries were subsequently re-equilibrated with the initial H<sub>2</sub>O/ACN mixture (70/30, v/v), that was used for the extraction step, delivered at 200 nL min<sup>-1</sup> by the syringe pump before being re-used. In order to confirm the complete elution of the analytes from the monolithic MIP/NIP, blanks were regularly performed to verify that the potential analyte residues led to concentrations level below the detection limit.

#### ***II.3.2.6. Preparation of plasma and saliva samples***

Human plasma was provided by the French Blood Establishment (Ivry-sur-Seine, France). 500 µL of plasma sample were first mixed with ACN (50%, %v/v) for protein precipitation. After vortex mixing, samples were centrifuged during 5 min at 6000 x g at 4°C. The supernatant was then recovered, filtered, and stored at 4°C until need. This treated plasma samples were either analyzed directly or spiked with cocaine to obtain a concentration of 50 ng mL<sup>-1</sup> in the supernatant, which corresponds to 100 ng mL<sup>-1</sup> in plasma equivalent. A volume of 50 nL was analyzed by SPE on MIP or NIP and nanoLC-UV.

Saliva samples were collected using Salivettes from Sarstedt (Numbrecht, Germany) designed with cotton swab without preparation from healthy individual and were free of cocaine and BZE. Saliva was filtered with 0.45 µm pore size Millex® Syringe filters from Merck (Darmstadt, Germany) and stored at -20°C until use. The treated saliva samples were either analyzed directly or spiked with cocaine to obtain a concentration of 50 ng mL<sup>-1</sup> and a volume of 50 nL was analyzed by SPE on MIP or NIP and nanoLC-UV.

### **II.3.3. Results and discussion**

#### ***II.3.3.1. Preliminary studies for the choice of the reagents***

In the present study, cocaine was chosen as model molecule to evaluate the possibility to synthesize a monolithic MIP in a capillary and to couple it on-line to nanoLC for the selective extraction of this compound from complex biological samples. For this, it was necessary to produce a MIP that

was sufficiently permeable to allow the percolation of solutions, including the nanoLC mobile phase, without generating a high back-pressure. The MIP must also possess specific cavities to provide a high selectivity for the extraction procedure. As previously mentioned, MIP showing a high selectivity towards cocaine and its metabolites, BZE and ecgonine methyl ester, was synthesized by our group in ACN using MAA as monomer, EGDMA as CL, and AIBN as radical initiator [133,134]. The acidic MAA was also here selected as monomer because of its strong interaction with the template that possesses a basic amino group. However, even if EGDMA was previously used, TRIM, a tri-functional monomer so-called “three arm cross-linker”, was also considered as CL in this work. Indeed, TRIM has been reported to give rise to macroporous polymers under some conditions [169,170] and this is particularly important for the imprinted monoliths since they should present good flow-through pores. The use of TRIM may also lead to monoliths with well-defined recognition sites, favoring a high selectivity and a high loading capacity [171]. Therefore, the first step of this work focused on the comparison of the impact of EGDMA and TRIM on the monolithic structure.

Sorbent porosity also depends on the careful tuning of some parameters such as the nature of the porogenic solvent. Depending on whether a good or a poor solvent is used as porogen, a large difference of the monolith porosity can be observed, since the porogen affects the polymer chain solvation in the reaction medium during the early stage of the polymerization [172,173]. Thus, the porogen composition is a key factor that may enable the tuning of the monolith porosity without changing its final chemical composition. A solvent is good when its solubility parameter is the same as the polymer’s one [174]. In such a solvent, the polymer exhibits low pore volume and high swelling, whereas a polymer prepared in a poor solvent exhibits permanent porosity and low swelling. To promote pore formation in the case of organic monoliths [175], common solvents are cyclohexanol/dodecanol mixtures. However, these solvents are forbidden for the synthesis of MAA-based imprinted monoliths because they inhibit hydrogen bonds between this monomer and the template. This is why the most common solvents used in molecular imprinting are dichloromethane, chloroform, ACN, and toluene. In the present study ACN was selected because of the high selectivity previously obtained when preparing a MIP with it by bulk polymerization for cocaine [133]. Reinholdssom *et al.* [169] and Schweitz *et al.* [37,38] suggested the addition of a low amount of isoctane, a solvent of low dissolving capacity, to the porogen in order to tune the porosity of the resulting monolith. The effect of the addition of 10% of isoctane was then evaluated. At last, the thermal initiation has shown its potential for the bulk polymerization of a MIP for cocaine [133] and is easier to set up than UV polymerization for this type of format. This is why, a thermal initiation of the reaction at 60°C was used.

To limit the template consumption, these preliminary evaluations were carried out by synthesizing only non-imprinted monoliths. Therefore, they were prepared using a polymerization mixture containing MAA as monomer (M) and EGDMA or TRIM as CL with a (M+CL)/P ratio of 20/80 or 15/85 (v/v, with a M/CL ratio of 1/5, mol/mol) introduced in a 15 cm-long capillary. The capillary was next cut in 5 cm-long capillaries and their permeability was measured by determining the back-pressure ( $\Delta P$ ) they generate while pumping ACN (200 nL min<sup>-1</sup>). A back-pressure close to 4 bar, exhibited by the nanoLC system itself when a 5 cm-long empty capillary is connected, was subtracted from the back pressure measured with the capillary containing the monolith.

For a 20/80 ratio and EGDMA, a back-pressure of 46 bar was measured, demonstrating that this monolith was not enough permeable. The use of a larger amount of porogen to favor macropores ((M+CL)/P of 15/85 instead of 20/80), gave rise to a higher permeability ( $\Delta P = 7$  bar). When using TRIM, the back-pressure was 8 and 2 bar for the 20/80 and 15/85 ratio, respectively, thus showing a very satisfactory permeability whatever the ratio. TRIM was therefore selected.

These preliminary experiments were followed by three independent syntheses of monolithic MIPs and NIPs with TRIM and using the two (M+CL)/P ratios. The back-pressure generated and the permeability of each monolith were measured by applying various flow rates of ACN, as shown in **Figure S1, (Appendix 3)**. With the 20/80 ratio, the permeability K of the MIP, determined following the **Equation 1**, was  $1.2 \times 10^{-15}$  m<sup>2</sup> (RSD = 10%, n = 3) and  $9.1 \times 10^{-15}$  m<sup>2</sup> (RSD = 7%, n = 3) for the NIP. For the 15/85 ratio, K values of  $3.3 \times 10^{-15}$  m<sup>2</sup> (RSD = 3%, n = 3) for the MIP and of  $3.7 \times 10^{-14}$  m<sup>2</sup> (RSD = 17%, n = 3) for the NIP were obtained. First of all, the permeability of NIP is always higher than the permeability of MIP thus showing the effect of the template molecules on the structure of the monolith. Finally, a higher permeability was obtained for both monolithic MIPs and NIPs with the 15/85 ratio. These more permeable supports are thus more suitable for on-line coupling with nanoLC column in order to limit the back-pressure that could damage the monolith. To confirm these results, the inter-day permeability was studied by synthesizing three independent monolithic MIPs and NIPs each day for three days. The inter-day permeability was  $2.8 \times 10^{-15}$  m<sup>2</sup> (RSD = 17%, n = 3) for the MIP and  $2.6 \times 10^{-15}$  m<sup>2</sup> (RSD = 37%, n = 3) for the NIP.

These monolithic MIPs and NIPs were also observed by SEM to obtain complementary information related to the homogeneity of the monolith and its attachment to the capillary wall (**Figure 11**). As shown by these pictures, monolithic MIP and NIP occupied the whole section of the capillary and were well anchored to its surface. It is worthwhile to notice that identical SEM observations were made for the monolith synthesized with the 20/80 ratio (data not shown).

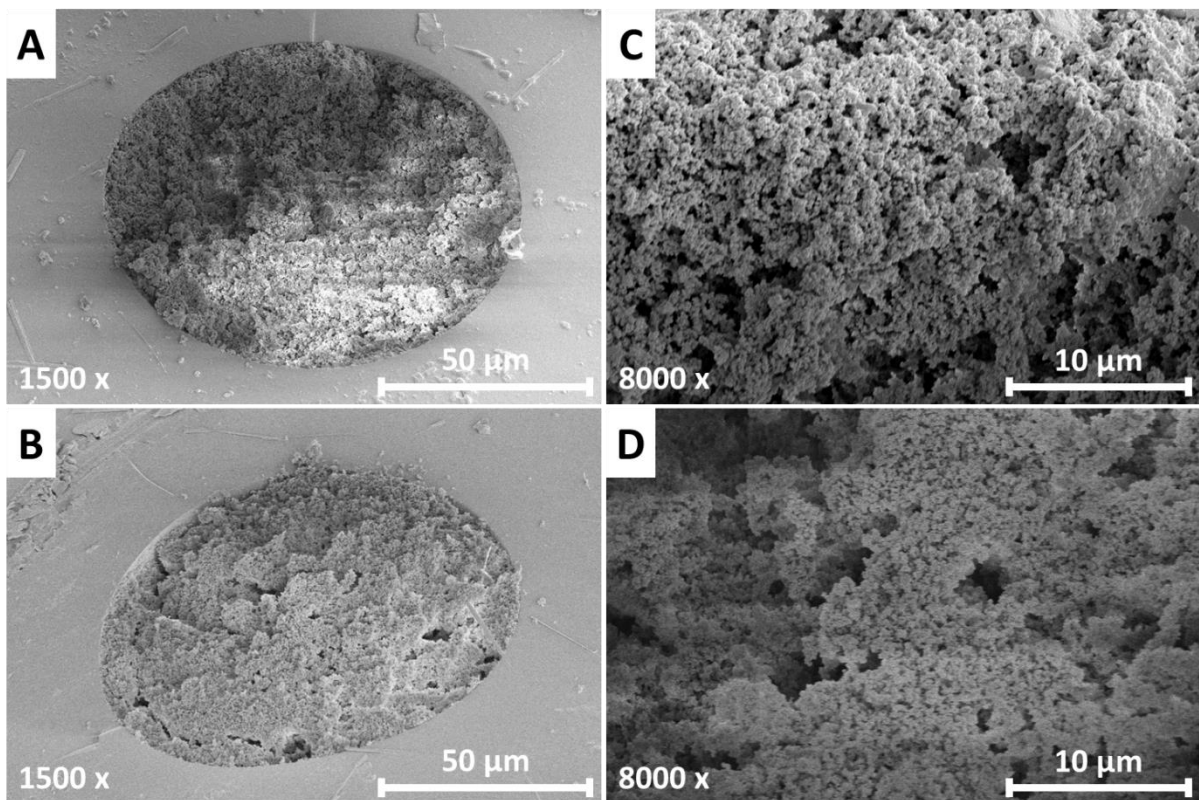


**Figure 11.** Scanning electron micrographs of the cross section of a 100  $\mu\text{m}$  i.d. capillary containing a monolithic (A, C) MIP or (B, D) NIP synthesized with the (M+CL)/P ratio of 15/85.

#### II.3.3.2. Evaluation of the selectivity studying retention properties in nanoLC

The selectivity of the monoliths obtained with both (M+CL)/P ratios was next characterized by studying the retention of cocaine and BZE injected on each MIP and its corresponding NIP in nanoLC with capillary length of 5 cm and a flow rate of 200  $\text{nL min}^{-1}$ . The injection of acetone on each monolith allowed the determination of the  $t_0$  value and then the calculation of the retention and imprinted factors. The evaluation was carried out in ACN because, as often mentioned in the literature related to MIP, the selectivity should be optimal when the solvent used is close to the porogen, *i.e.* ACN containing 10% isoctane here [161]. Moreover, the MIP previously prepared by bulk polymerization using cocaine, MAA, and EGDMA instead of TRIM was very selective towards cocaine and BZE in this solvent with recoveries higher than 80% on the MIP and lower than 10% on the NIP [134].

Retention factors and IFs measured on MIPs and their corresponding NIPs from three independent syntheses for the two different synthesis ratios are reported in **Table 13** and the chromatograms are provided as supplementary material (**Figure S2, Appendix 3**). First, RSD values of

retention factor for cocaine measured on three independent MIPs lower than 19% confirm the repeatability of the synthesis procedure already demonstrated by the permeability measurements. This repeatability is highly satisfactory because it implies both the repeatability of the activation step and of the polymer synthesis itself. It is also important to notice that the broad shape of the peaks has a strong impact on measurement accuracy. Moreover, cocaine is significantly more retained on MIPs than on the corresponding NIPs, thus attesting the presence of cavities specific to cocaine on MIP. In addition, these cavities are also able to selectively retain BZE, since it has a higher retention on MIP than on NIP too. This first evaluation of the selectivity confirmed that TRIM can be associated to MAA to generate specific cavities.

**Table 13.** Retention factors and imprinted factors of cocaine and BZE measured on three independent MIPs and NIPs synthesis for two different (M+CL)/P ratios. Injections of 50 nL of acetone, cocaine (COC, 25 µg mL<sup>-1</sup>), and BZE (25 µg mL<sup>-1</sup>) on 5 cm-long capillary filled with the monolithic MIP or NIP. Mobile phase: ACN.

Compound	Ratio 20/80, (M+CL)/P			Ratio 15/85, (M+CL)/P		
	k <sub>MIP</sub> (RSD, n = 3)	k <sub>NIP</sub> (RSD, n = 3)	IF (RSD, n = 3)	k <sub>MIP</sub> (RSD, n = 3)	k <sub>NIP</sub> (RSD, n = 3)	IF (RSD, n = 3)
Cocaine	1.5 (4%)	0.4 (6%)	3.9 (5%)	1.0 (2%)	0.3 (19%)	3.2 (17%)
BZE	2.3 (4%)	1.3 (1%)	1.7 (3%)	1.7 (21%)	0.8 (9%)	2.2 (13%)

By focusing on IFs, both MIPs obtained either with a M+CL)/(P ratio of 20/80 or 15/85 are selective towards the template molecule, *i.e.* cocaine, as shown by values higher than 1. The MIP obtained with the 20/80 ratio exhibits the best selectivity for cocaine (IF = 3.9 ± 0.2, n = 3), but the one obtained with the 15/85 ratio seems more selective towards BZE (IF = 2.2 ± 0.3, n = 3) while maintaining a very good selectivity for cocaine (IF = 3.2 ± 0.5, n = 3). Finally, the monolith synthesized with a ratio of 15/85 seems to correspond to the best compromise between permeability (K) and selectivity (IF) for cocaine and its main metabolite. It was therefore selected for further studies.

### **II.3.3.3. On-line coupling of the capillary containing the monolithic MIP and the nanoLC-UV system**

Before evaluating the possibility to couple on-line the monolithic MIP with nanoLC-UV analysis, the performance of the nanoLC-UV analysis was first studied. For this, aqueous solutions of BZE and cocaine with five concentrations between 50 and 500 ng mL<sup>-1</sup> for each compound were injected ( $V_{inj} = 50$  nL) on the nanoLC column (Acclaim<sup>TM</sup> PepMap<sup>TM</sup> 100 C18). The calibration lines and the chromatogram corresponding to the separation of cocaine and BZE at 500 ng mL<sup>-1</sup> are presented in **Figure S3 (Appendix 3)**. The response was linear in the range of studied concentration with  $R^2$  of 0.97 and 0.99 for cocaine and BZE, respectively. The limits of detection (corresponding to a signal-to-noise ratio of 3) and quantification (signal-to-noise ratio of 10) were estimated to 10 and 34 ng mL<sup>-1</sup> for BZE, respectively, and 2 and 8 ng mL<sup>-1</sup> for cocaine, respectively.

The MIP capillary (5 cm x 100 µm i.d.) was then coupled on-line with nanoLC. For this, it was placed at the loop position of a six-port switching valve and connected between a first valve having the injection loop, the nanoLC pump, and the nanoLC column as shown by the set-up presented in **Figure 10**. This set-up allows a back-flush elution of the compounds trapped on the MIP to nanoLC-UV system by the mobile-phase thus limiting some band broadening effects. The sample is first loaded in the loop (50 nL) present on valve 1 and next transferred by 1 µL of a hydro-organic solution (H<sub>2</sub>O/ACN, 90/10) to the MIP connected to valve 2. The composition of the transfer media was selected according to previous studies achieved on the MIP synthesized with cocaine, MAA, and EGDMA, showing that it should ensure the retention of cocaine and BZE on the MIP [134].

Typical chromatograms obtained by coupling on-line the MIP or the NIP to nanoLC-UV for the analysis of cocaine and BZE (50 nL, 1 µg mL<sup>-1</sup>) are presented in **Figure 12 B** and **C**, respectively. The comparison with the direct injection in nanoLC of both molecules (50 nL, 500 ng mL<sup>-1</sup>) (**Figure 12 A**) shows that the on-line coupling generates an increase in the retention time that can be explained by additional extra-column volumes due to the length of the connection capillaries used to fix the 5 cm-long capillary containing the monolith. The apparent efficiency of the resulting peaks were calculated and the values are for BZE  $98,100 \pm 3,200$  and  $93,000 \pm 2,700$  plates for direct injection and on-line MIP extraction, respectively, and for cocaine  $108,800 \pm 4,100$  and  $115,100 \pm 3,400$  plates for direct injection and on-line MIP extraction, respectively.

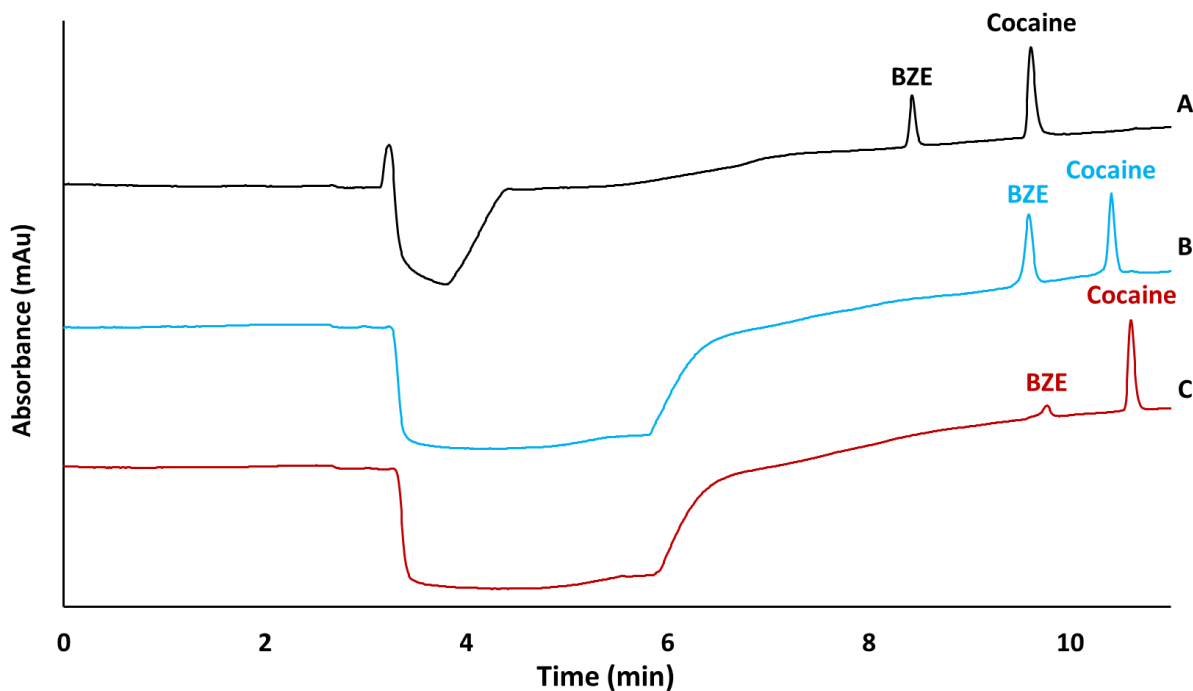


**Figure 12.** Chromatograms obtained by direct injection of cocaine and BZE ( $500 \text{ ng mL}^{-1}$  each) (A) and by on-line coupling of the extraction of water spiked at  $1 \mu\text{g mL}^{-1}$  with cocaine and BZE on monolithic MIP (B) and NIP (C) synthesized with  $(M+CL)/P$  ratio of 15/85.  $V_{inj} = 50 \text{ nL}$ , UV detection at 233 nm,  $V_{washing} = 1000 \text{ nL}$  ( $\text{H}_2\text{O}/\text{ACN}, 90/10, \text{v/v}$ ) for on-line extraction.

A one-factor variance analysis was performed for each compound and revealed that these values are not significantly different (ANOVA for BZE,  $p$  value =  $0.10 > 0.05$ ; ANOVA for cocaine,  $p$  value =  $0.11 > 0.05$ ). Therefore, this coupling is performant. If we now compare the chromatograms obtained with the MIP and its corresponding NIP (Figure 12 B and C, respectively) under the same conditions, the selectivity contribution of the monolithic MIP is not obvious, especially for cocaine, since the recovery yields are similar on both supports. Moreover, comparing the chromatogram obtained with the direct injection and the one after preconcentration on MIP, similar peak heights were obtained for cocaine whereas there is an injected amount ratio of 2, which indicates an extraction recovery of about 50%. This highlights the necessity to optimize the extraction protocol on the monolithic MIP in order to enhance the selectivity for cocaine and BZE and their extraction recoveries.

#### II.3.3.4. Optimization of the on-line MIP extraction and nanoLC-UV analysis protocol

The optimization of the extraction procedure consisted in studying the effect of the composition and volume of the solution that ensures the transfer of the sample from the loop to the

monolithic MIP or NIP and the washing step, promoting cocaine retention on the MIP while decreasing its retention on the NIP in order to obtain an optimal selectivity. The water sample was spiked at  $1 \mu\text{g mL}^{-1}$  with cocaine. Three different compositions for the transfer/washing solution were studied: 10%, 20%, and 30% of ACN in  $\text{H}_2\text{O}$ .

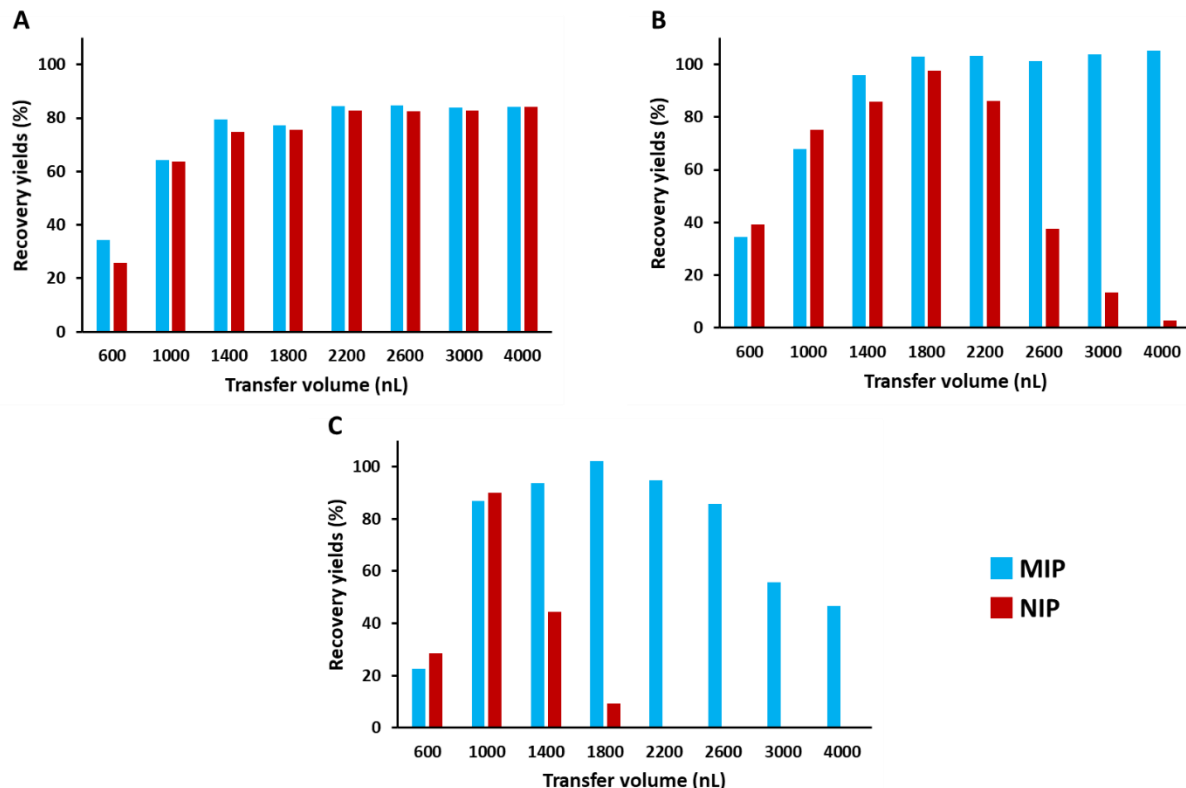


**Figure 13.** Effect of the volume and the composition of the transfer and washing solution, a  $\text{H}_2\text{O}/\text{ACN}$  mixture with a ratio (A) 90/10, (B) 80/20, or (C) 70/30 (v/v), on the extraction recovery of cocaine on MIP and on NIP, synthesized with a  $(\text{M}+\text{CL})/\text{P}$  ratio of 15/85, after the injection of 50 nL of water spiked with cocaine ( $1 \mu\text{g mL}^{-1}$ ).

The resulting histograms, reported in **Figure 13**, show first an increase of the extraction recoveries of cocaine with an increase in the volume of the solution, whatever its ACN content, indicating that the presence of a void volume in the set-up (mainly due to connecting capillaries) necessitates the use of a volume of solution higher than 1000 nL to ensure the whole transfer of the sample from the loop to the MIP or NIP. For a solution containing 10% of ACN (**Figure 13 A**), the elution strength is too weak to remove cocaine from the NIP. With a higher elution strength using 20% of ACN, cocaine is gradually eluted from the NIP with a washing volume of more than 2200 nL while it is still

retained on the MIP, highlighting the selective contribution of the MIP cavities in the retention process (**Figure 13 B**). The optimal washing volume for cocaine is between 3000 and 4000 nL, since it is possible to observe an almost total loss of cocaine from the NIP (recovery of only 3-13%) keeping a recovery of about 100% on the MIP. In addition, when the elution strength is still increased up to 30% of ACN, a recovery close to 100% is still obtained on the MIP while it is reduced to 9% on the NIP for a volume of 1800 nL (**Figure 13 C**). With a volume higher than 1800 nL, the breakthrough volume of cocaine is exceeded on both sorbents. Finally, a washing volume of 1800 nL with H<sub>2</sub>O/ACN mixture (70/30, v/v), was selected for extraction of cocaine from biological matrices corresponding to the condition giving rise to an optimal selectivity with a minimal washing volume.

Similar experiments were next carried out with BZE. Results reported on **Figure 14** show that the retained conditions of washing for cocaine extraction (1800 nL, H<sub>2</sub>O/ACN mixture (70/30, v/v)) caused the breakthrough of BZE on both sorbents.

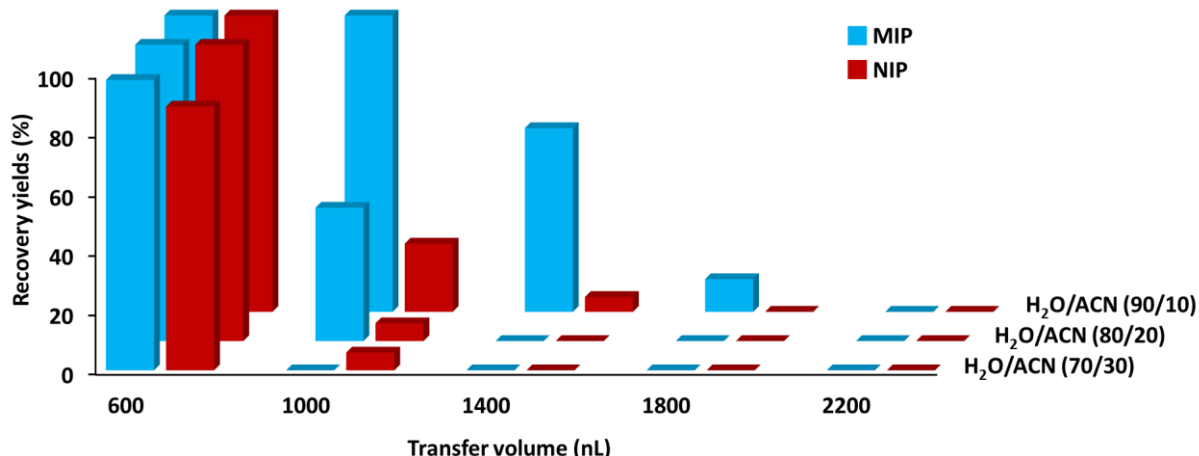


**Figure 14.** Effect of the volume and of the composition of the transfer and washing solution, a H<sub>2</sub>O/ACN mixture with a ratio 90/10, 80/20 or 70/30 (v/v), on the extraction recovery of BZE on MIP and on NIP, synthesized with a (M+CL)/P ratio of 15/85, after the injection of 50 nL of water spiked with BZE (1 µg mL<sup>-1</sup>).

It was therefore imperative to reduce the elution strength of the washing solution and the best results were obtained with a solution containing 10% of ACN and a volume of 1000 nL. Indeed, in that case, the retention of BZE on the MIP is total while the recovery is only 23% on the NIP. This difference confirms the selectivity of the monolithic MIP for this metabolite, already demonstrated by the

imprinted factor value. It is also worthwhile to notice that the MIP made with cocaine as template molecule has a lower affinity for BZE than for cocaine. This confirms previous results obtained using conventional cocaine-based MIP particles packed in a SPE cartridge [134]. The optimal selective extraction of BZE is then achieved with a solution whose volume and elution strength are much lower than those of cocaine, making the protocols for each analyte incompatible.

#### ***II.3.3.5. Applications to biological samples***

The potential of the monolithic MIP coupled on-line to nanoLC-UV analysis was first evaluated for the extraction of cocaine from human plasma sample. The plasma was treated with ACN (50%, v/v) for protein precipitation and centrifuged. This treated plasma sample was either analyzed directly or after spiking with cocaine to obtain a concentration of  $50 \text{ ng mL}^{-1}$  in the supernatant, which corresponds to  $100 \text{ ng mL}^{-1}$  in plasma equivalent. A volume of 50 nL was injected and transferred to the monolithic MIP with 1800 nL of a  $\text{H}_2\text{O}/\text{ACN}$  mixture (70/30, v/v), that was further eluted by the mobile phase to the nanoLC column. The resulting chromatogram is presented **Figure 15 A**. By comparing it with the chromatogram obtained for a blank plasma (**Figure 15 C**) under the same conditions, it appears that cocaine is extracted from the plasma sample and can be easily quantified. Moreover, the selectivity of the monolithic MIP allows the removal of the interfering compounds present in plasma, as both chromatograms have a clean baseline. The selectivity is further demonstrated with the extraction of the same spiked plasma sample on the NIP (**Figure 15 B**). The peak corresponding to cocaine is much less intense on the NIP than on the MIP, reflecting results consistent with those obtained previously in spiked water.

To evaluate the potential of this on-line coupling, the extraction recoveries were determined by injecting the spiked plasma sample in triplicate on the monolithic MIPs and NIPs resulting from three independent syntheses. The recoveries are reported in **Table 14**. For MIPs, they are similar to those obtained with pure spiked water ( $96.9 \pm 4.6\%$ ,  $n = 3$ ), thus showing no matrix effects. In the case of the NIPs, recoveries were not reported in **Table 14** as peak heights of cocaine were below the LOQ value previously determined ( $8 \text{ ng mL}^{-1}$ ), which corresponds to recoveries lower than 16%. The difference between the recovery values obtained for MIP and NIP demonstrates that the high selectivity of the MIP for cocaine, already demonstrated in pure media, is preserved in this biological fluid and allows the removal of interfering compounds. This removal is definitely a strong advantage for the possible future coupling of this nanoLC device to mass spectrometry. Indeed, despite its high sensitivity, this detection mode suffers from matrix effects. The use of a MIP will reduce the risk of ion

suppression often observed while applying such a detection device to trace analysis of a compound in a complex sample.

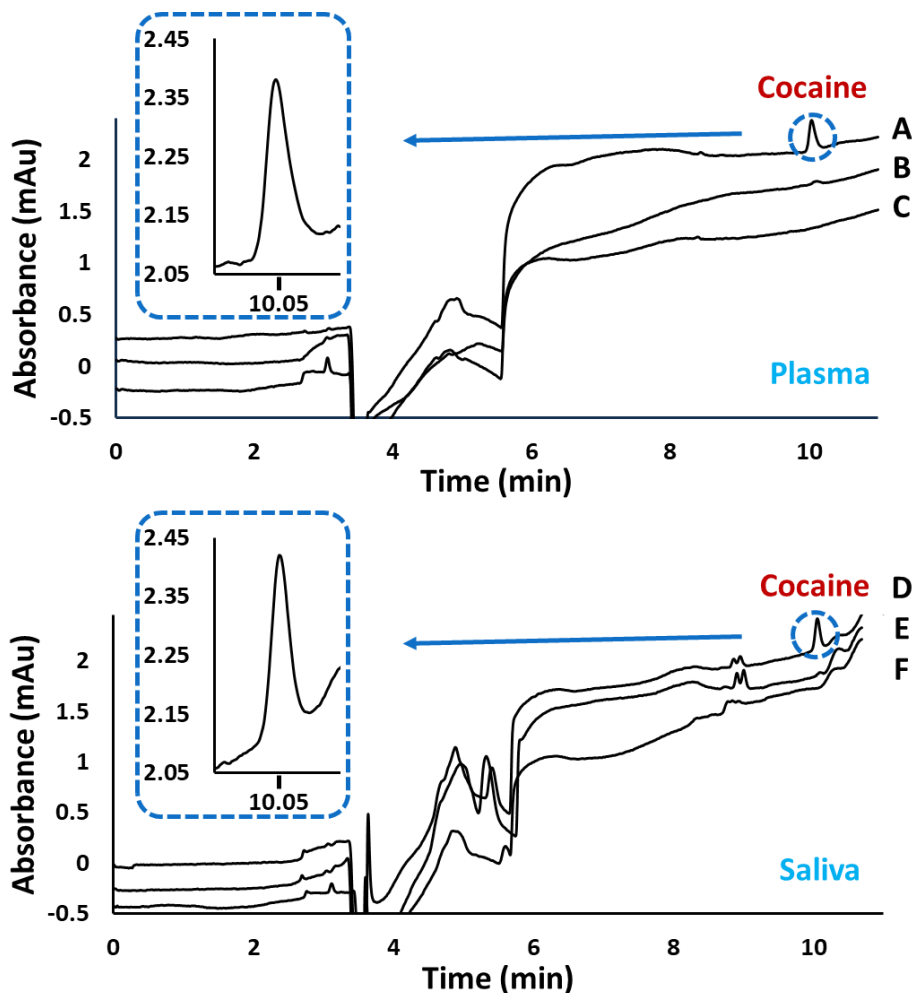


**Figure 15.** Chromatograms obtained after the extraction on MIP (A) and NIP (B) of 50 nL of plasma spiked with cocaine (equivalent to 100 ng mL<sup>-1</sup> in plasma) compared to the blank plasma (C) on MIP and chromatograms obtained after the extraction on MIP (D) and NIP (E) of 50 nL of saliva spiked at 50 ng mL<sup>-1</sup> with cocaine compared to the blank saliva (F) on MIP. Transfer and washing step: 1800 nL of H<sub>2</sub>O/ACN (70/30, v/v).

Focusing on repeatability, the recoveries have low RSD values, between 3.8 and 5.8%, for three extractions on one given monolithic MIP, and 7.5% for the intermediate reproducibility. Therefore, the repeatability of the synthesis of this miniaturized sorbent and of the SPE procedure is fully satisfactory.

**Table 14.** Repeatability and intermediate reproducibility of the extraction recoveries of cocaine obtained for the analysis in triplicate of 50 nL of the spiked plasma sample (equivalent to 100 ng mL<sup>-1</sup> in plasma).

MIP synthesis number	Repeatability of the extraction recoveries		Intermediate reproducibility of the extraction recoveries	
	Average extraction recovery (%)	RSD, n = 3 (%)	Average extraction recovery (%)	RSD, n = 3 (%)
1	98.7	4.9		
2	85.4	5.8	92.3	7.5
3	92.8	3.8		

It is important to confront the performance of our miniaturized analytical method with the concentration levels of cocaine commonly found in consumer samples. Gameiro *et al.* conducted a study on blood samples obtained *in vivo* or post-mortem and cocaine concentrations ranged from 14 to 12,111 ng mL<sup>-1</sup> (31 cases) [176]. For Fiorentin *et al.*, the average concentration in salivary, urinary or plasma samples was 144.7 ng mL<sup>-1</sup> with an amplitude of 19,272 ng mL<sup>-1</sup> (93 cases) [177]. In addition, a French decree defines a positivity threshold of 10 ng mL<sup>-1</sup> for the screening of cocaine in saliva and blood matrices [153]. It is therefore necessary to target cocaine in low concentrations to comply with the current legislation but with a wide linear range. In this sense, the optimized protocol based on a miniaturized monolithic MIP was evaluated by injecting in triplicate the plasma sample spiked with different concentrations of cocaine ranging from 10 to 1,000 ng mL<sup>-1</sup>, corresponding to 20–2,000 ng mL<sup>-1</sup> in plasma equivalent. Obtained recoveries and RSD values are reported in **Table 15**. The plotting of the concentration determined as a function of the injected concentration from 100 to 2,000 ng mL<sup>-1</sup> (not shown) had a linear shape with a R<sup>2</sup> of 0.999, thus indicating that the MIP capacity was not reached for these injected amounts. The LOD and LOQ were estimated for cocaine at 7.7 and 25.5 ng mL<sup>-1</sup> in plasma equivalent, respectively. These limits can be improved by increasing the injection volume up to 100 nL of plasma sample. In that case, LOD and LOQ values of 4.3 and 14.5 ng mL<sup>-1</sup> were obtained, respectively. Therefore, it is possible to conclude that the developed approach fulfills the application requirements.

To further evaluate the potential of the monolithic MIP, another biological matrix, saliva, was studied. Injections were carried out with filtered saliva samples, spiked at 10 and 50 ng mL<sup>-1</sup> with cocaine. The same transfer/washing procedure as for plasma was applied. Chromatogram obtained for

an injection of 50 nL of saliva spiked at 50 ng mL<sup>-1</sup> with cocaine is available in **Figure 15 D**. Cocaine peak can be clearly identified by comparison with the blank saliva performed with the same conditions (**Figure 15 F**). Once again, the baseline of the resulting chromatogram is cleaned of the majority of the interfering components from the biological matrix. In addition, selectivity is demonstrated by the extraction of the same spiked saliva sample on the NIP (**Figure 15 E**). The peak corresponding to cocaine is much less intense on the NIP than on the MIP, reflecting coherent results with those obtained previously. LOD and LOQ for MIP of 1.8 and 6.1 ng mL<sup>-1</sup>, respectively, were obtained for cocaine in saliva sample for an injected volume of 100 nL. Recovery values achieved for cocaine at two spiking levels and injected volumes are available in **Table 15**.

**Table 15.** Determination of cocaine in spiked plasma or saliva samples by selective extraction on the monolithic MIP coupled on-line to nanoLC-UV

Nature of matrix	V <sub>inj</sub> (nL)	Spiked concentration (ng mL <sup>-1</sup> )	Average recovery (%)	RSD n = 3 (%)	LOD (ng mL <sup>-1</sup> )	LOQ (ng mL <sup>-1</sup> )
Water	50	1000	96.9	4.7	3.6	12.0
Plasma	100	20*	89.8	5.2	4.3	14.5
	50	100*	98.7	4.9	7.7	25.5
		200*	96.4	3.1		
		400*	98.8	1.6		
		2000*	100.4	1.2		
Saliva	100	10	88.6	11.1	1.8	6.1
	50	50	92.6	4.7	4.2	13.9

\* Concentration in plasma equivalent

Similar performances as for plasma samples were obtained in terms of recovery and of repeatability, demonstrating the high potential brought by this approach for the selective extraction of cocaine from saliva too. A one-factor variance analysis (nature of the matrix, *i.e.* water, plasma, or saliva) was performed and revealed no significant difference between the three matrices (ANOVA, *p* value = 0.08 > 0.05), confirming the absence of matrix effect. However, for the future of the project

and more particularly the analysis of samples from consumers, it should be necessary to apply a corrective factor taking into account the recovery yields obtained in this work. But before that, it will be interesting to transfer the developed device to a microchip format in order to fully exploit the potential of this work.

#### **II.3.4. Conclusion**

The objective of this work was to demonstrate the possibility to couple on-line a selective extraction on a monolithic MIP prepared in a 100 µm i.d. capillary with nanoLC for the analysis of a targeted compound at trace level in a complex sample. For this, cocaine was taken as model molecule for the *in situ* synthesis of the monolithic MIP in a capillary. The most promising monolithic MIP resulting from the use of MAA, TRIM, and ACN containing 10% isoctane for its synthesis, demonstrated a high selectivity in pure media for the retention of cocaine and its main metabolite, BZE. Furthermore, particular care has been taken to evaluate the repeatability of permeability and selectivity for independent syntheses.

To optimize the selectivity of the extraction on the MIP coupled on-line with nanoLC-UV, various compositions and volumes of the washing solution were studied to transfer samples spiked with both targeted analytes to the MIP while reducing the contribution of non-specific interactions (controlled by the use of the NIP in parallel). The optimized conditions were further applied to the on-line analysis of cocaine from 50 or 100 nL of spiked plasma or saliva samples and the resulting chromatograms showed very clean baselines.

This study has showed the important contribution of the monolithic MIP for the on-line selective extraction and nanoLC separation of cocaine and its main metabolite. Some limitations were encountered in aqueous media for the extraction of BZE, but further investigations will be carried out for the synthesis of a MIP with BZE as template molecule in order to obtain stronger retention of this analyte in plasma and saliva but also in urine samples. Finally, the successful miniaturized coupling of the monolithic MIP to nanoLC paves the way for the integration of this technology into a microfluidic chip for the development of a lab-on-chip with a possible UV, fluorescent, or electrochemical detection to provide a miniaturized and portable device. In addition, this miniaturized approach could target other applications and analytes, by modifying the nature of the molecular template used for the synthesis of the monolithic MIP.

### II.3.5. Etude complémentaire en vue d'améliorer la rétention de la BZE

Des essais complémentaires ont été menés pour tenter d'augmenter la rétention de la BZE sur le MIP en conservant la sélectivité. Pour cela, le pH de la solution assurant le transfert des analytes cibles de la boucle d'injection vers le MIP et le lavage a été étudié. En effet, le groupement acide de la BZE est déprotoné au pH physiologique faisant de cette espèce un composé zwitterionique. En se plaçant en conditions acides, cette fonction est protonée et alors neutre et il serait donc possible de renforcer les interactions entre la BZE et les cavités spécifiques du MIP en développant davantage les interactions par liaisons hydrogène et en réduisant les répulsions électrostatiques entre la charge négative de la BZE et celles également moins présentes alors à la surface du polymère et des cavités.

Afin de se placer dans des conditions pouvant satisfaire une rétention sélective simultanée de la cocaïne et de la BZE sur le MIP, une solution de transfert et de lavage acidifiée à pH 3 et contenant 20% d'ACN a été utilisée pour extraire des échantillons de 50 nL d'eau dopée à  $1 \mu\text{g mL}^{-1}$ . Différents volumes de cette solution de transfert et de lavage ont été testés (de 600 à 1800 nL) puis la désorption-séparation en ligne a été réalisée dans les conditions déterminées précédemment. Les résultats obtenus sont reportés sous forme d'histogrammes en **Figure 16**. Dans ces conditions, le profil de rétention de la BZE sur le MIP est similaire à celui obtenu avec la même solution de transfert et de lavage à pH neutre (**Figure 14**). En revanche, ce protocole d'extraction n'est pas sélectif puisque les mêmes performances sont obtenues pour le NIP.

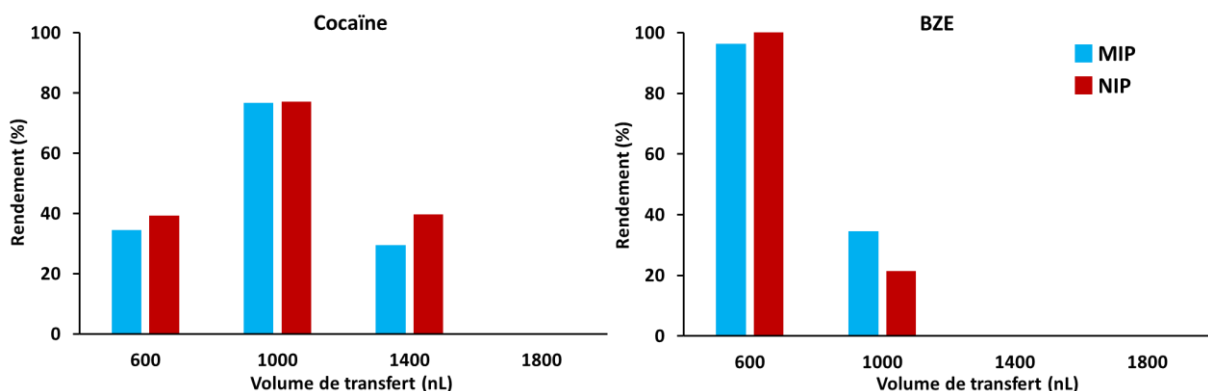


**Figure 16.** Effet du volume d'une solution de transfert et de lavage acidifiée à pH 3 et contenant 20% d'ACN sur les rendements d'extraction de la cocaïne et de la BZE ( $1 \mu\text{g mL}^{-1}$  dans l'eau) sur le MIP et le NP synthétisés avec un rapport  $(M+CL)/P$  de 15/85.

Par ailleurs, la rétention de la cocaïne sur le MIP est drastiquement réduite par rapport aux conditions utilisant une solution à pH neutre. En effet, il est possible d'observer la perte de cocaïne sur le MIP et le NIP dès 1400 nL de solution de transfert et de lavage alors que les résultats obtenus précédemment montraient une rétention de celle-ci jusqu'à 1800 nL pour le NIP et supérieur à 4000 nL pour le MIP (**Figure 13**). Comme l'état de charge de la cocaïne n'a pas été modifié entre un pH neutre et une valeur de 3 (une charge positive), c'est sans doute la diminution du degré d'ionisation, et donc de la charge négative, des groupements présents à la surface des polymères et des cavités avec le pH qui a eu un rôle prédominant. Il semble donc que les interactions électrostatiques aient un rôle clé dans le mécanisme de rétention.

L'utilisation d'une solution de transfert et de lavage acidifiée pour favoriser la rétention de la BZE lors de l'étape d'extraction n'a donc pas permis d'apporter une amélioration. De plus, une détérioration de la rétention et de la sélectivité a été constatée pour la cocaïne. Des travaux complémentaires sur la voie de synthèse semblent donc nécessaires afin de résoudre cette problématique.

## II.4. Conclusion

L'étude réalisée dans ce chapitre a permis d'obtenir un MIP monolithique miniaturisé pour extraire sélectivement la cocaïne avant un couplage en ligne à la nanoLC pour son analyse à l'état de trace dans des échantillons biologiques. Après avoir étudié les voies de synthèse privilégiées pour extraire de façon exhaustive la cocaïne et la BZE au format conventionnel, la cocaïne a été sélectionnée comme molécule empreinte pour la synthèse *in situ* dans des capillaires de 100 µm de diamètre interne. Les MIP monolithiques les plus prometteurs ont été synthétisés avec le MAA comme monomère fonctionnel, le TRIM en tant qu'agent réticulant, un solvant porogène constitué d'ACN contenant 10% d'isooctane et un ratio molaire T/M/CL de 1/4/20. Le ratio (M+CL)/P a quant à lui été fixé à 15/85 (v/v) après des études de perméabilité et de facteur d'impression. Ce support a démontré une grande sélectivité en milieu pur pour la rétention de la cocaïne et de la BZE ainsi que des répétabilités très satisfaisantes pour les différentes caractérisations menées sur des synthèses indépendantes.

Le MIP a ensuite été couplé en ligne à la nanoLC-UV. Diverses compositions et volumes de solution ont été étudiés pour transférer et extraire sélectivement la cocaïne et la BZE d'échantillons aqueux dopés. Dans le cas de la cocaïne, les conditions optimisées ont ensuite été appliquées à son analyse en ligne à partir de 50 ou 100 nL d'échantillons de plasma ou de salive dopés et les

chromatogrammes obtenus ont montré une élimination de la majorité des interférents. En revanche, certaines limitations ont été rencontrées pour l'extraction de la BZE en milieu pur. Malgré l'acidification de la solution de transfert et de lavage pour favoriser la rétention de cette dernière, il semble que le développement d'une autre voie de synthèse soit nécessaire.

## **CHAPITRE III**

**Monolithes à empreintes moléculaires pour la détection  
directe de la benzoylecggonine**



## **CHAPITRE III – Monolithes à empreintes moléculaires pour la détection directe de la benzoylecgonine**

Dans le chapitre précédent, un monolithe imprimé et miniaturisé a été intégré avec succès dans un montage en ligne afin d'extraire sélectivement la cocaïne dans des échantillons d'urine et de plasma humain avant une séparation en nanoLC. En revanche, le protocole d'extraction optimisé en milieu pur pour la BZE n'était pas suffisamment rétentif pour permettre l'extraction simultanée de ce métabolite avec la cocaïne dans des échantillons biologiques. Toutefois, le MIP synthétisé a démontré une sélectivité en milieu pur pour la BZE puisqu'un facteur d'impression de  $2,2 \pm 0,3$  a été déterminé.

Dans ce chapitre, il a donc été décidé de tirer avantage de la sélectivité du monolithe imprimé pour la BZE afin de simplifier le dispositif en supprimant la colonne analytique et en couplant directement l'extraction sur le MIP à la détection UV.

Ce chapitre se présente sous la forme d'un article rédigé en anglais, en cours de soumission : « Simplified miniaturized set-up based on molecularly imprinted polymer for the determination of benzoylecgonine in urine samples », T. Bouvarel, N. Delaunay, V. Pichon.



---

## **Article 2 : Simplified miniaturized set-up based on molecularly imprinted polymer for the determination of benzoylecgonine in urine samples**

Thomas Bouvarel<sup>a</sup>, Nathalie Delaunay<sup>a</sup>, Valérie Pichon<sup>a,b</sup>

<sup>a</sup> Laboratoire des Sciences Analytiques, Bioanalytiques et Miniaturisation - UMR Chimie Biologie Innovation 8231, ESPCI Paris, CNRS, PSL University, 75005 Paris, France

<sup>b</sup> Sorbonne Université, 75005 Paris, France

---

### **III.1. Abstract**

A simple, selective, and sensitive method involving solid phase extraction with molecularly imprinted polymer (MIP) directly coupled on-line to UV detection was developed for the determination of benzoylecgonine (BZE) in complex biological samples. Monolithic MIPs were prepared into 100 µm internal diameter fused-silica capillaries by UV polymerization using cocaine as dummy template, methacrylic acid as functional monomer, and trimethylolpropane trimethacrylate as cross-linker. The homogeneous morphology of the monolithic MIP was evaluated by scanning electron microscopy prior to measuring its permeability. Its selectivity was evaluated using the monolithic MIP as a stationary phase in nanoLC, leading to imprinting factors of  $4.0 \pm 0.6$  and  $2.7 \pm 0.1$  for cocaine and BZE, respectively, on polymers resulting from three independent syntheses, showing both the high selectivity of the MIP and the reproducibility of its synthesis. After selecting the appropriate capillary length and the set-up configuration and optimizing the extraction protocol to promote selectivity, the extraction of BZE present in spiked human urine samples was successfully carried out on the monolithic MIP and coupled on-line with a UV detection. The very clean-baseline of the resulting chromatogram revealing only the peak of interest for BZE illustrated the high selectivity brought by the monolithic MIP. Limits of detection and quantification of  $56.4 \text{ ng mL}^{-1}$  and  $188.0 \text{ ng mL}^{-1}$  were achieved in urine samples, respectively. It is therefore possible to achieve analytical thresholds in accordance with the legislation on cocaine consumption without the need for an additional chromatographic separation, allowing further simplification and miniaturization of the set-up.

### III.2. Introduction

Miniaturization has become a major issue in analytical chemistry whatever the field of application, be it clinical, environmental, food, toxicological, etc. and whatever the nature of the target compounds. The potential benefits of miniaturization are enormous, following the principle that small-scale processes consume less time, samples, and reagents [30]. One of the main objectives is to achieve a micro total analytical system ( $\mu$ -TAS), concept introduced by Manz *et al.* [31] in the 90's and also called lab-on-chip, with integration of the various steps of the analytical methods including sampling, sample handling, separation, and detection in a single device. However, in some cases, miniaturization can have detrimental effects on separation, because the reduction of the separation lengths can lead to a loss of separation power, which is crucial to overcome the complexity of samples, especially when target analytes are present at trace levels. In this context, the introduction of a selective sample pre-treatment step into miniaturized devices seems very interesting.

Solid phase extraction (SPE) is routinely used for the extraction of compounds from liquid samples or solid matrix extracts [178,179]. Many works have demonstrated the feasibility of miniaturization for this technique by the possibility to *in situ* synthesize organic monolith into capillary or chip channel [180–185]. However, the extraction on polymeric sorbent results from non-selective interactions dependent on the polarity of the molecules, which lead to co-extraction of compounds with polarities similar to the targets. To overcome this lack of selectivity, various extraction supports leading to a molecular recognition mechanism have been developed such as molecular imprinted polymers (MIPs). These sorbents are synthetic polymers possessing specific cavities with steric and functional complementarity towards a template molecule. They offer many advantages including chemical and thermal stability but also easy, cheap, and rapid preparation for a wide variety of applications such as drug delivery [3–5], sensors [6–9], biomimetic catalyst in organic synthesis [10], separation of structural analogs and enantiomers [16], or extraction [18].

The use of MIPs as selective extraction sorbents was first described by Sellergren and co-workers in 1994 for the extraction of pentamidine from urine [186]. Since then, there has been a growing interest in this field, whether for the selective recognition of small molecules, such as drugs, pesticides, or other environmental pollutants [19–24], of proteins [25–27], or even of microorganisms [28]. MIPs for extraction applications have been mainly used in particles form for off-line extraction by packing these particles into a cartridge between frits or by dispersing these particles in samples [18].

MIPs can also be integrated into miniaturized devices in order to incorporate selective processing steps, especially when the template, essential for MIP synthesis, is expensive or difficult to

synthesize. Several authors succeeded in introducing imprinted phases for exhaustive and miniaturized extraction in SPE by the synthesis of thin films [64,65], by packing MIP particles in specially designed chips [67,68], or by grafting MIP on the surface of a core monolith [49,88,124]. Another approach consists in synthesizing a monolithic porous imprinted polymer directly inside capillaries and chip microchannels. Indeed, monoliths are a way of overcoming the constraints related to the use of particles (immobilization, homogeneous packing...) or thin films (low amount of phase).

Miniaturized monolithic MIPs were first reported for chiral separations in capillary electrochromatography by Schweitz *et al.* [37,38] before being applied to extraction purposes. Recently, monolithic MIPs were developed for extractions in different miniaturized devices, such as pipet-tips [128,132], hollow-fiber membranes [167], or capillaries with internal diameter (i.d.) of 500 µm [47,117,119] used off-line before conventional analysis. Another significant part of the studies focused on the on-line coupling of monolithic MIPs prepared in capillaries of 250-530 µm i.d. [45,91,92,94] with separation columns with conventional i.d. of 2.1 [94] or 4.6 mm [45,91,92]. Besides, to our knowledge, only two works are related to the on-line coupling of a capillary containing a MIP (100 µm i.d.) with a capillary separation column [49,90]. One of them described the synthesis of a MIP grafted on the surface of a poly(trimethylolpropane trimethacrylate) core monolith [49]. The second one, reported by our group, is related to the direct *in situ* synthesis of a monolithic MIP filling the entire section of the capillary [90].

In this last case, the monolithic MIP (50 mm x 100 µm i.d.) was coupled on-line with nano-liquid chromatography (nanoLC) for the determination of cocaine in plasma and saliva samples [90]. The MIP was obtained with methacrylic acid (MAA) as monomer, trimethylolpropane trimethacrylate (TRIM) as cross-linker, acetonitrile (ACN) containing 10% isoctane as porogen, and thermal initiation at 60°C. Retention measurements in pure media showed the high selectivity of this MIP for cocaine and its main metabolite benzoylecgonine (BZE). The on-line coupling of this MIP with nanoLC-UV allowed the determination of cocaine with a limit of quantification (LOQ) of 6.1 and 14.5 ng mL<sup>-1</sup> while injecting only 100 nL of saliva or 2 times diluted plasma, respectively.

In a constant effort to miniaturize and simplify the analytical device, the aim of this work was to take maximum advantage of the selectivity of the monolithic MIP to remove the separation column and to on-line couple the monolithic MIP directly for selective extraction of target analytes from biological fluids with UV detection. As the previous study mainly showed the potential of MIP for cocaine [90], this study focused on the possibility to develop a system adapted to the survey of cocaine consumers by developing an analytical device allowing the detection of BZE, the main urinary metabolite of cocaine. First, the cocaine imprinted poly(MAA-co-TRIM) monolith from the previous

study [90] was employed to investigate the feasibility of such a simple device applied to a pure medium. In order to reduce the length of the monolith, thermal initiation was replaced by UV initiation. The resulting monoliths were compared in terms of permeability and selectivity. Then, a 10 mm length monolithic MIP was coupled on-line with UV detection and analyses of BZE present in spiked urine samples were carried out.

### **III.3. Experimental**

#### **III.3.1. Chemicals and reagents**

Stock solutions at 1 mg mL<sup>-1</sup> of BZE in MeOH and cocaine base were provided by Sigma-Aldrich (Saint-Quentin-Fallavier, France). The working solutions at 1 µg mL<sup>-1</sup> were obtained by dilution of the stock solution (1 mg mL<sup>-1</sup>) in HPLC-grade ACN (Carlo Erba, Val-de-Reuil, France). These solutions were stored at -20°C. MeOH, EtOH, and isoctane were purchased from Carlo Erba. Acetic acid and anhydrous ACN were provided by Sigma-Aldrich. 1 M NaOH and 0.1 M HCl were obtained using deionized water (Milli-Q purification system, Millipore, Molsheim, France) and Titrisol solutions from Merck (Darmstadt, Germany).

MAA, TRIM, and 3-(trimethoxysilyl)propyl methacrylate ( $\gamma$ -MAPS) were purchased from Sigma-Aldrich. Azo-*N,N'*-diisobutyronitrile (AIBN) was purchased from Acros Organics (Noisy-le-Grand, France). MAA was distilled under vacuum in order to remove inhibitors and stored at -20°C. TRIM, AIBN, and  $\gamma$ -MAPS were of satisfactory purity so they were used without further purification. Fused-silica capillaries with a UV transparent fluorocarbon polymer coating (PTFE-coated silica capillaries, 100 µm i.d. x 375 µm o.d.) were purchased from Polymicro Technologies (Photon Lines, Saint Germain-en-Laye, France).

#### **III.3.2. *In situ* preparation of the monolithic polymers**

The monolithic polymers were prepared *in situ* in fused silica capillaries by a two-step method adapted from the procedure described in a previous work [90]. Prior to polymerization, the inner wall of the capillaries was activated to anchor the monolith with  $\gamma$ -MAPS. Briefly, the capillaries were first rinsed with water, then activated by flushing 1 M NaOH for 30 min. After a washing step with water, 0.1 M HCl was flushed for 30 min. The silanization was then achieved with 250 µL of  $\gamma$ -MAPS in 1 mL of EtOH, with a pH adjusted to 3.5 by acetic acid, for at least 1 h at room temperature. The capillaries were washed with EtOH and finally dried with nitrogen.

The template molecule (T, cocaine), functional monomer (M, MAA), cross-linking agent (CL, TRIM), and radical initiator (AIBN) were dissolved in porogen (P, ACN containing 10% isoctane) with a molar ratio T/M/CL of 1/4/20. Then the polymerization mixture was purged with nitrogen for 5 min to get rid of oxygen and introduced in 150 mm-long capillaries. After sealing both ends of the capillaries with rubber septa, two initiation modes were performed. For thermal initiation, the capillaries were immersed in a thermostated water bath at 60°C and the polymerization was allowed to proceed during 24 h. For UV initiation, the capillaries were protected with a mask so that the imprinted monolith was located only in the part of 10, 25, or 50 mm exposed to UV light. They were then placed into a Spectrolinker XL-1500 UV crosslinker from Spectronics Corporation (Westbury, NY, USA), equipped with 6 UV lamps (6 x 155 W, 365 nm), for a cycle of 30 min at room temperature. After polymerization, the capillaries containing the monolithic MIPs were connected to a nano-pump and rinsed thoroughly with several capillary volumes of ACN/acetic acid (98/2, v/v) to remove the template molecules and other residual reagents. The monolithic NIPs were obtained by performing the same procedure in the absence of the template. The resulting capillaries from the thermal initiation were cut to obtain 50 mm-long capillaries while those resulting from the UV initiation were cut to obtain 100 mm-long capillaries containing a 10, 25 or 50 mm-long monolithic MIP having its extremity at 10 mm from the outlet.

### III.3.3. Characterization of the monoliths by SEM and nanoLC

The cross section of the capillaries containing the polymer was observed by SEM, with a Quattro S environmental scanning electron microscope (ThermoFisher Scientific, Le Pecq, France).

Permeability measurements were carried out with an Ultimate<sup>TM</sup> RSLCnano 3000 system (ThermoFisher Scientific, Le Pecq, France), composed of a nanoLC pump delivering 100% ACN ( $\eta = 0.316 \text{ mPa s}$  at 35°C) at a constant temperature of 35°C with different flow rates and allowing to record the generated backpressure. The permeability was calculated using Darcy's law (**Equation 1**):

$$K = \frac{4\eta LF}{\pi d_i^2 \Delta P} \quad (\text{Equation 1})$$

K is the permeability ( $\text{m}^2$ ), F the applied flow rate ( $\text{m}^3 \text{ s}^{-1}$ ),  $\eta$  the viscosity of the solvent ( $\text{Pa s}$ ), L the length of the capillary (m),  $\Delta P$  the measured backpressure (Pa), and  $d_i$  the capillary inner diameter (m).

For retention studies, cocaine ( $5 \mu\text{g mL}^{-1}$ ) and BZE ( $5 \mu\text{g mL}^{-1}$ ) were injected on the monolithic MIP or NIP contained in a capillary connected to a nanoLC system composed of a six-port switching nano-valve (Cheminert nanovolume 6 ports 2 pos 1/32", manual CN2-4346, Vici Valco Instruments Inc. Co., Houston, TX, USA) connected to a home-made injection loop (50 nL), to a nano-pump (NCP-3200RS Nano Pump, ThermoFisher Scientific Dionex, controlled by Chromeleon 6.80 SR12) and to a diode array detector (VWD 3100 Detector, ThermoFisher Scientific Dionex) with a flow cell of 3 nL. The capillaries containing the MIP or NIP were maintained at  $35^\circ\text{C}$  with a column oven (TCC 3000SD column compartment, ThermoFisher Scientific Dionex). Compounds were detected at 233 nm. The flow rate of ACN was set at  $400 \text{ nL min}^{-1}$ . The marker used to determine the dead volume was acetone. Imprinting factors (IF) and retention factors  $k$  were calculated using the following **Equation 2** and **Equation 3**:

$$\text{IF} = \frac{k_{\text{MIP}}}{k_{\text{NIP}}} \quad (\text{Equation 2})$$

where  $k_{\text{MIP}}$  and  $k_{\text{NIP}}$  are the retention factors obtained on the MIP and the NIP monolithic columns, respectively.

$$k = \frac{t_r - t_0}{t_0} \quad (\text{Equation 3})$$

where  $t_r$  and  $t_0$  are the retention times of cocaine or BZE and of acetone, respectively.

### III.3.4. On-line coupling of MIP or NIP extraction with direct UV detection

Preliminary studies were performed with the on-line set-up previously designed [90] and allowing the coupling of monolithic MIP/NIP thermally synthesized to the nanoLC-UV device as presented in **Figure S4 (Appendix 4)**. Briefly, it consisted in a syringe pump (Standard Infuse/Withdraw PHD ULTRA™ 4400 Programmable Syringe Pump, Harvard apparatus, Les Ulis, France) connected to a six-port switching nano-valve (valve 1). Valve 1, was connected to an injection loop and to another six-port switching nano-valve (valve 2). Valve 2 was connected to a nanoLC pump (Ultimate™ NanoFlow RSLC system, ThermoFisher Scientific Dionex), to the MIP or the NIP (50 mm x 100  $\mu\text{m}$  i.d., associated with an empty capillary (80 mm x 26  $\mu\text{m}$  i.d.) to allow their connection to the valve), and to the analytical column (Acclaim™ PepMap™ 100 C18, 150 x 0.075 mm, 3  $\mu\text{m}$ , ThermoFisher Scientific).

In the first step of the extraction procedure, 50 nL of sample were transferred from the loop to the monolithic MIP/NIP capillary using 1000 nL of a  $\text{H}_2\text{O}/\text{ACN}$  mixture (90/10, v/v), delivered by the syringe pump at a flow rate of  $200 \text{ nL min}^{-1}$ . The valve 2 was then switched allowing the elution of the

trapped compounds from the monolithic MIP/NIP to the nanoLC analytical column by the mobile phase delivered by the nanoLC pump at  $200 \text{ nL min}^{-1}$ , *i.e.* ammonium formate 10 mM pH 3.1 adjusted with formic acid (A) and ACN (B). The gradient started with 10% B, increased to 25% B in 1.5 min, then reached 40% B in 5.6 min, increased to 80% B in 0.8 min, and remained for 2.4 min. Finally, the composition of B was set back to 10% to let the system equilibrate.

The on-line set-up allowing the coupling of the extraction with the monolithic MIP or NIP directly to the UV detection in a nano-flow device is presented in **Figure 17 A**. The solution of transfer and washing, and next the elution solution were percolated owing to a nanoLC pump (Ultimate<sup>TM</sup> NanoFlow RSLC system, ThermoFisher Scientific Dionex) connected to the two six-port switching nano-valves, valve 1 and valve 2. Valve 1 was connected to home-made injection loops (150, 300, or 600 nL) and to valve 2. Valve 2 was connected to the MIP or the NIP capillary and to the UV detector. For the 50 mm-long MIP and NIP obtained by thermal initiation, they were associated with an empty capillary (80 mm x 26  $\mu\text{m}$  i.d.) downstream of them to allow their connection to the valve as presented in **Figure 17 B1**. For monoliths synthesized by UV photo-polymerization, the monolithic part was 10 mm-long and has its extremity at 10 mm from the outlet of the capillary (100 mm x 100  $\mu\text{m}$ ). Two positions of the capillary containing the monolithic MIP/NIP was studied, as shown in the **Figure 17 B2** and **B3**. All the connections were achieved with 26  $\mu\text{m}$  i.d. fused-silica capillaries (Polymicro Technologies, 360  $\mu\text{m}$  o.d.) and microtight unions PEEK (Upchurch Scientific).

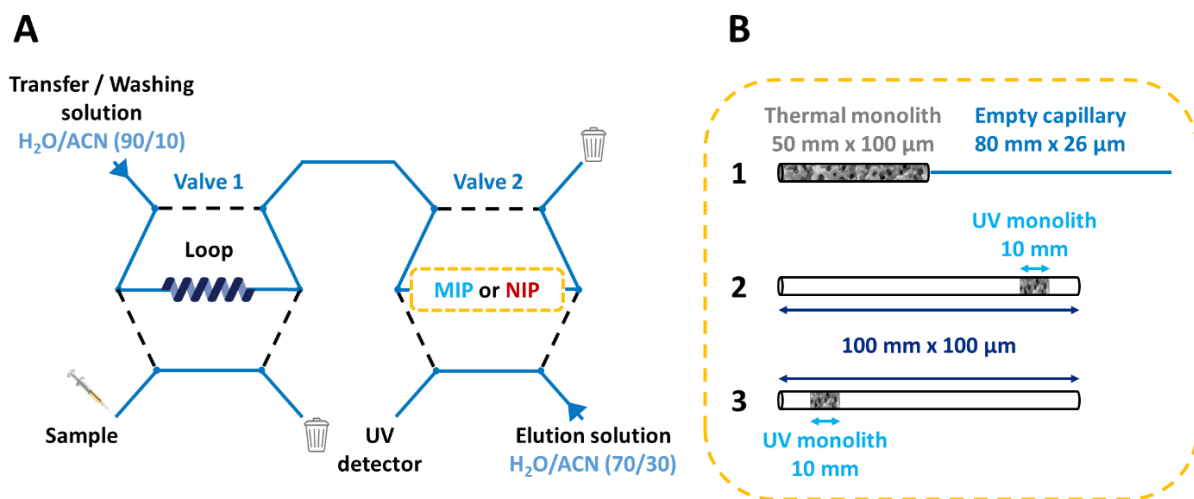


**Figure 17.** (A) On-line set-up of the monolithic MIP or NIP directly coupled to UV detection for an extraction-purification step and a subsequent elution-detection step with (B) enlargement of the monolith connection whether it results from (1) thermal or (2, 3) UV initiation of the polymerization.

In the first step of the extraction procedure, sample was loaded into the loop (150-600 nL) (valve 1). In parallel, the nanoLC pump connected to the same valve allows the conditioning of the monolith with a H<sub>2</sub>O/ACN (90/10, v/v) mixture. Then, the valve 1 was switched in order to transfer the sample to the monolithic MIP/NIP for extraction using the transfer and washing solution delivered by the nanoLC pump through the sample loop at a flow rate of 400 nL min<sup>-1</sup> with a volume that was varied between 900 and 1750 nL (optimized value used for applications: 1300 nL). In a second step, the nanoLC pump was connected to the valve 2 and the detector was conditioned with a solution of H<sub>2</sub>O/ACN (70/30, v/v). At the last step, the valve 2 was switched allowing thus the desorption of the trapped compounds from the monolithic MIP/NIP to the UV detector by the elution solution delivered by the nanoLC pump. After each analysis, the MIP/NIP monolith was re-equilibrated with the initial H<sub>2</sub>O/ACN mixture (90/10, v/v), that was used for the transfer and washing step, delivered at 400 nL min<sup>-1</sup> by the nanoLC pump before being re-used.

### **III.3.5. Preparation of biological samples**

Urine samples were collected from healthy individual and were free of cocaine and BZE. 500 µL of urine sample were first diluted with H<sub>2</sub>O (x2). The sample was then filtered with 0.45 µm pore size Millex® syringe filters from Merck (Darmstadt, Germany) and stored at -20°C until use. The treated urine samples were either directly analyzed or spiked with BZE to obtain a concentration of 150 ng mL<sup>-1</sup> in the diluted sample, which corresponds to 300 ng mL<sup>-1</sup> in urine. A volume of 600 nL was analyzed by SPE on MIP or NIP and UV detection.

## **III.4. Results and discussion**

### **III.4.1. Preliminary study on the potential of an on-line set-up for direct extraction and detection of BZE**

The objective was to couple directly the extraction-purification step of BZE on a MIP with UV detection, without any separation step to simplify the analytical set-up. Nevertheless, the use of BZE seems to be complicated as template for MIP synthesis as it is only commercially available in solvents such as MeOH or water, that are protic solvents preventing the development of hydrogen bonds between the monomer and the template which are necessary during the polymerization step to give rise to specific cavities. However, in a previous study, a cocaine imprinted poly(MAA-co-TRIM) monolith was *in situ* synthesized using cocaine as template in a fused-silica capillary (50 mm x 100 µm

i.d.) by thermal polymerization at 60°C for 24 h in ACN containing 10% isoctane, leading to imprinting factors of  $3.2 \pm 0.5$  and  $2.2 \pm 0.3$  for cocaine and BZE, respectively [90]. Since this previous monolith showed a high selectivity for BZE, the synthesis conditions of this MIP imprinted with cocaine were selected for this study and new monoliths were synthesized. To check their retention property, they were placed at a loop position of a six-port switching valve to be connected, as in the previous study [90], to an injection loop and to the nanoLC-UV system (see set-up in **Figure S4, Appendix 4**). The extraction procedure previously optimized to promote BZE retention on the MIP while decreasing its retention on the NIP in order to obtain an optimal selectivity was again applied. It consisted in injecting 50 nL of water spiked with BZE at  $1 \mu\text{g mL}^{-1}$  followed by a transfer/washing step using 1000 nL of a mixture of H<sub>2</sub>O/ACN (90/10, v/v), the elution being further ensured by the nanoLC mobile phase to elute BZE from the monolith to the analytical column. With these conditions, the same results were obtained for BZE as it was totally recovered on the MIP and the extraction recovery was only 25% on the NIP. Those preliminary results confirmed the repeatability of the MIP synthesis and its selectivity towards BZE. This MIP was therefore adapted for studying the development of a set-up without any analytical column.

A two-valve set-up was then designed as described in **Figure 17 A**. It involves a sample loop connected to valve 1 and the capillary containing the MIP or NIP connected to valve 2. Due to instrumental constraints making the length of the capillary entirely filled by the monolith (50 mm) insufficient to connect the two ports of valve 2, this capillary was associated with an empty capillary (80 mm x 26 µm i.d.) downstream of it to allow its connection (see **Figure 17 B1**). A volume of 150 nL, instead of 50 nL previously used, of water spiked with BZE at  $10 \mu\text{g mL}^{-1}$  was introduced in the loop in order to prevent detection limit problems caused by the removal of the analytical column and thus the lack of concentration effect of the elution fraction at the top of the column. Consequently, the volume of the transfer/washing solution (H<sub>2</sub>O/ACN, 90/10, v/v) was reduced from 1000 nL to 900 nL in order to maintain a constant volume adding the volumes of the sample and of the transfer/washing solution flowing through the monolith. Finally, a back-flush elution towards the UV detector of the analytes fixed on the monolith was performed with a H<sub>2</sub>O/ACN (70/30, v/v) mixture. The chromatograms resulting from this procedure applied in triplicate on the MIP and NIP are shown in **Figure 18**. Focusing on repeatability, the peak heights have low RSD values of 2.0 and 9.3% ( $n = 3$ ) for MIP and NIP, respectively. Average peak heights of 4.83 and 0.43 mAU were obtained for the MIP and NIP, respectively. The selectivity of the MIP is thus maintained with a peak height more than 11 times higher using the imprinted monolith than using the non-imprinted one. If an extraction recovery of 100% is assumed for the MIP, as previously obtained [90], this would mean that a recovery of only 9% was obtained for the NIP. This hypothesis was further investigated by injecting on the MIP the same spiked

sample but diluted 10 times ( $1 \mu\text{g mL}^{-1}$ ). A height of 0.43 mAU was obtained, similar to the values obtained with the NIP reflecting the fact that only an amount of approximately 10% was retained on the monolithic NIP and thus confirming the selectivity of the monolithic MIP in this set-up.

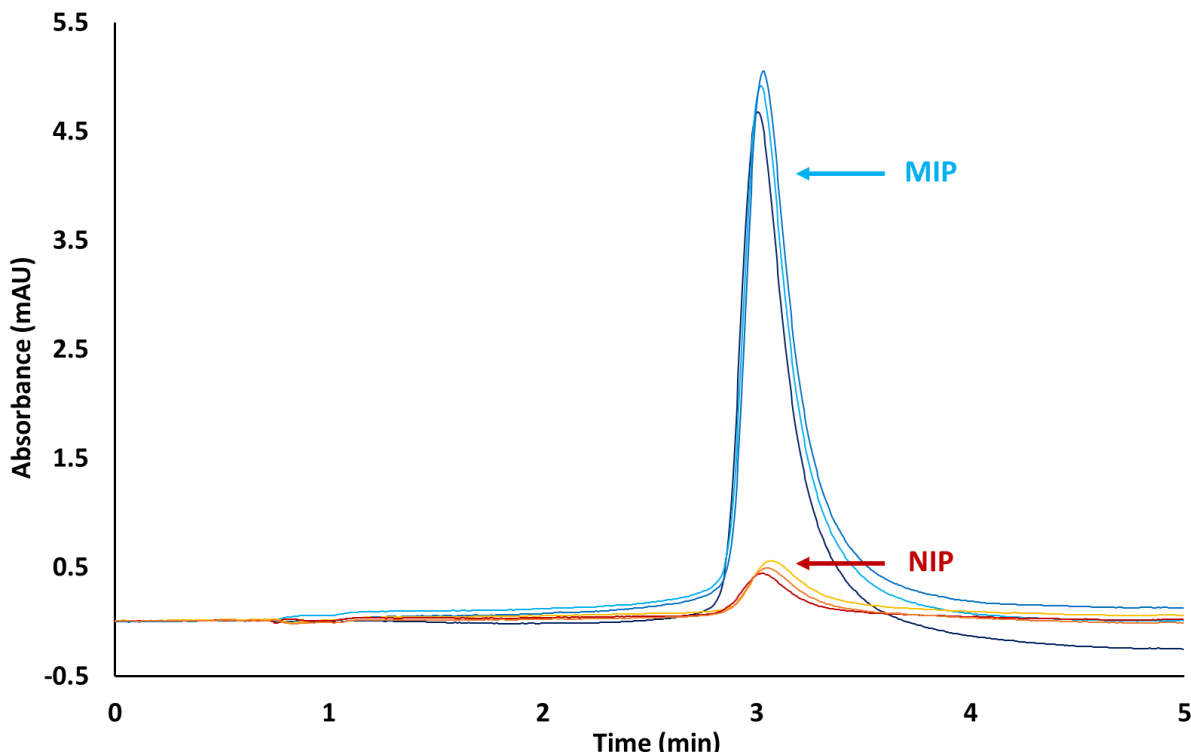


**Figure 18.** Chromatograms obtained by the direct on-line coupling of the monolithic MIP/NIP (50 mm  $\times 100 \mu\text{m}$ ) synthesized using thermal initiation with UV detection.  $V_{\text{inj}} = 150 \text{ nL}$  (BZE at  $10 \mu\text{g mL}^{-1}$  in water),  $V_{\text{washing}} = 900 \text{ nL}$  ( $\text{H}_2\text{O}/\text{ACN}$ , 90/10, v/v), UV detection at 233 nm. Other conditions: see Section III.3.4.

Despite the high selectivity obtained, the lengths of the monoliths used were still too long to develop miniaturized extraction systems. As the capacity of the 50 mm-long monolithic MIP did not seem to be reached even with a concentrated sample ( $10 \mu\text{g mL}^{-1}$ ), it was therefore possible to reduce the length of the monolith. If it is possible to have a small final length (< 50 mm) of a capillary entirely filled with a monolith obtained with thermal polymerization in a bath, it is however impossible to connect it to a valve from one extremity and to the second one to an empty capillary to get the final sufficient length to connect it in the loop position due to the minimal length of the required liners. Therefore, it was necessary to develop another approach based on the use of a single capillary partially filled with a monolith obtained by initiation of polymerization under UV using mask to get a monolith

with a small length (< 50 mm). However, since the MIP synthesis pathway was modified, it was necessary to verify the characteristics of the monolith in terms of permeability and selectivity.

### III.4.2. Study of the synthesis conditions

With regard to initiation conditions, our group has already compared the thermal and photo-polymerization using AIBN as initiator for the synthesis of MIPs in bulk with cocaine as template [133]. The extraction recoveries for BZE of the polymers produced by the two modes were similar for the MIPs:  $89 \pm 9\%$  and  $85 \pm 3\%$ , but not for the NIPs:  $4 \pm 3\%$  and  $12 \pm 4\%$  for UV and thermal initiation, respectively. A decrease in undesirable non-specific interactions for the polymer obtained by UV was therefore observed. Another significant advantage provided by UV initiation is the reduction of the synthesis time since thermal initiation was previously performed for 24 h while the UV exposure was only performed for few minutes or hours. In addition, UV polymerization provides an answer to instrumental issues, as previously mentioned, because it allows to obtain monoliths of any length in a capillary of sufficient length to fix it on a valve, since the monolithic length depends only on the capillary window exposed to UV light. It is for all these reasons that this way of synthesis appeared as an excellent option. Nevertheless, it was necessary to adapt it to the miniaturized capillary format, which had not yet been done.

To limit the template consumption, preliminary evaluations of the effect of exposure time to UV irradiation (15, 30, 60 or 120 min) on the resulting monolith were carried out by synthesizing one non-imprinted polymer for each photo-polymerization time. Therefore, they were prepared using the same polymerization mixture (MAA, TRIM, and ACN containing 10% isoctane) with a M/CL ratio of 1/5 (mol/mol) and a (M+CL)/P ratio of 15/85 (v/v) introduced in 150 mm-long capillaries (100  $\mu\text{m}$  i.d.). Masks with windows of different lengths, *i.e.* 10, 25, or 50 mm, were used, while ensuring that the window was at a minimum of 10 mm from the capillary end. After the monolith synthesis, the capillaries were then cut to a length of 100 mm, with the monolith still being at 10 mm from one extremity. The back-pressure generated by each capillary maintained at 35°C was then measured while pumping ACN at 200  $\text{nL min}^{-1}$ . A back-pressure close to 5 bar, generated by the nanoLC system itself when a 100 mm-long empty capillary is connected, was subtracted from the back pressure measured with the capillary containing the monolith.

For a polymerization time of 15 min, back-pressure values of 5, 9, and 34 bar were obtained for monolithic NIPs of 10, 25, and 50 mm, respectively. Those values were significantly lower than the ones obtained for longer exposure times whatever the length of the monolith, indicating that

polymerization was incomplete or that the monolith was incorrectly attached to the capillary inner surface. This was confirmed by SEM observations (**Figure S5, Appendix 4**). Indeed, it appears on the pictures that the monolithic NIPs synthesized with a UV irradiation of only 15 min did not occupy the entire section of the capillary, indicating incomplete polymerization (**Figure S5 B**). In return, the monoliths synthesized with 30 min of UV exposure occupied the whole section of the capillary and were well anchored to its surface (**Figure S5 D**). It is worthwhile to notice that identical SEM observations can be made for the thermally synthesized NIPs (**Figure S5 F**). Concerning the exposure times of 30, 60, and 120 min, the same back-pressure value of 7 bar was measured for the monolithic NIPs of 10 mm. In addition, back-pressure values of 17, 15, and 20 bar were obtained for 25 mm-long NIPs, whereas values of 43, 40, and 54 bar were obtained for 50 mm-long NIPs with polymerization time of 30, 60, and 120 min, respectively. In summary, average values of  $7 \pm 0$ ,  $17 \pm 3$ , and  $46 \pm 7$  bar were measured for monolithic lengths of 10, 25, and 50 mm, respectively, whatever the polymerization time value of 30, 60, or 120 min. These results suggested that polymerization was complete after only 30 min of UV irradiation, and this duration was retained for the rest of the study.

These preliminary experiments related to NIP were followed by three independent syntheses of MIPs and NIPs for each of the three lengths, with a UV irradiation time of 30 min. The same observations were made for the SEM images of the MIPs as for the corresponding NIPs discussed above (**Figure S5**). The permeability of each monolith was estimated by applying various flow rates of ACN. Knowing  $\eta$ , the permeability can be deduced from  $\Delta P$  measurements as explained in **Section III.3.3**. The results obtained are reported in the **Table 16**. First of all, the permeability of NIP was always higher than that of MIP thus showing the effect of the presence of the template molecules during the polymerization on the structure of the resulting monolith. Moreover, RSD values on permeability were between 2 and 19% ( $n = 3$ ), indicating a good repeatability of the synthesis whatever the length of the monolith. Subsequently, one-factor variance analyses were performed to assess the impact of the length (10, 25, or 50 mm) on the permeabilities of MIP and NIP monoliths. No significant differences were observed (ANOVA,  $p$  value =  $0.83 > 0.05$  and  $0.49 > 0.05$  for MIP and NIP, respectively). Finally, the average permeabilities were  $0.65 \times 10^{-15} \text{ m}^2$  (RSD = 8%,  $n = 9$ ) and  $1.67 \times 10^{-15} \text{ m}^2$  (RSD = 13%,  $n = 9$ ) for the MIPs and NIPs obtained under UV irradiation, respectively. Comparing these values with those obtained by thermal initiation with the same reaction mixture, a five-fold lower permeability can be observed for photo-polymerized MIPs. As a direct consequence, the monolithic MIPs with a length of 50 mm generated a back-pressure of  $105 \pm 3$  bar for a flow rate of  $200 \text{ nL min}^{-1}$ . In order to limit excessive back-pressure preventing the future replacement of expensive nanoLC pumps by less expensive syringe pumps, only monolithic MIPs and NIPs having a length of 10 and 25 mm were therefore selected for further investigations.

**Table 16.** Permeabilities measured on MIPs and NIPs having a length of 10, 25 or 50 mm and obtained by photo-initiation for 30 min and comparison with the results obtained previously [90] with the monoliths obtained by thermal syntheses with the same polymerization mixture recipe and having a length of 50 mm (three syntheses for each length).

	Monolithic length (mm)	K ( $10^{-15} \text{ m}^2$ )	RSD, n = 3 (%)	K average ( $10^{-15} \text{ m}^2$ )	RSD, n = 3 (%)
MIP (UV initiation)	10	0.63	14		
	25	0.66	6	0.65	8
	50	0.64	2		
MIP (Thermal initiation) [90]	50	3.27	3	-	-
NIP (UV initiation)	10	1.72	19		
	25	1.75	11	1.67	13
	50	1.54	3		
NIP (Thermal initiation) [90]	50	36.57	17	-	-

### III.4.3. Evaluation of the selectivity studying retention properties in nanoLC

The selectivity of the MIPs obtained by UV irradiation was next characterized by studying the retention of cocaine (template molecule) and BZE on both monolithic MIPs and NIPs. The compounds were injected on each MIP and its corresponding NIP having a length of 10 or 25 mm within a 100 mm x 100 µm i.d. capillary. The injection of acetone on each monolith allowed the determination of the  $t_0$  value and then the calculation of the retention and imprinted factors. The evaluation was carried out in ACN because, as often mentioned in literature, the selectivity should be optimal when the solvent used is close to the porogen, *i.e.* ACN containing 10% isoctane here. Moreover, the cocaine imprinted poly(MAA-co-TRIM) monolith previously prepared by thermal polymerization was very selective towards cocaine and BZE in this solvent [90].

As an example, the chromatograms obtained for a 10 mm-long MIP and its corresponding NIP are provided in **Figure 19**. IF values measured on MIPs and their corresponding NIPs from three

independent syntheses for the two different monolith lengths are reported in **Table 17** and compared with values previously obtained for the MIP and NIP synthesized with the same conditions except the polymerization mode (thermal) [90]. The template cocaine was significantly more retained on MIPs than on the corresponding NIPs giving rise to IF values above 3, independently of the length of the monolith, thus attesting the presence of cavities specific to cocaine in MIPs. In addition, these cavities were also able to selectively retain BZE, since imprinted factors higher than 2 were obtained. These results confirmed that both thermal and UV initiation modes can give MIPs with specific cavities. Moreover, RSD values of imprinted factor for cocaine and BZE measured on three independent MIPs obtained with UV irradiation were lower than 14%, which confirmed the repeatability of the synthesis procedure already demonstrated by the permeability measurements, despite the broad shape of the peaks that has a strong impact on measurement accuracy.

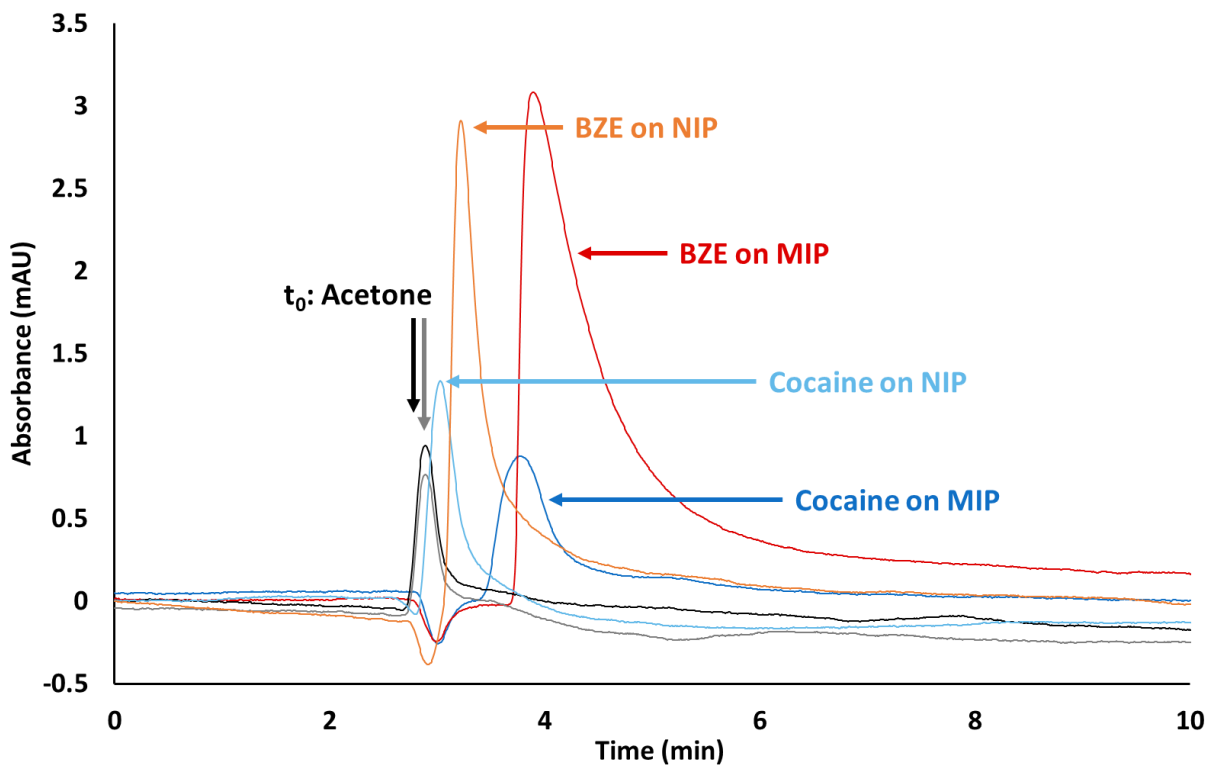


**Figure 19.** Chromatograms obtained after the injection of acetone, cocaine ( $5 \mu\text{g mL}^{-1}$ ), or BZE ( $5 \mu\text{g mL}^{-1}$ ) on monolithic MIP and NIP ( $10 \text{ mm} \times 100 \mu\text{m i.d.}$ ) synthesized with UV irradiation for 30 min in a  $100 \text{ mm} \times 100 \mu\text{m i.d.}$  capillary.  $V_{\text{inj}} = 50 \text{ nL}$ . Mobile phase: ACN,  $400 \text{ nL min}^{-1}$ . UV detection at 233 nm.

In addition, for the monoliths obtained by UV irradiation, a one-factor variance analysis was performed to evaluate the potential impact of the monolith length (10 or 25 mm) on IF values of cocaine and BZE. No significant differences were observed (ANOVA,  $p$  value =  $0.28 > 0.05$  and  $0.07 > 0.05$  for cocaine and BZE, respectively), resulting in final average IF values of  $4.0 \pm 0.6$  and  $2.7 \pm 0.1$  for cocaine and BZE, respectively. Considering then the influence of the initiation mode (thermal or UV) on the IFs, one-factor variance analyses were also carried out. For cocaine there is no significant difference between the two initiation modes (ANOVA,  $p$  value =  $0.09 > 0.05$ ), whereas there is a significant difference for BZE (ANOVA,  $p$  value =  $0.006 < 0.05$ ), demonstrating the selectivity enhancement for BZE of the monolithic MIPs obtained by UV irradiation.

**Table 17.** Imprinted factors of cocaine and BZE measured on three different MIPs and NIPs synthesized with UV irradiation or with thermal polymerization [90]. Experimental conditions: see

**Figure 19.**

	Monolith (10 mm, UV irradiation)		Monolith (25 mm, UV irradiation)		Monolith (50 mm, thermal synthesis) [90]	
	IF	RSD, n = 3 (%)	IF	RSD, n = 3 (%)	IF	RSD, n = 3 (%)
Cocaine	3.7	14	4.3	13	3.2	17
BZE	2.6	2	2.8	5	2.2	13

In conclusion, as selectivity was preserved, the monolithic MIPs of long dimension obtained by thermal initiation in capillaries can be replaced by MIPs obtained by photo-initiation, allowing to vary their dimension more easily.

#### III.4.4. Optimization of the on-line MIP extraction and UV detection analysis protocol

After having demonstrated the selectivity of the monolithic MIP using it as a separation column, a new set-up was developed to use it as an extraction sorbent, coupled on-line directly with UV detection. The capillary (100 mm x 100  $\mu\text{m}$  i.d.) containing the monolithic MIP or NIP was placed at the loop position of a valve (valve 2) and connected between another valve where is the sample injection loop (valve 1) and the UV detector as shown in **Figure 17 A**. This set-up allowed a back-flush elution of the compounds trapped on the monolith to the UV detector, thus limiting band broadening. To limit the elution volume required for the desorption and then the peak width, the shortest

monoliths of 10 mm-long were selected. Initially, it was chosen to place the monolith at the outlet of the extraction step, *i.e.* at the inlet of the elution-detection step (**Figure 17 B2**).

The sample was first loaded in the loop (150 nL) and next transferred by an H<sub>2</sub>O/ACN (90/10, v/v) mixture to the monolith, *i.e.* the mixture used in the preliminary tests with the monoliths synthesized thermally. To estimate the volume required for the transfer from the loop to the monolith and the washing, a calculation was performed, taking into account the difference in dead volume between the injection loop and the MIP for the current set-up and the one previously used in **Section III.4.1**. Given the transfer/washing volume of 900 nL applied for the application with the thermally synthesized monolithic MIP, a minimal volume of 1230 nL has to be applied in this new set-up. Different other volumes were tested (1400, 1600, and 1800 nL) and a decrease in the BZE peak height was only observed with a volume of 1800 nL. Finally, it was possible to increase this transfer/washing volume up to 1750 nL with no impact on the peak height for BZE (150 nL, 1 µg mL<sup>-1</sup> in water) using the monolithic MIP. This higher volume of transfer/washing confirmed an improvement in retention provided by the monolithic MIP obtained by photo-polymerization.

For the back-flush elution from the monolith to UV detection, a H<sub>2</sub>O/ACN (70/30, v/v) mixture was used as in the preliminary study. A chromatogram obtained by the on-line coupling of MIP extraction and UV detection for the analysis of BZE (150 nL, 1 µg mL<sup>-1</sup> in water) is presented **Figure 20 A**. The optimized volume of transfer of 1750 nL was used. A peak height of 0.45 mAU was observed, in agreement with the value of 0.43 mAU previously obtained in **Section III.4.1** with the same sample and the 50 mm thermally-initiated monolithic MIP.

In order to increase the sensitivity of this method, the injected volume was increased. Volumes of 300 and 600 nL containing BZE at 1 µg mL<sup>-1</sup> were percolated through the monolithic MIP, while still adapting the volume of the transfer/washing solution in each extraction protocol to ensure that the overall volume (sample plus transfer/washing solution) flowing through the monolithic MIP was kept constant. Volumes of the transfer and washing solution of 1600 and 1300 nL were therefore used, respectively, and the chromatograms obtained are presented in **Figure 20 A** together with the chromatogram corresponding to an injected sample of 150 nL. The BZE peak height increase shows a linearity with respect to the injection volume ( $R^2 = 0.0998$ ), indicating that the capacity of the monolithic MIP was not reached despite its reduced length (10 mm). An injected sample volume of 600 nL was therefore selected for subsequent analyses.

The selectivity of the monolithic MIP was then investigated by studying the retention of BZE on the corresponding NIP under the same conditions. Water spiked at 1 µg mL<sup>-1</sup> with BZE was

introduced in the injection loop of 600 nL and next transferred on the monolithic MIP or NIP with a volume of 1300 nL of H<sub>2</sub>O/ACN (70/30, v/v). The resulting chromatograms demonstrated that this procedure promoted BZE retention on the MIP while giving rise to a low retention on the NIP (**Figure 20 B**). Indeed, peak heights of 1.80 and 0.25 mAU were obtained on the MIP and NIP, respectively. A factor of more than 7 in peak height was therefore obtained between the two supports confirming the selectivity brought by the specific cavities of the monolithic MIP.

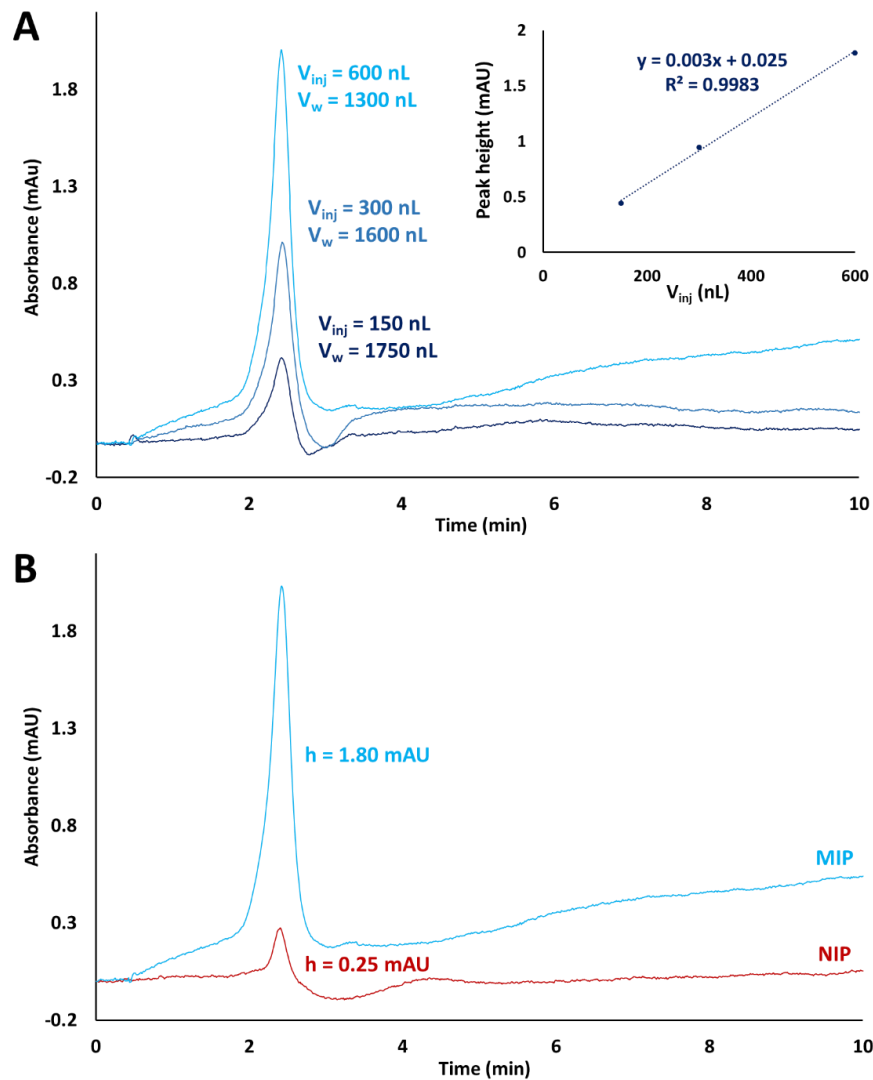


**Figure 20.** Chromatograms obtained by on-line coupling of the extraction of water spiked with BZE at 1  $\mu\text{g mL}^{-1}$  on monoliths (10 mm x 100  $\mu\text{m}$  i.d.) synthesized in a 100 mm x 100  $\mu\text{m}$  i.d. capillary under UV, showing (A) the influence of the percolated sample volume ( $V_{\text{inj}}$ ) by modifying appropriately the volume of the transfer/washing solution ( $V_w$ ) on MIP (insert: BZE peak height vs percolated sample volume) and (B) the selectivity by comparing the performances obtained on MIP and NIP for an injection of 600 nL ( $V_w$  of 1300 nL). Transfer/washing solution: H<sub>2</sub>O/ACN (90/10, v/v). UV detection at 233 nm. Other conditions: see **Section III.3.4**.

Finally, the position of the monolith on the valve was investigated. Indeed, in the current position (**Figure 17 B2**), the analytes retained on the MIP must flow through a large volume of empty capillary (80 mm x 100  $\mu\text{m}$  i.d., 628 nL) before reaching the detector during the elution step. By switching the capillary orientation (**Figure 17 B3**), this volume can be reduced (10 mm x 100  $\mu\text{m}$  i.d., 79 nL), which could have an influence on the shape of the peak. To assess this hypothesis, 300 nL of water spiked with BZE at 1  $\mu\text{g mL}^{-1}$  was injected in both configurations. The injection volume was reduced from 600 to 300 nL here in order to limit the BZE amount on the monolith and thus achieve an accurate observation of the peak spreading. Once again, the volume of the transfer/washing solution was adapted to take into account variations in dead volume. When the monolith was implemented at the outlet of the extraction step (**Figure 17 B2**), the transfer and washing were achieved with 1600 nL while in the reversed position the volume applied was 1050 nL. The chromatograms obtained are reported in **Figure 21 A**. The shape and height of the peak do not seem to be affected by the position of the monolith in the valve. However, it will be important to confirm this observation by applying a much more complex sample, such as urine.

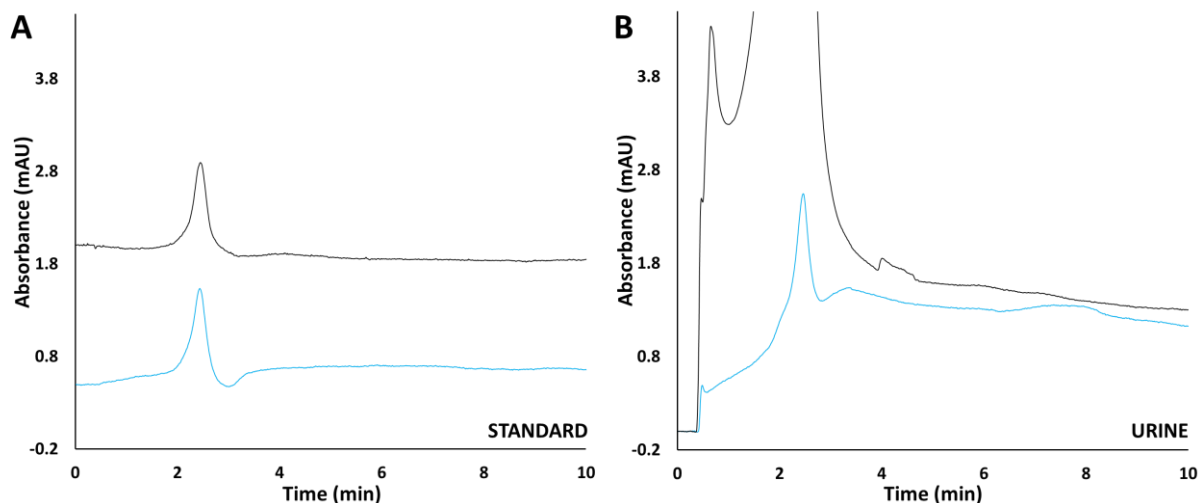


**Figure 21.** Chromatograms obtained after the extraction on monolithic MIP (10 mm x 100  $\mu\text{m}$  i.d.) of 300 nL of (A) water spiked with BZE at 1  $\mu\text{g mL}^{-1}$  or (B) 2x diluted and filtered urine spiked with BZE at 1  $\mu\text{g mL}^{-1}$  (equivalent to 2  $\mu\text{g mL}^{-1}$  in urine) for set-up implementing the monolith at the outlet of the extraction step (configuration **Figure 17 B2**) (Blue) or at the inlet of the extraction step (configuration **Figure 17 B3**) (Black). Transfer/washing step: 1600 nL (Blue) or 1050 nL (Black) of H<sub>2</sub>O/ACN (90/10, v/v). Other conditions: see **Section III.3.4**.

### III.4.5. Applications to urinary samples

The potential of the extraction/purification step with a monolithic MIP coupled on-line to UV detection was evaluated for the extraction of BZE from human urine samples. For this, urine was diluted with H<sub>2</sub>O (x2) and filtered. This sample was then spiked with BZE at 1 µg mL<sup>-1</sup>, which corresponds to a concentration level of 2 µg mL<sup>-1</sup> in urine. In order to check the influence of the monolith position in the set-up, the same protocol as above was applied with an injection of 300 nL, using the two possible configurations. The resulting chromatograms are presented in **Figure 21 B**.

While for spiked water no difference between the chromatograms was observed using both configurations, it was not the case when analyzing a much more complex sample, *i.e.* diluted urine. Indeed, when the monolith was positioned on the side of the injection loop (**Figure 17 B3**), a huge peak of interfering compounds was observed, preventing the identification of BZE. In this configuration, the volume of transfer/washing solution (1050 nL of H<sub>2</sub>O/ACN, 90/10, v/v) was not efficient to remove the interferents still present in the void volume of the empty capillary and that affect next the baseline of the chromatogram. In this position, even if there are no more interfering compounds retained on the MIP, there is still a large volume of empty capillary to be covered by the analytes before their elimination in the waste (80 mm x 100 µm i.d., 628 nL). Therefore, during back-flush elution, the remaining interfering analytes were redirected to the monolithic MIP, without being retained owing to the elution strength of the solution containing 30% ACN, and then passed in the UV detection cell. On the other hand, when the monolith was located at the outlet of the capillary during the extraction step (**Figure 17 B2**), the selectivity of the monolithic MIP allowed the removal of the interfering compounds present in urine and the 1600 nL of transfer/washing solution were enough to take the interfering analytes to waste. The resulting chromatogram exhibited a clean baseline with only one peak corresponding to BZE, similar to the one obtained with spiked water, thus showing no more matrix effect. The last configuration was therefore selected for further applications with urinary samples.

To evaluate the final potential of this on-line coupling, it was important to evaluate the concentration levels that could be quantified in biological samples. A French decree defines a positivity threshold of 300 ng mL<sup>-1</sup> for the screening of BZE in urine matrices [153]. It was therefore necessary to target BZE at these low concentrations to comply with the current legislation. In this sense, to improve the sensitivity of the method, the 300 nL loop was replaced by the 600 nL loop. Urine samples spiked with three concentrations levels, *i.e.* 150, 250, and 500 ng mL<sup>-1</sup> (equivalent to 300, 500, and 1000 ng mL<sup>-1</sup> in urine), were injected and transferred to the monolithic MIP with 1300 nL of a H<sub>2</sub>O/ACN

solution (90/10, v/v). BZE was back-flush eluted with the H<sub>2</sub>O/ACN mixture (70/30, v/v). The resulting chromatograms are presented in **Figure 22**. By comparing them with the chromatogram obtained for a blank urine (**Figure 22 E**) under the same conditions, it appears that BZE was extracted from urine and could be easily detected for each concentration. Moreover, owing to the selectivity of the monolithic MIP, the baseline of the resulting chromatogram was cleaned of the majority of the interfering components from the biological matrix. The high selectivity of the monolithic MIP in this biological fluid was further demonstrated with the extraction on the monolithic NIP of the same urine sample spiked with BZE at the highest tested concentration value with the MIP (1 µg mL<sup>-1</sup> in urine equivalent) (**Figure 22 D**). The peak corresponding to BZE was not detected after extraction on the NIP, which highlighted again the selectivity of the MIP extraction procedure, these results being also consistent with those obtained previously in spiked water.

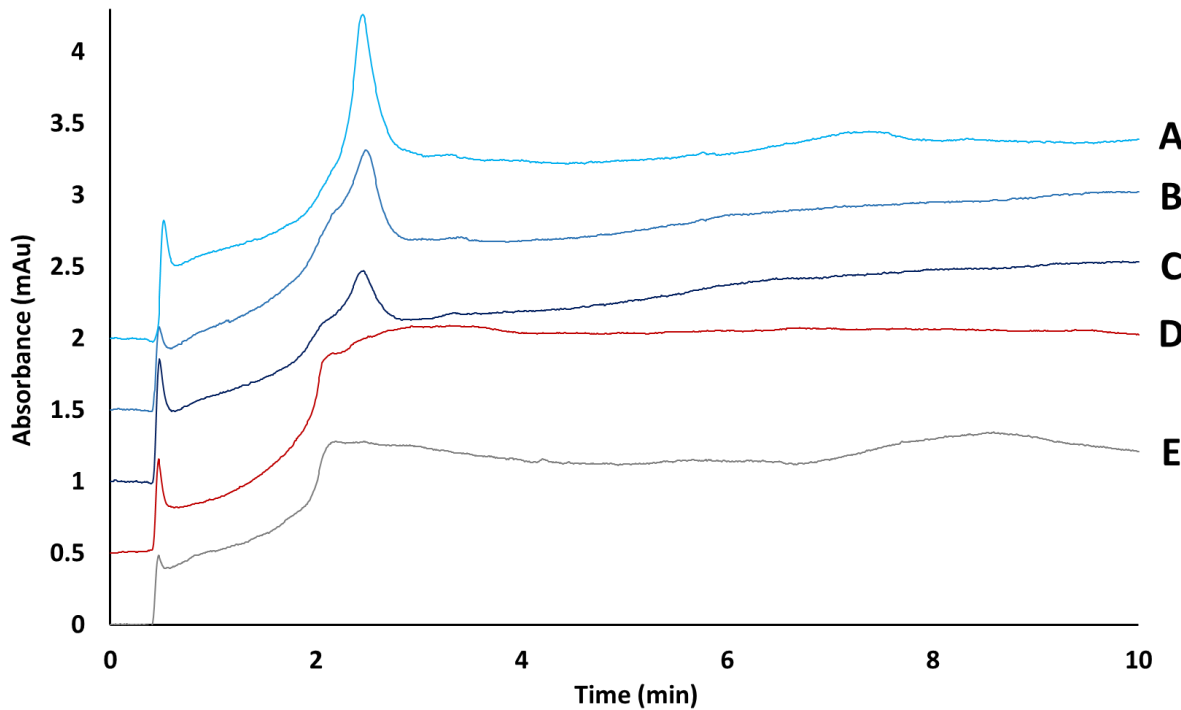


**Figure 22.** Chromatograms obtained after extraction on the monolith (10 mm x 100 µm i.d.) coupled with UV detection (configuration **Figure 17 B2**) of 600 nL of diluted urine (x2) spiked with BZE at (A) 500 ng mL<sup>-1</sup> on MIP, (B) 250 ng mL<sup>-1</sup> on MIP, (C) 150 ng mL<sup>-1</sup> on MIP, and (D) 500 ng mL<sup>-1</sup> on NIP or (E) of 600 nL of diluted urine (x2) (blank) on MIP. Transfer/washing step: 1300 nL of H<sub>2</sub>O/ACN (90/10, v/v). Other conditions: see **Section III.3.4**.

The analytical performances obtained for each concentration with triplicate injections are reported in **Table 18**. The curves plotting the peak height and area as a function of the BZE concentration in urine from 300 to 1,000 ng mL<sup>-1</sup> (**Figure S6, Appendix 4**) had a linear shape with R<sup>2</sup> of 0.9999 and 0.9994, respectively, thus indicating that the MIP capacity was not reached for these injected amounts. The LOD and LOQ were estimated for BZE at 56.4 and 188.0 ng mL<sup>-1</sup> in urine equivalent, respectively. Therefore, it is possible to conclude that the developed approach fulfills the application requirements for the thresholds established by the legislation. Focusing on repeatability, low RSD values (n = 3) were obtained for peak height (2.1-6.3%) and peak area (2.1-4.4%), for three extractions on one given monolithic MIP. Therefore, the repeatability of the synthesis of this miniaturized monolithic MIP demonstrated in **Section III.4.2** and of the on-line extraction-detection procedure is fully satisfactory. In the case of the monolithic NIP, the analytical performances obtained for the urine sample spiked at 1 µg mL<sup>-1</sup> were not reported in **Table 18** as peak heights of BZE were below the LOD value previously determined (56.4 ng mL<sup>-1</sup>), which corresponds to recoveries lower than 6% thus confirming results obtained in pure media.

**Table 18.** Analytical performances obtained for BZE in diluted (x2) urine spiked samples.

Spiked concentration (ng mL <sup>-1</sup> )	Average peak height (mAU)	RSD (peak height), n = 3 (%)	Average area (mAU x min)	RSD (area), n = 3 (%)	LOD (ng mL <sup>-1</sup> )	LOQ (ng mL <sup>-1</sup> )
300*	0.32	6.3	0.064	4.4	56.4	188.0
500*	0.50	3.1	0.127	2.9	-	-
1,000*	0.96	2.1	0.302	2.1	-	-

\* Concentration in urine equivalent

### III.5. Conclusion

The objective of this work was to demonstrate the possibility to directly couple a selective extraction step involving a monolithic MIP prepared in a 100 µm i.d. capillary with a UV detector for the analysis of BZE at trace level in a complex sample, in order to achieve another step towards the development of a µ-TAS. First, a cocaine imprinted poly(MAA-co-TRIM) monolith of a length of 50 mm, previously described by our group and synthesized by thermal polymerization, was first implemented

to evaluate the feasibility of this set-up. In order to gain flexibility on monolithic MIP length, the polymerization under UV irradiation was studied as it allows, by applying adapted mask, the synthesis of monolithic MIPs of various lengths ( $\leq 50$  mm) in a longer capillary allowing to connect it on a valve. The shorter resulting monolithic MIPs selected for their permeability and synthesized under UV exposure of 30 min instead of 24 h for thermal initiation, demonstrated a high selectivity in pure medium for BZE retention. Particular care was taken to evaluate synthesis repeatability in parallel of permeability and selectivity characterizations for independent syntheses.

To optimize the performances of this simple set-up consisting of a MIP coupled on-line with a UV detector, various parameters were optimized, such as sample volume and position of the monolith in the set-up. The optimized conditions were further applied to the on-line extraction of BZE from 600 nL of spiked urine samples and the resulting chromatograms showed very clean baselines. The repeatability of the analytical performances was assessed in urine samples and the legal thresholds for the detection of cocaine *via* BZE in this kind of biological sample were achieved for an overall analysis time of less than 10 min.

These monolithic and miniaturized MIPs have proven to be an important contribution for the on-line selective determination of BZE. However, it would be possible to improve the set-up by implementing mass spectrometry detection instead of UV to improve the sensitivity of the device for real sample analysis without being affected by the risk of matrix effects, the interfering compounds being removed by the MIP. Another perspective in the continuity of all the progress made during this work is the integration of this technology into a microfluidic chip for the development of a lab-on-chip to provide a miniaturized and portable device. Indeed, during this work, the impact of connection dead volumes on the miniaturized system was highlighted. Therefore, a chip with a dedicated design integrating the different steps of the analysis would considerably reduce these issues.

## **CHAPITRE IV**

**Transfert de savoir-faire pour la production d'un monolithe  
à empreintes moléculaires pour l'extraction sélective et  
miniaturisée de neurotransmetteurs**



## **CHAPITRE IV – Transfert de savoir-faire pour la production d'un monolithe à empreintes moléculaires pour l'extraction sélective et miniaturisée de neurotransmetteurs**

Dans les chapitres précédents, des synthèses de MIP monolithiques dans des capillaires de 100 µm de diamètre interne pour l'extraction de la cocaïne et la BZE ont été réalisées, permettant l'introduction à terme de MIP dans des microsystèmes. Un ajustement des conditions de synthèse, que ce soit le volume de solvant, la nature de l'agent réticulant ou le mode d'initiation a permis l'obtention de MIP monolithiques ancrés aux parois du capillaire, perméables et présentant une forte sélectivité pour la cocaïne et son métabolite. De plus, une excellente répétabilité de synthèse en termes de morphologie et de sélectivité a été obtenue. Par ailleurs, ces monolithes ont ensuite pu être testés dans un couplage en ligne de l'extraction sélective avec la nanoLC associé à une détection UV en ciblant la cocaïne dans des échantillons de salive et de plasma humain. Des résultats très encourageants ont été obtenus puisque ce couplage a permis d'obtenir une importante purification des échantillons biologiques et ainsi d'observer un pic en UV correspondant à la cocaïne tout en éliminant la majorité des pics interférents de la ligne de base. Par la suite, une miniaturisation encore plus poussée a été réalisée avec le couplage en ligne de l'extraction sélective directement avec la détection UV en éliminant la colonne analytique afin de cibler la BZE dans des échantillons d'urine. Ceci a nécessité le développement de nouvelles conditions de synthèse basées sur une initiation de la polymérisation par irradiation UV. Après optimisation du protocole d'extraction et du montage, des résultats tout aussi encourageants ont été obtenus avec la possibilité de détecter la BZE au seuil imposé par la législation.

Dans ce chapitre, nous avons donc voulu évaluer la possibilité de transférer le savoir-faire précédemment acquis afin de développer une étape d'extraction sur MIP miniaturisée et couplée en ligne avec la nanoLC-UV pour une autre famille de molécules cibles. Pour cela, certains neurotransmetteurs comme la dopamine et l'octopamine ainsi que quelques analogues structuraux tels que l'éphédrine, la méthyléphédrine et la synéphrine (**Figure 23**) ont été sélectionnés comme molécules cibles. Il s'agit d'un panel de molécules déjà disponibles au sein du laboratoire et nécessitant un suivi analytique en raison de leur usage médical pour diverses pathologies mais aussi de la réglementation mise en place pour ces composés dans de nombreux pays. Par ailleurs, des travaux de recherche ont déjà été menés sur l'élaboration de MIP en bloc pour leur extraction sélective [187–194], dont l'un a été réalisé au laboratoire avec l'éphédrine comme molécule empreinte [187]. Pour ce dernier, la synthèse a été initiée par irradiation UV avec le MAA comme monomère fonctionnel et

l'EGDMA en tant qu'agent réticulant, avec un ratio molaire de chaque composé de 1/4/20 (T/M/CL). Ces conditions de synthèses étant identiques à celles établies pour le MIP en bloc ciblant la cocaïne et la BZE, il semble possible de transférer de la même façon le protocole de synthèse développé précédemment à un format miniaturisé pour ces nouveaux composés cibles.

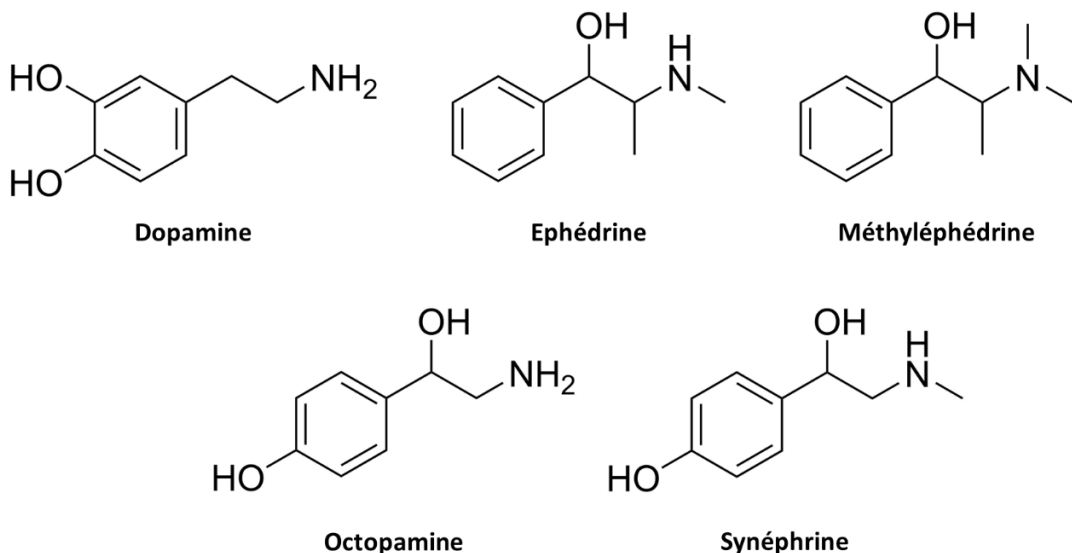


**Figure 23.** Structure chimique de l'éphédrine, la dopamine, la méthyléphédrine, l'octopamine et la synéphrine.

#### IV.1. Présentation des composés d'intérêt

L'éphédrine, la dopamine, la méthyléphédrine, l'octopamine et la synéphrine sont tous des alcaloïdes et des phénylethylamines. Tous ces composés, à l'exception de la méthyléphédrine, sont commercialisés en tant que médicament sympathicomimétique, une classe de médicaments dont les propriétés imitent la stimulation du système nerveux sympathique en accélérant la fréquence cardiaque, dilatant les bronchioles et provoquant en général une contraction des vaisseaux sanguins. Par conséquent, ces molécules sont également considérées comme stimulants dans le monde sportif et donc traitées comme produits dopants.

Elles sont constituées d'un squelette commun avec une région hydrophobe comprenant un noyau benzénique et une région hydrophile contenant une fonction amine. Les pKa de la fonction amine pour ces composés sont assez proches, entre 8,71 et 9,52, comme indiqué dans le **Tableau 19**. Il s'agit donc de bases faibles qui sont protonées dans les conditions physiologiques. Des groupements

hydroxy sont également présents, qui ont des propriétés d'acide faible, mais avec des valeurs de pKa très élevées. Concernant l'estimation de leur hydrophobie, des valeurs de log D<sub>oct</sub> allant de -0,82 à 1,73 sont répertoriées [195]. Ce sont donc des composés très polaires, et ceci est encore plus vrai lorsqu'ils sont ionisés.

**Tableau 19.** Valeurs des pKa (fonction amine en gras) et des coefficients de distribution octanol/H<sub>2</sub>O pour l'éphédrine et ses analogues structuraux [195].

Composé	M (g mol <sup>-1</sup> )	pKa	Log D <sub>oct</sub>
Ephédrine	165,23	<b>9,52 / 13,89</b>	1,32
Dopamine	153,18	<b>8,71 / 10,90 / 13,68</b>	-0,98
Méthyléphédrine	179,26	<b>8,86 / 13,88</b>	1,73
Octopamine	153,18	<b>8,98 / 9,64 / 14,28</b>	-0,32
Synéphrine	167,21	<b>9,15 / 9,76 / 14,27</b>	-0,62

#### IV.2. Etat de l'art sur les MIP pour l'extraction exhaustive non miniaturisée de l'éphédrine, la méthyléphédrine, la dopamine, l'octopamine et la synéphrine

De nombreuses études ont d'ores et déjà été réalisées sur la synthèse de MIP pour l'extraction exhaustive à l'échelle conventionnelle de ces molécules [187–194,196–202]. Les différentes conditions de synthèse ainsi que les performances obtenues avec ces supports sont résumées dans le **Tableau 20**.

**Tableau 20.** Conditions de synthèse et performances des MIP développés pour l'extraction exhaustive non miniaturisée de l'éphédrine, la méthyléphédrine, la dopamine, l'octopamine et la synéphrine.

Molécule cible *	M/CL/Solvant (v:v)	Ratio molaire T/M/CL	Initiation	Dimension	Echantillon	Capacité (MIP/NIP)	Sélectivité (MIP/NIP)	Rendement (CV)	Réf.
Dopamine, Sérotonine, Salbutamol, Isoprotérénol, Epinéphrine	MAA + Acrylamide/ MBAA/MeOH:H <sub>2</sub> O (80:20)	1/2+2/10	AIBN / 60°C, 24 h	Cartouche SPE (25 mg)	Urine (Dilution x2,2 dans MeOH/H <sub>2</sub> O, 82/18)	-	IF = 1,7	70-106% (2-10%, n = 3)	[192]
Dopamine (5-[2-(allyldithio)éthyl]-2-(4-vinylphényl)benzo[1,3,2]dioxaborole)	Styrène/DVB/ Chloroforme	1/5/25	AIBN / UV, 5°C 24 h puis 80°C 3 h	-	Milieu pur	-	-	-	[194]
Dopamine, 3-Méthoxytyramine, Sérotonine	AFFINIMIP Catécholamine & Métanéphrine (MIP commercial)	-	-	Cartouche SPE (100 mg)	Urine (Dilution x9 dans tampon ammoniac-acide acétique, pH 4)	-	-	-	[201]
Dopamine, 3-Méthoxytyramine, Epinéphrine, Norépinéphrine, Normétanéphrine, Sérotonine	AFFINIMIP Catécholamine & Métanéphrine (MIP commercial)	-	-	Cartouche SPE (100 mg)	Sérum (Dilution x10 dans H <sub>2</sub> O)	-	IF = 3,0-20,8	64-98% (< 6%, n = 4)	[202]
Dopamine (2-(3,4-Diméthoxy phényl)éthylamine)	MAA/EGDMA/ Toluène	1/4/16	AIBN / 88°C, 24 h	Cartouche SPE (25 mg)	Banane (Extrait dans MeOH)	Batch : 1,09/0,3 µg g <sup>-1</sup>	IF = 4,08	88,5% (5,2%, n = 5) / 12,8% (18,8%, n = 5) (MIP/NIP)	[198]

Molécule cible *	M/CL/Solvant (v:v)	Ratio molaire T/M/CL	Initiation	Dimension	Echantillon	Capacité (MIP/NIP)	Sélectivité (MIP/NIP)	Rendement (CV)	Réf.
<u>Dopamine</u>	MAA/EGDMA/ MeOH:H <sub>2</sub> O (87,5:12,5)	1/8/60,6	AIBN / 64°C, 24 h	Cartouche SPE (56,2 mg)	Milieu pur	-	-	84,1 / 29,1% (MIP/NIP) (3%, n = 3)	[190]
Dopamine (4-(2-Aminoéthyl) aniline))	MAA/EGDMA/ MeOH	1/4/20	AIBN / 64°C, 24 h	Cartouche SPE (50 mg)	Urine artificielle	9,6/0,66 µmol g <sup>-1</sup>	IF = 22,96	57,5-61,8% (6-7%, n = 3) / 13,7-18,2% (10-22%, n = 3) (MIP/NIP)	[188]
Dopamine, Epinéphrine, Norépinéphrine (Catéchol)	Acide carboxyphényl boronique/EGDMA /ACN	1/5/25	AIBN / 43°C 12 h puis 60°C 24 h et 85°C 6 h	Cartouche SPE (150 mg)	Urine (Diluée avec PBS)	-	IF = 10,21-10,70	63,4-106,2% (0,3-1,9%, n = 3)	[199]
<u>Ephédrine</u> , Pseudoéphédrine, Méthyléphédrine, Méthylpseudo éphédrine, Noréphédrine, Norpseudoéphédrine	MAA/EGDMA/ACN	1/4/20	AIBN / UV, 366 nm, Température ambiante, 24 h	Cartouche SPE (500 mg)	Ephédra chinois (Extrait dans chloroforme)	4,16/1,68 mg g <sup>-1</sup>	-	100,8-102,5% (2,7-3,3%, n = 5)	[189]
<u>Ephédrine</u> , Noréphédrine, caféine, Paracétamol, Epinéphrine, Noradrénaline	MAA/EGDMA/ Chloroforme	1/4/20	AIBN / UV, 15°C, 24 h	Cartouche SPE (100 mg)	Plasma humain (Dilution x2 dans ACN)	> 1 mg g <sup>-1</sup> /-	-	68 / 0% (MIP/NIP)	[187]
<u>Ephédrine</u>	Mélamine-Urée- Formaldéhyde	-	Température ambiante 1 nuit puis 60°C 24 h	Colonne de 8 mL, 40 x 15 mm (1 g)	Ephédra (Extrait dans EtOH/H <sub>2</sub> O, 80/20)	1,74/0,39 mg g <sup>-1</sup>	Adsorption : 96,7 / 24,1% (MIP avec Ephédrine / Pseudoéphédrine)	84,6%	[193]

Molécule cible *	M/CL/Solvant (v:v)	Ratio molaire T/M/CL	Initiation	Dimension	Echantillon	Capacité (MIP/NIP)	Sélectivité (MIP/NIP)	Rendement (CV)	Réf.
<u>Ephédrine</u>	Méthacrylate de glycidyle/EGDMA/ EtOH	1/20/17	Agitation, 75°C, 12 h	Cartouche SPE (200 mg)	Herbes médicinales	Batch : 5,76/≈ 4,50 mg g <sup>-1</sup>	-	87-104% (2,1-5,4%, n = 5)	[200]
<u>Synéphrine</u> , Octopamine, Tyramine	MAA/EGDMA/ACN	1/4/20	AIBN / 60°C, 24 h	Cartouche SPE (100 mg)	<i>Aurantii Fructus Immaturus</i> (Extrait dans EtOH/H <sub>2</sub> O, 68/32)	Batch : 155,5/64,4 μmol g <sup>-1</sup>	-	85,8-89,6% (3,0-3,9%, n = 5)	[191]

\* Molécule empreinte indiquée entre parenthèses lorsqu'elle est différente de la molécule d'intérêt ou soulignée dans le cas d'un mélange de plusieurs molécules cibles.

Différentes approches ont été mises en œuvre pour obtenir des particules de MIP, comme par exemple la polymérisation par précipitation [196–198]. Des études ont également rapporté la synthèse de MIP dans des formats différents de l'approche particulaire classique tels que des particules de MIP creuses [199] ou bien encore en synthétisant une couche de MIP à la surface de particules de silice recouvertes d'un liquide ionique [200]. Cependant, ces formats sont très peu représentés dans la bibliographie puisque la majorité des études se sont orientées vers le développement de MIP en bloc.

En utilisant ce mode de synthèse en bloc, Suedee *et al.* ont développé un MIP thermosensible par copolymérisation du MAA et de l'acrylamide avec le N,N-méthylène-bis-acrylamide comme agent réticulant et la dopamine comme molécule empreinte [192]. Ce matériau a la propriété de pouvoir gonfler de façon réversible sous l'influence de la température, permettant de moduler le nombre de sites pouvant interagir avec les molécules cibles. Une autre équipe a synthétisé un MIP avec l'éphédrine comme molécule empreinte dans un mélange mélamine-urée-formaldéhyde [193]. Cependant, ces voies de synthèses sont anecdotiques au vu de la tendance générale qu'il est possible d'observer dans la bibliographie sur le mode de synthèse en bloc.

Les réactifs employés majoritairement sont le MAA comme monomère fonctionnel [187–192] et l'EGDMA en tant qu'agent réticulant [187–191] avec un ratio molaire T/M/CL de 1/4/20 [187–189,191]. Afin de favoriser la formation du complexe molécule empreinte-monomère, des solvants faiblement polaires et aprotiques ont été principalement sélectionnés tels que le toluène, le chloroforme et l'ACN.

Luliński *et al.* ont rapporté la production de MIP ciblant la dopamine en comparant l'utilisation du MAA par rapport à six autres monomères fonctionnels (acide 4-vinylbenzoïque, allylamine, 2-phénylpropène, AA, VP et IA) [188]. Pour chaque synthèse, la 4-(2-aminoéthyl)aniline a été sélectionnée en tant que molécule empreinte analogue et l'EGDMA comme agent réticulant. Chaque support a ensuite été évalué en déterminant sa capacité et sa sélectivité pour des échantillons de MeOH/H<sub>2</sub>O (86/15, v/v) dopés à 50 µmol L<sup>-1</sup> avec la 4-(2-aminoéthyl)aniline et la dopamine. Les IF calculés pour tous les polymères avec la molécule empreinte indiquent une faible voire aucune sélectivité, à l'exception du MIP obtenu avec le MAA, avec des valeurs comprises entre 0,65 et 1,33. En revanche, des IF de 5,5 et 22,96 ont été déterminés respectivement pour la molécule empreinte et la dopamine sur le MIP à base de MAA, témoignant de la grande sélectivité de ce support. Une capacité supérieure a été obtenue sur ce MIP avec des valeurs de  $7,6 \pm 0,2$  et  $9,6 \pm 0,4$  µmol g<sup>-1</sup> ( $n = 5$ ) respectivement pour la molécule empreinte et la dopamine, contre  $2,2 \pm 0,03$  et  $0,7 \pm 0,003$  µmol g<sup>-1</sup> sur le NIP. Ensuite, la surface spécifique a été mesurée par adsorption du bleu de méthylène et des valeurs de  $99 \pm 16$  et  $63 \pm 3$  m<sup>2</sup> g<sup>-1</sup> ont été obtenues respectivement pour le MIP et le NIP, résultats en

adéquation avec les valeurs de capacité. Après optimisation du protocole SPE, des échantillons de 2 mL d'urines artificielles dopées avec la dopamine à 740 ng mL<sup>-1</sup> ont été percolés sur le MIP et le NIP. Un lavage avec 1 mL d'eau a ensuite été réalisé ainsi qu'une élution avec 1 mL d'une solution de MeOH/acétate d'ammonium 0,04 M (70/30, v/v). Des rendements d'extraction de 57,5-61,8% (CV : 6-7%, n = 3) ont été obtenus sur le MIP contre 13,7-18,2% (CV : 10-22%, n = 3) sur le NIP. Afin de démontrer davantage les performances du MIP, le protocole SPE a également été appliqué sur trois supports commerciaux, *i.e.* C18, Florisil (phase polaire) et MCX Oasis (phase d'échange d'ions). Ces supports se sont avérés être inefficaces pour la rétention de la dopamine dans ce type d'échantillon puisque des quantités inférieures à la LOQ ont été obtenues après l'étape d'élution sur les cartouches C18 et MCX Oasis et un rendement de seulement 7,8% a été calculé pour la cartouche Florisil.

Différentes synthèses en bloc utilisant le MAA et l'EGDMA ont également été rapportées pour d'autres cibles. Fan *et al.* ont développé un MIP avec la synéphrine comme molécule empreinte et l'ACN comme porogène [191]. La sélectivité a été déterminée *via* la mesure de la capacité pour des solutions de synéphrine dans l'ACN et des valeurs de 155,5 et 64,4 µmol g<sup>-1</sup> ont été respectivement obtenues pour le MIP et le NIP. Ce support a ensuite été appliqué en SPE à des échantillons d'extraits d'*Aurantii Fructus Immaturus* dopés à 20 µg mL<sup>-1</sup> avec la synéphrine. Après la percolation, une étape de lavage a été effectuée avec une solution d'acétate d'éthyle/ACN (90/10, v/v) puis un mélange MeOH/acide acétique (90/10, v/v) a été appliqué pour l'élution. De très bons rendements d'extraction ont été obtenus, entre 85,8 et 89,6%, avec des valeurs de CV de 3,0-3,9% (n = 5). De plus, un facteur d'enrichissement supérieur à 24 a été calculé. De la même façon, Dong *et al.* ont obtenu un MIP avec l'éphédrine comme molécule empreinte en utilisant de nouveau l'ACN comme porogène [189]. La capacité a été mesurée dans des extraits d'éphédra chinois dopés avec l'éphédrine à 322 µg mL<sup>-1</sup>. Des valeurs moyennes sur deux mesures de 4,16 mg g<sup>-1</sup> pour le MIP contre 1,68 mg g<sup>-1</sup> pour le NIP ont été obtenues et témoignent de la sélectivité du MIP. Après optimisation du protocole SPE, 0,5 mL d'extrait d'éphédra chinois dopé avec l'éphédrine entre 29 et 100 µg mL<sup>-1</sup> a été percolé sur le MIP. Un lavage avec 10 mL d'ACN a ensuite été réalisé suivi d'une élution avec 5 mL de MeOH + 5% TFA. Des rendements d'extraction compris entre 100,8 et 102,5% ont été obtenus avec des CV de 2,7-3,3% (n = 5).

Dans la continuité de tous ces travaux ayant démontré la sélectivité des MIP en bloc obtenus avec le MAA et l'EGDMA pour les neurotransmetteurs et les analogues ciblés, notre groupe a synthétisé des MIP reprenant ces conditions de synthèse [187]. L'éphédrine a été sélectionnée comme molécule empreinte, le chloroforme comme porogène et un ratio molaire T/M/CL de 1/4/20 a été appliqué. Des premières expériences d'extraction ont été menées avec 1 mL d'eau dopée avec

l'éphédrine à 500 ng mL<sup>-1</sup>. Un lavage avec 1 mL d'ACN a été effectué suivi de 1,5 mL d'ACN + 0,01% TFA puis l'élution a été réalisée avec 3 mL d'ACN + 0,025% TFA. L'effet d'impression a été démontré par la différence des rendements d'extraction obtenus pour le MIP de 74% et le NIP de 7% (n = 2). La capacité des supports a ensuite été évaluée avec des échantillons aqueux dopés avec diverses concentrations d'éphédrine (0,1-100 µg mL<sup>-1</sup>). Cependant, le plateau n'a pas été atteint pour le MIP dans l'intervalle étudié, mettant en évidence le fait que la capacité n'a pas été atteinte (< 1 mg g<sup>-1</sup>). En revanche, la rétention de l'éphédrine sur le NIP était faible avec un taux de récupération constant de 2% confirmant ainsi la présence de cavités spécifiques sur le MIP. Suite à l'optimisation du protocole d'extraction, des échantillons de 1 mL de plasma humain dilué dans l'ACN (x2) et dopé avec l'éphédrine à 500 ng mL<sup>-1</sup> ont été percolés sur le MIP et le NIP. Des lavages de 1 mL d'ACN et 3,5 mL d'ACN + 0,025% TFA ont été réalisés puis 2,5 mL d'ACN + 0,05% TFA ont été appliqués pour l'élution. Des rendements de 68% (n = 2) ont été obtenus sur le MIP alors qu'aucune rétention n'a été observée sur le NIP. Cette sélectivité du MIP a ainsi permis d'obtenir des chromatogrammes après séparation LC-UV montrant une ligne de base plus propre et l'absence de nombreux composés interférents. Des LOD et LOQ de respectivement 36 et 120 ng mL<sup>-1</sup> ont été estimés.

Ces études ont donc montré la faisabilité des MIP pour la reconnaissance spécifique des neurotransmetteurs et de leurs analogues structuraux ciblés dans ce chapitre. La voie de synthèse en bloc utilisant comme réactif le MAA et l'EGDMA avec un ratio molaire T/M/CL de 1/4/20 est prédominante dans la bibliographie et a démontré son potentiel dans l'extraction exhaustive en milieu réel. Il paraît donc judicieux de s'en inspirer pour la synthèse de monolithes imprimés miniaturisés.

### **IV.3. Synthèse de monolithes imprimés miniaturisés avec l'éphédrine et premières caractérisations**

L'objectif de ce chapitre est d'évaluer la possibilité de transférer facilement la méthode de synthèse thermique de MIP monolithique développée précédemment pour la cocaïne et la BZE à une autre famille de composés. Les supports monolithiques obtenus pourraient ainsi mener, de la même façon que pour la cocaïne, à un couplage en ligne de l'extraction miniaturisée avec la nanoLC-UV.

Dans la continuité des travaux menés au laboratoire sur les MIP en bloc pour l'extraction de neurotransmetteurs [187], l'éphédrine a été choisie comme molécule empreinte et les réactifs adéquats à la synthèse d'un MIP monolithique miniaturisé ont été repris des synthèses précédentes ciblant la cocaïne et la BZE. Le MAA a donc été utilisé comme monomère fonctionnel et le mélange d'ACN avec 10% d'isoctane a été conservé comme solvant porogène. Cependant, il a été décidé de

se concentrer sur l'impact de l'EGDMA ou du TRIM comme agent réticulant sur la structure monolithique, en réalisant par conséquent deux types de synthèse différents. Concernant la proportion de chacun des réactifs, un ratio molaire 1/4/20 a été conservé, correspondant respectivement à la molécule empreinte, au monomère et à l'agent réticulant. Par ailleurs, un ratio de 15/85 a été respecté entre le volume de monomère et d'agent réticulant et celui de porogène. Avec ces conditions de synthèse, des MIP monolithiques ont été préparés *in situ* par une polymérisation thermique à 60°C pendant 24 h dans des capillaires de 15 cm et 100 µm de diamètre interne selon le protocole utilisé dans le **Chapitre II** (Article 1) et décrit en **Annexe 2**. En parallèle des MIP, les supports NIP correspondants à chaque mélange réactionnel ont été synthétisés en absence de molécule empreinte. De plus, chaque synthèse de MIP ou NIP a été répétée indépendamment trois fois. Finalement, les capillaires contenant les monolithes ont été coupés pour obtenir des longueurs de 5 cm afin de caractériser les monolithes et comparer leurs propriétés et performances.

#### IV.3.1. Evaluation de la perméabilité des monolithes

Dans l'objectif de sélectionner la voie de synthèse la plus adaptée à un futur couplage en ligne de l'étape d'extraction sur le monolithe avec une séparation en nanoLC, une première étude sur la perméabilité des monolithes a été menée. En effet, ce paramètre est crucial pour l'avenir du projet puisque le MIP monolithique doit être suffisamment perméable pour permettre le passage de solutions telles que les phases mobiles sans générer une contre-pression trop importante.

Pour effectuer cette évaluation, chaque capillaire contenant un monolithe (5 cm x 100 µm i.d.) a été connecté à une pompe nanoLC délivrant de l'ACN et la température du montage a été fixée à 35°C. En faisant varier le débit délivré et en enregistrant la contre-pression générée par chaque MIP et NIP (**Figure 24**), la loi de Darcy a permis de calculer la perméabilité de chaque monolithe indiquée dans le **Tableau 21**. Pour les monolithes synthétisés avec l'EGDMA, la perméabilité est de  $1,82 \times 10^{-15} \text{ m}^2$  (CV = 7%, n = 3) pour le MIP et de  $10,16 \times 10^{-15} \text{ m}^2$  (CV = 8%, n = 3) pour le NIP. Pour les synthèses avec le TRIM, des valeurs de  $2,61 \times 10^{-15} \text{ m}^2$  (CV = 5%, n = 3) et  $6,33 \times 10^{-15} \text{ m}^2$  (CV = 16%, n = 3) ont été respectivement obtenues pour le MIP et le NIP. Dans chaque cas, la perméabilité du NIP est supérieure à celle du MIP, comme cela a déjà été observé lors de l'étude sur la cocaïne et la BZE (**Tableau 21**), témoignant de l'effet de la molécule empreinte sur la structure du monolithe. D'autre part, la perméabilité est plus grande en utilisant le TRIM plutôt que l'EGDMA comme agent réticulant, ce qui confirme l'intérêt de ce monomère trifonctionnel. En effet, il a déjà été rapporté que ce réactif pouvait donner lieu à des polymères macroporeux [169,170], ce qui est particulièrement intéressant pour la synthèse de monolithes miniaturisés afin de pouvoir y assurer l'écoulement de solutions lors de leur

utilisation. Les monolithes synthétisés avec le TRIM comme agent réticulant ont donc été sélectionnés pour la suite de l'étude et leur sélectivité a donc ensuite été évaluée.

**Tableau 21.** Perméabilités mesurées sur les MIP et les NIP synthétisés avec l'EGDMA ou le TRIM comme agent réticulant et comparées avec les résultats obtenus précédemment [90] pour les supports avec la cocaïne comme molécule empreinte et le TRIM (3 synthèses indépendantes pour chaque support).

T/M/CL	MIP		NIP	
	K ( $10^{-15} \text{ m}^2$ )	CV, n = 3 (%)	K ( $10^{-15} \text{ m}^2$ )	CV, n = 3 (%)
Ephédrine/MAA/EGDMA	1,82	7	10,16	8
Ephédrine/MAA/TRIM	2,61	5	6,33	16
Cocaïne/MAA/TRIM	3,27	3	36,57	17

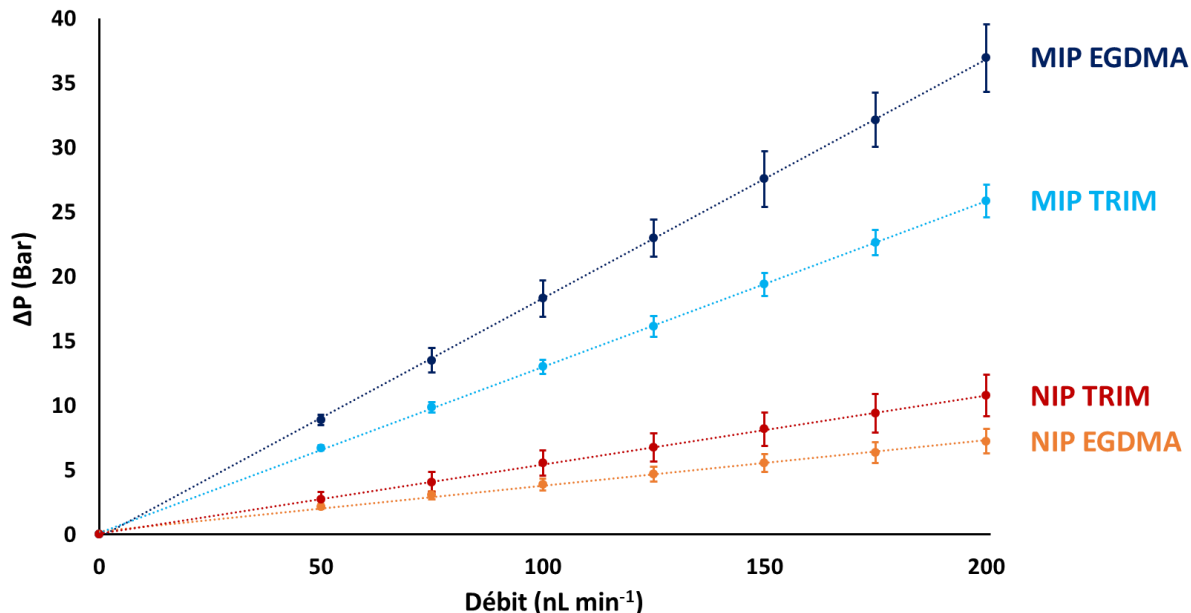


**Figure 24.** Contre-pression générée en fonction du débit de phase mobile appliquée sur le capillaire (5 cm x 100 µm i.d.) contenant le MIP ou le NIP monolithique synthétisés avec l'EGDMA ou le TRIM comme agent réticulant. Phase mobile : ACN, n = 3 synthèses indépendantes. Autres conditions : voir Annexe 5.

#### IV.3.2. Evaluation de la sélectivité des monolithes à base de TRIM

Puisque la caractérisation de la rétention de tous les composés d'intérêt sur les monolithes est particulièrement chronophage, il a été choisi d'étudier en priorité deux composés, *i.e.* l'éphédrine et la dopamine, à savoir la molécule empreinte ainsi que l'analogue structural ayant la polarité et la structure la plus éloignée de cette dernière. L'éphédrine et la dopamine, à  $100 \mu\text{g mL}^{-1}$  dans l'ACN, ont donc été injectées *via* une boucle d'injection de 50 nL montée sur une vanne 6 voies sur le MIP ou le NIP correspondant (50 mm x 100 µm i.d.). La phase mobile était composée d'ACN car une sélectivité optimale est en général obtenue avec un solvant proche du porogène employé lors de la synthèse (ACN/Isooctane, 90/10, v/v). De plus, le MIP monolithique synthétisé précédemment pour la cocaïne et la BZE a démontré une très forte sélectivité dans ce solvant. Cependant, un volume de 10% d' $\text{H}_2\text{O}$  a dû être ajouté dans la phase mobile afin de permettre l'élution de l'éphédrine du MIP, composé le plus retenu sur ce support. Par ailleurs de l'acétone a également été injectée afin de déterminer le temps de rétention nulle. Des exemples de chromatogrammes obtenus avec le MIP et le NIP sont présentés

**Figure 25.**

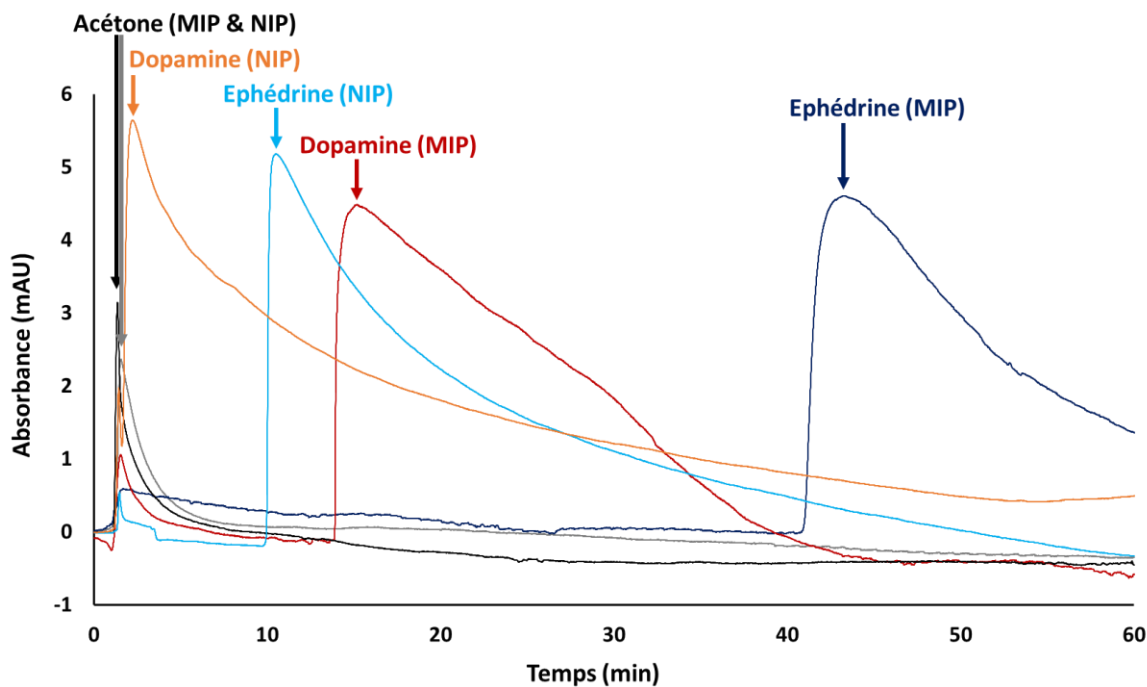


**Figure 25.** Chromatogrammes obtenus après injection de 50 nL d'acétone, d'éphédrine ( $100 \mu\text{g mL}^{-1}$ ) ou de dopamine ( $100 \mu\text{g mL}^{-1}$ ) sur les MIP et NIP monolithiques (50 mm x 100 µm i.d.). Phase mobile : ACN/ $\text{H}_2\text{O}$  (90/10, v/v),  $400 \text{ nL min}^{-1}$ , détection UV à 200 nm.

De toute évidence, la rétention de l'éphédrine et de la dopamine sur le MIP est plus importante que sur le NIP. Cette différence de rétention sur les deux supports témoigne de la sélectivité du MIP pour les deux composés. Malgré l'asymétrie des pics obtenus, les temps de rétention de l'acétone et des deux analytes ont été déterminés au sommet du pic. Les facteurs de rétention et d'impression de l'éphédrine et la dopamine ont ainsi été calculés et ils sont donnés dans le **Tableau 22**.

**Tableau 22.** Facteurs de rétention et facteurs d'impression pour l'éphédrine et la dopamine mesurés sur trois couples MIP/NIP issus de synthèses indépendantes. Injection de 50 nL d'acétone, d'éphédrine ( $100 \mu\text{g mL}^{-1}$ ) ou de dopamine ( $100 \mu\text{g mL}^{-1}$ ) sur un capillaire rempli de MIP ou NIP monolithique (50 mm x 100  $\mu\text{m}$  i.d.). Phase mobile : ACN/ $\text{H}_2\text{O}$  (90/10, v/v).

	$k_{\text{MIP}}$ (CV, n = 3)	$k_{\text{NIP}}$ (CV, n = 3)	IF (CV, n = 3)
Ephédrine	26,8 (1%)	6,7 (3%)	4,0 (2%)
Dopamine	8,4 (4%)	0,7 (11%)	11,7 (7%)

La forte sélectivité des MIP indépendamment synthétisés est confirmée pour les deux molécules dans le milieu ACN/ $\text{H}_2\text{O}$  (90/10, v/v) puisque les IF sont largement supérieurs à 1, avec des valeurs de respectivement  $4,0 \pm 0,1$  et  $11,7 \pm 0,8$  pour l'éphédrine et la dopamine. Enfin, les valeurs de CV (n = 3) mesurées sur les facteurs de rétention pour les deux analytes sont inférieures à 11%. Ces résultats confirment la répétabilité du protocole de synthèse. Ceci montre qu'il est possible d'obtenir *in situ* dans des capillaires de 100  $\mu\text{m}$  de diamètre interne des MIP monolithiques à la fois sélectifs et répétables avec des protocoles génériques pouvant s'adapter à différentes natures de molécule empreinte. Le couplage en ligne de l'extraction des cinq composés cibles sur ces supports et leur séparation en nanoLC a donc été envisagée.

#### IV.4. Séparation analytique de l'éphédrine et de ses analogues structuraux

Avant d'évaluer la possibilité d'analyser l'éphédrine et ses analogues structuraux en nanoLC-UV et de coupler en ligne cette méthode avec une extraction sur le MIP monolithique, la méthode d'analyse LC-UV a d'abord été développée en format conventionnel. En raison de la grande polarité des composés (cf. **Tableau 19**), un mode de séparation par chromatographie d'interaction hydrophile (HILIC) a été choisi.

#### IV.4.1. Séparation HILIC au format conventionnel

Une colonne analytique ZIC-HILIC (150 x 2,1 mm, 3,5 µm, Merck) a été sélectionnée pour la séparation d'un mélange des cinq composés à une concentration de  $100 \mu\text{g mL}^{-1}$  dans un mélange  $\text{H}_2\text{O}/\text{ACN}$  (30/70, v/v). Ce type de colonne est constitué d'une phase stationnaire avec des groupements zwitterioniques permettant un mécanisme de rétention mixte. La séparation a été réalisée dans les conditions décrites en **Annexe 6**, à une température de 35°C, un débit de  $300 \mu\text{L min}^{-1}$ , un volume d'injection de 5 µL et des phases mobiles composées de formiate d'ammonium à 10 mM et ajusté à pH 3 avec de l'acide formique (A) et ACN (B). Un premier gradient linéaire a été appliqué comme indiqué dans l'**Annexe 6**. Brièvement, une composition de 95 à 75% de phase mobile B a été balayée en 15 min. Le chromatogramme obtenu est présenté dans la **Figure 26 A**. Une forte dérive de la ligne de base est observable, en particulier à partir de 17 min, interférant avec la séparation des analytes. De plus, des composés issus probablement d'une dégradation de la solution injectée sont co-élués avec l'octopamine.

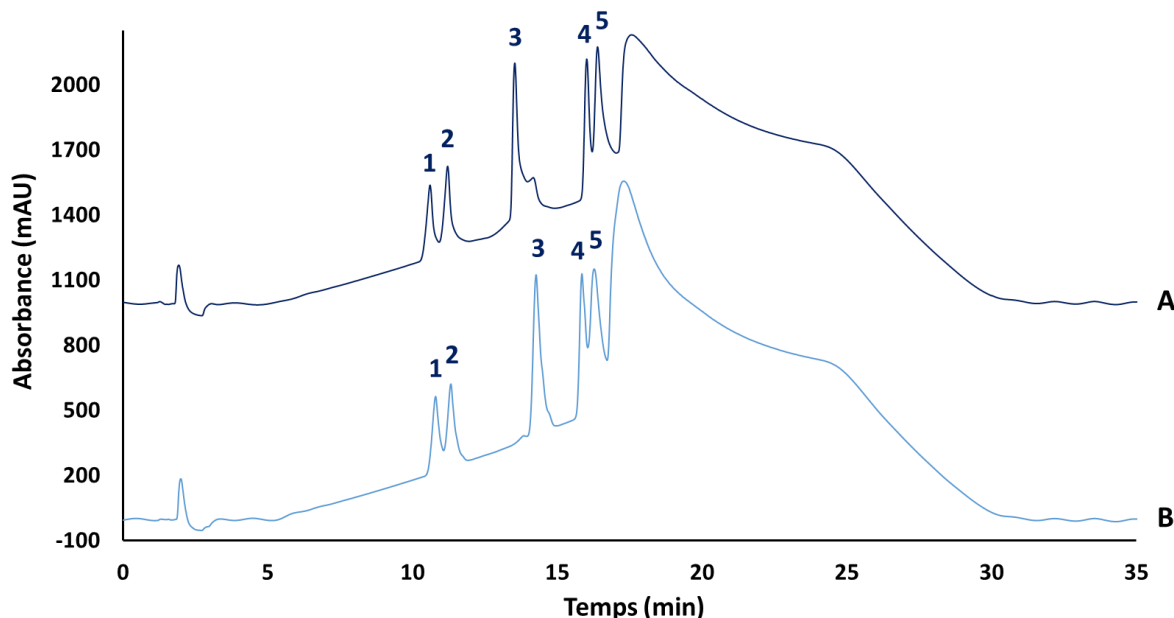


**Figure 26.** Chromatogrammes obtenus lors de la séparation en HILIC d'un mélange de méthyléphédrine (1), éphédrine (2), synéphrine (3), d'octopamine (4) et dopamine (5) à  $100 \mu\text{g mL}^{-1}$  dans  $\text{H}_2\text{O}/\text{ACN}$  (30/70, v/v) (A) ou  $\text{HCl} 0,05 \text{ M}/\text{ACN}$  (30/70, v/v). Colonne ZIC-HILIC (150 x 2,1 mm, 3,5 µm),  $V_{inj} = 5 \mu\text{L}$ , phase mobile : formiate d'ammonium 10 mM pH 3/ACN,  $300 \mu\text{L min}^{-1}$ , détection UV à 200 nm.

Afin d'éliminer ces interférents, une nouvelle solution a été préparée en veillant à acidifier le milieu comme reporté dans l'**Annexe 6**. Le chromatogramme correspondant à ce mélange (**Figure 26 B**) montre l'élimination des composés interférents, confirmant l'hypothèse d'un problème de stabilité des échantillons. Un suivi de la dégradation des solutions préparées a par conséquent été réalisé ensuite (**Section IV.4.2**) pour garantir la stabilité des solutions acidifiées dans le temps. En revanche, le phénomène de dérive de la ligne de base n'a pas été résolu et semble même s'être aggravé. Ce phénomène pourrait avoir comme origine le gradient de sel induit lors de la séparation, puisque ceux-ci sont uniquement présents dans la phase mobile aqueuse (A). Les conditions de la séparation ont donc été modifiées pour conserver une concentration en sel constante tout au long de l'analyse. Pour cela, les phases mobiles ont été modifiées comme indiqué dans l'**Annexe 6** (formiate d'ammonium 50 mM à pH 3/ACN (5:95) (A) et formiate d'ammonium 10 mM pH 3/ACN (25:75) (B)) et la programmation du gradient a été adaptée afin de conserver un ratio de phase aqueuse/organique identique par rapport aux séparations précédentes. Un gradient passant de 0 à 100% de B en 15 min a donc été appliqué et le chromatogramme résultant est présenté dans la **Figure 27**.

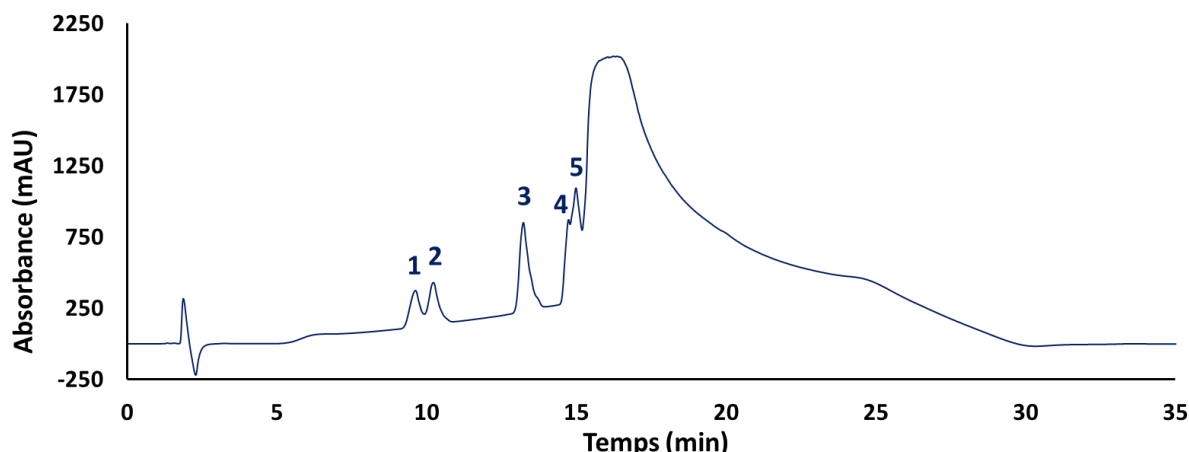


**Figure 27.** Chromatogramme obtenu lors de la séparation en HILIC avec un gradient maintenant une teneur en sel constante d'un mélange de méthyléphédrine (1), éphédrine (2), synéphrine (3), d'octopamine (4) et dopamine (5) à  $100 \mu\text{g mL}^{-1}$  dans  $\text{HCl } 0,05 \text{ M/ACN (30/70, v/v)}$ . Colonne ZIC-HILIC (150 x 2,1 mm, 3,5  $\mu\text{m}$ ),  $V_{\text{inj}} = 5 \mu\text{L}$ , phase mobile : formiate d'ammonium 50 mM pH 3:ACN (5:95)/formiate d'ammonium 10 mM pH 3:ACN (25:75),  $300 \mu\text{L min}^{-1}$ , détection UV à 200 nm.

Le phénomène de dérive a malheureusement été amplifié avec ces nouvelles conditions et il semble donc difficile de mener à bien l'analyse de ce mélange avec cette colonne. Il a donc été choisi de s'orienter vers un autre mode chromatographique pour réaliser la séparation des cinq composés.

#### **IV.4.2. Séparation avec une phase stationnaire PGC au format conventionnel et transfert de méthode**

Etant donné les phénomènes observés lors des séparations en HILIC, il a été choisi de réaliser la séparation de l'éphédrine et de ses analogues structuraux avec un autre mode chromatographique. Un mode de séparation de partage à polarité de phases inversée intégrant une phase stationnaire à base de carbone graphite poreux a été choisi. Une colonne analytique Hypercarb (150 x 3 mm, 5 µm, ThermoFisher Scientific), dont la phase stationnaire est également disponible à l'échelle nano, a été sélectionnée afin de faciliter le futur transfert de la méthode au format miniaturisé.

Dans un premier temps, la stabilité des analytes en solution a été étudiée. Pour cela, une solution des cinq composés à une concentration de 100 µg mL<sup>-1</sup> a été préparée dans un mélange H<sub>2</sub>O/ACN (80/20, v/v). Trois injections de cette solution ont alors été réalisées sur le système LC-UV avec un écart de 6 h entre chaque séparation afin de suivre la possible dégradation de cette dernière dans le temps. La séparation a été réalisée dans les conditions décrites en **Annexe 6**, à une température de 35°C, un débit de 400 µL min<sup>-1</sup>, un volume d'injection de 5 µL et des phases mobiles composées de H<sub>2</sub>O + 0,1% TFA (A) et d'ACN (B). Un gradient simple a été mis en place, allant de 2 à 20% de B en 22,5 min. Les chromatogrammes obtenus sont présentés dans la **Figure 28**. Il est possible d'observer une dégradation de la solution au cours du temps, en particulier pour la dopamine. En effet, son pic diminue progressivement et de nouveaux composés de rétention supérieure sont détectés. Afin d'éviter ce phénomène, une nouvelle solution a été préparée à l'identique mais cette fois en acidifiant le milieu (HCl 0,05 M/ACN (80/20, v/v), **Annexe 6**). Trois injections ont ensuite été réalisées dans les mêmes conditions que précédemment et l'expérience a été répétée une seconde fois deux jours plus tard. Les six chromatogrammes obtenus sont similaires et ne révèlent aucune dégradation. Ces conditions de préparation ont donc été sélectionnées pour la suite de l'étude. Toutefois, de nouvelles solutions ont été préparées tous les 3 jours afin d'éviter une possible dégradation en dehors de l'intervalle de temps étudié.

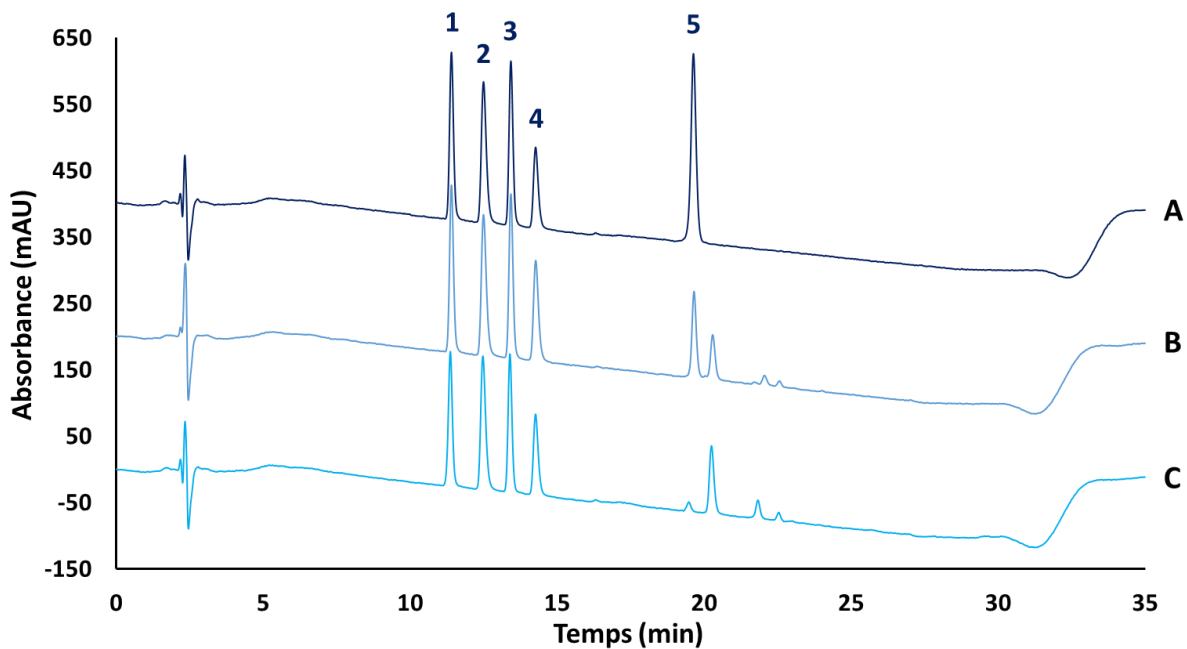


**Figure 28.** Chromatogrammes obtenus immédiatement (A), 6 h (B) et 12 h (C) après la préparation d'un mélange d'octopamine (1), éphédrine (2), synéphrine (3), méthyléphédrine (4) et dopamine (5) à  $100 \mu\text{g mL}^{-1}$  dans un mélange  $\text{H}_2\text{O}/\text{ACN}$  (80/20, v/v). Colonne Hypercarb (150 x 3 mm, 5  $\mu\text{m}$ ).

$V_{inj} = 5 \mu\text{L}$ , phase mobile :  $\text{H}_2\text{O} + 0,1\%$  TFA/ACN,  $400 \mu\text{L min}^{-1}$ , détection UV à 200 nm.

La séparation a ensuite été étudiée plus en détail en diminuant la concentration de TFA de 0,1% à 0,05% dans la phase mobile. En effet, cet acide fortement corrosif pourrait générer des effets néfastes sur le montage en ligne du monolithe avec la nanoLC. De plus, dans le cas d'une éventuelle détection par spectrométrie de masse, la réduction du TFA est également bénéfique puisqu'il est responsable de phénomènes de suppression de signal. Dans un premier temps, un gradient linéaire (Gradient 1, **Annexe 6**) a été testé en passant de 2 à 20% d'ACN en 15 min. Le chromatogramme obtenu présenté dans la **Figure 29 A** montre une co-élution de l'éphédrine et de la synéphrine. Le gradient a donc été modifié comme décrit dans l'**Annexe 6** (Gradient 2). Brièvement, la phase mobile passe de 2 à 5% d'ACN en 1 min, puis une première rupture de pente est réalisée en augmentant le ratio d'ACN dans la phase mobile de seulement 3% en 7,5 min. La force éluante est donc plus faible dans cette zone par rapport au premier gradient, permettant une meilleure séparation des deux analytes précédemment co-élués. Ensuite, une deuxième rupture de pente est réalisée pour atteindre 20% d'ACN en 5 min. Finalement, le chromatogramme présenté **Figure 29 B** a été obtenu avec un retour à la ligne de base entre chaque analyte. Ces conditions de séparation sont donc satisfaisantes.

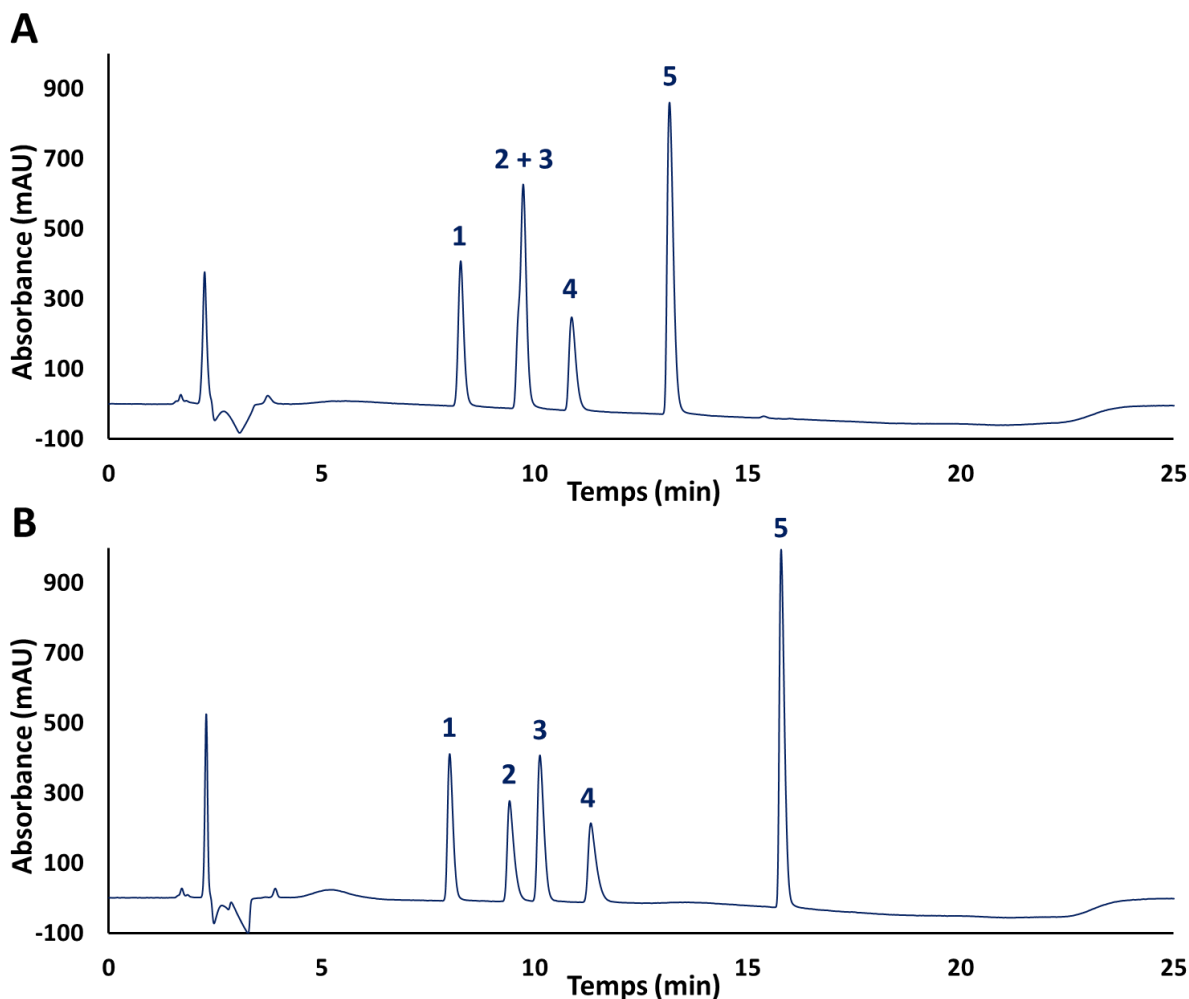


**Figure 29.** Chromatogrammes obtenus pour un mélange d'octopamine (1), éphédrine (2), synéphrine (3), méthyléphédrine (4) et dopamine (5) ( $100 \mu\text{g mL}^{-1}$  dans  $\text{HCl } 0,05 \text{ M/ACN (80/20, v/v)}$ ). Colonne Hypercarb ( $150 \times 3 \text{ mm}, 5 \mu\text{m}$ ).  $V_{\text{inj}} = 5 \mu\text{L}$ , phase mobile :  $\text{H}_2\text{O} + 0,05\%$  TFA/ACN,  $400 \mu\text{L min}^{-1}$ , gradient 1 (A) ou gradient 2 (B), détection UV à 200 nm.

Il est donc dorénavant possible d'envisager le transfert de cette méthode analytique à l'échelle nano sur une colonne Hypercarb de dimension  $50 \times 0,075 \text{ mm}$  ( $5 \mu\text{m}$ ). Pour ce qui concerne le gradient de séparation, un calculateur intégrant les équations fondamentales de la chromatographie a été utilisé [203]. Pour ce faire, il a été nécessaire de renseigner les dimensions de la colonne et le débit de phase mobile, qui a été alors fixé à  $300 \text{ nL min}^{-1}$ . Le gradient ainsi proposé est décrit dans la **Figure 30**. Malheureusement, en raison d'un délai de livraison très important, le transfert de la séparation à l'échelle miniaturisée n'a pas pu être fait.

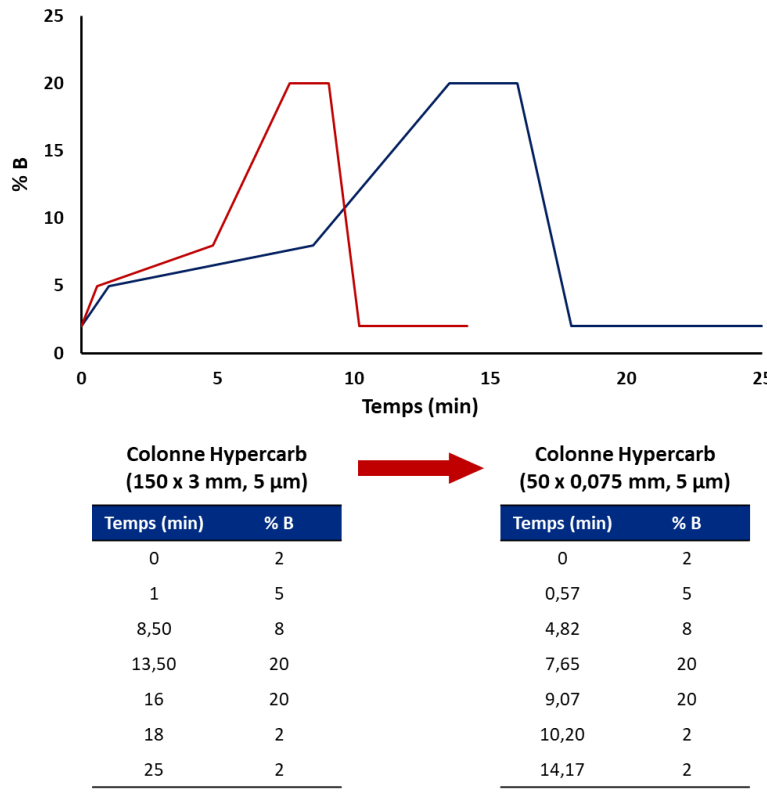


**Figure 30.** Transfert du gradient de séparation des composés d'intérêt d'une colonne Hypercarb de dimension 150 x 3 mm (5 µm) avec un débit de  $400 \mu\text{L}.\text{min}^{-1}$  (Bleu) vers une colonne Hypercarb de dimension 50 x 0,075 mm (5 µm) avec un débit de  $300 \text{nL}.\text{min}^{-1}$  (Rouge).

#### IV.5. Conclusion

Dans ce dernier chapitre, des MIP monolithiques et miniaturisés ont été synthétisés pour extraire de nouvelles cibles, des neurotransmetteurs et leurs analogues structuraux, en s'appuyant sur les acquis précédemment obtenus avec la cocaïne et la BZE. En prenant l'éphédrine comme molécule empreinte, le MAA comme monomère et en reprenant le ratio molaire T/M/CL de 1/4/20 ainsi que le ratio (M+CL)/P de 15/85 (v/v) déterminés lors des précédentes synthèses, deux agents réticulants ont été testés, le TRIM et l'EGDMA. La mesure de la perméabilité de chaque monolithe a montré que le TRIM permettait d'obtenir des monolithes plus perméables et donc plus compatibles avec un couplage en ligne avec un système générant de fortes pressions. Par la suite, une évaluation de la rétention de l'éphédrine et de la dopamine sur les monolithes a démontré la sélectivité des MIP avec l'obtention de facteurs d'impression de respectivement  $4,0 \pm 0,1$  et  $11,7 \pm 0,8$ . De plus, la répétabilité de synthèse a de nouveau été démontrée. Ces résultats viennent donc confirmer la possibilité de transférer la

méthode de synthèse de MIP monolithiques miniaturisés développée pour la cocaïne et la BZE pour d'autres familles de composés tout en conservant une excellente sélectivité.

Par manque de temps, il n'a pas été possible ensuite d'approfondir l'étude du potentiel d'extraction sélective des MIP et de leur couplage en ligne avec une séparation en nanoLC pour analyser les cinq composés ciblés dans divers échantillons biologiques.





## CONCLUSION GENERALE ET PERSPECTIVES

Au regard de l'évolution des méthodes séparatives, la miniaturisation associée au concept de  $\mu$ -TAS est une tendance qui ne cesse de prendre de l'ampleur. Dans ce cadre, le développement et la mise en œuvre d'outils intégrant les étapes de traitement de l'échantillon, séparation et détection au format capillaire représente une première voie d'élaboration de systèmes miniaturisés. Ce format capillaire offre les avantages d'être directement intégrable sur des appareils commerciaux et de limiter les coûts liés au développement de puces tel que le prototypage. L'objectif de ce travail était donc de développer des MIP miniaturisés et synthétisés *in situ* et de mettre en place des méthodes permettant leur intégration dans des systèmes en ligne afin d'extraire et d'analyser divers composés présents à l'état de trace dans des échantillons biologiques.

Après une étude de l'état de l'art, dans une première approche, la cocaïne et son métabolite principal, la BZE, ont été sélectionnés comme molécules d'intérêt. Différentes conditions de synthèses ont été ciblées pour identifier celles conduisant au MIP le plus sélectif mais également ayant la plus grande perméabilité afin d'envisager un couplage en ligne de l'étape d'extraction avec l'étape de séparation et/ou de détection. Le support monolithique le plus prometteur a été obtenu avec la cocaïne comme molécule empreinte, le MAA en tant que monomère et le TRIM comme agent réticulant avec un ratio 1/4/20 de ces réactifs. De plus, le ratio volumique des réactifs (monomère et agent réticulant) sur le porogène a été fixé à une valeur de 15/85. Ce support a été caractérisé par une observation au MEB et la détermination des perméabilités et des facteurs d'impression tout en prenant soin également d'évaluer la répétabilité des synthèses. L'étape d'extraction avec le monolithe imprimé a ensuite été couplée en ligne à une analyse en nanoLC-UV. La sélectivité de l'extraction sur le MIP a été optimisée en milieu pur avec diverses compositions et volumes de la solution de lavage. Certaines limitations ont été rencontrées en milieu aqueux pour l'extraction de la BZE mais des rendements proches de 100% ont été obtenus pour la cocaïne sur le MIP contre seulement 9% sur le NIP, témoignant de la sélectivité de la procédure SPE. Les conditions optimisées ont ensuite été appliquées à l'analyse en ligne de la cocaïne à partir de 100 nL d'échantillons de plasma ou de salive dopés et des LOQ de respectivement 14,5 et 6,1 ng mL<sup>-1</sup> ont été obtenues.

Dans la seconde approche, une miniaturisation encore plus poussée du système mis en place a été réalisée en couplant directement l'étape d'extraction avec celle de détection en UV pour l'analyse de la BZE. Pour ce faire, la voie de synthèse a été modifiée avec une initiation photochimique pour pouvoir réduire la longueur du MIP monolithique. Il a donc été nécessaire de caractériser à nouveau

la morphologie et la perméabilité du monolithe ainsi que la répétabilité de synthèse. De plus, il a été observé que ces MIP obtenus par irradiation UV offraient une meilleure sélectivité en milieu pur pour la BZE ( $IF = 2,7 \pm 0,1$ ) que ceux obtenus par initiation thermique. Par la suite, la sélectivité de l'étape d'extraction pour son couplage en ligne avec la nanoLC-UV a été optimisée en milieu pur en étudiant l'influence du volume d'injection et de la position du monolithe dans le montage. En raison de la sélectivité accrue du MIP monolithique par rapport à la première approche, il a été possible de procéder à une étape de lavage plus intense, ce qui a permis de réduire davantage la contribution des interactions non spécifiques. Les conditions optimisées ont ensuite été appliquées à l'extraction en ligne de la BZE à partir de 600 nL d'échantillons d'urine dopés et des limites de détection et de quantification de respectivement 56,4 et 188,0 ng mL<sup>-1</sup> ont été estimées. Il a donc été possible d'exploiter la forte sélectivité du monolithe afin de mettre en place un montage simple couplant uniquement l'extraction sur MIP à la détection et permettant la purification d'échantillons urinaires afin de détecter un seul pic correspondant à la BZE à des valeurs compatibles avec la législation française sur le dépistage de la consommation de cocaïne.

Compte tenu de la sélectivité des MIP monolithiques miniaturisés obtenus dans les précédentes études, un MIP monolithique miniaturisé a ensuite été développé en exploitant le savoir-faire acquis pour de nouvelles cibles, *i.e.* l'éphédrine, la méthyléphédrine, la dopamine, l'octopamine et la synéphrine. Des conditions de synthèses similaires à celles utilisées pour la cocaïne ont été mises en œuvre. Cependant, la nature de l'agent réticulant a été étudiée et il a été confirmé que le TRIM donnait des MIP plus perméables. Ensuite, d'excellentes valeurs de facteur d'impression ont été déterminées en milieu pur pour l'éphédrine et la dopamine (respectivement  $4,0 \pm 0,1$  et  $11,7 \pm 0,8$ ). Malheureusement, le couplage en ligne de l'extraction sur MIP avec une analyse en nanoLC-UV n'a pas pu être réalisé en raison de complication dans l'approvisionnement de la colonne analytique.

La présente étude a donc montré la faisabilité d'une synthèse de MIP monolithiques miniaturisés, synthétisés *in situ*, pour deux panels de molécules cibles différents ainsi que la possibilité de réaliser divers montages en ligne miniaturisés intégrant ces supports sélectifs pour l'analyse de traces dans des échantillons salivaires, plasmatiques ou urinaires. Toutefois, ces systèmes miniaturisés ont l'inconvénient majeur d'être relativement complexe à mettre en place puisque cela nécessite une attention particulière au niveau des multiples connexions et des volumes morts pour pouvoir obtenir des analyses répétables et performantes. Ces problèmes pourraient être allégés, voire supprimés, par l'utilisation d'une puce dédiée, où les étapes d'extraction et de séparation sont intégrées. L'intégration d'un monolithe imprimé dans un tel système pourrait donc être une perspective intéressante, notamment si l'on considère que les synthèses effectuées *in situ* au cours de ce travail de thèse ont

présenté une répétabilité très satisfaisante, aussi bien pour la morphologie des MIP obtenus que pour leurs propriétés de rétention sélective que ce soit en milieu pur ou avec des échantillons biologiques. Des optimisations seront néanmoins à prévoir pour mener à bien leur intégration dans des puces, notamment le traitement de la surface des canaux du microsystème pour le bon ancrage du MIP. Une étape intermédiaire pourrait également être envisagée, en réalisant une puce hybride dans laquelle le capillaire permettant l'extraction serait intégré directement. Cette technologie permettrait de conserver le savoir-faire des synthèses de monolithes imprimés ainsi que leur répétabilité pour se concentrer davantage sur l'optimisation des modules environnants.



---

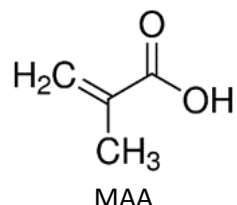
## **ANNEXES**

---



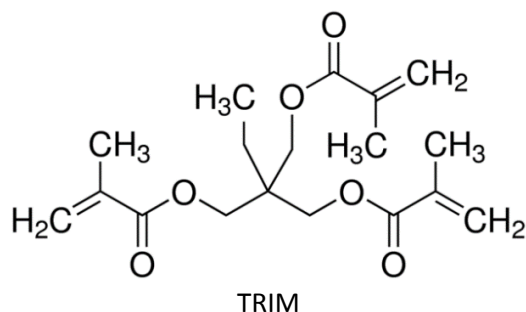
## Annexe 1 : Structure chimique des réactifs

**Monomère :**

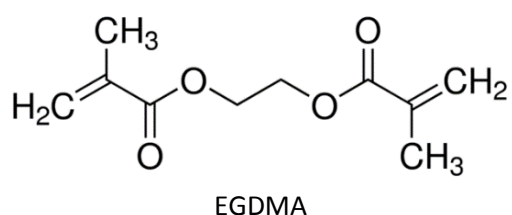


Acide méthacrylique

**Agents réticulants :**

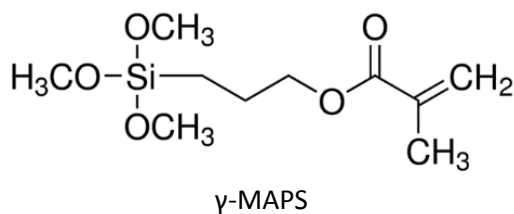


Triméthylolpropane triméthacrylate



Ethylèneglycol diméthacrylate

**Activateur :**



$\gamma$ -(Triméthoxysilyl)propyl méthacrylate

## **Annexe 2 : Protocole de synthèse d'un MIP dans un capillaire**

Les synthèses ont été réalisées avec une bobine de capillaire en silice vierge de  $100 \pm 4 \mu\text{m}$  de diamètre interne et  $363 \pm 10 \mu\text{m}$  de diamètre externe avec une gaine de Téflon® AF transparente aux UV (TSU 100375, Polymicro Molex). Le protocole suivant a été utilisé pour 1 m de capillaire.

### **Pré-traitement du capillaire :**

- Acétone : élimination des impuretés ( $\approx 100 \mu\text{L}$  injection manuelle)
- H<sub>2</sub>O : rinçage ( $\approx 100 \mu\text{L}$  injection manuelle)
- NaOH 1 M : rupture des ponts siloxane et activation des groupements silanols (injection manuelle jusqu'à pH basique sur bandelette puis pousse-seringue :  $0.25 \mu\text{L min}^{-1}$ , 30 min)
- H<sub>2</sub>O : rinçage (injection manuelle jusqu'à pH neutre sur bandelette)
- HCl 0.1 M : élimination des impuretés métalliques (injection manuelle jusqu'à pH acide sur bandelette puis pousse-seringue :  $0.25 \mu\text{L min}^{-1}$ , 30 min)
- EtOH : conditionnement ( $\approx 100 \mu\text{L}$  injection manuelle)
- 20% de 3-(triméthoxysilyl)propyl méthacrylate dans EtOH (pH = 3.5 Acide Acétique) ( $\approx 100 \mu\text{L}$  injection manuelle puis pousse-seringue :  $0.25 \mu\text{L min}^{-1}$ , 60 min)
- EtOH : lavage ( $300 \mu\text{L}$  injection manuelle)
- Séchage sous flux d'azote ( $t = 3 \text{ h}$ )

### **Synthèse du monolithe :**

Le capillaire est découpé afin d'obtenir des longueurs de 15 cm. Suite au calcul des quantités requises pour chacun des réactifs, la synthèse a été effectuée de la façon suivante :

- Mélange de la molécule empreinte, du monomère et du mélange de solvants.
- Le flacon est fermé, agité et placé au réfrigérateur pendant 1 h.
- Ajout de l'agent réticulant et de l'initiateur dans le flacon précédemment plongé dans un bain de glace.
- Dégazage sous flux d'azote pendant 5 min dans le bain de glace. Pour ce faire, le septum est percé d'une part avec une aiguille reliée à la rampe d'azote puis d'une autre part avec une seconde aiguille venant faire contre pression.
- Le capillaire est rempli par capillarité en venant percer le septum.
- Le capillaire est bouché de part et d'autre par des bouchons de GC.

- La polymérisation est initiée de la façon suivante :
  - Polymérisation thermique : bain thermostaté à 60°C pendant 24 h.
  - Polymérisation UV : chambre d'irradiation Spectrolinker XL-1500 UV crosslinker (Spectronics Corporation) comportant 6 lampes UV (6 x 155 W) de 365 nm à température ambiante pendant 30 min.
- Les polymères obtenus sont lavés avec ACN/Acide Acétique (98/2, v/v) pour éliminer l'empreinte avec un volume équivalent à dix fois celui du capillaire et un débit de 0.2 µL min<sup>-1</sup>.

### Annexe 3 : Supplementary materials – Chapitre II - Article 1

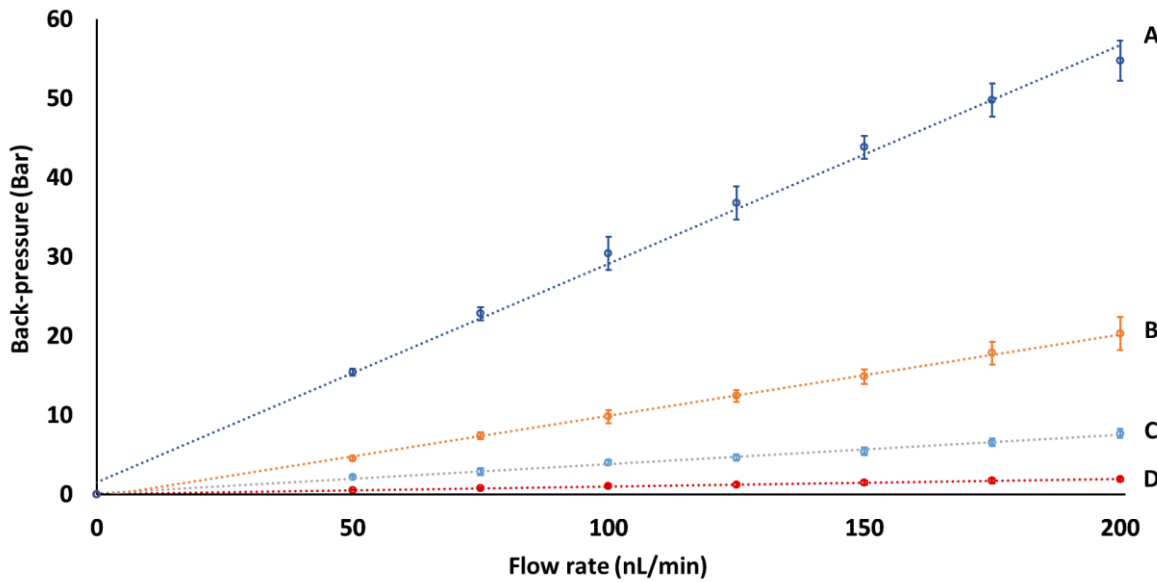


**Figure S1.** Effect of flow rate on the back-pressure generated by the capillary (5 cm-long) containing the monolithic MIP (A) and NIP (C) synthesized with (M+CL)/P ratio of 20/80 and the monolithic MIP (B) and NIP (D) synthesized with (M+CL)/P ratio of 15/85. Mobile phase: ACN,  $n = 3$ .

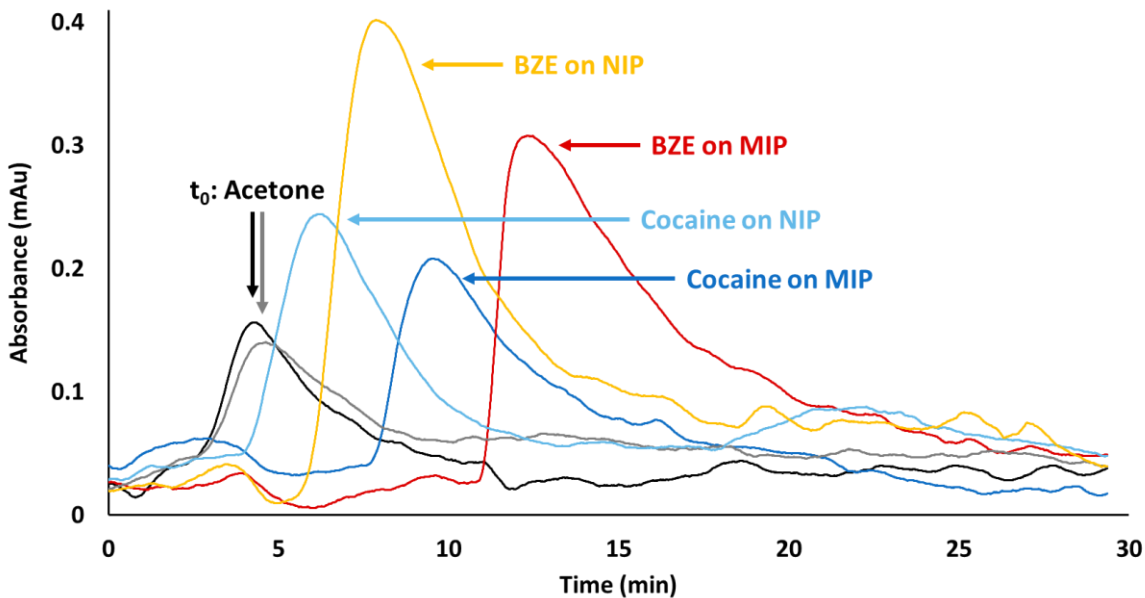


**Figure S2.** Chromatograms obtained after the injection of acetone, cocaine (COC, 50 nL,  $25 \mu\text{g mL}^{-1}$ ), and BZE (50 nL,  $25 \mu\text{g mL}^{-1}$ ) on monolithic MIP and NIP (50 mm x 100  $\mu\text{m}$  i.d.) synthesized with a ratio 15/85 ((M+CL)/P). Mobile phase: ACN,  $200 \text{ nL min}^{-1}$ , UV detection at 233 nm.

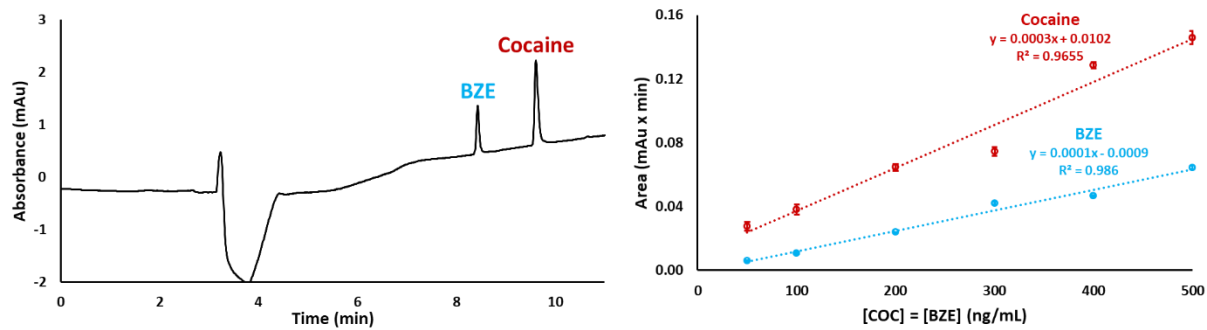


**Figure S3.** Chromatogram and calibration lines obtained for the direct injection of cocaine and BZE at  $500 \text{ ng mL}^{-1}$  on the Acclaim<sup>TM</sup> PepMap<sup>TM</sup> 100 C18 ( $150 \times 0.075 \text{ mm}$ ,  $3 \mu\text{m}$ ).  $V_{inj} = 50 \text{ nL}$ , Mobile phase: ammonium formate  $10 \text{ mM}$  pH 3.1 adjusted with formic acid (A) / ACN (B),  $200 \text{ nL min}^{-1}$ , UV detection at  $233 \text{ nm}$ .

## Annexe 4 : Supplementary materials – Chapitre III - Article 2

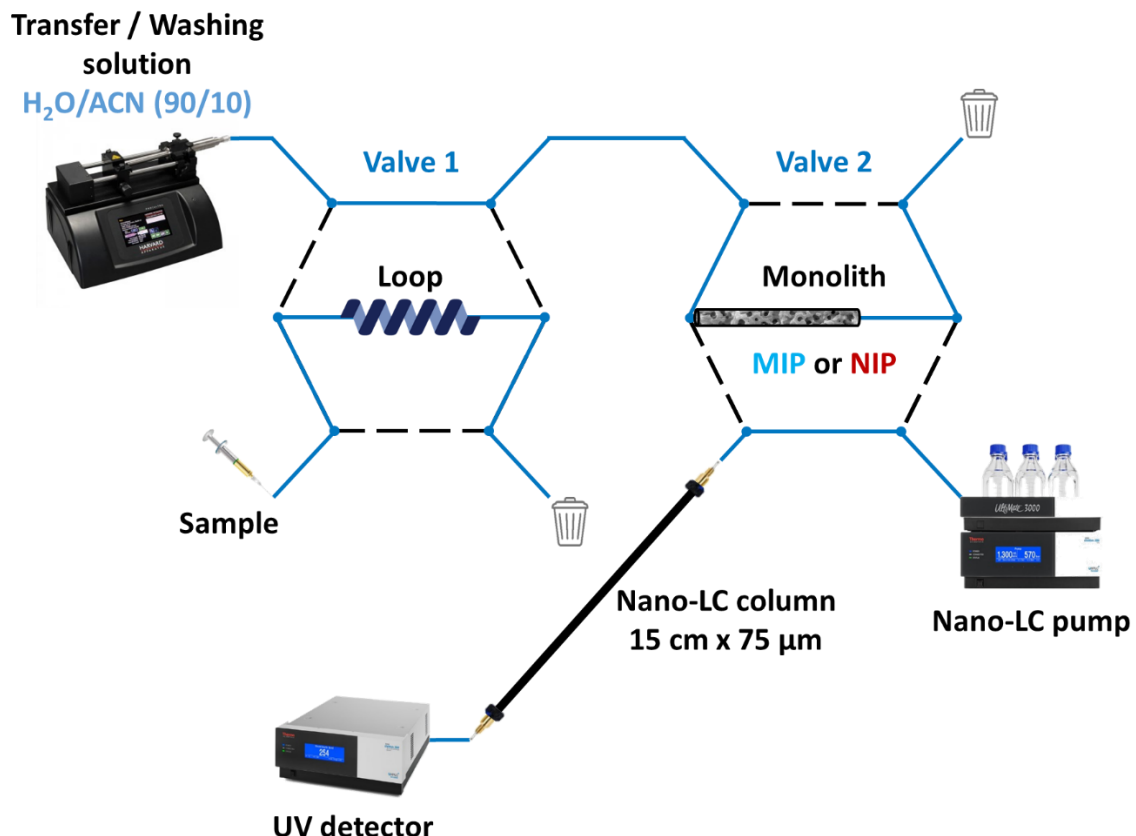


**Figure S4.** Set-up of the on-line coupling of the monolithic MIP/NIP (50 mm x 100 µm i.d.) synthesized using thermal initiation with nanoLC-UV.

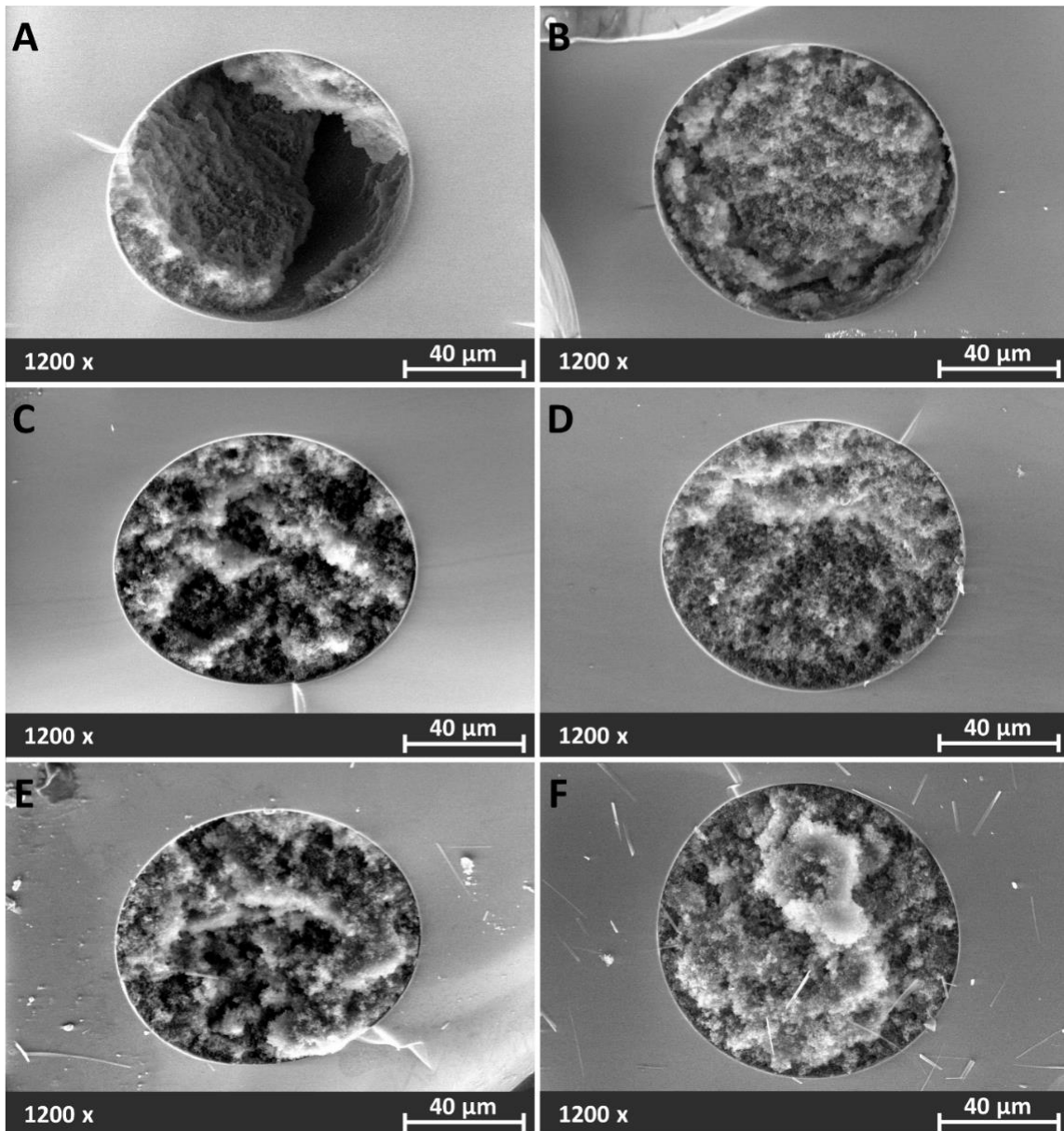


**Figure S5.** Scanning electron micrographs of the cross section of a 100  $\mu\text{m}$  i.d. capillary containing a monolithic (A, C, E) MIP or (B, D, F) NIP synthesized with UV initiation at room temperature during 15 min (A, B) and 30 min (C, D) or thermal initiation at 60°C during 24h (E, F).

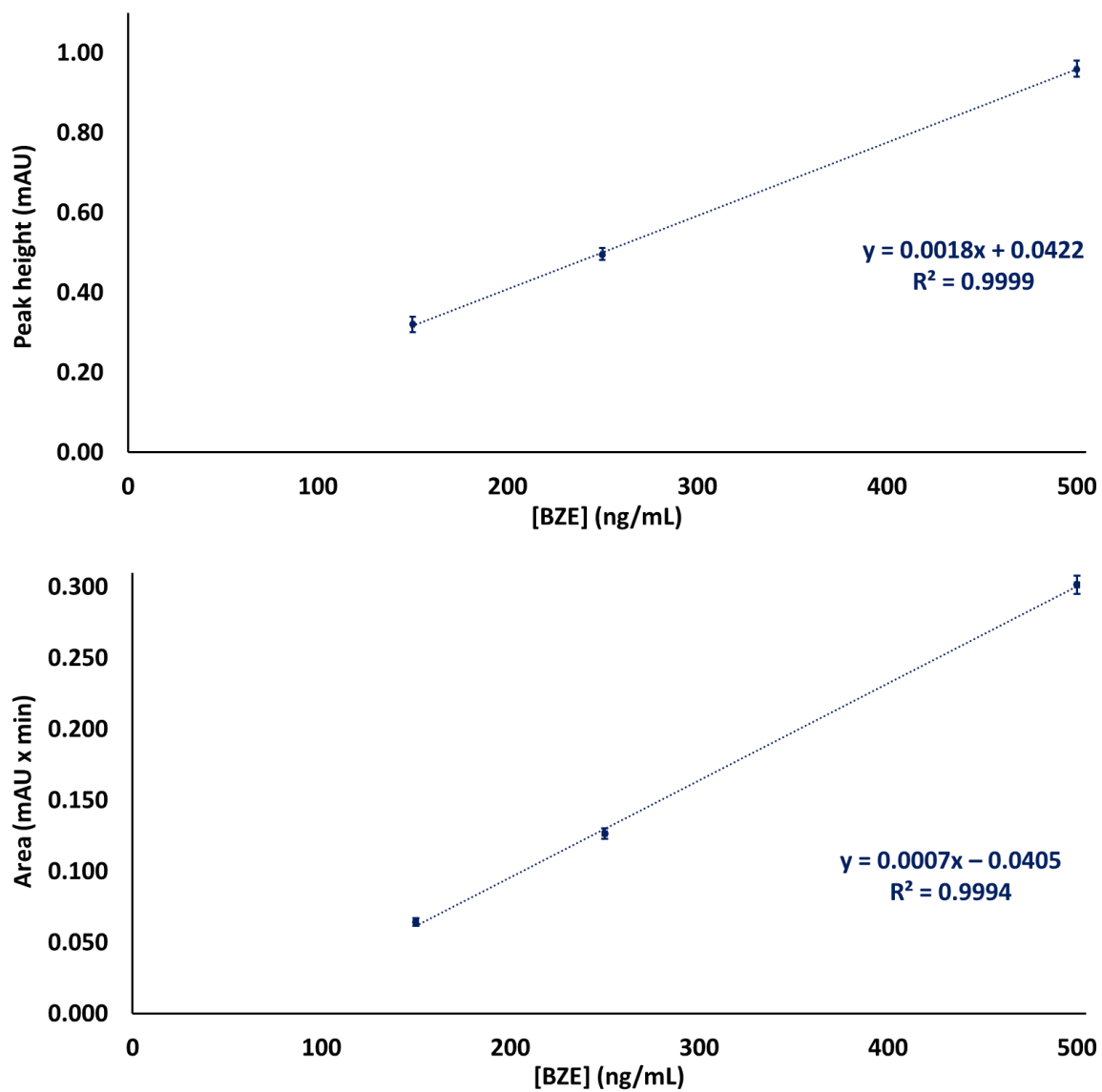


**Figure S6.** Curves plotting (Top) the peak height and (Down) peak area as a function of the BZE concentration from 150 to 500 ng mL<sup>-1</sup> in 600 nL of spiked diluted urine (x2).

## **Annexe 5 : Conditions expérimentales pour la synthèse et la caractérisation des monolithes imprimés miniaturisés avec l'éphédrine**

### **Composition du mélange réactionnel de synthèse :**

Les synthèses ont été réalisées par voie thermique avec le protocole décrit en **Annexe 2** et le mélange réactionnel suivant :

T : Ephédrine

M : MAA

CL : EGDMA ou TRIM

P : ACN/Isooctane (90/10, v/v)

Initiateur : AIBN, 1,5% M+CL (w/w)

Ratio molaire T/M/CL : 1/4/20

Ratio (M+CL)/P : 15/85 (v/v)

### **Caractérisation de la perméabilité :**

Les mesures de contre-pression ont été effectuées avec un système UltimateTM RSLCnano 3000 (ThermoFisher Scientific, Le Pecq, France), composé d'une pompe nanoLC délivrant 100% d'ACN ( $\eta = 0,316 \text{ mPa s}$  à  $35^\circ\text{C}$ ) à différents débits en maintenant le monolithe à une température constante de  $35^\circ\text{C}$  avec un four à colonne (TCC 3000SD column compartment, ThermoFisher Scientific Dionex).

La perméabilité a été calculée en utilisant la loi de Darcy :

$$K = \frac{4\eta LF}{\pi d_i^2 \Delta P} \quad (\text{Equation 1})$$

où K est la perméabilité ( $\text{m}^2$ ), F le débit appliqué ( $\text{m}^3 \text{ s}^{-1}$ ),  $\eta$  la viscosité du solvant ( $\text{Pa s}$ ), L la longueur du capillaire (m),  $\Delta P$  la contre-pression mesurée (Pa) et  $d_i$  le diamètre intérieur du capillaire (m)

### **Evaluation de la sélectivité :**

Des injections de cocaïne et de BZE ( $100 \mu\text{g mL}^{-1}$  dans l'ACN) ont été réalisées sur les capillaires contenant les MIP/NIP *via* un système nanoLC composé d'une nano-vanne à six ports (Cheminert nanovolume 6 ports 2 pos 1/32", manuel CN2-4346, Vici Valco Instruments Inc. Co., Houston, TX, USA) connectée à une boucle d'injection de 50 nL, à une nano-pompe (NCP-3200RS Nano Pump, ThermoFisher Scientific Dionex, contrôlée par Chromeleon 6.80 SR12) délivrant la phase mobile ACN/H<sub>2</sub>O (90/10, v/v) à un débit de  $400 \text{ nL min}^{-1}$  et à un détecteur à barrettes de diodes (VWD 3100

Detector, ThermoFisher Scientific Dionex) avec une cellule de détection de 3 nL. Les capillaires contenant les MIP/NIP ont été maintenus à 35°C avec un four à colonne (TCC 3000SD column compartment, ThermoFisher Scientific Dionex). Les composés ont été détectés à 200 nm et l'acétone a été utilisée comme marqueur pour déterminer le volume mort. Les facteurs d'impression (IF) et de rétention (k) ont été calculés à l'aide des équations suivantes :

$$IF = \frac{k_{MIP}}{k_{NIP}} \quad (\textbf{Equation 2})$$

où  $k_{MIP}$  et  $k_{NIP}$  sont les facteurs de rétention obtenus respectivement sur les colonnes de MIP et NIP monolithiques

$$k = \frac{t_r - t_0}{t_0} \quad (\textbf{Equation 3})$$

où  $t_r$  et  $t_0$  sont les temps de rétention respectivement de la dopamine ou l'éphédrine et de l'acétone

## Annexe 6 : Méthode d'analyse LC-UV pour l'éphédrine et ses analogues structuraux

### Préparation des solutions :

Des solutions stocks ont d'abord été préparées pour chaque analyte (éphédrine, méthyléphédrine, dopamine, octopamine, synéphrine) à une concentration de  $1000 \mu\text{g mL}^{-1}$  dans un mélange HCl 0,05 M/ACN dont le ratio varie en fonction de la solubilité de l'analyte de 10/90 (v/v) pour l'éphédrine et la méthyléphédrine à 90/10 (v/v) pour la dopamine, la synéphrine et l'octopamine. Ensuite, une solution du mélange des cinq composés a été préparée à une concentration de  $100 \mu\text{g mL}^{-1}$  dans un mélange final HCl 0,05 M/ACN avec un ratio de 30/70 (v/v) pour les séparations HILIC et 80/20 (v/v) pour les séparations PGC.

### Conditions d'analyses :

Pour la méthode LC-UV, une chaîne Agilent 1200 a été utilisée avec un détecteur à barrette de diodes, selon les conditions suivantes :

#### ➤ Séparation HILIC

Colonne analytique : SeQuant® ZIC®-HILIC (150 x 2,1 mm, 3,5 µm, Merck)

Débit :  $300 \mu\text{L min}^{-1}$

Température du four :  $35^\circ\text{C}$

Volume injecté : 5 µL

Détection : UV à 200 nm

- Phase mobile : (A) : Formiate d'ammonium 10 mM pH 3 ajusté avec l'acide formique (A)  
(B) : ACN

Temps (min)	%B
0	95
15	75
20	75
25	95
35	95

- Phase mobile : (A) : Formiate d'ammonium 50 mM pH 3 ajusté avec l'acide formique/ACN (5/95)
- (B) : Formiate d'ammonium 10 mM pH 3 ajusté avec l'acide formique/ACN (25/75)

Temps (min)	%B
0	0
15	100
20	100
25	0
35	0

#### ➤ Séparation PGC

Colonne analytique : Hypercarb™ (150 x 3 mm, 5 µm, ThermoFisher Scientific)

Débit : 400 µL min<sup>-1</sup>

Température du four : 35°C

Volume injecté : 5 µL

Détection : UV à 200 nm

- Phase mobile : (A) : H<sub>2</sub>O + 0,1% TFA  
(B) : ACN

Temps (min)	%B
0	2
22,5	20
26	20
27	2
35	2

- Phase mobile : (A) : H<sub>2</sub>O + 0,05% TFA  
(B) : ACN

**Gradient 1 :**

Temps (min)	%B
0	2
15	20
17	20
19	2
25	2

**Gradient 2 :**

Temps (min)	%B
0	2
1	5
8,5	8
13,5	20
16	20
18	2
25	2



## LISTE DES TABLEAUX ET FIGURES

### Liste des figures

- Figure 1.** Open tubular CEC separation with a MIP stationary phase in a capillary (50 µm i.d.) with a length of 1 m (A), 2 m (B), and 3 m (C). CEC conditions: ACN/sodium acetate 60 mM at pH 3.5 (92/8 (v/v)), applied voltage of +30 kV, UV detection at 214 nm. Peaks attribution: Acetone (1), Racemic naproxen (2), Racemic ibuprofen (3), Racemic fenoprofen (4), R-ketoprofen (5), and S-ketoprofen (6). Scanning electron micrograph of the MIP synthesized with S-ketoprofen in the capillary cross section (I) and enlargement in the region of the capillary wall (II). Adapted from [56]..... 37
- Figure 2.** (Left) MIP magnetic nanoparticles used in a chip device and (Right) chromatograms of the CEC separation of R,S-ofloxacin in a microchannel empty (A) or filled with a NIP (B) or a MIP (C). CEC conditions: ACN/acetate buffer 40 mM at pH 4.0 (9/1 (v/v)), detection potential of +1.0 V, injection voltage of 200 V for 2 s and separation voltage of 1200 V. AE: Auxiliary electrode; BR: Buffer reservoir; DR: Detection reservoir; E1, E2, E3, and E4: Electrodes for applying sampling and separation voltages; RE: Reference electrode; SR: Sample reservoir; WE: Working electrode. Adapted from [72]. ..... 46
- Figure 3.** Preparation of a monolith imprinted with a glycoprotein, based on boronate functionalized monomer with poly(dopamine) coating, and its recognition mechanism toward glycoproteins. Adapted from [88]..... 59
- Figure 4.** (Left) Scanning electron micrograph of the trietazine imprinted poly(MAPA-co-EGDMA) and the corresponding NIP and (Right) separation performance on the monolithic MIP and NIP for template trietazine (1), analog cyanazine (2), and thiourea (\*, unretained marker) at 1.0 mg/mL in aqueous media. CEC conditions: ACN/PBS buffer 10 mM at pH 11.0 (9/1 (v/v)), injection voltage of 5 kV for 30 s and separation voltage of +10 kV, UV detection at 214 nm. Adapted from [112]. ..... 64
- Figure 5.** Set-up of the on-line coupling of the monolithic MIP/NIP (50 mm x 100 µm i.d.) with nanoLC-UV (Top). Chromatograms (Left) obtained after the extraction on MIP (A) and NIP (B) of 50 nL of plasma spiked with cocaine (equivalent to 100 ng mL<sup>-1</sup> in plasma) compared to the blank plasma (C) on MIP and chromatograms (Right) obtained after the extraction on MIP (D) and NIP (E) of 50 nL of saliva spiked with 50 ng mL<sup>-1</sup> of cocaine compared to the blank plasma (F) on MIP. Adapted from [90]. .... 79
- Figure 6.** Structure chimique de la cocaïne et de la benzoylecgonine..... 91

<b>Figure 7.</b> Mécanisme d'action de la cocaïne sur le système nerveux. Adapté de [138].....	92
<b>Figure 8.</b> Principales voies métaboliques de la cocaïne dans le corps humain.....	94
<b>Figure 9.</b> Profils d'élution de la cocaïne et de la BZE ( $100 \text{ ng mL}^{-1}$ dans ACN) obtenus sur les différents MIP et NIP synthétisés en appliquant les protocoles optimisés correspondants décrits dans le <b>Tableau 12</b> [133]. .....	98
<b>Figure 10.</b> Set-up of the on-line coupling of the monolithic MIP/NIP (50 mm x $100 \mu\text{m}$ i.d.) with nanoLC-UV.....	109
<b>Figure 11.</b> Scanning electron micrographs of the cross section of a $100 \mu\text{m}$ i.d. capillary containing a monolithic (A, C) MIP or (B, D) NIP synthesized with the (M+CL)/P ratio of 15/85. ....	113
<b>Figure 12.</b> Chromatograms obtained by direct injection of cocaine and BZE ( $500 \text{ ng mL}^{-1}$ each) (A) and by on-line coupling of the extraction of water spiked at $1 \mu\text{g mL}^{-1}$ with cocaine and BZE on monolithic MIP (B) and NIP (C) synthesized with (M+CL)/P ratio of 15/85. $V_{\text{inj}} = 50 \text{ nL}$ , UV detection at 233 nm, $V_{\text{washing}} = 1000 \text{ nL}$ ( $\text{H}_2\text{O}/\text{ACN}, 90/10, \text{v/v}$ ) for on-line extraction.....	116
<b>Figure 13.</b> Effect of the volume and the composition of the transfer and washing solution, a $\text{H}_2\text{O}/\text{ACN}$ mixture with a ratio (A) 90/10, (B) 80/20, or (C) 70/30 (v/v), on the extraction recovery of cocaine on MIP and on NIP, synthesized with a (M+CL)/P ratio of 15/85, after the injection of 50 nL of water spiked with cocaine ( $1 \mu\text{g mL}^{-1}$ ). ....	117
<b>Figure 14.</b> Effect of the volume and of the composition of the transfer and washing solution, a $\text{H}_2\text{O}/\text{ACN}$ mixture with a ratio 90/10, 80/20 or 70/30 (v/v), on the extraction recovery of BZE on MIP and on NIP, synthesized with a (M+CL)/P ratio of 15/85, after the injection of 50 nL of water spiked with BZE ( $1 \mu\text{g mL}^{-1}$ ).....	118
<b>Figure 15.</b> Chromatograms obtained after the extraction on MIP (A) and NIP (B) of 50 nL of plasma spiked with cocaine (équivalent à $100 \text{ ng mL}^{-1}$ in plasma) compared to the blank plasma (C) on MIP and chromatograms obtained after the extraction on MIP (D) and NIP (E) of 50 nL of saliva spiked at $50 \text{ ng mL}^{-1}$ with cocaine compared to the blank saliva (F) on MIP. Transfer and washing step: 1800 nL of $\text{H}_2\text{O}/\text{ACN}$ (70/30, v/v).....	120
<b>Figure 16.</b> Effet du volume d'une solution de transfert et de lavage acidifiée à pH 3 et contenant 20% d'ACN sur les rendements d'extraction de la cocaïne et de la BZE ( $1 \mu\text{g mL}^{-1}$ dans l'eau) sur le MIP et le NP synthétisés avec un rapport (M+CL)/P de 15/85.....	124

**Figure 17.** (A) On-line set-up of the monolithic MIP or NIP directly coupled to UV detection for an extraction-purification step and a subsequent elution-detection step with (B) enlargement of the monolith connection whether it results from (1) thermal or (2, 3) UV initiation of the polymerization.

..... 137

**Figure 18.** Chromatograms obtained by the direct on-line coupling of the monolithic MIP/NIP (50 mm x 100 µm) synthesized using thermal initiation with UV detection.  $V_{inj} = 150$  nL (BZE at 10 µg mL<sup>-1</sup> in water),  $V_{washing} = 900$  nL (H<sub>2</sub>O/ACN, 90/10, v/v), UV detection at 233 nm. Other conditions: see **Section III.3.4.** ..... 140

**Figure 19.** Chromatograms obtained after the injection of acetone, cocaine (5 µg mL<sup>-1</sup>), or BZE (5 µg mL<sup>-1</sup>) on monolithic MIP and NIP (10 mm x 100 µm i.d.) synthesized with UV irradiation for 30 min in a 100 mm x 100 µm i.d. capillary.  $V_{inj} = 50$  nL. Mobile phase: ACN, 400 nL min<sup>-1</sup>. UV detection at 233 nm. ..... 144

**Figure 20.** Chromatograms obtained by on-line coupling of the extraction of water spiked with BZE at 1 µg mL<sup>-1</sup> on monoliths (10 mm x 100 µm i.d.) synthesized in a 100 mm x 100 µm i.d. capillary under UV, showing (A) the influence of the percolated sample volume ( $V_{inj}$ ) by modifying appropriately the volume of the transfer/washing solution ( $V_w$ ) on MIP (insert: BZE peak height vs percolated sample volume) and (B) the selectivity by comparing the performances obtained on MIP and NIP for an injection of 600 nL ( $V_w$  of 1300 nL). Transfer/washing solution: H<sub>2</sub>O/ACN (90/10, v/v). UV detection at 233 nm. Other conditions: see **Section III.3.4.** ..... 147

**Figure 21.** Chromatograms obtained after the extraction on monolithic MIP (10 mm x 100 µm i.d.) of 300 nL of (A) water spiked with BZE at 1 µg mL<sup>-1</sup> or (B) 2x diluted and filtered urine spiked with BZE at 1 µg mL<sup>-1</sup> (equivalent to 2 µg mL<sup>-1</sup> in urine) for set-up implementing the monolith at the outlet of the extraction step (configuration **Figure 17 B2**) (Blue) or at the inlet of the extraction step (configuration **Figure 17 B3**) (Black). Transfer/washing step: 1600 nL (Blue) or 1050 nL (Black) of H<sub>2</sub>O/ACN (90/10, v/v). Other conditions: see **Section III.3.4.** ..... 148

**Figure 22.** Chromatograms obtained after extraction on the monolith (10 mm x 100 µm i.d.) coupled with UV detection (configuration **Figure 17 B2**) of 600 nL of diluted urine (x2) spiked with BZE at (A) 500 ng mL<sup>-1</sup> on MIP, (B) 250 ng mL<sup>-1</sup> on MIP, (C) 150 ng mL<sup>-1</sup> on MIP, and (D) 500 ng mL<sup>-1</sup> on NIP or (E) of 600 nL of diluted urine (x2) (blank) on MIP. Transfer/washing step: 1300 nL of H<sub>2</sub>O/ACN (90/10, v/v). Other conditions: see **Section III.3.4.** ..... 150

<b>Figure 23.</b> Structure chimique de l'éphédrine, la dopamine, la méthyléphédrine, l'octopamine et la synéphrine.....	156
<b>Figure 24.</b> Contre-pression générée en fonction du débit de phase mobile appliquée sur le capillaire (5 cm x 100 µm i.d.) contenant le MIP ou le NIP monolithique synthétisés avec l'EGDMA ou le TRIM comme agent réticulant. Phase mobile : ACN, n = 3 synthèses indépendantes. Autres conditions : voir Annexe 5. ....	165
<b>Figure 25.</b> Chromatogrammes obtenus après injection de 50 nL d'acétone, d'éphédrine ( $100 \mu\text{g mL}^{-1}$ ) ou de dopamine ( $100 \mu\text{g mL}^{-1}$ ) sur les MIP et NIP monolithiques (50 mm x 100 µm i.d.). Phase mobile : ACN/H <sub>2</sub> O (90/10, v/v), 400 nL min <sup>-1</sup> , détection UV à 200 nm.....	166
<b>Figure 26.</b> Chromatogrammes obtenus lors de la séparation en HILIC d'un mélange de méthyléphédrine (1), éphédrine (2), synéphrine (3), d'octopamine (4) et dopamine (5) à $100 \mu\text{g mL}^{-1}$ dans H <sub>2</sub> O/ACN (30/70, v/v) (A) ou HCl 0,05 M/ACN (30/70, v/v). Colonne ZIC-HILIC (150 x 2,1 mm, 3,5 µm), V <sub>inj</sub> = 5 µL, phase mobile : formiate d'ammonium 10 mM pH 3/ACN, 300 µL min <sup>-1</sup> , détection UV à 200 nm.....	168
<b>Figure 27.</b> Chromatogramme obtenu lors de la séparation en HILIC avec un gradient maintenant une teneur en sel constante d'un mélange de méthyléphédrine (1), éphédrine (2), synéphrine (3), d'octopamine (4) et dopamine (5) à $100 \mu\text{g mL}^{-1}$ dans HCl 0,05 M/ACN (30/70, v/v). Colonne ZIC-HILIC (150 x 2,1 mm, 3,5 µm), V <sub>inj</sub> = 5 µL, phase mobile : formiate d'ammonium 50 mM pH 3:ACN (5:95)/formiate d'ammonium 10 mM pH 3:ACN (25:75), 300 µL min <sup>-1</sup> , détection UV à 200 nm.....	169
<b>Figure 28.</b> Chromatogrammes obtenus immédiatement (A), 6 h (B) et 12 h (C) après la préparation d'un mélange d'octopamine (1), éphédrine (2), synéphrine (3), méthyléphédrine (4) et dopamine (5) à $100 \mu\text{g mL}^{-1}$ dans un mélange H <sub>2</sub> O/ACN (80/20, v/v). Colonne Hypercarb (150 x 3 mm, 5 µm). V <sub>inj</sub> = 5 µL, phase mobile : H <sub>2</sub> O + 0,1% TFA/ACN, 400 µL min <sup>-1</sup> , détection UV à 200 nm.....	171
<b>Figure 29.</b> Chromatogrammes obtenus pour un mélange d'octopamine (1), éphédrine (2), synéphrine (3), méthyléphédrine (4) et dopamine (5) ( $100 \mu\text{g mL}^{-1}$ dans HCl 0,05 M/ACN (80/20, v/v)). Colonne Hypercarb (150 x 3 mm, 5 µm). V <sub>inj</sub> = 5 µL, phase mobile : H <sub>2</sub> O + 0,05% TFA/ACN, 400 µL min <sup>-1</sup> , gradient 1 (A) ou gradient 2 (B), détection UV à 200 nm. ....	172
<b>Figure 30.</b> Transfert du gradient de séparation des composés d'intérêt d'une colonne Hypercarb de dimension 150 x 3 mm (5 µm) avec un débit de 400 µL.min <sup>-1</sup> (Bleu) vers une colonne Hypercarb de dimension 50 x 0,075 mm (5 µm) avec un débit de 300 nL.min <sup>-1</sup> (Rouge). ....	173

## Liste des tableaux

<b>Table 1.</b> Conditions of synthesis and performances of MIPs in open tubular format.....	33
<b>Table 2.</b> Conditions of synthesis and performances of MIPs particles.....	41
<b>Table 3.</b> Conditions of synthesis and performances of MIPs by imprinting the surface of core particles.	
.....	44
<b>Table 4.</b> Conditions of in situ synthesis of monolithic MIPs in capillaries. ....	53
<b>Table 5.</b> Conditions of synthesis of MIPs by surface functionalization on core monolith. ....	61
<b>Table 6.</b> Performances of monolithic MIPs used as stationary phase for separation. ....	67
<b>Table 7.</b> Conditions of synthesis and performances of monolithic MIPs in pipette tips. ....	74
<b>Table 8.</b> Performances of monolithic MIPs prepared in capillaries, used as extraction sorbent, and ordered by the successive separation methods.....	81
<b>Tableau 9.</b> Valeurs des pKa (fonction amine en gras) et des coefficients de distribution octanol/eau pour la cocaïne et son principal métabolite, la BZE [148].....	95
<b>Tableau 10.</b> Durées de détectabilité et seuils de positivité pour la consommation de cocaïne en France dans les matrices biologiques couramment analysées [144,153,154]. ....	96
<b>Tableau 11.</b> Conditions de synthèse des MIP en bloc pour l'extraction de la cocaïne et la BZE [133].	97
<b>Tableau 12.</b> Conditions de lavage optimisées pour les différents MIP/NIP dans des cartouches remplies avec 25 mg de phase [133].....	97
<b>Table 13.</b> Retention factors and imprinted factors of cocaine and BZE measured on three independent MIPs and NIPs synthesis for two different (M+CL)/P ratios. Injections of 50 nL of acetone, cocaine (COC, 25 µg mL <sup>-1</sup> ), and BZE (25 µg mL <sup>-1</sup> ) on 5 cm-long capillary filled with the monolithic MIP or NIP. Mobile phase: ACN. ....	114
<b>Table 14.</b> Repeatability and intermediate reproducibility of the extraction recoveries of cocaine obtained for the analysis in triplicate of 50 nL of the spiked plasma sample (equivalent to 100 ng mL <sup>-1</sup> in plasma). ....	121

<b>Table 15.</b> Determination of cocaine in spiked plasma or saliva samples by selective extraction on the monolithic MIP coupled on-line to nanoLC-UV.....	122
<b>Table 16.</b> Permeabilities measured on MIPs and NIPs having a length of 10, 25 or 50 mm and obtained by photo-initiation for 30 min and comparison with the results obtained previously [90] with the monoliths obtained by thermal syntheses with the same polymerization mixture recipe and having a length of 50 mm (three syntheses for each length).....	143
<b>Table 17.</b> Imprinted factors of cocaine and BZE measured on three different MIPs and NIPs synthesized with UV irradiation or with thermal polymerization [90]. Experimental conditions: see <b>Figure 19</b> ... .....	145
<b>Table 18.</b> Analytical performances obtained for BZE in diluted (x2) urine spiked samples.....	151
<b>Tableau 19.</b> Valeurs des pKa (fonction amine en gras) et des coefficients de distribution octanol/H <sub>2</sub> O pour l'éphédrine et ses analogues structuraux [195]. .....	157
<b>Tableau 20.</b> Conditions de synthèse et performances des MIP développés pour l'extraction exhaustive non miniaturisée de l'éphédrine, la méthyléphédrine, la dopamine, l'octopamine et la synéphrine. ....	158
<b>Tableau 21.</b> Perméabilités mesurées sur les MIP et les NIP synthétisés avec l'EGDMA ou le TRIM comme agent réticulant et comparées avec les résultats obtenus précédemment [90] pour les supports avec la cocaïne comme molécule empreinte et le TRIM (3 synthèses indépendantes pour chaque support). ....	165
<b>Tableau 22.</b> Facteurs de rétention et facteurs d'impression pour l'éphédrine et la dopamine mesurés sur trois couples MIP/NIP issus de synthèses indépendantes. Injection de 50 nL d'acétone, d'éphédrine (100 µg mL <sup>-1</sup> ) ou de dopamine (100 µg mL <sup>-1</sup> ) sur un capillaire rempli de MIP ou NIP monolithique (50 mm x 100 µm i.d.). Phase mobile : ACN/H <sub>2</sub> O (90/10, v/v). ....	167

## REFERENCES

1. Polyakov, M.V. Adsorption properties and structure of silica gel. *Zhurnal Fiz. Khimii* **1931**, *2*, 799–805.
2. Wulff, G.; Sarhan, A. Use of polymers with enzyme-analogues structures for resolution of racemates. *Angew. Chem. Int. Ed.* **1972**, *11*, 341–344.
3. Luliński, P. Molecularly imprinted polymers based drug delivery devices: a way to application in modern pharmacotherapy. A review. *Mater. Sci. Eng. C* **2017**, *76*, 1344–1353, doi:10.1016/j.msec.2017.02.138.
4. Piletsky, S.; Canfarotta, F.; Poma, A.; Bossi, A.M.; Piletsky, S. Molecularly Imprinted Polymers for Cell Recognition. *Trends Biotechnol.* **2019**, doi:10.1016/j.tibtech.2019.10.002.
5. Tuwahatu, C.A.; Yeung, C.C.; Lam, Y.W.; Roy, V.A.L. The molecularly imprinted polymer essentials: curation of anticancer, ophthalmic, and projected gene therapy drug delivery systems. *J. Controlled Release* **2018**, *287*, 24–34, doi:10.1016/j.jconrel.2018.08.023.
6. Cao, Y.; Feng, T.; Xu, J.; Xue, C. Recent advances of molecularly imprinted polymer-based sensors in the detection of food safety hazard factors. *Biosens. Bioelectron.* **2019**, *141*, 111447, doi:10.1016/j.bios.2019.111447.
7. Saylan, Y.; Akgönüllü, S.; Yavuz, H.; Ünal, S.; Denizli, A. Molecularly Imprinted Polymer Based Sensors for Medical Applications. *Sensors* **2019**, *19*, doi:10.3390/s19061279.
8. Ahmad, O.S.; Bedwell, T.S.; Esen, C.; Garcia-Cruz, A.; Piletsky, S.A. Molecularly Imprinted Polymers in Electrochemical and Optical Sensors. *Trends Biotechnol.* **2019**, *37*, 294–309, doi:10.1016/j.tibtech.2018.08.009.
9. BelBruno, J.J. Molecularly Imprinted Polymers. *Chem. Rev.* **2019**, *119*, 94–119, doi:10.1021/acs.chemrev.8b00171.
10. Yin, Y.; Dong, Z.; Luo, Q.; Liu, J. Biomimetic catalysts designed on macromolecular scaffolds. *Prog. Polym. Sci.* **2012**, *37*, 1476–1509, doi:10.1016/j.progpolymsci.2012.04.001.
11. Wei, Z.-H.; Mu, L.-N.; Huang, Y.-P.; Liu, Z.-S. Imprinted monoliths: Recent significant progress in analysis field. *TrAC Trends Anal. Chem.* **2017**, *86*, 84–92, doi:10.1016/j.trac.2016.10.009.
12. Cheong, W.J.; Ali, F.; Choi, J.H.; Lee, J.O.; Yune Sung, K. Recent applications of molecular imprinted polymers for enantio-selective recognition. *Talanta* **2013**, *106*, 45–59, doi:10.1016/j.talanta.2012.11.049.
13. Zheng, C.; Huang, Y.-P.; Liu, Z.-S. Synthesis and theoretical study of molecularly imprinted monoliths for HPLC. *Anal. Bioanal. Chem.* **2013**, *405*, 2147–2161, doi:10.1007/s00216-012-6639-6.
14. Iacob, B.C.; Bodoki, E.; Oprean, R. Recent advances in capillary electrochromatography using molecularly imprinted polymers: CE and CEC. *Electrophoresis* **2014**, *35*, 2722–2732, doi:10.1002/elps.201400253.

15. Mu, L.-N.; Wei, Z.-H.; Liu, Z.-S. Current trends in the development of molecularly imprinted polymers in CEC: CE and CEC. *Electrophoresis* **2015**, *36*, 764–772, doi:10.1002/elps.201400389.
16. Rutkowska, M.; Płotka-Wasylka, J.; Morrison, C.; Wieczorek, P.P.; Namieśnik, J.; Marć, M. Application of molecularly imprinted polymers in analytical chiral separations and analysis. *TrAC Trends Anal. Chem.* **2018**, *102*, 91–102, doi:10.1016/j.trac.2018.01.011.
17. Xu, X.; Zhu, L.; Chen, L. Separation and screening of compounds of biological origin using molecularly imprinted polymers. *J. Chromatogr. B* **2004**, *804*, 61–69, doi:10.1016/j.jchromb.2004.02.012.
18. Pichon, V.; Delaunay, N.; Combes, A. Sample preparation using molecularly imprinted polymers. *Anal. Chem.* **2019**, doi:10.1021/acs.analchem.9b04816.
19. Gama, M.R.; Bottoli, C.B.G. Molecularly imprinted polymers for bioanalytical sample preparation. *J. Chromatogr. B* **2017**, *1043*, 107–121, doi:10.1016/j.jchromb.2016.09.045.
20. Pichon, V.; Chapuis-Hugon, F. Role of molecularly imprinted polymers for selective determination of environmental pollutants-A review. *Anal. Chim. Acta* **2008**, *622*, 48–61, doi:10.1016/j.aca.2008.05.057.
21. Beltran, A.; Borrull, F.; Marcé, R.M.; Cormack, P.A.G. Molecularly-imprinted polymers: useful sorbents for selective extractions. *TrAC Trends Anal. Chem.* **2010**, *29*, 1363–1375, doi:10.1016/j.trac.2010.07.020.
22. Farooq, S.; Nie, J.; Cheng, Y.; Yan, Z.; Li, J.; Bacha, S.A.S.; Mushtaq, A.; Zhang, H. Molecularly imprinted polymers' application in pesticide residue detection. *Analyst* **2018**, *143*, 3971–3989, doi:10.1039/C8AN00907D.
23. Ndunda, E.N.; Mizaikoff, B. Molecularly imprinted polymers for the analysis and removal of polychlorinated aromatic compounds in the environment: a review. *Analyst* **2016**, *141*, 3141–3156, doi:10.1039/C6AN00293E.
24. Boulanouar, S.; Mezzache, S.; Combès, A.; Pichon, V. Molecularly imprinted polymers for the determination of organophosphorus pesticides in complex samples. *Talanta* **2018**, *176*, 465–478, doi:10.1016/j.talanta.2017.08.067.
25. Boysen, R.I. Advances in the development of molecularly imprinted polymers for the separation and analysis of proteins with liquid chromatography. *J. Sep. Sci.* **2019**, *42*, 51–71, doi:10.1002/jssc.201800945.
26. Xing, R.; Wen, Y.; He, H.; Guo, Z.; Liu, Z. Recent progress in the combination of molecularly imprinted polymer-based affinity extraction and mass spectrometry for targeted proteomic analysis. *TrAC Trends Anal. Chem.* **2019**, *110*, 417–428, doi:10.1016/j.trac.2018.11.033.
27. Ansari, S.; Masoum, S. Molecularly imprinted polymers for capturing and sensing proteins: Current progress and future implications. *TrAC Trends Anal. Chem.* **2019**, *114*, 29–47, doi:10.1016/j.trac.2019.02.008.
28. Jia, M.; Zhang, Z.; Li, J.; Ma, X.; Chen, L.; Yang, X. Molecular imprinting technology for microorganism analysis. *TrAC Trends Anal. Chem.* **2018**, *106*, 190–201, doi:10.1016/j.trac.2018.07.011.

29. Matsui, Jun.; Kato, Teru.; Takeuchi, Toshifumi.; Suzuki, Masayasu.; Yokoyama, Kenji.; Tamiya, Eiichi.; Karube, Isao. Molecular recognition in continuous polymer rods prepared by a molecular imprinting technique. *Anal. Chem.* **1993**, *65*, 2223–2224, doi:10.1021/ac00065a009.
30. Reyes, D.R.; Iossifidis, D.; Auroux, P.-A.; Manz, A. Micro Total Analysis Systems. 1. Introduction, Theory, and Technology. *Anal. Chem.* **2002**, *74*, 2623–2636, doi:10.1021/ac0202435.
31. Manz, A.; Gruber, N.; Widmer, H.M. Miniaturized total chemical analysis systems: A novel concept for chemical sensing. *Sens. Actuators B Chem.* **1990**, *1*, 244–248, doi:[https://doi.org/10.1016/0925-4005\(90\)80209-I](https://doi.org/10.1016/0925-4005(90)80209-I).
32. Svec, F.; Huber, C.G. Monolithic Materials: Promises, Challenges, Achievements. *Anal. Chem.* **2006**, *78*, 2100–2107, doi:10.1021/ac069383v.
33. Guiochon, G. Monolithic columns in high-performance liquid chromatography. *J. Chromatogr. A* **2007**, *1168*, 101–168, doi:10.1016/j.chroma.2007.05.083.
34. Walsh, Z.; Paull, B.; Macka, M. Inorganic monoliths in separation science: A review. *Anal. Chim. Acta* **2012**, *750*, 28–47, doi:10.1016/j.aca.2012.04.029.
35. Namera, A.; Saito, T. Advances in monolithic materials for sample preparation in drug and pharmaceutical analysis. *TrAC Trends Anal. Chem.* **2013**, *45*, 182–196, doi:10.1016/j.trac.2012.10.017.
36. Hong, T.; Yang, X.; Xu, Y.; Ji, Y. Recent advances in the preparation and application of monolithic capillary columns in separation science. *Anal. Chim. Acta* **2016**, *931*, 1–24, doi:10.1016/j.aca.2016.05.013.
37. Schweitz, L.; Andersson, L.I.; Nilsson, S. Capillary electrochromatography with molecular imprint-based selectivity for enantiomer separation of local anaesthetics. *J. Chromatogr. A* **1997**, *792*, 401–409, doi:[https://doi.org/10.1016/S0021-9673\(97\)00895-9](https://doi.org/10.1016/S0021-9673(97)00895-9).
38. Schweitz, L.; Andersson, L.I.; Nilsson, S. Rapid electrochromatographic enantiomer separations on short molecularly imprinted polymer monoliths. *Anal. Chim. Acta* **2001**, *435*, 43–47, doi:10.1016/S0003-2670(00)01210-1.
39. Zhang, S.W.; Xing, J.; Cai, L.S.; Wu, C.Y. Molecularly imprinted monolith in-tube solid-phase microextraction coupled with HPLC/UV detection for determination of 8-hydroxy-2'-deoxyguanosine in urine. *Anal. Bioanal. Chem.* **2009**, *395*, 479–487, doi:10.1007/s00216-009-2964-9.
40. Masini, J.C.; Svec, F. Porous monoliths for on-line sample preparation: A review. *Anal. Chim. Acta* **2017**, *964*, 24–44, doi:10.1016/j.aca.2017.02.002.
41. Seidi, S.; Tajik, M.; Baharfar, M.; Rezazadeh, M. Micro solid-phase extraction (pipette tip and spin column) and thin film solid-phase microextraction: Miniaturized concepts for chromatographic analysis. *TrAC Trends Anal. Chem.* **2019**, *118*, 810–827, doi:10.1016/j.trac.2019.06.036.
42. Sarafraz-Yazdi, A.; Razavi, N. Application of molecularly-imprinted polymers in solid-phase microextraction techniques. *TrAC Trends Anal. Chem.* **2015**, *73*, 81–90, doi:10.1016/j.trac.2015.05.004.

43. Xu, C.-H.; Chen, G.-S.; Xiong, Z.-H.; Fan, Y.-X.; Wang, X.-C.; Liu, Y. Applications of solid-phase microextraction in food analysis. *TrAC Trends Anal. Chem.* **2016**, *80*, 12–29, doi:10.1016/j.trac.2016.02.022.
44. Ansari, S.; Karimi, M. Recent progress, challenges and trends in trace determination of drug analysis using molecularly imprinted solid-phase microextraction technology. *Talanta* **2017**, *164*, 612–625, doi:10.1016/j.talanta.2016.11.007.
45. Zhang, S.; Sun, X.; Wang, W.; Cai, L. Determination of urinary 8-hydroxy-2'-deoxyguanosine by a combination of on-line molecularly imprinted monolithic solid phase microextraction with high performance liquid chromatography-ultraviolet detection: Sample Preparation. *J. Sep. Sci.* **2013**, *36*, 752–757, doi:10.1002/jssc.201200735.
46. Zhang, S.; Song, X.; Zhang, W.; Luo, N.; Cai, L. Determination of low urinary 8-hydroxy-2'-deoxyguanosine excretion with capillary electrophoresis and molecularly imprinted monolith solid phase microextraction. *Sci. Total Environ.* **2013**, *450–451*, 266–270, doi:10.1016/j.scitotenv.2013.02.025.
47. Liang, G.; Zhai, H.; Huang, L.; Tan, X.; Zhou, Q.; Yu, X.; Lin, H. Synthesis of carbon quantum dots-doped dummy molecularly imprinted polymer monolithic column for selective enrichment and analysis of aflatoxin B1 in peanut. *J. Pharm. Biomed. Anal.* **2018**, *149*, 258–264, doi:10.1016/j.jpba.2017.11.012.
48. Wang, Q.; Zhang, X.; Li, J.; Xu, Z. Synthesis and Evaluation of Organic-Inorganic Hybrid Molecularly Imprinted Monolith Column for Selective Recognition of Acephate and Phosphamidon in Vegetables. *Adv. Polym. Technol.* **2015**, *36*, 401–408, doi:10.1002/adv.21620.
49. Szumski, M.; Grzywiński, D.; Prus, W.; Buszewski, B. Monolithic molecularly imprinted polymeric capillary columns for isolation of aflatoxins. *J. Chromatogr. A* **2014**, *1364*, 163–170, doi:10.1016/j.chroma.2014.08.078.
50. Zaidi, S.A. Dual-templates molecularly imprinted monolithic columns for the evaluation of serotonin and histamine in CEC: CE and CEC. *Electrophoresis* **2013**, *34*, 1375–1382, doi:10.1002/elps.201200640.
51. Qu, P.; Lei, J.; Sheng, J.; Zhang, L.; Ju, H. Simultaneous multiple enantioseparation with a one-pot imprinted microfluidic channel by microchip capillary electrochromatography. *The Analyst* **2011**, *136*, 920–926, doi:10.1039/C0AN00559B.
52. Huang, L.; Zhai, H.; Liang, G.; Su, Z.; Yuan, K.; Lu, G.; Pan, Y. Chip-based dual-molecularly imprinted monolithic capillary array columns coated Ag/GO for selective extraction and simultaneous determination of bisphenol A and nonyl phenol in fish samples. *J. Chromatogr. A* **2016**, *1474*, 14–22, doi:10.1016/j.chroma.2016.10.074.
53. Brüggemann, O.; Freitag, R.; Whitcombe, M.J.; Vulfson, E.N. Comparison of polymer coatings of capillaries for capillary electrophoresis with respect to their applicability to molecular imprinting and electrochromatography. *J. Chromatogr. A* **1997**, *781*, 43–53, doi:10.1016/S0021-9673(97)00288-4.
54. Tan, Z.J.; Remcho, V.T. Molecular imprint polymers as highly selective stationary phases for open tubular liquid chromatography and capillary electrochromatography. *Electrophoresis* **1998**, *19*, 2055–2060, doi:10.1002/elps.1150191203.

55. Qu, P.; Lei, J.; Ouyang, R.; Ju, H. Enantioseparation and Amperometric Detection of Chiral Compounds by in Situ Molecular Imprinting on the Microchannel Wall. *Anal. Chem.* **2009**, *81*, 9651–9656, doi:10.1021/ac902201a.
56. Zaidi, S.A.; Cheong, W.J. Long open tubular molecule imprinted polymer capillary columns with excellent separation efficiencies in chiral and non-chiral separation by capillary electrochromatography. *Electrophoresis* **2009**, *30*, 1603–1607, doi:10.1002/elps.200800541.
57. Zaidi, S.A.; Cheong, W.J. Preparation of an open-tubular capillary column with a monolithic layer of S-ketoprofen imprinted and 4-styrenesulfonic acid incorporated polymer and its enhanced chiral separation performance in capillary electrochromatography. *J. Chromatogr. A* **2009**, *1216*, 2947–2952, doi:10.1016/j.chroma.2008.08.015.
58. Jang, R.; Kim, K.H.; Zaidi, S.A.; Cheong, W.J.; Moon, M.H. Analysis of phospholipids using an open-tubular capillary column with a monolithic layer of molecularly imprinted polymer in capillary electrochromatography-electrospray ionization-tandem mass spectrometry. *Electrophoresis* **2011**, *32*, 2167–2173, doi:10.1002/elps.201100205.
59. Kulsing, C.; Knob, R.; Macka, M.; Junor, P.; Boysen, R.I.; Hearn, M.T.W. Molecular imprinted polymeric porous layers in open tubular capillaries for chiral separations. *J. Chromatogr. A* **2014**, *1354*, 85–91, doi:10.1016/j.chroma.2014.05.065.
60. Huang, Y.-C.; Lin, C.-C.; Liu, C.-Y. Preparation and evaluation of molecularly imprinted polymers based on 9-ethyladenine for the recognition of nucleotide bases in capillary electrochromatography. *Electrophoresis* **2004**, *25*, 554–561, doi:10.1002/elps.200305735.
61. Zhao, Q.-L.; Zhou, J.; Zhang, L.-S.; Huang, Y.-P.; Liu, Z.-S. Coatings of molecularly imprinted polymers based on polyhedral oligomeric silsesquioxane for open tubular capillary electrochromatography. *Talanta* **2016**, *152*, 277–282, doi:10.1016/j.talanta.2016.02.019.
62. Song, W.-F.; Zhao, Q.-L.; Zhou, X.-J.; Zhang, L.-S.; Huang, Y.-P.; Liu, Z.-S. A star-shaped molecularly imprinted polymer derived from polyhedral oligomeric silsesquioxanes with improved site accessibility and capacity for enantiomeric separation via capillary electrochromatography. *Microchim. Acta* **2019**, *186*, doi:10.1007/s00604-018-3151-5.
63. Wu, X.; Wei, Z.-H.; Huang, Y.-P.; Liu, Z.-S. Preparation of Molecularly Imprinted Coatings with Ternary Porogen for CEC. *Chromatographia* **2010**, *72*, 101–109, doi:10.1365/s10337-010-1627-5.
64. Zhang, X.; Xu, S.; Lee, Y.-I.; Soper, S.A. LED-induced in-column molecular imprinting for solid phase extraction/capillary electrophoresis. *The Analyst* **2013**, *138*, 2821, doi:10.1039/c3an00257h.
65. Zhang, X.; Zhu, D.; Huang, C.; Sun, Y.; Lee, Y.-I. Sensitive detection of bisphenol A in complex samples by in-column molecularly imprinted solid-phase extraction coupled with capillary electrophoresis. *Microchem. J.* **2015**, *121*, 1–5, doi:10.1016/j.microc.2015.01.012.
66. Schweitz, L. Molecularly Imprinted Polymer Coatings for Open-Tubular Capillary Electrochromatography Prepared by Surface Initiation. *Anal. Chem.* **2002**, *74*, 1192–1196, doi:10.1021/ac0156520.

67. He, D.; Zhang, Z.; Zhou, H.; Huang, Y. Micro flow sensor on a chip for the determination of terbutaline in human serum based on chemiluminescence and a molecularly imprinted polymer. *Talanta* **2006**, *69*, 1215–1220, doi:10.1016/j.talanta.2005.12.043.
68. Lei, J.D.; Tong, A.J. Preparation of Z-L-Phe-OH-NBD imprinted microchannel and its molecular recognition study. *Spectrochim. Acta. A. Mol. Biomol. Spectrosc.* **2005**, *61*, 1029–1033, doi:10.1016/j.saa.2004.06.001.
69. Lin, J.-M.; Nakagama, T.; Uchiyama, K.; Hobo, T. Enantioseparation of D, L-Phenylalanine By Molecularly Imprinted Polymer Particles Filled Capillary Electrochromatography. *J. Liq. Chromatogr. Relat. Technol.* **1997**, *20*, 1489–1506, doi:10.1080/10826079708010989.
70. Lara, F.J.; Lynen, F.; Sandra, P.; García-Campaña, A.M.; Alés-Barrero, F. Evaluation of a molecularly imprinted polymer as in-line concentrator in capillary electrophoresis. *Electrophoresis* **2008**, *29*, 3834–3841, doi:10.1002/elps.200700889.
71. Moreno-González, D.; Lara, F.J.; Gámiz-Gracia, L.; García-Campaña, A.M. Molecularly imprinted polymer as in-line concentrator in capillary electrophoresis coupled with mass spectrometry for the determination of quinolones in bovine milk samples. *J. Chromatogr. A* **2014**, *1360*, 1–8, doi:10.1016/j.chroma.2014.07.049.
72. Qu, P.; Lei, J.; Zhang, L.; Ouyang, R.; Ju, H. Molecularly imprinted magnetic nanoparticles as tunable stationary phase located in microfluidic channel for enantioseparation. *J. Chromatogr. A* **2010**, *1217*, 6115–6121, doi:10.1016/j.chroma.2010.07.063.
73. Wang, X.N.; Liang, R.P.; Meng, X.Y.; Qiu, J.D. One-step synthesis of mussel-inspired molecularly imprinted magnetic polymer as stationary phase for chip-based open tubular capillary electrochromatography enantioseparation. *J. Chromatogr. A* **2014**, *1362*, 301–308, doi:10.1016/j.chroma.2014.08.044.
74. Chen, J.; Liang, R.P.; Wang, X.N.; Qiu, J.D. A norepinephrine coated magnetic molecularly imprinted polymer for simultaneous multiple chiral recognition. *J. Chromatogr. A* **2015**, *1409*, 268–276, doi:10.1016/j.chroma.2015.07.052.
75. Wu, L.-L.; Liang, R.-P.; Chen, J.; Qiu, J.-D. Separation of chiral compounds using magnetic molecularly imprinted polymer nanoparticles as stationary phase by microchip capillary electrochromatography. *Electrophoresis* **2018**, *39*, 356–362, doi:10.1002/elps.201700334.
76. Oxelbark, J.; Legido-Quigley, C.; Aureliano, C.S.A.; Titirici, M.-M.; Schillinger, E.; Sellergren, B.; Courtois, J.; Irgum, K.; Dambies, L.; Cormack, P.A.G.; et al. Chromatographic comparison of bupivacaine imprinted polymers prepared in crushed monolith, microsphere, silica-based composite and capillary monolith formats. *J. Chromatogr. A* **2007**, *1160*, 215–226, doi:10.1016/j.chroma.2007.05.057.
77. Zhou, T.; Ding, L.; Che, G.; Jiang, W.; Sang, L. Recent advances and trends of molecularly imprinted polymers for specific recognition in aqueous matrix: Preparation and application in sample pretreatment. *TrAC Trends Anal. Chem.* **2019**, *114*, 11–28, doi:10.1016/j.trac.2019.02.028.
78. Wackerlig, J.; Lieberzeit, P.A. Molecularly imprinted polymer nanoparticles in chemical sensing – Synthesis, characterisation and application. *Sens. Actuators B Chem.* **2015**, *207*, 144–157, doi:10.1016/j.snb.2014.09.094.

79. Azizi, A.; Bottaro, C.S. A critical review of molecularly imprinted polymers for the analysis of organic pollutants in environmental water samples. *J. Chromatogr. A* **2020**, *1614*, 460603, doi:10.1016/j.chroma.2019.460603.
80. Capriotti, A.L.; Cavaliere, C.; La Barbera, G.; Montone, C.M.; Piovesana, S.; Laganà, A. Recent Applications of Magnetic Solid-phase Extraction for Sample Preparation. *Chromatographia* **2019**, *82*, 1251–1274, doi:10.1007/s10337-019-03721-0.
81. Ansari, S.; Karimi, M. Recent configurations and progressive uses of magnetic molecularly imprinted polymers for drug analysis. *Talanta* **2017**, *167*, 470–485, doi:10.1016/j.talanta.2017.02.049.
82. Ou, J.; Kong, L.; Pan, C.; Su, X.; Lei, X.; Zou, H. Determination of dl-tetrahydropalmatine in Corydalis yanhusuo by l-tetrahydropalmatine imprinted monolithic column coupling with reversed-phase high performance liquid chromatography. *J. Chromatogr. A* **2006**, *1117*, 163–169, doi:10.1016/j.chroma.2006.03.084.
83. Ou, J.; Hu, L.; Hu, L.; Li, X.; Zou, H. Determination of phenolic compounds in river water with on-line coupling bisphenol A imprinted monolithic precolumn with high performance liquid chromatography. *Talanta* **2006**, *69*, 1001–1006, doi:10.1016/j.talanta.2005.12.003.
84. Wang, S.; Li, D.; Hua, Z.; Zhao, M. Molecularly imprinted monolith coupled on-line with high performance liquid chromatography for simultaneous quantitative determination of cyromazine and melamine. *The Analyst* **2011**, *136*, 3672, doi:10.1039/c1an15086c.
85. Javanbakht, M.; Moein, M.M.; Akbari-adergani, B. On-line clean-up and determination of tramadol in human plasma and urine samples using molecularly imprinted monolithic column coupling with HPLC. *J. Chromatogr. B* **2012**, *911*, 49–54, doi:10.1016/j.jchromb.2012.10.019.
86. Lv, Y.K.; Yang, L.; Liu, X.H.; Guo, Z.Y.; Sun, H.W. Preparation and evaluation of a novel molecularly imprinted hybrid composite monolithic column for on-line solid-phase extraction coupled with HPLC to detect trace fluoroquinolone residues in milk. *Anal. Methods* **2013**, *5*, 1848, doi:10.1039/c3ay26431a.
87. Li, X.; Zhou, M.; Turson, M.; Lin, S.; Jiang, P.; Dong, X. Preparation of clenbuterol imprinted monolithic polymer with hydrophilic outer layers by reversible addition–fragmentation chain transfer radical polymerization and its application in the clenbuterol determination from human serum by on-line solid-phase extraction/HPLC analysis. *The Analyst* **2013**, *138*, 3066–3074, doi:10.1039/c3an36801g.
88. Lin, Z.; Wang, J.; Tan, X.; Sun, L.; Yu, R.; Yang, H.; Chen, G. Preparation of boronate-functionalized molecularly imprinted monolithic column with polydopamine coating for glycoprotein recognition and enrichment. *J. Chromatogr. A* **2013**, *1319*, 141–147, doi:10.1016/j.chroma.2013.10.059.
89. Lin, Z.; Lin, Y.; Sun, X.; Yang, H.; Zhang, L.; Chen, G. One-pot preparation of a molecularly imprinted hybrid monolithic capillary column for selective recognition and capture of lysozyme. *J. Chromatogr. A* **2013**, *1284*, 8–16, doi:10.1016/j.chroma.2013.02.042.
90. Bouvarel, T.; Delaunay, N.; Pichon, V. Selective extraction of cocaine from biological samples with a miniaturized monolithic molecularly imprinted polymer and on-line analysis in nano-liquid chromatography. *Anal. Chim. Acta* **2020**, *1096*, 89–99, doi:10.1016/j.aca.2019.10.046.

91. Bi, X.; Tian, W.; Wang, X.; Cao, W.; Gao, L.; Fan, S.; Wang, Y.; Wang, M.; Niu, L. Preparation of a POSS-hybridized molecularly imprinted monolith for the analysis of baicalin and its analogues in a microwave-assisted extract from *Scutellaria baicalensis* by means of on-line SPME-HPLC and off-line LC-MS/MS. *Anal. Methods* **2019**, *11*, 2351–2361, doi:10.1039/C9AY00568D.
92. Zhang, Q.; Xiao, X.; Li, G. Porous molecularly imprinted monolithic capillary column for on-line extraction coupled to high-performance liquid chromatography for trace analysis of antimicrobials in food samples. *Talanta* **2014**, *123*, 63–70, doi:10.1016/j.talanta.2014.02.010.
93. Zheng, M.M.; Gong, R.; Zhao, X.; Feng, Y.-Q. Selective sample pretreatment by molecularly imprinted polymer monolith for the analysis of fluoroquinolones from milk samples. *J. Chromatogr. A* **2010**, *1217*, 2075–2081, doi:10.1016/j.chroma.2010.02.011.
94. Marchioni, C.; Vieira, T.M.; Miller Crotti, A.E.; Crippa, J.A.; Costa Queiroz, M.E. In-tube solid-phase microextraction with a dummy molecularly imprinted monolithic capillary coupled to ultra-performance liquid chromatography-tandem mass spectrometry to determine cannabinoids in plasma samples. *Anal. Chim. Acta* **2020**, *1099*, 145–154, doi:10.1016/j.aca.2019.11.017.
95. Liao, S.; Wang, X.; Lin, X.; Wu, X.; Xie, Z. A molecularly imprinted monolith for the fast chiral separation of antiparasitic drugs by pressurized CEC. *J. Sep. Sci.* **2010**, *33*, 2123–2130, doi:10.1002/jssc.200900855.
96. He, J.; Fang, G.; Deng, Q.; Wang, S. Preparation, characterization and application of organic–inorganic hybrid ractopamine multi-template molecularly imprinted capillary monolithic column. *Anal. Chim. Acta* **2011**, *692*, 57–62, doi:10.1016/j.aca.2011.02.056.
97. Qu, P.; Zhang, L.; Sheng, J.; Lei, J.; Ju, H. Convenient enantioseparation by monolithic imprinted capillary clamped in a chip with electrochemical detection. *Electrophoresis* **2011**, *32*, 1522–1529, doi:10.1002/elps.201000655.
98. Li, M.; Lin, X.; Xie, Z. Investigation of enantiomer recognition of molecularly imprinted polymeric monoliths in pressurized capillary electrochromatography screening the amino acids and their derivatives. *J. Chromatogr. A* **2009**, *1216*, 5320–5326, doi:10.1016/j.chroma.2009.05.012.
99. Yuan, K.; Wang, J.; Zhai, H.; Chen, Z.; Huang, L.; Su, Z. Sensitive determination of rose bengal in brown sugar by a molecularly imprinted solid-phase extraction monolithic capillary column coupled with capillary electrophoresis. *Anal. Methods* **2015**, *7*, 8297–8303, doi:10.1039/C5AY01838B.
100. Zhai, H.; Li, J.; Chen, Z.; Su, Z.; Liu, Z.; Yu, X. A glass/PDMS electrophoresis microchip embedded with molecular imprinting SPE monolith for contactless conductivity detection. *Microchem. J.* **2014**, *114*, 223–228, doi:10.1016/j.microc.2014.01.006.
101. Su, Z.; Zhai, H.; Chen, Z.; Zhou, Q.; Li, J.; Liu, Z. Molecularly imprinted solid-phase extraction monolithic capillary column for selective extraction and sensitive determination of safranine T in wolfberry. *Anal. Bioanal. Chem.* **2014**, *406*, 1551–1556, doi:10.1007/s00216-013-7541-6.
102. Yan, W.; Gao, R.; Zhang, Z.; Wang, Q.; Jiang, C.V.; Yan, C. Capillary electrochromatographic separation of ionizable compounds with a molecular imprinted monolithic cationic exchange column. *J. Sep. Sci.* **2003**, *26*, 555–561, doi:<https://doi.org/10.1002/jssc.200390076>.

103. Cacho, C.; Schweitz, L.; Turiel, E.; Pérez-Conde, C. Molecularly imprinted capillary electrochromatography for selective determination of thiabendazole in citrus samples. *J. Chromatogr. A* **2008**, *1179*, 216–223, doi:10.1016/j.chroma.2007.11.097.
104. Li, J.; Zhai, H.; Chen, Z.; Zhou, Q.; Liu, Z.; Su, Z. Preparation and evaluation of a novel molecularly imprinted SPE monolithic capillary column for the determination of auramine O in shrimp: Sample Preparation. *J. Sep. Sci.* **2013**, *36*, 3608–3614, doi:10.1002/jssc.201300681.
105. Tan, J.; Jiang, Z.-T.; Li, R.; Yan, X.-P. Molecularly-imprinted monoliths for sample treatment and separation. *TrAC Trends Anal. Chem.* **2012**, *39*, 207–217, doi:10.1016/j.trac.2012.05.009.
106. Liao, S.; Wang, X.; Lin, X.; Xie, Z. Preparation and characterization of a molecularly imprinted monolithic column for pressure-assisted CEC separation of nitroimidazole drugs. *Electrophoresis* **2010**, *31*, 2822–2830, doi:10.1002/elps.201000035.
107. Ou, J.; Dong, J.; Tian, T.; Hu, J.; Ye, M.; Zou, H. Enantioseparation of tetrahydropalmatine and Tröger's base by molecularly imprinted monolith in capillary electrochromatography. *J. Biochem. Biophys. Methods* **2007**, *70*, 71–76, doi:10.1016/j.jbbm.2006.07.003.
108. Zheng, C.; Liu, Z.; Gao, R.; Zhang, L.; Zhang, Y. Recognition of oxytocin by capillary electrochromatography with monolithic tetrapeptide-imprinted polymer used as the stationary phase. *Anal. Bioanal. Chem.* **2007**, *388*, 1137–1145, doi:10.1007/s00216-007-1325-9.
109. Zheng, C.; Liu, Z.-S.; Gao, R.-Y.; Zhang, Y.-K. Mechanism of Molecular Recognition on Tetrapetide-imprinted Monolith by Capillary Electrochromatography. *Chin. J. Chem.* **2008**, *26*, 1857–1862, doi:10.1002/cjoc.200890335.
110. He, J.-X.; Fang, G.; Yao, Y.; Wang, S. Preparation and characterization of molecularly imprinted silica monolith for screening sulfamethazine. *J. Sep. Sci.* **2010**, *33*, 3263–3271, doi:10.1002/jssc.200900650.
111. Zhao, T.; Wang, Q.; Li, J.; Qiao, X.; Xu, Z. Study on an electrochromatography method based on organic-inorganic hybrid molecularly imprinted monolith for determination of trace trichlorfon in vegetables: Determination of trichlorfon in vegetables. *J. Sci. Food Agric.* **2014**, *94*, 1974–1980, doi:10.1002/jsfa.6511.
112. Aşır, S.; Derazshamshir, A.; Yılmaz, F.; Denizli, A. Triazine herbicide imprinted monolithic column for capillary electrochromatography: CE and CEC. *Electrophoresis* **2015**, *36*, 2888–2895, doi:10.1002/elps.201500232.
113. Aşır, S.; Sari, D.; Derazshamshir, A.; Yılmaz, F.; Şarkaya, K.; Denizli, A. Dopamine-imprinted monolithic column for capillary electrochromatography. *Electrophoresis* **2017**, *38*, 3003–3012, doi:10.1002/elps.201700228.
114. Şarkaya, K.; Aşır, S.; Göktürk, I.; Yılmaz, F.; Yavuz, H.; Denizli, A. Electrochromatographic separation of hydrophobic amino acid enantiomers by molecularly imprinted capillary columns. *Process Biochem.* **2020**, *92*, 69–77, doi:10.1016/j.procbio.2020.02.033.
115. Zhang, C.; Cai, J.; Duan, Y.; Xu, L.; Fang, G.; Wang, S. Synthesis, characterization and application of organic-inorganic hybrid and carbaryl-imprinted capillary monolithic column. *Chem. Res. Chin. Univ.* **2014**, *30*, 374–378, doi:10.1007/s40242-014-3420-8.

116. Wang, H.-F.; Zhu, Y.-Z.; Yan, X.-P.; Gao, R.-Y.; Zheng, J.-Y. A Room Temperature Ionic Liquid (RTIL)-Mediated, Non-Hydrolytic Sol–Gel Methodology to Prepare Molecularly Imprinted, Silica-Based Hybrid Monoliths for Chiral Separation. *Adv. Mater.* **2006**, *18*, 3266–3270, doi:10.1002/adma.200601024.
117. Zhai, H.; Liang, G.; Guo, X.; Chen, Z.; Yu, J.; Lin, H.; Zhou, Q. Novel coordination imprinted polymer monolithic column applied to the solid-phase extraction of flumequine from fish samples. *J. Chromatogr. B* **2019**, *1118–1119*, 55–62, doi:10.1016/j.jchromb.2019.04.023.
118. Zhai, H.; Huang, L.; Chen, Z.; Su, Z.; Yuan, K.; Liang, G.; Pan, Y. Chip-based molecularly imprinted monolithic capillary array columns coated GO/SiO<sub>2</sub> for selective extraction and sensitive determination of rhodamine B in chili powder. *Food Chem.* **2017**, *214*, 664–669, doi:10.1016/j.foodchem.2016.07.124.
119. Liang, G.; Guo, X.; Tan, X.; Mai, S.; Chen, Z.; Zhai, H. Molecularly imprinted monolithic column based on functionalized β-cyclodextrin and multi-walled carbon nanotubes for selective recognition of benzimidazole residues in citrus samples. *Microchem. J.* **2019**, *146*, 1285–1294, doi:10.1016/j.microc.2019.02.064.
120. Huang, B.-Y.; Chen, Y.-C.; Wang, G.-R.; Liu, C.-Y. Preparation and evaluation of a monolithic molecularly imprinted polymer for the chiral separation of neurotransmitters and their analogues by capillary electrochromatography. *J. Chromatogr. A* **2011**, *1218*, 849–855, doi:10.1016/j.chroma.2010.12.054.
121. Ou, J.; Li, X.; Feng, S.; Dong, J.; Dong, X.; Kong, L.; Ye, M.; Zou, H. Preparation and Evaluation of a Molecularly Imprinted Polymer Derivatized Silica Monolithic Column for Capillary Electrochromatography and Capillary Liquid Chromatography. *Anal. Chem.* **2007**, *79*, 639–646, doi:10.1021/ac061475x.
122. Courtois, J.; Fischer, G.; Sellergren, B.; Irgum, K. Molecularly imprinted polymers grafted to flow through poly(trimethylolpropane trimethacrylate) monoliths for capillary-based solid-phase extraction. *J. Chromatogr. A* **2006**, *1109*, 92–99, doi:10.1016/j.chroma.2005.12.014.
123. Wei, Z.H.; Mu, L.N.; Pang, Q.Q.; Huang, Y.P.; Liu, Z.S. Preparation and characterization of grafted imprinted monolith for capillary electrochromatography: CE and CEC. *Electrophoresis* **2012**, *33*, 3021–3027, doi:10.1002/elps.201200042.
124. Wen, L.; Tan, X.; Sun, Q.; Svec, F.; Lv, Y. “Smart” molecularly imprinted monoliths for the selective capture and easy release of proteins: Other Techniques. *J. Sep. Sci.* **2016**, *39*, 3267–3273, doi:10.1002/jssc.201600576.
125. Du, T.; Cheng, J.; Wu, M.; Wang, X.; Zhou, H.; Cheng, M. Pipette tip-based molecularly imprinted monolith for selective micro-solid-phase extraction of methomyl in environmental water. *Anal. Methods* **2014**, *6*, 6375–6380, doi:10.1039/C4AY00766B.
126. Li, H.; Ji, X.; Wei, L. Preparation of Cholecystokinin Molecularly Imprinted Polymer Monolith and its Application in Solid Phase Microextraction and HPLC Analysis. *Chin. J. Anal. Chem.* **2015**, *43*, 1130–1135, doi:10.1016/S1872-2040(15)60844-1.
127. Zhu, J.; Chen, D.; Ai, Y.; Dang, X.; Huang, J.; Chen, H. A dummy molecularly imprinted monolith for selective solid-phase microextraction of vanillin and methyl vanillin prior to their determination by HPLC. *Microchim. Acta* **2017**, *184*, 1161–1167, doi:10.1007/s00604-017-2107-5.

128. Song, X.; Zhou, T.; Zhang, J.; Su, Y.; Zhou, H.; He, L. Preparation and Application of Molecularly Imprinted Monolithic Extraction Column for the Selective Microextraction of Multiple Macrolide Antibiotics from Animal Muscles. *Polymers* **2019**, *11*, 1109, doi:10.3390/polym11071109.
129. Zhang, W.; Chen, Z. Preparation of micropipette tip-based molecularly imprinted monolith for selective micro-solid phase extraction of berberine in plasma and urine samples. *Talanta* **2013**, *103*, 103–109, doi:10.1016/j.talanta.2012.10.014.
130. Liu, X.; Zhu, Q.; Chen, H.; Zhou, L.; Dang, X.; Huang, J. Preparation of 2,4-dichlorophenoxyacetic acid imprinted organic–inorganic hybrid monolithic column and application to selective solid-phase microextraction. *J. Chromatogr. B* **2014**, *951–952*, 32–37, doi:10.1016/j.jchromb.2014.01.010.
131. Cao, J.; Yan, H.; Shen, S.; Bai, L.; Liu, H.; Qiao, F. Hydrophilic molecularly imprinted melamine–urea-formaldehyde monolithic resin prepared in water for selective recognition of plant growth regulators. *Anal. Chim. Acta* **2016**, *943*, 136–145, doi:10.1016/j.aca.2016.09.016.
132. Arabi, M.; Ghaedi, M.; Ostovan, A. Synthesis and application of in-situ molecularly imprinted silica monolithic in pipette-tip solid-phase microextraction for the separation and determination of gallic acid in orange juice samples. *J. Chromatogr. B* **2017**, *1048*, 102–110, doi:10.1016/j.jchromb.2017.02.016.
133. Thibert, V.; Legeay, P.; Chapuis-Hugon, F.; Pichon, V. Synthesis and characterization of molecularly imprinted polymers for the selective extraction of cocaine and its metabolite benzoylecgonine from hair extract before LC–MS analysis. *Talanta* **2012**, *88*, 412–419, doi:10.1016/j.talanta.2011.11.009.
134. Thibert, V.; Legeay, P.; Chapuis-Hugon, F.; Pichon, V. Molecularly imprinted polymer for the selective extraction of cocaine and its metabolites, benzoylecgonine and ecgonine methyl ester, from biological fluids before LC–MS analysis. *J. Chromatogr. B* **2014**, *949–950*, 16–23, doi:10.1016/j.jchromb.2013.11.051.
135. United Nations Office on Drugs and Crime *The International Drug Control Conventions*; 1961;
136. United Nations Office on Drugs and Crime *World Drug Report 2020*; United Nations publication: Vienna, 2020; ISBN 978-92-1-148345-1.
137. Shanti, C.M.; Lucas, C.E. Cocaine and the critical care challenge. *Crit. Care Med.* **2003**, *31*, 1851–1859, doi:10.1097/01.CCM.0000063258.68159.71.
138. Cocaine, ecstasy, heroine, cannabis : effets sur le système nerveux Available online: <http://neurobranches.chez-alice.fr/flash/effdrog.html> (accessed on Sep 29, 2020).
139. Goldstein, R.A.; DesLauriers, C.; Burda, A.M.; Johnson-Arbor, K. Cocaine: history, social implications, and toxicity: a review. *Semin. Diagn. Pathol.* **2009**, *26*, 10–17, doi:10.1053/j.semdp.2008.12.001.
140. Gérôme, C.; Cadet-Taïrou, A.; Gandilhon, M.; Milhet, M.; Detrez, V.; Martinez, M. Usagers, marchés et substances : évolutions récentes (2018-2019). *Obs. Fr. Drogue Toxicom.* **2019**, *136*, 1–8.
141. Jufer, R.A.; Darwin, W.D.; Cone, E.J. Current methods for the separation and analysis of cocaine analytes. *Handb. Anal. Sep.* **2000**, *2*, 67–106, doi:10.1016/S1567-7192(00)80052-2.

142. Knuth, M.; Temme, O.; Daldrup, T.; Pawlik, E. Analysis of cocaine adulterants in human brain in cases of drug-related death. *Forensic Sci. Int.* **2018**, *285*, 86–92, doi:10.1016/j.forsciint.2018.02.001.
143. Alvarez, J.-C.; Boyer, J.-C.; Verstraete, A.G.; Pelissier-Alicot, A.-L. Conduite automobile et cocaïne : bases bibliographiques pour un consensus de la Société française de toxicologie analytique. *Toxicol. Anal. Clin.* **2015**, *27*, 165–183, doi:10.1016/j.toxac.2015.07.006.
144. Feliu, C.; Fouley, A.; Millart, H.; Gozalo, C.; Marty, H.; Djerada, Z. Clinical and analytical toxicology of opiate, cocaine and amphetamine. *Ann. Biol. Clin. (Paris)* **2015**, *54*–69, doi:10.1684/abc.2014.1009.
145. Baselt, R.C. *Disposition of toxic drugs and chemicals in man*; 11th edition; Biomedical Publications.; Seal Beach, CA, 2011; ISBN 978-0-692-77499-1.
146. Kolbrich, E.A.; Barnes, A.J.; Gorelick, D.A.; Boyd, S.J.; Cone, E.J.; Huestis, M.A. Major and Minor Metabolites of Cocaine in Human Plasma following Controlled Subcutaneous Cocaine Administration. *J. Anal. Toxicol.* **2006**, *30*, 501–510, doi:10.1093/jat/30.8.501.
147. Jagerdeo, E.; Abdel-Rehim, M. Screening of cocaine and its metabolites in human urine samples by direct analysis in real-time source coupled to time-of-flight mass spectrometry after online preconcentration utilizing microextraction by packed sorbent. *J. Am. Soc. Mass Spectrom.* **2009**, *20*, 891–899, doi:10.1016/j.jasms.2009.01.010.
148. Maquille, A.; Guillarme, D.; Rudaz, S.; Veuthey, J.-L. High-Throughput Screening of Drugs of Abuse in Urine by Supported Liquid–Liquid Extraction and UHPLC Coupled to Tandem MS. *Chromatographia* **2009**, *70*, 1373–1380, doi:10.1365/s10337-009-1337-z.
149. Follador, M.; Yonamine, M.; Moreau, R.; Silva, O. Detection of cocaine and cocaethylene in sweat by solid-phase microextraction and gas chromatography/mass spectrometry. *J. Chromatogr. B* **2004**, *811*, 37–40, doi:10.1016/j.jchromb.2004.03.071.
150. Valente-Campos, S.; Yonamine, M.; Moreau, R.L. de M.; Silva, O.A. Validation of a method to detect cocaine and its metabolites in nails by gas chromatography–mass spectrometry. *Forensic Sci. Int.* **2006**, *159*, 218–222, doi:10.1016/j.forsciint.2005.07.021.
151. D'Avila, F.B.; Ferreira, P.C.L.; Salazar, F.R.; Pereira, A.G.; Santos, M.K. dos; Pechansky, F.; Limberger, R.P.; Fröhlich, P.E. Analysis of cocaine/crack biomarkers in meconium by LC–MS. *J. Chromatogr. B* **2016**, *1012–1013*, 113–117, doi:10.1016/j.jchromb.2016.01.019.
152. Pellegrini, M.; Casá, A.; Marchei, E.; Pacifici, R.; Mayné, R.; Barbero, V.; Garcia-Algar, O.; Pichini, S. Development and validation of a gas chromatography–mass spectrometry assay for opiates and cocaine in human teeth. *J. Pharm. Biomed. Anal.* **2006**, *40*, 662–668, doi:10.1016/j.jpba.2005.07.003.
153. Arrêté du 13 décembre 2016 fixant les modalités du dépistage des substances témoignant de l'usage de stupéfiants, et des analyses et examens prévus par le code de la route et abrogeant l'arrêté du 5 septembre 2001 modifié fixant les modalités du dépistage des substances témoignant de l'usage de stupéfiants, et des analyses et examens prévus par le code de la route; 2016;

154. Tableau des durées de positivité Available online: <https://www.drogues-info-service.fr/Tout-savoir-sur-les-drogues/Le-depistage-des-drogues/Tableau-des-durees-de-positivite> (accessed on Sep 29, 2020).
155. Sorribes-Soriano, A.; Esteve-Turrillas, F.A.; Armenta, S.; de la Guardia, M.; Herrero-Martínez, J.M. Cocaine abuse determination by ion mobility spectrometry using molecular imprinting. *J. Chromatogr. A* **2017**, *1481*, 23–30, doi:10.1016/j.chroma.2016.12.041.
156. Brothier, F.; Pichon, V. Immobilized antibody on a hybrid organic–inorganic monolith: Capillary immunoextraction coupled on-line to nanoLC-UV for the analysis of microcystin-LR. *Anal. Chim. Acta* **2013**, *792*, 52–58, doi:10.1016/j.aca.2013.07.019.
157. Faure, K.; Delaunay, N.; Alloncle, G.; Cotte, S.; Rocca, J.-L. Optimization of in-situ monolithic synthesis for immunopreconcentration in capillary. *J. Chromatogr. A* **2007**, *1149*, 145–150, doi:10.1016/j.chroma.2007.03.031.
158. Brothier, F.; Pichon, V. Miniaturized DNA aptamer-based monolithic sorbent for selective extraction of a target analyte coupled on-line to nanoLC. *Anal. Bioanal. Chem.* **2014**, *406*, 7875–7886, doi:10.1007/s00216-014-8256-z.
159. Deng, N.; Liang, Z.; Liang, Y.; Sui, Z.; Zhang, L.; Wu, Q.; Yang, K.; Zhang, L.; Zhang, Y. Aptamer Modified Organic–Inorganic Hybrid Silica Monolithic Capillary Columns for Highly Selective Recognition of Thrombin. *Anal. Chem.* **2012**, *84*, 10186–10190, doi:10.1021/ac302779u.
160. Pichon, V.; Haupt, K. Affinity Separations on Molecularly Imprinted Polymers with Special Emphasis on Solid-Phase Extraction. *J. Liq. Chromatogr. Relat. Technol.* **2006**, *29*, 989–1023, doi:10.1080/10826070600574739.
161. Pichon, V. Selective sample treatment using molecularly imprinted polymers. *J. Chromatogr. A* **2007**, *1152*, 41–53, doi:10.1016/j.chroma.2007.02.109.
162. Chen, X.; Yang, W.; Zhou, Y.; Jiao, F. In situ synthesis of monolithic molecularly imprinted stationary phases for liquid chromatographic enantioseparation of dibenzoyl tartaric acid enantiomers. *J. Porous Mater.* **2012**, *19*, 587–595, doi:10.1007/s10934-011-9509-2.
163. Baykara, E.; Tunc, Y.; Ulubayram, K. Synthesis of monolithic HPLC stationary phase with self-assembled molecular recognition sites for 4-aminophenol. *J. Appl. Polym. Sci.* **2012**, *123*, 493–501, doi:10.1002/app.34460.
164. Turiel, E.; Martín-Esteban, A. Molecularly imprinted polymers-based microextraction techniques. *TrAC Trends Anal. Chem.* **2019**, *118*, 574–586, doi:10.1016/j.trac.2019.06.016.
165. Spégel, P.; Schweitz, L.; Nilsson, S. Molecularly imprinted polymers in capillary electrochromatography: Recent developments and future trends. *Electrophoresis* **2003**, *24*, 3892–3899, doi:10.1002/elps.200305665.
166. Zheng, C.; Huang, Y.-P.; Liu, Z.-S. Recent developments and applications of molecularly imprinted monolithic column for HPLC and CEC. *J. Sep. Sci.* **2011**, n/a-n/a, doi:10.1002/jssc.201100164.
167. Chen, J.; Bai, L.; Tian, M.; Zhou, X.; Zhang, Y. Hollow-fiber membrane tube embedded with a molecularly imprinted monolithic bar for the microextraction of triazine pesticides. *Anal Methods* **2014**, *6*, 602–608, doi:10.1039/C3AY41455H.

168. Hjertén, S. High-performance electrophoresis : Elimination of electroendosmosis and solute adsorption. *J. Chromatogr. A* **1985**, *347*, 191–198, doi:[https://doi.org/10.1016/S0021-9673\(01\)95485-8](https://doi.org/10.1016/S0021-9673(01)95485-8).
169. Reinholdsson, P.; Hargitai, T.; Isaksson, R.; Törnell, B. Preparation and properties of porous particles from trimethylolpropane trimethacrylate. *Angew. Makromol. Chem.* **1991**, *192*, 113–132, doi:[10.1002/apmc.1991.051920110](https://doi.org/10.1002/apmc.1991.051920110).
170. Rosenberg, J.E.; Flodin, P. Macroporous gels. 2. Polymerization of trimethylolpropane trimethacrylate in various solvents. *Macromolecules* **1987**, *20*, 1518–1522, doi:[10.1021/ma00173a013](https://doi.org/10.1021/ma00173a013).
171. Kempe, M. Antibody-Mimicking Polymers as Chiral Stationary Phases in HPLC. *Anal. Chem.* **1996**, *68*, 1948–1953, doi:[10.1021/ac9512160](https://doi.org/10.1021/ac9512160).
172. Santora, B.P.; Gagné, M.R.; Moloy, K.G.; Radu, N.S. Porogen and Cross-Linking Effects on the Surface Area, Pore Volume Distribution, and Morphology of Macroporous Polymers Obtained by Bulk Polymerization. *Macromolecules* **2001**, *34*, 658–661, doi:[10.1021/ma0004817](https://doi.org/10.1021/ma0004817).
173. Viklund, C.; Švec, F.; Fréchet, J.M.J.; Irgum, K. Monolithic, “Molded”, Porous Materials with High Flow Characteristics for Separations, Catalysis, or Solid-Phase Chemistry: Control of Porous Properties during Polymerization. *Chem. Mater.* **1996**, *8*, 744–750, doi:[10.1021/cm950437j](https://doi.org/10.1021/cm950437j).
174. Sellergren, B. *Molecularly Imprinted Polymers: Man-Made Mimics of Antibodies and their applications in analytical chemistry; Techniques and Instrumentation in Analytical Chemistry*; Elsevier: Amsterdam, 2001; Vol. 23; ISBN 978-0-444-82837-8.
175. Švec, F.; Tennikova, T.B.; Deyl, Z. *Monolithic Materials: Preparation, Properties and Applications*; Journal of Chromatography Library; Elsevier: Amsterdam, 2003; Vol. 67; ISBN 978-0-444-50879-9.
176. Gameiro, R.; Costa, S.; Barroso, M.; Franco, J.; Fonseca, S. Toxicological analysis of cocaine adulterants in blood samples. *Forensic Sci. Int.* **2019**, *299*, 95–102, doi:[10.1016/j.forsciint.2019.03.005](https://doi.org/10.1016/j.forsciint.2019.03.005).
177. Fiorentin, T.R.; D'Avila, F.B.; Comiran, E.; Zamboni, A.; Scherer, J.N.; Pechansky, F.; Borges, P.E.M.; Fröhlich, P.E.; Limberger, R.P. Simultaneous determination of cocaine/crack and its metabolites in oral fluid, urine and plasma by liquid chromatography-mass spectrometry and its application in drug users. *J. Pharmacol. Toxicol. Methods* **2017**, *86*, 60–66, doi:[10.1016/j.vascn.2017.04.003](https://doi.org/10.1016/j.vascn.2017.04.003).
178. Andrade-Eiroa, A.; Canle, M.; Leroy-Cancellieri, V.; Cerdà, V. Solid-phase extraction of organic compounds: A critical review (Part I). *TrAC Trends Anal. Chem.* **2016**, *80*, 641–654, doi:[10.1016/j.trac.2015.08.015](https://doi.org/10.1016/j.trac.2015.08.015).
179. Andrade-Eiroa, A.; Canle, M.; Leroy-Cancellieri, V.; Cerdà, V. Solid-phase extraction of organic compounds: A critical review. part II. *TrAC Trends Anal. Chem.* **2016**, *80*, 655–667, doi:[10.1016/j.trac.2015.08.014](https://doi.org/10.1016/j.trac.2015.08.014).
180. Lee, E.Z.; Huh, Y.S.; Jun, Y.-S.; Won, H.J.; Hong, Y.K.; Park, T.J.; Lee, S.Y.; Hong, W.H. Removal of bovine serum albumin using solid-phase extraction with in-situ polymerized stationary phase in a microfluidic device. *J. Chromatogr. A* **2008**, *1187*, 11–17, doi:[10.1016/j.chroma.2008.01.084](https://doi.org/10.1016/j.chroma.2008.01.084).

181. Proczek, G.; Augustin, V.; Descroix, S.; Hennion, M.-C. Integrated microdevice for preconcentration and separation of a wide variety of compounds by electrochromatography. *Electrophoresis* **2009**, *30*, 515–524, doi:10.1002/elps.200800308.
182. Cakal, C.; Ferrance, J.P.; Landers, J.P.; Caglar, P. Development of a micro-total analysis system ( $\mu$ -TAS) for the determination of catecholamines. *Anal. Bioanal. Chem.* **2010**, *398*, 1909–1917, doi:10.1007/s00216-010-3998-8.
183. Kang, Q.-S.; Li, Y.; Xu, J.-Q.; Su, L.-J.; Li, Y.-T.; Huang, W.-H. Polymer monolith-integrated multilayer poly(dimethylsiloxane) microchip for online microextraction and capillary electrophoresis. *Electrophoresis* **2010**, *31*, 3028–3034, doi:10.1002/elps.201000210.
184. Nordman, N.; Barrios-Lopez, B.; Laurén, S.; Suvanto, P.; Kotiaho, T.; Franssila, S.; Kostiainen, R.; Sikanen, T. Shape-anchored porous polymer monoliths for integrated online solid-phase extraction-microchip electrophoresis-electrospray ionization mass spectrometry: Microfluidics and Miniaturization. *Electrophoresis* **2015**, *36*, 428–432, doi:10.1002/elps.201400278.
185. Janků, S.; Komendová, M.; Urban, J. Development of an online solid-phase extraction with liquid chromatography method based on polymer monoliths for the determination of dopamine: Liquid Chromatography. *J. Sep. Sci.* **2016**, *39*, 4107–4115, doi:10.1002/jssc.201600818.
186. Sellergren, B. Direct drug determination by selective sample enrichment on an imprinted polymer. *Anal. Chem.* **1994**, *66*, 1578–1582, doi:<https://doi.org/10.1021/ac00081a036>.
187. Lasáková, M.; Thiébaut, D.; Jandera, P.; Pichon, V. Molecularly imprinted polymer for solid-phase extraction of ephedrine and analogs from human plasma. *J. Sep. Sci.* **2009**, *32*, 1036–1042, doi:10.1002/jssc.200800684.
188. Luliński, P.; Dana, M.; Maciejewska, D. Synthesis and characterization of 4-(2-aminoethyl)aniline imprinted polymer as a highly effective sorbent of dopamine. *Talanta* **2014**, *119*, 623–631, doi:10.1016/j.talanta.2013.11.060.
189. Dong, X.; Wang, W.; Ma, S.; Sun, H.; Li, Y.; Guo, J. Molecularly imprinted solid-phase extraction of (–)-ephedrine from Chinese Ephedra. *J. Chromatogr. A* **2005**, *1070*, 125–130, doi:10.1016/j.chroma.2005.03.017.
190. Luliński, P.; Maciejewska, D.; Bamburowicz-Klimkowska, M.; Szutowski, M. Dopamine-Imprinted Polymers: Template-Monomer Interactions, Analysis of Template Removal and Application to Solid Phase Extraction. *Molecules* **2007**, *12*, 2434–2449, doi:10.3390/12112434.
191. Fan, J.-P.; Zhang, L.; Zhang, X.-H.; Huang, J.; Tong, S.; Kong, T.; Tian, Z.-Y.; Zhu, J.-H. Molecularly imprinted polymers for selective extraction of synephrine from Aurantii Fructus Immaturus. *Anal. Bioanal. Chem.* **2012**, *402*, 1337–1346, doi:10.1007/s00216-011-5506-1.
192. Suedee, R.; Seechamnuntarakit, V.; Canyuk, B.; Ovatlarnporn, C.; Martin, G.P. Temperature sensitive dopamine-imprinted (N,N-methylene-bis-acrylamide cross-linked) polymer and its potential application to the selective extraction of adrenergic drugs from urine. *J. Chromatogr. A* **2006**, *1114*, 239–249, doi:10.1016/j.chroma.2006.02.033.
193. Tian, S.; Guo, Z.; Zhang, X.; Wu, X. Synthesis of molecularly imprinted co-polymers for recognition of ephedrine. *Anal. Methods* **2013**, *5*, 5179, doi:10.1039/c3ay41202d.

194. Takeuchi, T.; Murase, N.; Maki, H.; Mukawa, T.; Shinmori, H. Dopamine selective molecularly imprinted polymers via post-imprinting modification. *Org. Biomol. Chem.* **2006**, *4*, 565, doi:10.1039/b514432a.
195. *Chemicalize - Instant Cheminformatics Solutions*; ChemAxon, 2020;
196. Fan, J.-P.; Li, L.; Tian, Z.-Y.; Xie, C.-F.; Xue, Y.; Xie, Y.-L.; Xu, R.; Qin, Y.; Zhang, X.-H.; Zhu, J.-H. Synthesis and Evaluation of Uniformly Sized Synephrine-Imprinted Microparticles Prepared by Precipitation Polymerization. *Sep. Sci. Technol.* **2014**, *49*, 258–266, doi:10.1080/01496395.2013.837073.
197. Fan, J.-P.; Tian, Z.-Y.; Tong, S.; Zhang, X.-H.; Xie, Y.-L.; Xu, R.; Qin, Y.; Li, L.; Zhu, J.-H.; Ouyang, X.-K. A novel molecularly imprinted polymer of the specific ionic liquid monomer for selective separation of synephrine from methanol–water media. *Food Chem.* **2013**, *141*, 3578–3585, doi:10.1016/j.foodchem.2013.06.040.
198. Luliński, P.; Maciejewska, D. Effective separation of dopamine from bananas on 2-(3,4-dimethoxyphenyl)ethylamine imprinted polymer: Other Techniques. *J. Sep. Sci.* **2012**, *35*, 1050–1057, doi:10.1002/jssc.201100910.
199. Hou, X.; Huang, W.; Tong, Y.; Tian, M. Hollow dummy template imprinted boronate-modified polymers for extraction of norepinephrine, epinephrine and dopamine prior to quantitation by HPLC. *Microchim. Acta* **2019**, *186*, doi:10.1007/s00604-019-3801-2.
200. Fang, L.; Xie, J.; Lin, L.; Tian, M.; Row, K.H. Multi-phase extraction of ephedrine from *Pinellia ternata* and herbal medicine using molecular imprinted polymer coated ionic liquid-based silica. *Phytochem. Anal.* **2020**, *31*, 242–251, doi:10.1002/pca.2888.
201. Claude, B.; Nehmé, R.; Morin, P. Analysis of urinary neurotransmitters by capillary electrophoresis: Sensitivity enhancement using field-amplified sample injection and molecular imprinted polymer solid phase extraction. *Anal. Chim. Acta* **2011**, *699*, 242–248, doi:10.1016/j.aca.2011.05.014.
202. Claude, B.; Morin, P.; Denoroy, L. Selective solid-phase extraction of catecholamines and metanephrines from serum using a new molecularly imprinted polymer. *J. Liq. Chromatogr. Relat. Technol.* **2014**, *37*, 2624–2638, doi:10.1080/10826076.2013.853310.
203. Guillarme, D.; Nguyen, D.T.T.; Rudaz, S.; Veuthey, J.-L. Method transfer for fast liquid chromatography in pharmaceutical analysis: Application to short columns packed with small particle. Part II: Gradient experiments. *Eur. J. Pharm. Biopharm.* **2008**, *68*, 430–440, doi:10.1016/j.ejpb.2007.06.018.

---

## RESUME

Une des tendances actuelles de la recherche en chimie analytique est liée à la miniaturisation et l'intégration de différentes étapes de l'analyse dans un dispositif unique afin de répondre, entre autres, à des besoins de portabilité et d'automatisation. Cependant, des solutions pour l'analyse d'échantillons complexes de faibles volumes contenant des analytes d'intérêt de natures diverses à l'état de trace restent à développer. Une approche possible est la synthèse *in situ* de monolithes imprimés dans des capillaires et leur couplage en ligne avec l'étape de séparation et/ou de détection. C'est l'option qui a été étudiée lors de ce travail de thèse. Après une étude de l'état de l'art concernant l'intégration de polymères à empreintes moléculaires dans des dispositifs d'extraction et de séparation miniaturisés, le développement de supports monolithiques imprimés miniaturisés et leur couplage en ligne avec une séparation en nano-chromatographie en phase liquide ou bien directement avec une détection UV a été réalisé pour l'analyse d'échantillons biologiques. Différentes voies de synthèse ont été ciblées en faisant varier la nature des réactifs (molécule empreinte, agent réticulant et solvant), leur ratio et le mode d'initiation. La caractérisation des supports obtenus a été réalisée en termes de morphologie, de perméabilité et de répétabilité de synthèse. La sélectivité des monolithes imprimés a été évaluée par nano-chromatographie en phase liquide en confrontant leur potentiel d'extraction à celui de monolithes non imprimés synthétisés dans les mêmes conditions mais sans introduction de la molécule empreinte. Les protocoles d'extraction et conditions de couplages ont été optimisés avec succès permettant l'analyse de la cocaïne dans la salive et le plasma ou la détection de la benzoylecgonine dans l'urine (volume échantillon : 50-600 nL) avec des seuils de détection en accord avec la législation de l'ordre de la dizaine de ng mL<sup>-1</sup>. En exploitant le savoir-faire acquis, d'autres supports imprimés miniaturisés ont également été synthétisés afin de cibler des neurotransmetteurs ainsi que des analogues structuraux.

---

## ABSTRACT

An important part of the research in analytical chemistry is related to the miniaturization and integration of different analytical steps in a single device in order to meet, among other things, portability and automation issues. However, solutions for the analysis of complex samples with limited volumes containing various analytes of interest that may be found at trace levels are still required. One approach consists in the *in situ* synthesis of imprinted monoliths within capillaries and their on-line coupling with a separation and/or detection step. This was the objective of this thesis work. After the study of the state-of-the-art concerning the integration of molecularly imprinted polymers in miniaturized extraction and separation devices, the development of miniaturized imprinted monolithic supports and their on-line coupling with a nano-liquid chromatography separation or directly with UV detection were performed for biological applications. Different synthesis pathways were screened by varying the nature of the reagents (template, cross-linking agent, and solvent), their ratio and the mode of initiation. The characterization of the obtained supports was carried out in terms of morphology, permeability and synthesis repeatability. The selectivity of MIP monoliths was evaluated with nano-liquid chromatography by confronting their extraction potential with the one of non-imprinted monoliths synthesized in the same conditions but without the introduction of the template. The extraction protocols and coupling conditions were successfully optimized for the analysis of cocaine in saliva and plasma or the detection of benzoylecgonine in urine (sample volume: 50-600 nL) with detection thresholds in agreement with the legislation around tens of ng mL<sup>-1</sup>. By exploiting the know-how acquired, other miniaturized imprinted supports were also produced to target neurotransmitters and structural analogues.

---